UNIVERSITY OF SOUTHAMPTON

The relationship between zooplankton and their physico-chemical environment at the mesoscale

Alexander T Mustard

Submitted for the degree of Doctor of Philosophy

January 2001

ABSTRACT

The objective of this thesis is to examine what influences the distribution of different sized mesozooplankton at the mesoscale. Zooplankton distributions are influenced by both the physico-chemical environment and by biological processes. To study the relationship between these processes at the mesoscale, biological and physical variables were measured concurrently using a combination of the SeaSoar, fluorimeter, optical plankton counter (OPC) and EK500 echosounder instruments. These data were collected in March 1997, during a survey of the Strait of Hormuz, that connects the Arabian Gulf to the Gulf of Oman in the North West Indian Ocean.

OPC data were used to describe and study the distribution of mesozooplankton. The accuracy of the OPC's estimates of abundance and biovolume was determined by comparison with net samples of zooplankton collected by a Longhurst-Hardy Plankton Recorder (LHPR). The correlation of the OPC abundance data with the net samples showed an approximate 1:1 relationship, suggesting that the OPC was capable of reliably enumerating mesozooplankton. Biovolume was first calculated from the sizes of particles measured by the OPC using a spherical model for the zooplankton. The resulting OPC biovolume data were consistently larger than the biovolume measured in the net samples. The OPC biovolume was then calibrated using a spheroidal model, which better represented the zooplankton in the Strait and incorporated measurements of the dimensions of animals in the net samples. The resulting OPC biovolume was within the range of the net samples, although the OPC overestimated biovolume relative to the net at low *in situ* concentrations. The OPC biovolume and abundance were consistent with data from previous net surveys in the Strait, and the OPC biovolume calibration factor is close to factors determined empirically in other studies. A set of OPC biovolume calibration equations are defined. The calibrated OPC data were accepted as reliable for describing zooplankton distributions at the mesoscale.

The Strait of Hormuz is characterised by a two layer exchange of water between the Gulf of Oman and the Arabian Gulf. The SeaSoar survey revealed a mesoscale frontal region between these two flows, a sharp mesoscale front at the western boundary of this frontal region and sub-mesoscale internal waves in the eastern Strait. Changes in the distribution of zooplankton were correlated with all these features. The LHPR samples provided further detail of the zooplankton community, that was dominated by copepods (>80% of numbers) at both of the two stations in the Strait. The vertical distributions of different zooplankton taxa determined by the LHPR were at times strongly correlated with the water column structure, but at other times showed no correlation, indicating that both physical and biological mechanisms were influencing zooplankton distributions.

The mesoscale frontal water in the Strait had intermediate temperature and salinity characteristics of the two flows, but its biological properties differed dramatically from those

expected from conservative mixing. In the frontal water the chlorophyll *a* stock was double and the mesozooplankton abundance was only half that in the two flows. In the two flows mesozooplankton biovolume size spectrum was dominated by small (0.3-1.0 mm equivalent spherical diameter, ESD) zooplankton, whereas in the frontal water larger individuals dominated (2.3-4.5 mm ESD). Several, not necessarily exclusive, mechanisms were considered that may account for the observations. There was no evidence that the low stocks of small mesozooplankton were influenced by bottom-up or top-down mechanisms at the mesoscale, or that their distribution resulted from advection. A possible explanation is that the variability coupled with the large environmental gradients encountered in the frontal water made it unfavourable to zooplankton. However, all these mechanisms are simplistic for a natural system, where the interaction between many species in the ecotone (frontal region) makes the prediction of the resulting community difficult.

The standing stocks of the larger species of mesozooplankton (2.3-4.5 mm ESD) and the mean volume back scattering strength (MVBS) of macrozooplankton measured by the EK500 in the frontal water were intermediate in comparison with the two flows. This suggests that the larger species were influenced more by the physico-chemical environmental gradient across the whole Strait, rather than the mesoscale processes of the frontal region.

An abrupt change in the distribution of plankton was correlated with the sharp front at the western boundary of the frontal region, and allowed the effect of cross front mixing on different sized zooplankton to be examined. Across the front, small (0.4-1.6 mm ESD) zooplankton showed a gradient that was predominantly conservative with salinity, and hence mixing. The larger (1.6-4.0 mm ESD) zooplankton were aggregated on either side, but were at lower concentrations within the front.

On the eastern side of the Strait internal waves, with wavelengths <50 km, were observed as vertical perturbations in the water column structure and were correlated with similar changes in the zooplankton distributions. Spectral analysis of the variability revealed that the patchiness of small (0.4-1.0 mm ESD) zooplankton was correlated with the physical structure, while the patchiness of larger species was not.

These findings of this study indicate that physico-chemical processes at the mesoscale have a strong influence on the distribution of zooplankton. However, the analysis also indicates that different size classes of zooplankton have different distributions in relation to physical forcing at the mesoscale. Both physico-chemical and biological mechanisms that can account for these observations are discussed and assessed with reference to the observations and measurements made during the survey. The findings are also set in the context of other mesoscale studies.

CONTENTS

Chapter 1: Introduction, rationale and background to this thesis . . . 1
1.1 INTRODUCTION – RELEVANCE OF WORK 2
1.2 OBJECTIVES OF THIS THESIS 5
1.2.1 List of objectives 6
1.2.2 Work plan 6
1.2.3 Practical work undertaken by myself 8
1.3 PHYSICAL AND BIOLOGICAL MECHANISMS CAPABLE OF INFLUENCING ZOOPLANKTON DISTRIBUTIONS AT THE MESOSCALE 9
1.3.1 Interaction of the ecosystem with mesoscale environmental forcing . . . 10
1.3.2 Behavioural processes that influence zooplankton distributions . . . 13
1.3.3 Conclusion: physical and biological forcing at the mesoscale 14
1.4 TECHNIQUES FOR SAMPLING MESOSCALE ZOOPLANKTON DISTRIBUTIONS . . . 15
1.4.1 Traditional zooplankton sampling techniques 15
1.4.2 Modern technologies for describing zooplankton distributions 20
1.4.3 Conclusion: sampling technologies needed for mesoscale studies . . . 23

Chapter 2: The survey: review of previous studies in the survey area – the Strait of Hormuz, the Arabian Gulf and the Gulf of Oman, and data collection and processing from RRS *Charles Darwin* cruise 104 24
2.1 THE REGION: STRAIT OF HORMUZ, ARABIAN GULF AND GULF OF OMAN . . . 25
2.1.1 Physical conditions in the survey region 25
2.1.2 The phytoplankton community in the survey region 29
2.1.3 The zooplankton community in the survey region 31
2.1.4 Other aspects of the biology of the region 35
2.1.5 Summary of the findings of previous studies in the region 35
2.2 METHODS: RRS CHARLES DARWIN CRUISE 104 – COLLECTION OF DATA AND SAMPLES AND THEIR PROCESSING AND CALIBRATION 37
2.2.1 Introduction to the cruise and the sampling strategy 37
2.2.2 Hydrographic measurements made with a SeaSoar 38
2.2.3 Determining the distribution of chlorophyll *a* 40
2.2.4 Methods for processing Optical Plankton Counter data 43
2.2.5 Zooplankton samples collected with a Longhurst-Hardy plankton recorder . . 49
2.2.6 The measurement of bio-acoustic backscatter 53
2.2.7 The data collected by the profiling CTD 54

Chapter 3: The calibration of OPC data into accurate estimates of zooplankton abundance and biovolume in the Strait of Hormuz 56
3.1 COMPARISON OF ZOOPLANKTON ABUNDANCE FROM THE OPC WITH THE ABUNDANCE ENUMERATED FROM THE LHPR SAMPLES 58
3.1.1 Correction of the sampling biases of the OPC and LHPR 58
3.1.2 Further corrections required when using an OPC on SeaSoar 61
3.1.3 Comparison of zooplankton abundance from the OPC and LHPR samples . . 65
3.2 CALIBRATION OF ZOOPLANKTON BIOVOLUME FROM ESD MEASUREMENTS MADE BY THE OPC 72
3.2.1 Previous calibrations of biovolume and biomass from the OPC 73
3.2.2 Calibration equations for determining zooplankton biovolume with an OPC . . 74
3.2.3 Evaluation of errors associated with the calibration 79
3.3 COMPARISON OF CALIBRATED OPC BIOVOLUME WITH LHPR BIOVOLUME . . . 81
3.3.1 Comparison of OPC and LHPR biovolume before calibration 81
3.3.2 Comparison of calibrated OPC biovolume with the LHPR biovolume . . . 83

3.4 FURTHER EVALUATION OF CALIBRATED OPC BIOVOLUME 85
3.4.1 Comparison with previous studies in the region 85
3.42 Comparison with existing OPC calibration factors 86
3.4.3 Comparison between zooplankton and phytoplankton carbon biomass . . . 87
3.4.4 Summary of the evaluation of the calibrated OPC biovolume . . . 90

Chapter 4: Description of the physico-chemical environment and distribution of plankton in the Strait of Hormuz in March 1997 94
4.1 DATA COLLECTED WITH A SEASOAR AND A CTD IN THE STRAIT OF HORMUZ . . 95
4.1.1 Presentation of SeaSoar and CTD data 95
4.1.2 Hydrographic conditions in the Strait of Hormuz 97
4.1.3 Distribution of plankton in the Strait of Hormuz 118
4.1.4 Diel vertical migration of zooplankton in the Strait and Gulf of Oman . . . 121
4.1.5 Summary of hydrographic and biological observations made with SeaSoar . . 126
4.2 DATA COLLECTED WITH A LONGHURST HARDY PLANKTON RECORDER IN THE STRAIT . 127
4.2.1 Presentation of the data collected by the LHPR 128
4.2.2 Hydrographic conditions at both LHPR stations 136
4.2.3 Distribution of zooplankton measured by the LHPR 136
4.2.4 The distribution of euphausiids at stn 54007 140
4.2.5 Factors influencing the distribution of zooplankton at each station . . . 145
4.2.6 Summary of findings from LHPR data 146

Chapter 5: Analysis of the interrelationship between physical, chemical and biological environment and behavioural processes in determining the distribution of zooplankton in the Strait 148
5.1 THE INFLUENCE OF THE FORMATION OF THE STW ON THE DISTRIBUTION OF DIFFRERENT SIZED PLANKTON IN THE STRAIT OF HORMUZ 149
5.1.1 The concentration of chlorophyll *a* in each water type 150
5.1.2 Mesozooplankton abundance and biovolume measured by the OPC . . . 150
5.1.3 Mesozooplankton biomass size spectra measured by the OPC 154
5.1.4 Acoustic Backscatter from EK500 156
5.1.5 Summary and discussion of the influence of the formation of the STW on the distribution of plankton in the Strait 156
5.2 THE DISTRIBUTION OF PLANKTON AROUND THE FRONT BETWEEN THE AGO AND THE STW IN THE WESTERN STRAIT 157
5.2.1 A spatial description of the front and the associated plankton distributions . . 157
5.2.2 The influence of the physical processes at the front on the plankton . . . 160
5.2.3 The interrelationship between mesozooplankton and phytoplankton . . . 161
5.2.4 The relationship between meso- and macrozooplankton 168
5.2.5 Summary and discussion of observations and findings 168
5.3 THE AFFECT OF VARIABILITY CAUSED BY INTERNAL WAVES AT THE BOUNDARY BETWEEN THE GOS AND THE STW 169
5.3.1 Description of the physical structure and plankton distributions . . . 170
5.3.2 The impact of mesoscale and sub-mesoscale forcing on patchiness . . . 172
5.3.3 Spectral analysis of the variability of the temperature structure and the mesozooplankton and phytoplankton patchiness in the GOS 177
5.3.4 The importance of forcing mechanisms acting on the plankton . . . 180
5.3.5 Summary and conclusions 183

Chapter 6: Discussion of observations and findings 186
6.1 THE USE OF AN OPC TO DESCRIBE ZOOPLANKTON DISTRIBUTIONS AT THE MESOSCALE . 187
6.1.1 An assessment of the OPC calibration and improvements for future work . . 188
6.1.2 The use of the OPC in mesoscale studies, improvements in the collection of calibration and interpretation datasets 193
6.2 DISCUSSION OF THE FINDINGS OF THIS STUDY: THE EFFECT OF THE PHYSICOCHEMICAL ENVIRONMENT ON THE DISTRIBUTION OF ZOOPLANKTON 197
6.2.1 Summary of expected trophic interactions of plankton in the Strait . . . 198
6.2.2 Possible mechanisms impacting of zooplankton distributions in the three water types defined in the Strait of Hormuz 200
6.2.3 Mechanisms affecting plankton at the front between the STW and AGO . . 208
6.2.4 The importance of the internal waves in determining plankton distributions . . 209
6.3 IMPLICATIONS FOR THE RELATIONSHIP BETWEEN ZOOPLANKTON AND THEIR PHYSICO-CHEMICAL ENVIRONMENT AT THE MESOSCALE 210
6.3.1 The importance of different forcing mechanisms at the mesoscale . . . 210
6.3.2 Effect of zooplankton size on their relationship with the environment . . . 213
6.3.3 Implications for upper ocean productivity and biogeochemistry . . . 215

REFERENCES 217

APPENDICES 234
1 PEXEC processing of OPC data from CD 104 235
2 The relationship between the length and width of copepods 236
3 Quantifying and correcting the LHPR sample shrinkage 240
4 Comparison between biovolume to carbon conversions for zooplankton . . . 241
5 Relating ESD sizes to lengths and LHPR samples 243

LIST OF FIGURES

Chapter 2: The survey: review of previous studies in the survey area – the Strait of Hormuz, the Arabian Gulf and the Gulf of Oman, and data collection and processing from RRS Charles Darwin cruise 104

Figure 2.1.1.i The region of study: a map of the Strait of Hormuz, the Arabian Gulf and the Gulf of Oman 26
Figure 2.1.1.ii The circulation in the Arabian Gulf and the Strait of Hormuz. Also showing the gradient in species richness of phytoplankton and zooplankton 26
Figure 2.2.2.i A map showing the positions of the six transects of the SeaSoar survey and the LHPR biological stations in the Strait of Hormuz 39
Figure 2.2.2.ii SeaSoar fitted with an optical plankton counter 39
Figure 2.2.3.i The calibration graph for the CTD fluorimeter in the Gulf of Oman, showing the lack of quenching 42
Figure 2.2.4.i Histogram showing the counts in size classes in the raw OPC data . . 42

Chapter 3: The calibration of OPC data into accurate estimates of zooplankton abundance and biovolume in the Strait of Hormuz

Figure 3.1.2.i Profiles of mean particle concentration derived from OPC data from up and down profiles of SeaSoar in the Strait of Hormuz and in the Mediterranean . . . 64
Figure 3.1.3.i Zooplankton abundance from the OPC and the LHPR at station 54006 . . 68
Figure 3.1.3.ii Water column structure during SeaSoar and LHPR sampling at station 54006 . 68
Figure 3.1.3.iii Zooplankton abundance from the OPC and the LHPR at station 54007 . . 70
Figure 3.1.3.iv Water column structure during SeaSoar and LHPR sampling at station 54007 . 70
Figure 3.2.2.i Diagram representing the effect of orientation on shadow size . . . 76
Figure 3.2.2.ii Graph showing the CSA of a spheroid from Eq 3.2.3 at various angles . . 76
Figure 3.2.2.iii CF_{ran} to correct the measured CSA to the maximum CSA for spheroids with different values of r 76
Figure 3.2.3.i CF_{vol} for spherical model for spheroids with different values of r . . 76
Figure 3.3.1.i Uncalibrated zooplankton biovolume from the OPC and LHPR at station 54006 . 82
Figure 3.3.2.i Calibrated zooplankton biovolume from the OPC and LHPR at station 54006 . 82
Figure 3.4.2.i A comparison of the OPC biovolume calibration used in the Strait of Hormuz with calibration functions used in other studies 88
Figure 3.4.3.i Comparison of phytoplankton and mesozooplankton carbon biomass in a section of the survey from the west side of the Strait, plotted as a function of salinity . . . 88

Chapter 4: Description of the physico-chemical environment and distribution of plankton in the Strait of Hormuz in March 1997

Figure 4.1.1.i Contour plots of legs through the Strait of Hormuz (16 pp) . . . 98-113
Figure 4.1.1.ii Maps of the distribution of surface (9 m) salinity, temperature, chlorophyll *a*, OPC measured zooplankton abundance and biovolume, and MVBS at 120 kHz at 18m . . 114
Figure 4.1.1.iii Contoured CTD sections from the Strait of Hormuz 115
Figure 4.1.1.iv Full depth CTD data from line D: showing salinity, temperature and oxygen . 116
Figure 4.1.2.i Temperature as a function of salinity for the water sampled by the CTD in the Gulf of Oman and the Arabian Gulf and by the SeaSoar in the Strait 116
Figure 4.1.4.i Diel vertical migration of MVBS at 38 kHz 123
Figure 4.1.4.ii The vertical distribution of MVBS at 38 kHz over 24 hours in the Gulf of Oman 123
Figure 4.1.4.iii Day and night profiles of zooplankton biovolume in 4 OPC size classes in the GOS 124
Figure 4.1.4.iv Mesozooplankton biovolume in biovolume in each size class in the upper 30 m of the GOS 124

Figure 4.2.1.i The distribution of zooplankton biovolume with depth at station 54006: biovolume divided into size classes – profiles of temperature and salinity of the down profile also presented 129
Figure 4.2.1.ii The distribution of zooplankton biovolume with depth at station 54007: biovolume divided into size classes – profiles of temperature and salinity of the down profile also presented 129
Figure 4.2.1.iii The percentage of zooplankton abundance represented by each taxonomic group on the down profile at station 54006 (08/03/97) 130
Figure 4.2.1.iv The percentage of zooplankton abundance represented by each taxonomic group on the down profile at station 54007 (11/03/97) 131
Figure 4.2.1.v Abundance profiles of the dominant zooplankton groups at station 54006 . 132
Figure 4.2.1.vi Abundance profiles of the dominant zooplankton groups at station 54006 . 133
Figure 4.2.1.vii Abundance profiles of the dominant zooplankton groups at station 54007 . 134
Figure 4.2.1.viii Abundance profiles of the dominant zooplankton groups at station 54007 . 135
Figure 4.2.4.i Acoustic backscatter at 120 kHz contoured against time and depth at station 54007 142
Figure 4.2.4.ii Bars showing zooplankton biovolume in each two minute sample from the LHPR and lines showing concurrent acoustic backscatter at 120 and 200 kHz 142
Figure 4.2.1.iii Vertical profiles from the up cast at stn 54007 142

Chapter 5: Analysis of the interrelationship between the physical, chemical and biological environment and behavioural processes in determining the distribution of zooplankton in the Strait

Figure 5.1.1.i The surface position of the water types identified in the Strait of Hormuz . 151
Figure 5.1.1.ii Biological characteristics of the water types identified in the Strait of Hormuz . 152
Figure 5.1.1.iii Biomass size spectra for the upper 25 m of the GOS, STW and AGO water types 153
Figure 5.2.1.i The distribution of chlorophyll *a,* mesozooplankton and MVBS at the front between the AGO and STW 158
Figure 5.2.2.i Zooplankton biovolume in each size class and chlorophyll a integrated over the top 25 m, plotted as a function of the average salinity in the top 25 m 162
Figure 5.2.3.i The relationship between salinity and the ratio of phytoplankton carbon to zooplankton carbon in the upper 25 m of the front between the AGO and STW 163
Figure 5.2.3.ii The relationship between salinity and the ratio of phaeopigments to chlorophyll *a* in surface samples taken concurrently to those above 163
Figure 5.3.1.i Variability in thermal structure and zooplankton abundance in GOS water . 171
Figure 5.3.1.ii Zooplankton abundance (0.4-4.1 mm ESD) plotted as a function of potential temperature. Data from the east side of the Strait of Hormuz 171
Figure 5.3.2.i Variability in the depth of the 22.5°C isotherm and the zooplankton abundance integrated over the upper 50 m of the water column in the GOS 174
Figure 5.3.2.ii The relationship between the depth of the isotherm and zooplankton abundance (integrated over the upper 50 m) in the Gulf of Oman inflow 174
Figure 5.3.2.iii The Pearson Correlation Coefficient between mesozooplankton abundance in the upper 50 m and the depth of the 22.5°C isotherm, plotted as a function of organism size . . 175
Figure 5.3.3.i Power spectra of the spatial variability in the depth of the 22.5°C isotherm, chlorophyll *a*, and mesozooplankton abundance in each size class integrated over the upper 50m . . 179
Figure 5.3.4.i The relationship between phytoplankton and temperature in the eastern Strait . 175

List Of Abbreviations Used

ADCP – acoustic Doppler current profiler
AGO – Arabian Gulf outflow water, dense high salinity water flowing eastwards through the Strait of Hormuz
ANOVA – analysis of variance
ARIES – auto-sampling and recording instrumented environmental sampling system
CalCOFI – Californian Cooperative Oceanic Fisheries Investigation
CD 104 – R.R.S. *Charles Darwin* cruise 104
CF_{ran} – calibration factor required to correct the mean CSA of a particle measured by an OPC to a maximum CSA
CF_{vol} – calibration factor required to correct the volume of particle determined with a spherical model from OPC data to its actual volume
Chl*a* – Chlorophyll *a* concentration
CPR – continuous plankton recorder
CSA – cross sectional area
CTD – vertical profiling system, incorporating sensors such as the conductivity, temperature, depth sensor
DS – digital size, the output voltage from the OPC that represents the shadow size of a particle
DVM – diel vertical migration
ESD – equivalent spherical diameter
F_D – Door factor
FFT – Fast Fourier Transform
F_m – acidification coefficient
FRRF – fast repetition rate fluorimeter
GOS – Gulf of Oman surface inflow, warm water flowing westward into the Strait of Hormuz from the Gulf of Oman
GPS – the global positioning system
HC – herbivorous consumption
HPLC – high pressure liquid chromatography
I_{24} – ingestion of chlorophyll by a zooplankter in 24 hours
IAPSO –
IOSN – Indian Ocean Standard net
JGOFS – Joint Global Ocean Flux Study
LHPR – Longhurst-Hardy plankton recorder
LOPC – laser optical plankton counter
MAPS – multifrequency acoustic profiling system
MOCNESS – multiple opening/closing net and environmental sensing system
MVBS – mean volume backscattering strength
NORPAC – North Pacific plankton net
OAR – open area ratio
OPC – optical plankton counter
PAR – photosynthetically available radiation
PCC – Pearson's Correlation Coefficient
PSM – plankton sampling mechanism
r – the ratio of the length of the major to minor axis of a spheroid
R.R.S. – Royal Research Ship
RMT – rectangular midwater trawl
SOC – Southampton Oceanography Centre
stn – biological station
STW – Strait transition water, represents the frontal region between the AGO and GOS
TAPS – Tracor acoustic profiling system
TUBA – towed undulating bio-acoustic instrument
UAE – the United Arab Emirates
UVP – underwater video profiler
VPR – video plankton recorder
WP-2 – working party two plankton net
§ - section

ACKNOWLEDGEMENTS

First, I would like to thank Dr Thomas Anderson for his supervision of my PhD, his efforts in reviewing the manuscript and specifically for his help with writing the OPC calibration equations in this thesis. I am also grateful to Professor Paul Tyler for his overall supervision of this work.

The main datasets presented and analysed in this thesis were collected during R.R.S. *Charles Darwin* cruise 104 (CD 104). I am grateful to the principal scientist Professor Howard Roe, Captain Robin Plumley, and the officers, crew and scientific complement. I would also like to thank Dr Raymond Pollard for writing FORTRAN programs for processing the data from the optical plankton counter, and particularly for the modifications to the programs that I requested. I am also grateful to Dr David Smeed, Dr John Allen and Mr Nick Crisp for their initial processing of the physical hydrographic variables measured from SeaSoar and the CTD during CD 104. Individually, I would like to thank Dr David Smeed for his advice and discussions concerning the physical oceanography of the study region, Dr John Allen for his help in understanding the problems associated with the use of an optical plankton counter on SeaSoar, and Mr Nick Crisp for calculating the mean volume backscattering strength from the EK 500 echosounder. I would also like to acknowledge the work of Ms Penny Howell, Ms Jenny Bull, Dr Peter Herring, Dr Pat Hargreaves and Dr Phil Pugh in processing the rectangular midwater trawl (RMT) samples collected during the cruise. I am grateful to Ms Sophie Fielding, Ms Gabriella Malzone and Dr Peter Herring for their advice in sorting the zooplankton samples collected by the Longhurst-Hardy plankton recorder. I would also like to thank Drs Meric Srokosz, Brian Bett, Richard Lampitt, Peter Challenor and Mr Ben Rabe for useful discussions relating to this PhD.

I would also like to thank my examiners Dr Jonathon Watkins and Dr John Williams for their advice, ideas and review of this thesis, and an enjoyable discussion of the work.

I am also grateful for the support of my family and friends during my studentship and writing of this thesis.

CHAPTER 1

Introduction, rationale and background to this thesis

1.1 INTRODUCTION – RELEVANCE OF WORK 2
1.2 OBJECTIVES OF THIS THESIS 5
1.3 PHYSICAL AND BIOLOGICAL MECHANISMS CAPABLE OF INFLUENCING ZOOPLANKTON DISTRIBUTIONS AT THE MESOSCALE 9
1.4 TECHNIQUES FOR SAMPLING MESOSCALE ZOOPLANKTON DISTRIBUTIONS . . 15

1.1 INTRODUCTION – RELEVANCE OF WORK

Within the ocean, superimposed on top of the large scale currents and gyres there is mesoscale variability. Mesoscale physical features are widespread, and have a strong influence on the plankton community because they operate at spatial and temporal scales that are significant to the biological processes of plankton populations. The mesoscale covers scales between 10 and 100 km and includes physical features such as eddies, fronts, jets and filaments. These features typically persist for weeks to months, but may last for more than a year. A number of studies have investigated the impact of these features on the distribution of phytoplankton and primary production, but less is known about the impact of these processes on the distribution of zooplankton, the secondary producers.

Processes that influence the distribution of zooplankton at the mesoscale

At the mesoscale both physical and biological forcing can affect zooplankton distributions (Haury *et al.*, 1978), see section 1.3 (§1.3). The geostrophic and ageostrophic circulation associated with physical features can advect, accumulate and disperse both phytoplankton and zooplankton (Denmann and Powell, 1984; Franks, 1992). Physical processes at the mesoscale also have an important indirect impact on zooplankton by forcing the ecosystem. Upwelling induced by mesoscale features can result in bottom-up forcing by supplying new nutrients to the euphotic zone (Falkowski *et al.*, 1991; Strass, 1992; Pollard and Regier, 1992). In the open ocean nutrients often limit primary production, so upwelling increases phytoplankton production and provides a food source for zooplankton. Bottom-up forcing can influence the degree of trophic coupling in the ecosystem, and results in a shift away from a "steady state" system dominated by tightly coupled microheterotrophs to a "classic" food chain where a higher proportion of the primary production is assimilated by mesozooplankton (§1.3). The distribution of zooplankton can also be controlled by top-down processes, such as an increased density of predators, accumulated by physical or biological processes (Wiebe and Boyd, 1978; Wishner *et al.*, 1988). The behaviour of zooplankton can also influence their distributions, and at the mesoscale this interacts with physical processes because both operate over similar spatial and temporal scales (Haury *et al.*, 1978). Examples of behavioural processes are vertical migration, mating and feeding (§1.3).

Several important aspects of zooplankton biology are correlated with body size, such as swimming ability, population doubling times, prey selection and trophic status

(e.g. Sheldon *et al.*, 1972; Platt, 1985; Steele, 1991). These factors can influence the impact of these forcing processes on zooplankton distributions. As a result mesoscale forcing can be expected to have different affects on different sized zooplankton.

Impact of mesoscale processes on upper ocean biogeochemistry

Recent studies have demonstrated that physical processes at the mesoscale may have an important impact on biogeochemical cycling in the upper ocean. For example, calculations have shown that physical processes associated with mesoscale eddies in the Sargasso Sea may provide around 60% of the new nitrogen available for phytoplankton production in the euphotic zone (McGillicuddy and Robinson, 1997). In addition, zooplankton feeding impacts on geochemical processes in the upper ocean, for example by recycling nutrients for phytoplankton, and by exporting production to deeper waters as faecal pellets (Lampitt *et al.*, 1990). The export flux to the deep ocean is greater when larger zooplankton are the dominant grazers, as these produce faster sinking faecal pellets. Mesoscale physical features may influence the size distribution of zooplankton communities and so are important in determining the export of atmospheric carbon dioxide to the deep ocean, which in a steady state system is balanced by new nutrient supply, because of their impact on primary production and community structure (Watson *et al.*, 1991). In addition it is important to evaluate the role of mesozooplankton when determining the sustainable harvest of the ocean as they ultimately lead to fish production, rather than the primary production being recycled through the microbial loop (Cushing, 1989).

An elucidation of the relationship between different sized plankton and the mesoscale physical and chemical environment is necessary for increasing understanding, modelling and predicting a range of biogeochemical processes in the upper ocean.

Determining mesoscale zooplankton distributions

It is well established that zooplankton are not evenly or randomly distributed in space, but show spatial (and temporal) heterogeneity, known as "patchiness", from megascales (10^4 km) down to nannoscales (10^{-4} km), (e.g. Steele, 1978; Mackas *et al.*, 1985; Krembs *et al.*, 1998). Despite their patchy distribution, zooplankton have traditionally been sampled by techniques that are limited in their spatial resolution and coverage (Hardy, 1956).

Relatively recently zooplankton sensing techniques have been developed with the appropriate resolution and coverage to determine the spatial heterogeneity of

zooplankton at the mesoscale (§1.4). These include acoustic echosounders which measure the backscatter from macrozooplankton and micronekton (Flagg and Smith, 1989) and the optical plankton counter (OPC) which counts and sizes mesozooplankton (Herman, 1992). These techniques allow the distributions of different size zooplankton to be described at the same time and space scales as physical hydrographic and chlorophyll measurements. This concurrent sampling is fundamental in the robust study of the interaction between environmental variability and biological processes at the mesoscale (Roe *et al.*, 1996). The measurements made with acoustic and optical zooplankton sensing technologies must be validated by comparison with established sampling technologies, such as nets. In addition to calibration data, the nets can provide samples for taxonomic and process studies.

Such a multidisciplinary dataset, incorporating concurrent measurements of zooplankton distribution, is central to this thesis in observing and studying the relationship between different sized zooplankton and their mesoscale physico-chemical environment.

1.2 Objectives of this Thesis

Background

Three main tasks were completed in order to study the importance of the mesoscale physico-chemical environment in determining observed zooplankton distributions. (1) A multidisciplinary (hydrographic and biological) dataset was collected on RRS *Charles Darwin* cruise 104 (CD 104), in February and March 1997, in the Gulf of Oman, Strait of Hormuz and Arabian Gulf (see methods §2.2). (2) Net samples were analysed after the cruise and used to calibrate observations made with an optical plankton counter. (3) The distributions of different sized zooplankton were described and analysed in relation to the physico-chemical environment at the mesoscale.

The SeaSoar survey within the Strait of Hormuz revealed physical variability on scales of 5 to more than 100 km. The Strait of Hormuz is characterised by a two layer exchange, whereby lower salinity water from the Gulf of Oman, overlies high salinity water from the Arabian Gulf (see §2.1 for more detail and references). This study defined a third water type in the Strait (differentiated by temperature and salinity characteristics not found elsewhere in the region) which was formed by the mixing of water from the Gulf of Oman and Arabian Gulf. The formation of this water occurred at a scale of ≈100 km and thus represents a mesoscale frontal region between the two layers. Other features identified in this study are a more sharply defined mesoscale front (50-80 km) which forms part of this larger frontal region and marks the western boundary of the water formed in the Strait, and meso- and sub-mesoscale variability primarily resulting from internal waves on the east side of the Strait.

The acoustic and optical sampling technologies were used to determine distributions of different sized zooplankton in relation to these features. It was hypothesised that because of differences in their behaviour and physiology, the various sizes of zooplankton would show distinct interactions with the environmental forcing. This thesis concentrates on discerning the importance of the mesoscale physico-chemical environment in determining the distribution of different sized zooplankton (with their associated differences in behaviour) in the Strait of Hormuz.

1.2.1 List of objectives

a) Describe the distribution of zooplankton (in size classes and taxonomic groups) in relation to physical features and water column structure in the Strait of Hormuz.

b) Assess the importance of physical forcing mechanisms on zooplankton, in particular at the mesoscale, in the Strait.

c) Compare the importance of physical forcing mechanisms and biological forcing mechanisms at the mesoscale, and investigate how they interact.

d) Examine how the impact of the size of zooplankton varies with mesoscale forcing.

e) Examine the accuracy and value of the data produced by modern zooplankton sampling technologies, specifically from an optical plankton counter, using net samples.

1.2.2 Work plan of the thesis

1.2.2.1 Introduction and literature review. Chapter 1

Introduce the subject area, and the relevance and rationale of this work. Also list primary objectives and the work carried out to achieve these. Subsequently there are literature reviews detailing the physical environmental and biological mechanisms capable of influencing zooplankton distributions at the mesoscale, and the advances in sampling technologies that allow more robust studies of the mesoscale distribution of zooplankton.

1.2.2.2 The survey region, and data collection methods. Chapter 2

Introduce the survey region, and review previous hydrographic and pelagic biology studies, setting the Strait of Hormuz in context of the Arabian Gulf and Gulf of Oman. This is followed by a description of the collection, processing and calibration of multidisciplinary data from CD 104, and additional background information on the optical plankton counter (OPC) and the Longhurst Hardy plankton recorder (LHPR).

1.2.2.3 Calibration and evaluation of the OPC data. Chapter 3

Comparison of the zooplankton abundance counted by the OPC with the abundance enumerated in LHPR samples. Quantify and correct sampling biases of both instruments to produce a standardised calibration dataset. Theoretical calibration of OPC size measurements into biovolume accounting for shape, orientation, translucency and appendages of zooplankton. Comparison of calibrated biovolume with biovolume measured in LHPR samples. Additional evaluation of OPC biovolume calibration with (1) zooplankton net samples from previous surveys in the region, (2) previous calibration factors determined for the OPC, and (3) after conversion into biomass, with concurrent measurements of phytoplankton biomass.

1.2.2.4 The hydrography and distribution of zooplankton in the Strait. Chapter 4

Presentation of contour plots of physical structure and the distribution of plankton measured during the SeaSoar survey in the Strait. Description of major hydrographic features such as the exchange between Gulf of Oman and Arabian Gulf, the water types present and the mesoscale and sub-mesoscale variability. Description of the distribution of phytoplankton and meso- and macrozooplankton in relation to physical and chemical environment. Investigation of macrozooplankton diel vertical migration (DVM) in the Gulf of Oman and Strait of Hormuz. Investigation of mesozooplankton DVM in the Strait of Hormuz. Description of the vertical distribution of zooplankton taxonomic groups measured by the LHPR in the Strait. These distributions are discussed in relation to depth, water column structure and water type.

1.2.2.5 Analysis of the impact of mesoscale physical and biological driving forces on distribution of zooplankton in the Strait. Chapter 5

This chapter examines the interrelationship between the physical, chemical and biological environment and behavioural processes in determining the distribution of zooplankton at various scales in the Strait of Hormuz. Determine the biological characteristics of the water types present in the Strait at >100 km scale. Estimate potential zooplankton herbivory in the Strait. Investigate the distribution of different sized zooplankton in relation to a front in the western Strait. Examine the effect of sub-mesoscale variability in the eastern Strait, that primarily results from internal waves, on different sized plankton.

1.2.2.6 Discussion of findings. Chapter 6

Discuss the use of an optical plankton counter as a tool to describe the distribution of zooplankton at the mesoscale. Evaluate OPC calibration in terms of zooplankton

abundance and biovolume. Discuss errors associated with OPC and suggest solutions. List limitations of the calibration dataset used in this study and propose an improved methodology. Compare the main features of the distribution of zooplankton in relation to the mesoscale environment in the Strait of Hormuz with previous studies in this area. Examine environmental and behavioural mechanisms that may determine mesoscale plankton distributions in the Strait. Evaluate these in context of observations and other mesoscale studies. Discuss the implications of the findings of this study on the impact of mesoscale forcing on the role of different size zooplankton in biogeochemical processes in the upper ocean.

1.2.3 Practical work undertaken by myself

I participated in R.R.S. Discovery cruise 223 in the North Atlantic, although as a result of equipment failure, there were no data collected on this cruise by the optical plankton counter, and therefore no data from this cruise are presented in this thesis. Subsequently, I went to sea on R.R.S. *Charles Darwin* cruise 104, to the Gulf of Oman, Strait of Hormuz and Arabian Gulf, to collect the datasets that are presented and analysed in this thesis. As a late addition to the scientific complement and as a PhD student I did not have any influence of cruise strategy and survey design during the cruise. My responsibilities and duties at sea included processing OPC data, analysing oxygen and chlorophyll samples, and collecting zooplankton samples with net systems including the LHPR, CPR, RMT and WP-2 nets. On land, I identified the major taxonomic groups and measured the abundance and biovolume of zooplankton in the LHPR samples. I also calibrated and re-processed the OPC data, and calibrated the fluorimeters into chlorophyll *a* concentration. I was also involved in producing several deliverable reports resulting from the datasets from these cruises: Mustard (1997), Crisp *et al.* (1998) and Rabe *et al.* (1998).

1.3 PHYSICAL AND BIOLOGICAL MECHANISMS CAPABLE OF INFLUENCING ZOOPLANKTON DISTRIBUTIONS AT THE MESOSCALE

The mesoscale is thought to be important in the ocean because ubiquitous environmental variability has been observed at this scale in physical, chemical and biological parameters. Several reviews have demonstrated the impact of the physico-chemical environment on the distribution of plankton at the mesoscale (e.g. reviewed by Haury *et al.*, 1978; Herman and Platt, 1980; Owen, 1981; Denmann and Powell, 1984). In more recent studies and reviews, the increasing importance of the behaviour of zooplankton has been noted, and the current prevailing opinion is that distribution of zooplankton, at the mesoscale, results from the interaction of biological processes with the physical forcing, (e.g. Haury *et al.*, 1978; Pinel-Alloul, 1995; Folt and Burns, 1999). However, only recently have zooplankton sampling technologies had the adequate resolution and coverage to collect the data needed to observe this interaction (see §1.4). This section reviews the ways in which zooplankton populations are affected by and interact with mesoscale physical processes.

Forcing of zooplankton at different scales

Various physical and biological processes interacting over wide range of scales influence the distribution of zooplankton in the ocean (Haury *et al.*, 1978). Variability in the forcing leads to spatial heterogeneity in the plankton populations at that scale, a phenomenon known as patchiness. Patchiness is well established as a fundamental feature of plankton populations (e.g. Hardy and Gunther, 1935; Cassie, 1963; Steele, 1978; Mackas *et al.*, 1985; Kils, 1993) and is observable from the megascale (10^4 km) to the nanoscale (10^{-8} km) (Conversi and Hameed, 1998; Krembs *et al.*, 1998).

Pinel-Alloul (1995) summarises that "over large geographic scales, abiotic forces should be prominent and, in contrast, the biotic forces should have the primacy at small spatial scales". At the megascale (>10^3 km) physical forcing, such as from the climate and circulation of ocean gyres, dominates in determining the geographic distribution of primary production and consequently the zooplankton. These large scale physical processes persist over many generations of plankton, which leads to the formation of stable faunal provinces: the basis of zoogeography (Fager and McGowan, 1963; Spoel and Heyman, 1983; Pierrot-Bults *et al.*, 1986; Barry and Dayton, 1991). At the finescale (<1 km) biological mechanisms, with their smaller spatial and temporal scales, are more dominant in determining zooplankton spatial heterogeneity. Behaviours such as migration, predator prey interactions and

reproductive behaviour have been identified as driving forces (Cassie, 1959; Burns and Folt, 1999). The mesoscale (10s to 100s km, weeks to months in duration) falls between these scales, and is characterised by physical features such as eddies and fronts. The mesoscale is interesting because the distribution of zooplankton is determined by both the widespread physical features and their interaction with biological processes (Haury *et al.*, 1978; Roe *et al.*, 1996). This interaction occurs at the mesoscale because physical forcing mechanisms exist on temporal and spatial scales that coincide with the scales of biological processes of plankton populations (Steele, 1991; Dickey, 1991; Hitchcock *et al.*, 1993).

1.3.1 Interaction of the ecosystem with mesoscale environmental forcing

The impact of mesoscale physical forcing can be divided into direct affects on the zooplankton and indirect affects that influence the zooplankton through other aspects of the planktic[1] community. Direct affects are the physical redistribution of plankton caused by flow field associated with mesoscale phenomena. Indirect affects include physico-chemical processes that result in bottom-up forcing of the community.

1.3.1.1 The direct physical redistribution of plankton by mesoscale circulation

Mesoscale features, such as eddies and fronts, contain kinetic energy equivalent to major currents, and an order of magnitude larger than the mean flow (Richards and Gould, 1996). Examples of this flow are the rotation and advection of eddies, convergence and divergence at fronts and flow along frontal jets. This flow field can directly influence zooplankton distributions by aggregating, dispersing, isolating, redistributing and advecting zooplankton populations (Wiebe *et al.*, 1976a; the Ring Group, 1981; Owen, 1981; Franks, 1992; Govoni and Grimes, 1992) and can also directly alter zooplankton behaviour (Wiebe *et al.*, 1976a; Haury *et al.*, 1990).

Mesoscale features can also contain ageostrophic vertical velocities, for example as an eddy rotates upwelling and downwelling is induced on either side (Allen and Smeed, 1996). Vertical motion can also redistribute, concentrate and disperse both phytoplankton and zooplankton (Denmann and Powell, 1984). At the Almeria-Oran front, in the western Mediterranean, ageostrophic subduction, induced by the front, transports phytoplankton out of the euphotic zone (Allen *et al.*, submitted; Fielding *et al.*, submitted).

[1] The adjective planktic is used in this thesis instead of planktonic following the recommendation in Harris *et al.* (2000) page 2.

The mobility of the plankton will determine the extent to which they can resist being redistributed by the flow field. In general, the swimming ability of plankton is related to their size. Phytoplankton and microzooplankton are not capable of significant locomotion on these scales, but larger zooplankton become more capable of maintaining their ideal position in the face of stronger mixing (Mackas and Boyd, 1979; Haury *et al.*, 1990; Piotkovski *et al.*, 1997). Gallager *et al.* (1996) concluded that in water around the George's Bank weak swimmers were aggregated in stratified regions with high vertical stability, while strong swimmers were aggregated in either areas of low or high vertical stability. Populations of small organisms can nevertheless persist in advective regimes if their doubling rates are sufficiently high (e.g. Kierstead and Slobodkin, 1953). The size of a zooplankton, which in general is related to its mobility, will partly determine the influence of direct physical forcing.

1.3.1.2 The indirect forcing of zooplankton at the mesoscale

Indirect mesoscale forcing involves physical mechanisms that influence other aspects of the planktic community, which in turn modify the distribution of zooplankton. Bottom-up mechanisms involve physico-chemical processes that increase autotrophic production and may lead to secondary production and thus influence zooplankton distributions. Bottom-up forcing can also occur when plankton are aggregated and dispersed by the flow field changing the availability of food for the zooplankton.

Primary production is often limited by the lack of nutrients in the oligotrophic mixed layer of the open ocean (Cushing, 1959). The upward ageostrophic vertical circulation and the doming of isopycnals induced by mesoscale physical features provide mechanisms to supply nutrients from below the mixed layer into the euphotic zone. In this way mesoscale features can enhance primary production (e.g. Prier *et al.*, 1993; Videau *et al.*, 1994; Fernández and Pingree, 1996). Ageostrophic vertical motions within mesoscale features, have been determined to be of the order of several tens of metres per day, which is approximately an order of magnitude larger than velocities in coastal upwelling areas, although mesoscale upwelling is more confined spatially and temporally (Pollard and Regier, 1992; Allen and Smeed, 1996; Rudrick, 1996). Eddy pumping is another mechanism that can raise isopycnals and consequently nutrients into the euphotic zone. Eddy pumping occurs when a cyclonic mesoscale eddy is formed or intensified (Falkowski *et al.*, 1991; McGillicuddy and Robinson, 1997; McGillicuddy *et al.*, 1998).

The addition of nutrients by physical processes can influence the fate of primary production by changing the trophic pathway of the ecosystem. The trophic pathways in the open ocean vary from the "classic" food chain (e.g. Hardy 1924; Steele and Frost, 1977) to the "microbial loop" (Azam *et al.*, 1983). Typically, the microbial loop prevails in the oligotrophic open ocean, where autotrophic picoplankton dominate, by out-competing larger cells in the uptake of recycled nutrients (these dynamics are typified by a low *f* ratio: Eppley and Peterson, 1979). The primary production is utilised and recycled by heterotrophic microzooplankton and therefore little energy is passed up to the mesozooplankton (Cushing, 1989). The microheterotrophs have population doubling times similar to phytoplankton (day-days), and their high grazing rate maintains relatively constant levels of primary production and standing stock.

Larger autotrophic cells (such as diatoms) are favoured when new nutrients are injected into the euphotic zone by mesoscale physical processes (these dynamics show higher *f* ratios). Larger phytoplankton are a more suitable food for mesozooplankton, thus favouring classic food web dynamics, with production more efficiently passed up to higher levels (Cushing, 1959; Ryther, 1969; Thibault *et al.*, 1994; Legendre *et al.*, 1999). Herbivorous mesozooplankton populations have longer doubling times (days-weeks) than phytoplankton (Sheldon *et al.*, 1972; Steele, 1991), and as a result may be decoupled from the transient and spatially confined primary production at the mesoscale. However, when mesozooplankton are aggregated at high densities (by both physical and behavioural processes) they are capable of rapid grazing of phytoplankton biomass, leading to the fluctuation of the biomass of producers and grazers.

Top-down mechanisms influence zooplankton distributions by altering the predation pressure on the zooplankton (Verity and Smetacek, 1996; Pitta *et al.*, 1998). Mesoscale circulation may result in high densities of planktivores, such as at fronts (Laurs *et al.*, 1994) or in eddies (Wiebe and Boyd, 1978), but aggregations of zooplanktivores may also result from their behaviour (§1.3.2). Predation and grazing pressure acting on pelagic organisms can substantially alter their distribution by directly reducing their standing stock, which can result in gaps or grazing holes in their distributions (Wishner *et al.*, 1988: Folt *et al.*, 1993; Macaulay *et al.*, 1995) and can also change the composition and structure of the community (Behrends and Schneider, 1995).

1.3.2 Behavioural processes that influence zooplankton distributions

In order to study mesoscale forcing it is important to determine what aspects of zooplankton distributions are controlled by their behaviour. Folt and Burns (1999) suggest four mechanisms that are responsible for behaviourally mediated patchiness. These are diel vertical migration, predator avoidance, finding food and mating.

It is well established that many zooplankton populations have different vertical distributions during the day and night, and the movement between these, usually towards the surface in the evening and away from it at dawn, is termed diel vertical migration – DVM (e.g. Murray and Hjort, 1912; Russell, 1927; Roe, 1974; Angel, 1986). DVM often results in a large proportion of the biomass of zooplankton moving over 10s to 100s of meters and aggregating in a predictable way at a specific depths. The swimming and migration ability of many zooplankton species is broadly related to their size, with larger more mobile species generally migrating furthest.

The DVM of a species can be influenced by biological variables such as food, predators, endogenous rhythms (Dagg *et al.*, 1997; Lampert, 1993), and physico-chemical properties of the water such as temperature, oxygen concentration (Herring *et al.*, 1997) and water depth. Additionally, recent studies have also been able to resolve diel vertical migration behaviour interacting with physical forcing caused by mesoscale features (Roe *et al.*, 1996). Fielding *et al.* (submitted) observed part of the migrating community of macrozooplankton altering their usual cycle, and aggregating in a subducted streamer of phytoplankton rich surface water, drawn down at a front.

Predation activity may also alter the distribution of zooplankton by causing escape behaviour which can result in dispersal and aggregation of populations, and diel migration is thought to be driven by predator avoidance. Some zooplankton do not utilise a surface food source during the day, remaining deeper in the water column, to avoid their visual predators (Lampert, 1993). Experiments with freshwater species have demonstrated aggregation responses in cladocerans in the presence of kairomones, chemicals from their predators, (Pijanowski and Kowalczewski, 1997), but similar mechanisms have not been detected in marine zooplankton (Bollens *et al.*, 1994; Folt and Burns, 1999).

Zooplankton might be aggregated in a food source as a result of their behaviour (Folt and Burns, 1999). Tiselius (1992) reports that in high food levels the copepod *Acartia tonsa* increases turning thus remaining within the food, while at low food levels it swims much straighter, increasing its chances of finding a new source.

Copepods can also detect food by its odour and chemical exudates (Poulet *et al.*, 1991).

The need to reproduce is a dominant driving force in the lives of all organisms, and because a randomly distributed zooplankton population is fairly sparsely spread, aggregation is considered important to reproductive success. This is because the high density of the population will increase encounters between males and females, essential for fertilisation (Strickler, 1998). Recent studies have shown that copepods can track mates by following pheromones or by the mechanical disturbance caused by mating signals (Van Duren and Videler, 1996). Such processes can lead to patchiness at small scales, but are thought to be of little consequence at larger scales (Davis *et al.*, 1992a). Physical forcing interacts with these processes: chemical and mechanical signals are broken down by weak mixing and aggregations are dispersed by stronger turbulence.

1.3.3 Conclusion: physical and biological forcing at the mesoscale

At the mesoscale physical and biological mechanisms interact to determine the distribution of zooplankton. The flow associated with mesoscale physical features can redistribute zooplankton, but also provide mechanisms (ageostrophic vertical velocities and eddy pumping) that can influence ecosystem dynamics and zooplankton distributions by bottom-up forcing. Behavioural processes such as DVM, feeding and mating also affect the distribution of zooplankton. Top-down mechanisms can also impact on zooplankton distributions and community structure.

Many aspects of zooplankton biology are correlated with their body size: for example population doubling times, mobility, trophic status, and preferred food size (Eberhardt, 1969; Sheldon *et al.*, 1972; Banse, 1976, 1982; Platt and Denmann, 1978; Steele, 1991). As a result of the physical and biological forcing mechanisms that operate at the mesoscale can be expected to have a different influence on different sized zooplankton. For example, the new nutrients supplied by physical forcing favour larger phytoplankton and mesozooplankton herbivores. However, bottom-up forcing at the mesoscale can be localised and ephemeral events which do not provide adequate time for mesozooplankton populations to increase, and these species may not be closely coupled with the primary production. It is a central objective of this thesis to examine how physical and biological forcing at the mesoscale varies with different sized zooplankton.

1.4 TECHNIQUES FOR SAMPLING MESOSCALE ZOOPLANKTON DISTRIBUTIONS

The study of marine zooplankton was one of the first disciplines in oceanography to be investigated by scientists (Hensen, 1887), and as a result a wide range of techniques have been developed to describe the distribution of zooplankton. These methods can be divided into traditional techniques, such as nets, bottles and pumps, that involve the filtering of seawater to produce a sample of zooplankton, and modern techniques, such as optical and acoustic methods, which measure population densities *in situ*, without the collection of samples.

The study of the relationship between the mesoscale environment and the distribution of zooplankton requires the assimilation of a suitable multidisciplinary dataset. First, physical and biological variables must be measured concurrently, so that comparisons between them are not biased by temporal and spatial discrepancies in the data. Second, the resolution of sampling must be fine enough to reveal the details of the features, while coverage must be large enough to quasi-synoptically encompass them. Thirdly, instruments and nets must collect useful data, that can be related to the abundance, biomass, species and size distribution of the zooplankton. It must also be practical to collect the data within the usual constraints of a survey.

The problem of sampling the mesoscale physical environment can currently be addressed by using a towed undulating vehicle, such as a SeaSoar (Pollard, 1986), in addition to hull mounted sensors such as an ADCP. To sample the biology both traditional and modern zooplankton sampling methods are needed. Recently developed technologies (§1.4.2), can be used synchronously with the physical survey to provide concurrent biological data at the appropriate spatial and temporal resolution and coverage. Traditional techniques (§1.4.1) provide the taxonomic detail and provide established measurements of abundance and biomass to compare and calibrate the modern technologies. However, there are particular short comings and biases associated with each technology which must be considered when the instruments are combined in a survey. In this section both traditional and modern techniques are described and compared for their suitability for a multidisciplinary mesoscale survey.

1.4.1 Traditional zooplankton sampling techniques

Traditional sampling methods are not capable of resolving mesoscale heterogeneity in zooplankton distributions because within quasi-synoptic time limits, these methods cannot achieve spatial coverage with the appropriate vertical and horizontal resolution

(Hardy, 1956). In addition, the taxonomic sorting and species identification are time consuming, and limit the feasible number of samples that can be processed. These methods typically lack concurrent physical measurements, and even when these are taken they are not at a suitable resolution and coverage for mesoscale studies. However, traditional methods are needed in a multidisciplinary survey of mesoscale features to collect actual samples of zooplankton for identification, and to produce measurements of zooplankton abundance and biomass for comparison.

1.4.1.1. Zooplankton nets

Zooplankton nets come in many forms, ranging from simple conical nets such as the WP-2 (Fraser, 1968), to opening and closing multi-nets such as the MOCNESS (Wiebe *et al.*, 1976b), to serial samplers such as the LHPR (Longhurst *et al.*, 1966). A list of common net systems is given in Table 1.4.1a. Nets are the most widely used devices for sampling zooplankton and in their basic form are simple to use. In comparison to other technologies nets are inexpensive and reliably filter a large volume of water, producing large samples, but in doing so integrate the structure of the zooplankton distribution over the range that they are towed.

Table 1.4.1a A list of some zooplankton nets in common usage

Net Name	Description	Reference
WP-2	Conical net	Fraser 1968
NORPAC	Conical net	Motoda 1959
Indian Ocean Standard	Conical net	Currie 1963
CalCOFI Standard	Conical net	Smith *et al.* 1968,
Tropical Juday	Conical net	Bogorov 1959
Bongo	Paired, closing net	McGowan and Brown 1966
Clarke-Bumpus sampler	Opening and closing net	Clarke and Bumpus 1950
RMT1 and RMT8	Opening and closing nets	Clarke 1969; Roe and Shale 1979
MOCNESS	Opening and closing multinet	Wiebe *et al.* 1976b
BIONESS	Opening and closing multinet	Sameoto *et al.* 1977
CPR	Continuous serial sampler	Hardy 1936, Warner and Hays 1994
LHPR	Discrete serial sampler	Longhurst *et al.* 1966, Williams 1983
ARIES	Discrete serial sampler	Dunn *et al.* 1983
U-Tow	Serial sampler	Hays *et al.* 1998
Gulf III	Sequential net sampler	Gehringer 1952

There are several problems and biases associated with obtaining quantitative samples from simple nets, and overcoming these has led to the development of a wide range of samplers. Accurate measurements from nets are especially important when the data are used to calibrate data from other sources, such as modern sampling technologies.

The first problem is that to accurately quantify population densities, nets must reliably filter water and the amount that has been filtered must be determined. The

filtration efficiency of a net is calculated as the percentage of water actually filtered of the theoretical volume filtered (the mouth area multiplied by the distance of the tow). For a standard conical net the efficiency is usually around 80-90%, but can be increased with the addition of a reducing mouth cone or flares behind the mouth to 110-120% (Omori and Ikeda, 1992). Tranter and Heron (1967) reported that a 14° flare behind the mouth of a Clarke-Bumpus sampler increased the efficiency from 81 to 115%. With such variations in efficiency it is crucial to measure the flow through the net. The filtration efficiency of a net is determined by the open area ratio (*OAR*), which is the ratio between the area of pores in the net to the size of the mouth.

The filtration efficiency of a net can be greatly reduced by clogging as the net fills with plankton, which can be a major source of error (e.g. Smith *et al.*, 1968). Tranter and Smith (1968) recommend that a net should have an open area ratio of at least 6. The amount of water filtered by a net is measured with a flowmeter placed in its mouth, allowing the density of zooplankton to be accurately calculated (Mahnken and Jossi, 1967; Fraser, 1968).

The second problem with a simple conical plankton net is that zooplankton distributions are integrated over the distance of the tow, and consequently horizontal and vertical patchiness and gradients are not resolved. This problem has been overcome by nets that can collect multiple zooplankton samples in a single tow. There are two main solutions, the first uses multiple opening and closing nets (e.g. MOCNESS and BIONESS) and the second uses a single net collecting a series of samples on a strip of filtering silk with a modified cod-end (e.g. CPR and LHPR).

The third problem associated with nets is the loss of smaller zooplankton through the mesh. The mechanisms can be divided into passive escapement where the organism is small enough to pass through the mesh and active escapement where the behaviour of the organisms enables them to move through the mesh (Saville, 1958; Vannucci, 1965). Escapement is enhanced by a positive pressure gradient inside the net, which increases as the net is towed faster, forcing larger plankton through the mesh. Saville (1958) showed that glass beads with a diameter of 0.261 mm were lost through a mesh of 0.222 mm. Active escapement mechanisms allow zooplankton that are considerably larger than the mesh size to escape through it. Vannucci (1965) determined that copepods with a width of 0.35 mm passed through a 0.33 mm mesh net, but once preserved they could be retained by a 0.4 mm mesh, and Timonin (1983) measured a 50% escapement of 0.8 mm long copepods through a 0.18 mm mesh.

Barnes and Tranter (1965) determined the minimum retention sizes of three meshes and recommend a 0.33 mm mesh for copepods with a length of 1 mm, a 0.27 mm mesh for a length of 0.8 mm and a 0.17 mm mesh for a body of 0.6 mm. The results of Nichols and Thompson (1991) indicate that 95% of copepods are retained by a mesh size 75% of their width.

A fourth problem that affects quantitative measurements is that large motile species can avoid the net (Fleminger and Clutter, 1965; Clutter and Anraku, 1968; Hillmann-Kitalong and Birkland, 1987). Many studies have showed that faster towing speeds (up to 10 ms^{-1}) continue to increase the catch of species such as euphausiids, decapods and ichthyoplankton (Omori *et al.*, 1965; Clutter and Anraku, 1968; Bernard *et al.*, 1973). However, the faster a net is towed the less efficiently it filters seawater and as a result the open area ratio of the net must be increased. An additional problem of fast towing speeds is that zooplankton are damaged as they are filtered, which can limit identification, and lower measurements of their biovolume.

The previous two factors demonstrate that a net, with a particular mesh size and towing speed will only catch a selective range of plankton sizes. In order to catch small individuals a fine mesh is needed, which must be towed slowly, but to capture larger more motile zooplankton the net must be towed more quickly which necessitates a coarser mesh. Additionally, population abundance is related to size, with smaller zooplankton more abundant than larger ones (Sheldon and Parsons, 1967), and consequently to sample populations of larger zooplankton, a greater volume of water must be filtered. Therefore, to effectively sample the zooplankton community, several nets are needed, biased to different size ranges.

In a multidisciplinary survey the limitations and biases of plankton nets must be carefully considered and as far as possible quantified, when zooplankton data from modern sampling technologies are compared with them (Skjoldal *et al.*, 2000).

1.4.1.2. Water bottles for sampling zooplankton

Water bottles are used less commonly than plankton nets and while solving some of the problems and biases of nets are limited in their application. Water bottles take spatially discrete and precise samples, and the volume of water sampled is accurately known. However bottles sample a much smaller volume of water than nets – a large bottle has a capacity of 150 l, but a short 50 m vertical net haul with a 50 cm diameter net will filter 10,000 l. As a consequence, sparse populations are not sampled reliably

by bottles, which will limit statistically robust sampling to smaller more abundant species (Van Dorn, 1957; Vinogradov and Shushkina, 1983; Vinogradov *et al.*, 1987).

Several studies have demonstrated that nets do not reliably catch smaller species, and bottles can produce more accurate measurements (e.g. Tutubalin *et al.*, 1987; Vinogradov and Shushkina, 1983). For example, Musaeva and Nezlin (1996) compared the catch of a 180 μm Juday net and 30 l bottle: the bottle samples contained 4 to 5 times the abundance of 1-3 mm copepods and 20 to 30 times the abundance of 1-3 mm euphausiids and chaetognaths than the net. The authors concluded that the net underestimated zooplankton abundance because of loss through the mesh, incomplete filtration due to clogging and avoidance.

Bottles measure spatially discrete samples, and are a time consuming method with which to measure the patchy distribution of zooplankton. Bottles can be used to collect reliable point samples of small zooplankton, but do not provide the quasi-synoptic coverage needed for mesoscale studies.

1.4.1.3. Water pumps for sampling zooplankton

Pumps offer some advantages over nets as they are capable of high spatial resolution, do not suffer from clogging and the volume of water filtered can be measured precisely (Hensen, 1887, Aron, 1958; Taggart and Leggett, 1984; and Møhlenberg, 1987). Pumps can be either mounted on the ship collecting samples with a hose, or can be submersible filtering *in situ*. However, there are several specific problems that limit the applications of pumps. First, pumps sample low volumes of water in comparison to nets (typical rates are 100-2000 l min^{-1}, Wiborg, 1948; Mullin and Brooks, 1976), which limits reliable sampling to high density populations (Miller and Judkins, 1981). Second, friction in the intake hose limits the depth to which samples can be taken, although this can be overcome by very large pumps with wide bore hoses (Snyder, 1983; Bishop *et al.*, 1992) and *in situ* pumps, which can operate at any depth (Waite and O'Grady, 1980; Solemdal and Ellertsen, 1984; Møhlenberg, 1987). The final problem that has discouraged many users, is that pumps can potentially damage organisms (Lenz, 1972; Gale and Mohr, 1978).

Zooplankton pumps offer few advantages over advanced nets systems and therefore are not widely used in oceanographic surveys. Pumps are commonly used for underway surface sampling of phytoplankton and zooplankton populations, sometimes in conjunction with modern sampling technologies (e.g. Gallienne *et al.*, 1996; Checkley *et al.*, 1997).

1.4.2 Modern technologies for describing zooplankton distributions

There are several modern technologies that provide data at the appropriate spatial coverage and resolution to study the relationship between the mesoscale environment and the distribution of zooplankton. Not all modern technologies collect data that are required in this type of study, for example, the spatial information preservation method is designed to look at nannoscale patchiness (Krembs *et al.*, 1998) and the laser lit, 3D video system is tailored to the scales needed to observe copepod mating (Strickler, 1998). Therefore, this section will concentrate only on those capable of collecting data concurrently with physical environmental measurements. These technologies can be divided into acoustical or optical methods (Harris *et al.*, 2000).

1.4.2.1 Bio-acoustic sensing methods

Acoustics have been used for several decades to determine the distribution of pelagic biology (Clay and Medwin, 1977) and are in common use by fisherman, who use echosounders to locate schools of fish (e.g. Maclennan, 1990). Measurements of the acoustic backscatter from zooplankton are obtained from sonars; either acoustic Doppler current profilers (ADCPs) or purpose built biological echosounders (e.g. Bary, 1966; Holliday, 1977; Smith *et al.*, 1992; and Roe *et al.*, 1996). Zooplankton are detected when the sound emitted from the sonar is scattered or reflected by their bodies back to the receiver. The sonar is usually fixed to the hull of the ship, or in a tow-fish deployed just below the surface, which allows data to be obtained concurrently with that from other instruments (Roe and Griffiths, 1993). Using this technique the acoustic backscatter of zooplankton targets, with the appropriate horizontal and vertical spatial resolution can be rapidly measured. However, there are several disadvantages and biases that arise from this methodology.

The main drawback of acoustic measurements of zooplankton distributions is the difficulty in assessing population densities in terms of abundance, biomass or species. This problem can be solved for fish stocks, where a single species, with a known target strength, is the dominant scatterer (Holliday and Pieper, 1995). Unlike fish shoals, zooplankton communities are typically diverse containing a wide range of species with varied backscattering characteristics (Kogeler *et al.*, 1987). For example, Stanton *et al.* (1994) demonstrated that a 2 mm pteropod will return 20000 times more sound than 25 mm salp. As a result the relationship between backscatter and biomass (or abundance) is highly variable in natural communities. This relationship can be more reliably quantified with net samples, by comparing the measured backscatter

with the backscatter predicted from the abundance of major anatomical groups, with different scattering abilities, in the samples (Stanton *et al.*, 1996; Wiebe *et al.*, 1996).

A second limitation of acoustics is the trade off between the minimum detection size of zooplankton and the depth penetration of a particular frequency. Higher acoustic frequencies will be scattered by smaller particles, but will also be dissipated by the water at shallower depths. Single frequency acoustic devices are compromised by these limitations: ADCPs typically operate at 150 kHz and resolve macrozooplankton larger than 2 cm, at a depth down to 400 to 500 m (Flagg and Smith, 1989; Heywood *et al*, 1991; Roe and Griffiths, 1993). To address this problem multifrequency acoustic systems have been developed (Holliday, 1980; Holiday *et al.*, 1989; Pieper *et al.*, 1990). An example is the Simrad EK500, which operates at three frequencies: 38, 120 and 200 kHz (Bodholt *et al.*, 1989). The minimum zooplankton size detection limits and water column penetrations of these are approximately 7.5mm and 100 m for the 200 kHz frequency, 1 cm and 350 m for the 120 kHz and 4 cm and 800 m for the 38 kHz (Griffiths *et al.*, 1996). The upper limits cannot be defined as precisely, as they depend on the scattering characteristics of the organism.

For this reason, acoustic instruments that remain on the surface cannot determine the distribution of the smaller mesozooplankton, in the size range approximately between 0.2–5 mm. This is an important size range because it contains the herbivorous copepods that are the link between primary production and larger organisms. It is clear that it is important to sample this trophic level to observe the effect of bottom-up forcing, driven by mesoscale physical processes, on the pelagic ecosystem. As a result acoustic instruments, operating at the higher frequencies needed to sample small mesozooplankton, must be profiled through the water column because of the rapid dissipation of sound at these frequencies. The multifrequency acoustic profiling system (MAPS), which operates at 21 frequencies between 100-10000 kHz (Pieper *et al.*, 1990), is used on station and as a result is not capable of adequate spatial resolution and quasi-synoptic coverage to study mesoscale processes. Both the Tracor acoustic profiling system (TAPS) and the towed undulating bio-acoustic sensor (TUBA) are designed to be deployed on a SeaSoar body (McGehee *et al.*, 2000; Griffiths *et al.*, 1997). TAPS operates at 6 frequencies between 265-3000 kHz and TUBA operates at 7 frequencies between 175-2400 kHz. These instruments are currently not widely available, but do offer a technology suited to resolve mesozooplankton distributions concurrently with physical measurements.

1.4.2.2 Optical zooplankton sensing methods

A wide range of optical instrumentation has been developed for studying the distribution of zooplankton at a variety of scales (e.g. Strickler, 1977; Kils, 1992; van Duren and Videler, 1995; Tiselius, 1998; Strickler, 1998; Katz *et al.*, 1999). However, many of these systems have been developed to study zooplankton behaviour on microscales. The video plankton recorder (Davis *et al.*, 1992a) and the optical plankton counter (Herman, 1992) are the only instruments currently available that can be mounted on towed undulating bodies for multidisciplinary mesoscale studies.

The video plankton recorder (VPR) uses towed video-microscopy to identify and count mesozooplankton (Davis *et al.*, 1992a & 1992b). The identification of major taxonomic groups is predominantly automated, as images from the cameras are compared with a database of images. Zooplankton abundance is determined from the number of animals in the video sampling volume. The system can resolve particles in the size range 10 μm to 2 cm. The VPR is suited for studying microscale distributions, and analysis of the images can reveal behavioural information, even of delicate forms that are damaged in plankton nets, such as medusae, siphonophores and salp chains (Gallager *et al.*, 1996). However, the current VPR is large and significantly reduces the depth penetration of an undulating body. The underwater video profiler (UVP) has a comparable zooplankton size detection range to the VPR (Gorsky *et al.*, 1992), but is a profiling instrument and cannot be deployed with an undulating survey.

The optical plankton counter (OPC) sizes and counts mesozooplankton by measuring the amount of light blocked by each individual as it passes through a light beam, projected across the instrument's sampling tunnel (Herman, 1992; for more details see §2.2.4). The size and volume of each particle can be calculated from the shadow size, and the abundance and biovolume of zooplankton in size classes can be determined from the amount of water passing through the sampling tunnel. The OPC is sensitive to particles with an equivalent spherical diameter between 0.25 and 14 mm. The OPC is suited for concurrent sampling during a mesoscale physical survey as it can also be fixed onto a variety of platforms. However, the OPC has several limitations.

The measurements of the amount of light blocked by a particle determined by an OPC must be calibrated into useful measurements such as zooplankton abundance and biomass. This is problematic as the amount of light blocked varies with particle shape, orientation and translucency (see §3.2). An OPC also cannot distinguish between

zooplankton and other particles in this size range, nor can it directly distinguish between taxonomic groups. Second, when an OPC is configured for SeaSoar, the water sampling inlet is reduced to keep the count rate within the limits of the software to avoid coincidence counts. As a result of the reduced data rate, it is not possible to robustly sample the distribution of larger zooplankton. This imposes a reliable upper size limit of between 5 and 8 mm, dependant on the natural abundance of the zooplankton of these sizes (Mustard, 1997; Rabe *et al.*, 1998) which is a shortcoming of this system.

1.4.3 Conclusion: sampling technologies needed for mesoscale studies

Technologies are now available that can determine the distribution of phytoplankton (fluorimeter), mesozooplankton and macrozooplankton at the same resolution and concurrently with the physical measurements needed to study mesoscale processes. The main limitations of these modern acoustic and optical technologies are in relating the outputs of these instruments to accepted and useful measurements of zooplankton communities (species, taxonomic groups, size spectra, abundance and biomass). To this end, traditional methods, such as nets, must still constitute an integral part of any mesoscale multidisciplinary study. However, the traditional methods are not without their limitations and biases, and these must be carefully considered when comparisons or calibrations are made between methodologies.

It is a major aim of this thesis to examine the accuracy and value of the data produced by modern zooplankton sensing technologies - specifically from an optical plankton counter (§1.2.1).

CHAPTER 2

The survey: review of previous studies in the survey area: the Strait of Hormuz, the Arabian Gulf and the Gulf of Oman, and data collection and processing from R.R.S. *Charles Darwin* cruise 104

2.1 THE REGION: STRAIT OF HORMUZ, ARABIAN GULF AND GULF OF OMAN . . 25
2.2 METHODS: RRS CHARLES DARWIN CRUISE 104 – COLLECTION OF DATA AND SAMPLES AND THEIR PROCESSING AND CALIBRATION 37

FIGURES

2.1.1.i The region of study: a map of the Strait of Hormuz, the Arabian Gulf and the Gulf of Oman 26
2.1.1.ii The circulation in the Arabian Gulf and the Strait of Hormuz. Also showing gradient in species richness of phytoplankton and zooplankton 26
2.2.2.i A map showing the positions of the six transects of the SeaSoar survey and the LHPR biological stations in the Strait of Hormuz 39
2.2.2.ii SeaSoar fitted with optical plankton counter (OPC) 39
2.2.3.i The calibration The calibration graph for the CTD fluorimeter in the Gulf of Oman, showing the lack of quenching 42
2.2.4.i Histogram of counts in size classes in the raw OPC data 42

The data used in this thesis were collected during R.R.S. *Charles Darwin* cruise 104 (CD 104) in February and March 1997, in the north west Indian Ocean. The main dataset presented in this thesis is a high resolution, hydrographic survey made with a SeaSoar in the Strait of Hormuz. This region has received little oceanographic attention and previous work can be divided into the coastal studies of the Gulf States and a few international surveys that have set out to establish the regional large scale hydrographic and biological conditions (Emery, 1956; Leveau and Szekielda, 1968; Brewer and Dyrssen, 1985). Satellite observations have demonstrated that this region is rich in mesoscale features (Gundersen *et al.*, 1998; Bohm *et al.*, 1999) but CD104 was the first cruise to attempt to resolve the mesoscale variability. This chapter contains a review of the hydrography and pelagic biology of the survey region and a description of the sampling protocols, equipment and data processing on CD 104.

2.1 The Region: Strait of Hormuz, Arabian Gulf & Gulf of Oman

The Strait of Hormuz connects the Gulf of Oman and the Arabian Gulf. (**Fig 2.1.1.i**), and is the site of exchange and mixing between these two areas. The Gulf of Oman is an extension of the NW Indian Ocean, whereas the Arabian Gulf is a shallow, semi-enclosed shelf sea, that is strongly influence by the arid conditions of the region. It is important to understand the character of each area because both influence the conditions in the Strait. In this section there is a review of some of the previous studies in this region, which provide a background to the current work.

2.1.1 Physical conditions in the survey region

2.1.1.1 The monsoon

The Indian Ocean is dramatically seasonal, forced by a biannual reversal in the atmospheric circulation over the Arabian Sea. Known as the monsoons, the change in the winds causes a seasonal reversal in the ocean circulation (e.g. Yoder *et al.*, 1992; Burkill, 1999). The strong SW monsoon winds build up in May and last to September, driving the SW monsoon currents which are greatest in July and August and break down in October (Sastry and D'Souza, 1972; Wyrtki, 1973). Associated with the SW monsoon is intense wind driven upwelling along the Omani coast, south of the Gulf of Oman (Swallow, 1984; Currie, 1992). The upwelling increases primary production and zooplankton standing stock across the N Indian Ocean (Madhupratap *et al.*, 1996; Barlow *et al.*, 1999). The ocean currents of the weaker NE monsoon start to develop in

Figure 2.1.1.i The region of study:a map of the Strait of Hormuz, the Arabian Gulf and the Gulf of Oman

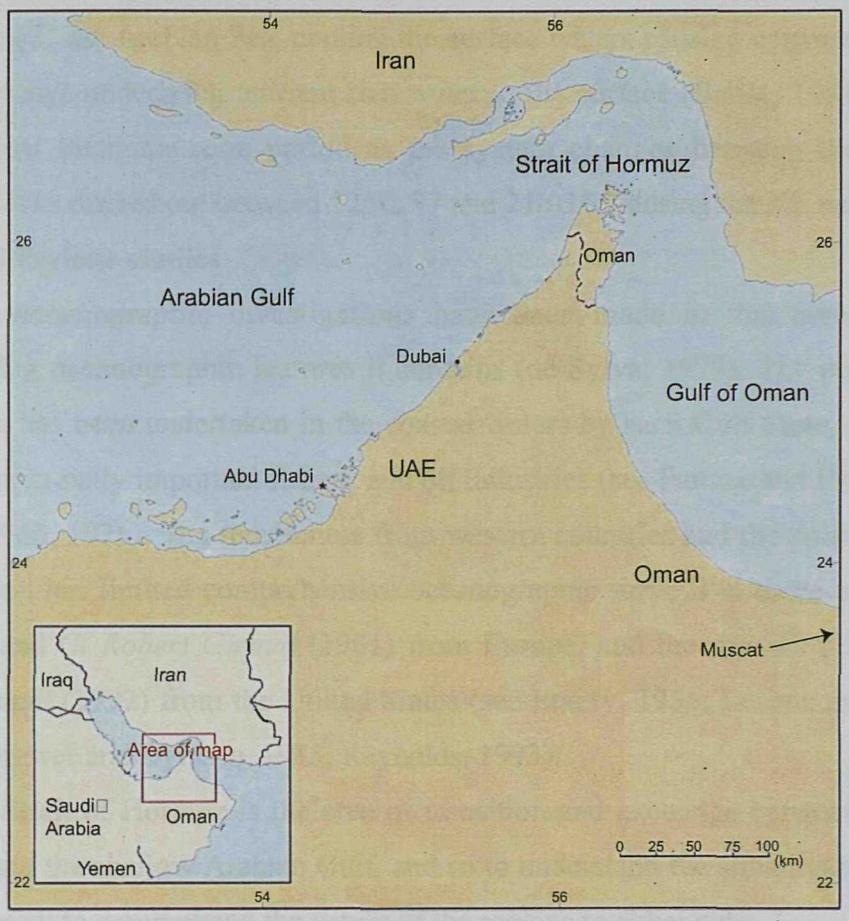

Figure 2.1.1.ii The circulation in the Arabian Gulf and the Strait of Hormuz. Also showing gradient in species richness of phytoplankton and zooplankton

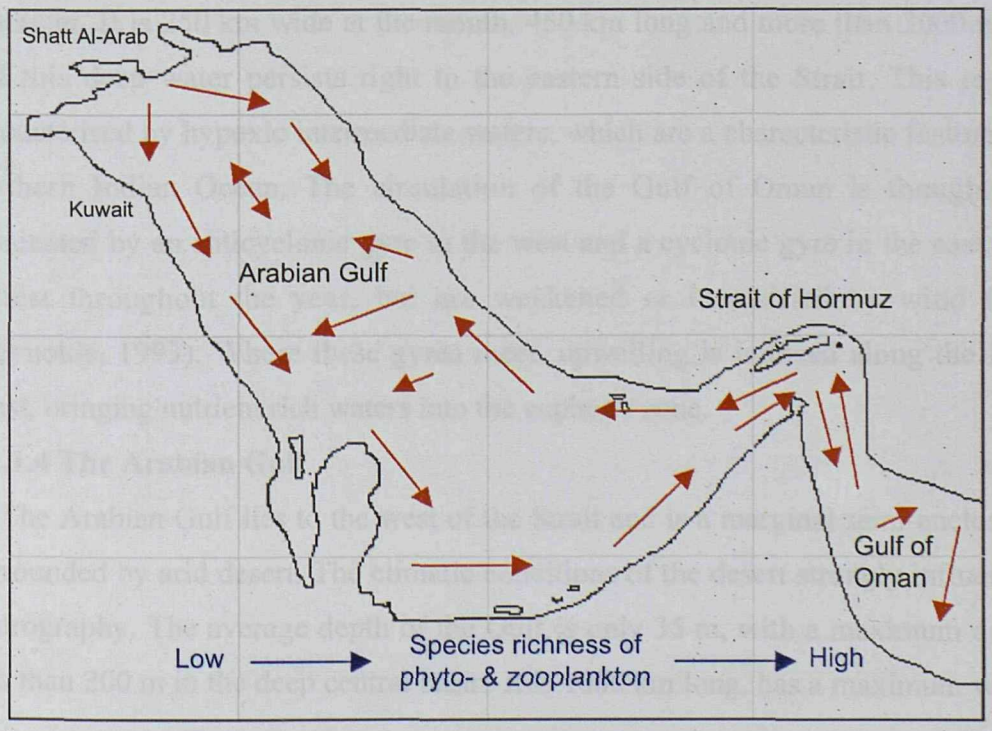

November, are strongest in February and can persist until April. Nutrients are also supplied to the euphotic zone during winter, when cool winds from the Himalayas blow across the Arabian Sea, cooling the surface waters causing convective overturn, which brings underlying nutrient rich water to the surface (Banse, 1984). There is a significant inter-monsoon period as the system changes between the two states. CD 104 was carried out between 12/02/97 and 21/03/97 during the NE monsoon.

2.1.1.2 Previous studies

Few oceanographic investigations have been made in this area despite the interesting oceanographic features it contains (de Sylva, 1979). The majority of the research has been undertaken in the coastal waters by each Gulf State, and concerns the commercially important fishery and oil industries (see Farmer and Docksey, 1983; FAO, 1966, 1976). The remoteness from western countries and the political unrest in the region has limited comprehensive oceanographic surveys to those of the *Meteor* (1948) and *Ct Robert Giraud* (1961) from Europe, and the *Atlantis* (1976) and the *Mt Mitchell* (1992) from the United States (see Emery, 1956; Leveau and Szekielda, 1968; Brewer and Dyrssen, 1985; Reynolds, 1993).

The Strait of Hormuz is the area of transition and exchange between the Gulf of Oman and the shallow Arabian Gulf, and so to understand the situation in the Strait it is important to comprehend the nature of the regions to either side.

2.1.1.3 The Gulf of Oman

The Gulf of Oman is a north western extension of the Arabian Sea and is oceanic in character. It is 250 km wide at the mouth, 450 km long and more than 3000 m deep, and this deep water persists right to the eastern side of the Strait. This region is characterised by hypoxic intermediate waters, which are a characteristic feature of the northern Indian Ocean. The circulation of the Gulf of Oman is thought to be dominated by an anticyclonic gyre in the west and a cyclonic gyre in the east, which persist throughout the year, but are weakened or intensified by wind forcing (Reynolds, 1993). Where these gyres meet, upwelling is induced along the Iranian coast, bringing nutrient rich waters into the euphotic zone.

2.1.1.4 The Arabian Gulf

The Arabian Gulf lies to the west of the Strait and is a marginal semi-enclosed sea surrounded by arid desert. The climatic conditions of the desert strongly influence the hydrography. The average depth of the Gulf is only 35 m, with a maximum depth of less than 200 m in the deep central basin. It is 1000 km long, has a maximum width of

338 km and a volume of 8,630 km^3 (Emery, 1956; Michel *et al.*, 1981a; Reynolds, 1993). The arid climate means that the evaporation is high at 200 cm yr^{-1} (Meshal and Hassan, 1987; Ahmad and Sultan, 1991), and rainfall and riverine inputs only replace about 25% of this loss: rivers contribute 46 cm yr^{-1} and rain 7 cm yr^{-1} (Reynolds, 1993). To balance this loss, water flows into the Arabian Gulf through the only opening, the Strait of Hormuz, from the Gulf of Oman.

Fig 2.1.1.ii shows the circulation pattern in the Arabian Gulf and the Strait. Within the Gulf, the inflow through the Strait of Hormuz forces a cyclonic circulation in the southern waters (Brewer *et al.*, 1978; Brewer and Dyrssen, 1985; Eid and Elgindy, 1998). In the northern part of the Gulf the freshwater from the Shatt Al-Arab maintains a cyclonic circulation, which would otherwise be anticyclonic (Reynolds 1993). The general circulation is driven by wind forcing, evaporation and the positive buoyancy of the inflow at the Strait of Hormuz (Al-Hajri *et al.*, 1997). The inflow stagnates in the centre of the Gulf, between Qatar and the UAE, where the high evaporation forms dense saline water which sinks and flows along the bottom out of the Strait of Hormuz. This water has an unusually high salinity, typically around 39-40 but as high as 44.3 (Saad, 1976; Jacob and Al-Muzani, 1990).

2.1.1.5 The Strait of Hormuz

A reverse flow estuarine circulation exists in the Strait of Hormuz, similar to the Strait of Gibraltar at the entrance of the Mediterranean. Warmer, fresher water moves in from the Gulf of Oman and below this, cooler saltier water flows out of the Arabian Gulf (Leveau and Szekielda, 1968). Coriolis force deflects these exchange currents, with the majority of the inflow being near the northern Iranian coast and the subsurface outflow being strongest on the southern Arabian side (Sultan and Elghribi, 1996). The Strait constricts to just 56 km wide, but there is no sill and it is generally about 90 m deep, although there is a depression close to the tip of the Masandam peninsula deeper than 100 m. This area is an important shipping route: at peak times a ship passes through the Strait every 6 minutes, including 60% of global ship borne oil transport (Al-Hajri, 1990).

In the Strait of Hormuz the high salinity outflow from the Arabian Gulf is diluted by entrainment of Gulf of Oman water, and the salinity is reduced to less than 40 (Banse, 1997). The mixing is enhanced by tidal forcing and by flowing over the uneven topography. The dilution results in the flow swelling to 3 times its original

volume, and in the northern Gulf of Oman the flow becomes neutrally buoyant and leaves the sea floor flowing southward along the Omani shelf (Smeed, 1997).

2.1.1.6 The affect of the seasons in the survey region

Seasonality, enforced by the monsoons, has a clear effect on the structure and circulation of the water in the Arabian Gulf and Strait of Hormuz. In winter, during the NE monsoon, convection occurs freely and increased wind and tidal forcing result in a well mixed water column throughout the Gulf, but not in the Strait of Hormuz. In addition, shamal winds weaken the westward inflow along the Iranian coast. In the summer, during the SW monsoon, strong solar heating produces a sharp thermocline (gradient 1.8 °C m^{-1}) in the Gulf which inhibits mixing between the two layers (Joseph and Lee, 1989). But the wind driven mixing remains strong enough to prevent low oxygen conditions developing in the lower layer (Seibold, 1973). The exchange is strongest during the summer because during the winter vertical mixing in the Arabian Gulf reduces the density of the outflow (Eid and Elgindy, 1998). In general there are stronger currents in Arabian Gulf and Strait of Hormuz during the SW monsoon (Hunter, 1983).

2.1.2 The phytoplankton community in the survey region

Studies on the phytoplankton community in this region (reviewed by Rao and Al-Yamani, 1998) have revealed clear gradients in several variables from the NW Arabian Gulf to the Gulf of Oman.

2.1.2.1 Phytoplankton standing stock and production

In general, phytoplankton standing stock is reduced with distance from the NW Arabian Gulf to the Gulf of Oman (Table 2.1.2a). The sparse measurements of primary production also show the highest values in the NW Arabian Gulf. The Shatt Al-Arab estuary (in the NW of the Gulf) contains the largest chlorophyll *a* concentration which varies annually between 0.52 and 3.25 mg m^{-3}, (Al-Saadi *et al.*, 1989; Huq *et al.*, 1981), although in the eutrophic canals used in the shrimp fishery it may be more than an order of magnitude larger up to 94 mg m^{-3} (Schiewer *et al.*, 1982; Al Mousawi *et al.*, 1990). In the north western Gulf values are also high 0.56-2.06 mg m^{-3} (Huq *et al.*, 1978), including Kuwaiti waters which support a high concentration of chlorophyll, especially during the winter months when nutrients are more plentiful (Jacob *et al.*, 1980). Despite recording a high maximum value (13.9 mg m^{-3}) Jacob *et al.* (1980) report that this region generally has a lower biomass than the estuary. Phytoplankton

production is also lower in Kuwait waters than the estuary: 0.87 compared with 3.2 mg C l^{-1} h^{-1} (Rao and Al-Yamani, 1998). This gradient continues in the eastern Arabian Gulf: El-Gindy and Dorgham (1992) recorded a mean chlorophyll *a* concentration in the top 10 m of 1.18 mg m^{-3} on the Arabian Gulf side of the Strait of Hormuz, and 0.55 mg m^{-3} on the Gulf of Oman side. This gradient in chlorophyll *a* concentration correlates with a lessening influence of the eutrophic fresh water input at the Shatt Al-Arab (Saad, 1976) and the increasing influence of oceanic waters. In addition, nutrients are remineralised more quickly in the shallow Arabian Gulf (Michel *et al.*, 1981; El-Gindy and Dorgham, 1992).

Table 2.1.2a Gradients of phytoplankton concentration, production and diversity in the Arabian Gulf and Gulf of Oman

Area	Chlorophyll *a* (mg m^{-3})	Primary Production (mg C l^{-1} h^{-1})	Number of species
Shatt Al-Arab	**0.52 – 3.25** Al-Saadi *et al.* (1989) Huq *et al.* (1981)	**upto 3.2** Rao & Al-Yamani (1998)	**116** Hadi *et al.* (1984)
NW Arabian Gulf and Kuwaiti waters	**0.56 – 2.06** Huq *et al.* (1978) Jacob *et al.* (1980)	**upto 0.87** Rao & Al-Yamani (1998)	**148** Al-Kaisi (1976) Jacob *et al.* (1980)
Eastern Arabian Gulf	**1.18 & 0.96** means: top 10m and 10-40m El-Gindy & Dorgham(1992)	No data	**390** Dorgham & Muftah (1986)
NW Gulf of Oman	**0.55 & 0.87** means: top 10m and 10-40m El-Gindy & Dorgham(1992)	No data	**527** Al-Saadi & Hadi (1987)

2.1.2.2 Species richness of the phytoplankton community

A gradient also exists in the species richness of the phytoplankton community (Table 2.1.2a) which is lowest in north west of the Arabian Gulf: furthest from typical ocean conditions (Rao and Al-Yamani, 1998). The Shatt Al-Arab contains the fewest species: Hulbert *et al.* (1981) recorded 90 and Hadi *et al.* (1984) measured 116 species. Kuwaiti waters support a greater species diversity: Al-Kaisi (1976) and Jacob *et al.* (1980) recorded 148 species. The diversity increases more in the offshore waters of the central Gulf, where Dorgham and Muftah (1986) recorded 390 species. The greatest diversity in the region is in the Strait of Hormuz and Gulf of Oman, where Al-Saadi and Hadi (1987) recorded 527 species. Most species present in the Arabian Gulf also exist outside in the Gulf of Oman, and diversity is reduced in the Arabian Gulf as some species cannot endure the harsh environmental conditions. Rao and Al-Yamani, (1998) postulate that the Gulf shows a gradient of increasing community maturity from the Shatt Al-Arab to the Strait of Hormuz.

2.1.3 The zooplankton community in the survey region

There have been several studies of zooplankton made in the Arabian Gulf, although most have been limited to coastal waters of a single country (e.g. Enomoto, 1971; Basson et al., 1977; Michel *et al.*, 1986a; Al-Yamani *et al.*, 1993). Only a few authors have surveyed (or reviewed) the entire region (Frontier, 1963a; Kimor, 1973; Yamazi, 1974; Gibson *et al.*, 1980; Michel *et al.*, 1986b). For comparison with the data presented in this thesis there must be an overlap between the datasets both seasonally and regionally. Only Gibson *et al.* (1980) and Frontier (1963a) have taken samples that geographically encompass the CD 104 SeaSoar survey, and only Gibson *et al.* (1980) and Michel *et al.* (1986b) sampled in the early spring.

2.1.3.1 The distribution of zooplankton biomass

In contrast to the phytoplankton, there does not appear to be a clear gradient in zooplankton biomass across the Gulf. Michel *et al.* (1986b) reported that the central region of the Gulf supported the lowest zooplankton biovolume (0.23-3.14 ml m^{-3})[1], but Gibson *et al.* (1980) determined that this region had the highest biovolume (0.31-1.48 ml m^{-3}). However the mean biovolume recorded by Gibson *et al.* (1980) in March 1977 in all areas, was lower than that measured by Michel *et al.* (1986b) in February/March 1980. The differences may have resulted from the different sampling equipment and techniques used to determine biovolume: Gibson *et al.* (1980) used a 243 μm mesh net, and Michel *et al.* (1986b) used a 110 μm net. The differences may also be caused by seasonal and annual changes in the region.

Gibson *et al.* (1980) reported a higher biovolume in Gulf of Oman (0.52-2.27 ml m^{-3}) than in the eastern Arabian Gulf (0.22-1.11 ml m^{-3}). Zooplankton abundance was also higher (978-2809 m^{-3}, mean:1732 m^{-3}) compared with the Arabian Gulf (79-2734 m^{-3} mean: 1436 m^{-3}). Frontier (1963a) measured zooplankton biomass[2] in May 1961 and found similar amounts in the Gulf of Oman and the Strait, but much larger biomass in the area west of the Strait in the Arabian Gulf, which was dominated by salps. Both Frontier (1963a) and Michel *et al.* (1986b) report lower biovolume in the NW Arabian Gulf than in the area west of the Strait. These measurements were taken at different times, in different locations and with different specified nets, and

[1] Converted to volume by assuming dry weight is 10% of wet weight, and the density of the zooplankton is to sea water.

[2] Frontier (1963a) records biomass standardised to the length of the tow, but does not provide the volume filtered. Therefore those numbers are not presented here

unsurprisingly have produced a range of biovolume estimates. From these data it is not possible to draw any robust conclusions in this apparently variable region.

Gibson *et al.* (1980) reported that there were no diurnal differences in biovolume within the Arabian Gulf. Recent studies (e.g. Al-Yamani *et al.*, 1993) have shown that the zooplankton community is distinctly patchy in this region, contrary to the findings of Grice and Gibson (1978).

2.1.3.2 The dominant zooplankton species in the region

Copepods have been found to be the numerically dominant taxa in all zooplankton surveys in the Strait of Hormuz and Arabian Gulf (e.g. Yamazi, 1974; Jacob *et al.*, 1980; Gibson *et al.*, 1980; Michel *et al.*, 1986b). Michel *et al.* (1986a) suggest that other studies have underestimated copepod abundance, because these studies have not used fine enough nets to capture the smaller species, such as *Oithona* spp. and *Paracalanus crassirostris*, that are particularly abundant in this region. The detailed study of Michel *et al.* (1986b) found that in the eastern Arabian Gulf in March, the numerically dominant copepods were *Oithona* spp., *Paracalanus crassirostis*, *P. aculeatus*, *Oncaea conifera*, *Euterpina acutifrons*, *Corycaeus* spp., and *Temora turbinata*. These seven species accounted for >80% (11894 m^{-3}) of the total measured zooplankton abundance (14512 m^{-3}). The high abundance of *Oithona* spp. and *Oncaea conifera* results in approximately equal numbers of calanoid and cyclopoid copepods in the eastern Arabian Gulf (Michel *et al.*, 1986b).

Although all the studies in the Arabian Gulf have found copepods to be the most abundant taxonomic group, each has determined a different order of abundance for the remaining groups (Table 2.1.3a). After copepods, Gibson *et al.* (1980) showed that ostracods were the next most abundant followed by chordata, cladocerans, and chaetognaths in the eastern Gulf. In the same area Michel *et al.* (1986b) found chordata to be the next most abundant, followed by cladocerans, mollusc larvae, chaetognaths and ostracods. Yamazi's (1974) survey of the whole Arabian Gulf ranked the taxa in the order copepods, cladocerans, chordata, chaetognaths. The majority of the chordata were *Oikopleura* spp., although Grice and Gibson (1978) reported large numbers of *Doliolum* spp. at some stations. The cladocerans were represented mainly by *Penilia avirostris* and *Evadne* sp., ostracods by *Euconchoecia* spp., molluscs by bivalve veliger larvae, and chaetognaths by *Sagitta enflata* and *S. neglecta* (Michel *et al.*, 1986b; Gibson *et al.*, 1980; Halim, 1984).

Table 2.1.3a Ranking the most abundant taxonomic groups of zooplankton in the Arabian Gulf

Abundance rank	Michel *et al.*, (1986)	Gibson *et al.*, (1980)	Yamazi (1974)
1	Copepoda	Copepoda	Copepoda
2	Cladocera	Ostracoda	Cladocera
3	Mollusca larvae	Chordata	Chordata
4	Chaetognatha	Cladocera	Chaetognatha
5	Ostracoda	Chaetognatha	

2.1.3.3 A gradient in zooplankton community species richness

There is a clear gradient in the number of zooplankton species across the region, which like the phytoplankton is lowest in the NW Arabian Gulf and largest in the Gulf of Oman (Kimor, 1973). The zooplankton communities of the Gulf are less diverse than those of the Gulf of Oman, and the main reduction occurs in the Strait of Hormuz (Tables 2.1.3b, c, d, e). Weigmann (1970) reported 24 species of euphausiids in the Arabian Sea, just 6 species in the Gulf of Oman and only a single species (*Pseudeuphausia latifrons*) in the Arabian Gulf. There are only three species of pteropods in the Arabian Gulf compared with more than 13 in the Gulf of Oman (Frontier, 1963b), and there is a reduction in the number of appendicularian species from 12 to 6 westward across the Strait (Fenaux, 1964; 1973). Ostracods also show the same pattern: Leveau (1968) recorded 6 species in the Gulf of Oman, but only two of these, *Euconchoecia aculeata* and *Cypridina chierchiae*, in the Arabian Gulf. This poverty of species in the Gulf extends to nearly all taxonomic groups, including copepods and chaetognaths (Bour and Frontier, 1974). Several epiplanktic species are found in the Gulf and act as indicators of oceanic water (e.g. the copepods *Eucalanus crassus*, *E. elongatus* and *Undiula vulgaris*) but there is no evidence that there are permanent breeding populations of these species in the Gulf (Michel *et al.*, 1986b; Yamazi, 1974).

Table 2.1.3.b Pelagic Ostracoda in the Gulf of Oman and Arabian Gulf (after Leveau, 1968)

Number of species	Species name	Present in the Gulf of Oman	Present in the Arabian Gulf
1	*Euconchoecia aculeata*	✓	✓
2	*Cypridina chierchiae*	✓	✓
3	*Conchoecia procera*	✓	
4	*Conchoecia elegans*	✓	
5	*Conchoecia alata*	✓	
6	*Archiconchoecia striata*	✓	

Table 2.1.3.c Appendicularia in the Gulf of Oman and Arabian Gulf (Fenaux, 1964)

Number of species	Species name	Number of stations in Gulf of Oman (out of 10)	Number of stations in Arabian Gulf (out of 11)
1	*Oikopleura longicauda*	9	11
2	*Oikopleura fusiformis*	8	2
3	*Oikopleura rufescens*	5	7
4	*Fritillaria formica*	5	2
5	*Stegosoma magnum*	2	2
6	*Megalocerus huxleyi*	1	1
7	*Fritillaria venusta*	5	
8	*Fritillaria pellucia*	3	
9	*Fritillaria borealis*	2	
10	*Oikopleura albicans*	1	
11	*O. fusiformis f. cornut.*	1	
12	*Folia gracilis*	1	

Table 2.1.3.d Euphausiacea in the Gulf of Oman and Arabian Gulf (Weigmann, 1970)

Number of Species	Species name	Present in the Gulf of Oman	Present in the Arabian Gulf
1	*Pseudeuphausia latifrons*	✓	✓
2	*Euphausia sazoi*	✓	
3	*Euphausia distinguenda*	✓	
4	*Euphausia diomedeae*	✓	
5	*Stylocheiron lomgicorne*	✓	
6	*Stylocheiron affine*	✓	

Table 2.1.3.e Pteropoda in the Gulf of Oman and Arabian Gulf (Frontier, 1963b)

Number of species	Species name	Present in the Gulf of Oman	Present in the Arabian Gulf
1	*Creseis virgula*	✓	✓
2	*Limacina inflata*	✓	✓
3	*Desmopterus papilio*	✓	✓
4	*Cavolinia* sp.	✓	✓
5	*Creseis acicula*	✓	✓ (rare)
6	*Hyalocyclix striata*	✓	✓ (rare)
7	*Clionina longicaudata*	✓	✓ (rare)
8	*Corolla* sp.	✓	✓ (rare)
9	*Limacina trochiformis*	✓	
10	*Euclio pyramidata*	✓	
11	*Limacina bulimoices*	✓	
12	*Desmopterus gardineri*	✓	
13	*Cymbulia* spp.	✓	

The main reason for the poverty of species in the Arabian Gulf is thought to be the high salinity of the water, which makes the area inhospitable to many species (Kimor, 1973). Another factor believed to be important is shallowness of the sea which precludes mesopelagic and bathypelagic species from the Gulf of Oman (Leveau and Szekielda, 1968). For example the mesopelagic chaetognath *Sagitta pacifica* does not penetrate into the Gulf, but *S. bedoti*, which is characteristic of surface waters, is

present (Furnestin and Codaccioni, 1968). The rectangular mid-water trawl (RMT) samples from CD 104 also showed this same pattern: these samples contained 38 species of fish and 21 species of decapods in the Gulf of Oman, but only 9 species of fish and 7 species of decapods above the continental slope on the east side of the Strait (Herring *et al.*, 1998).

The Arabian Gulf supports a subset of the more diverse fauna found in the Gulf of Oman and there are few endemic zooplankton species. The species that are present are those that can tolerate the extreme environmental conditions. Few.

2.1.4 Other aspects of the biology of the region

The biology of the region is unusual in other ways and there are certain features that should be considered briefly (Basson *et al.*, 1977; Sheppard *et al.*, 1992; Price *et al.*, 1993a). The bottom substrate of the Gulf consists usually of soft sediment which encourages plentiful growth of seagrass and algae beds (Price and Coles, 1992). Coral reefs are present in the Gulf, Strait and Gulf of Oman, but are sparse, and as with the plankton there are fewer species of corals than in the Indian Ocean. Mangrove swamps are also rare, and most of the total of about 125 km^2 is concentrated on the Iranian coast (IUCN, 1987). The number of fish species is much lower in the Gulf than outside and Price *et al.* (1993a) estimate that there are about 500 species present from Coad's survey (1993). The Gulf also contains a sizeable population of the seasnake *Hydrophis* (Gasperetti, 1988) cetaceans (e.g. Al-Robaae, 1969) and the rare marine mammal the dugong (Gallagher, 1975).

The Arabian Gulf has been of special interest recently because of the Gulf War in the early 1990s. This resulted in the release of about 6 million barrels of oil into the Gulf, as well as soot from the burning of wells. Many parts of the ecosystem have been affected, for example the abundance of larval penaeid shrimps (which form an important fishery) is greatly reduced, (Price *et al.*, 1993b). Al-Yamani *et al.* (1993) report that there has been no detectable effect on the zooplankton biomass.

2.1.5 Summary of the findings of previous studies in the region

In general, the conditions in the Gulf of Oman are typical of the NW Indian Ocean, however the shallow Arabian Gulf is characterised by high salinity water. The Strait of Hormuz is the only connection for the exchange and mixing of water between the these two areas. The exchange occurs as a two layer structure, with fresher water from

the Gulf of Oman overlying saltier water from the Arabian Gulf. In this way both the Arabian Gulf and the Gulf of Oman influence the conditions in the Strait. Satellite observations have revealed that mesoscale features are common in this region, but previous studies have not attempted to resolve their impact on the plankton.

Both the phytoplankton and zooplankton communities become less diverse with increasing distance into the Arabian Gulf and away from the Gulf of Oman. The high salinity and the shallow water of the Arabian Gulf are believed to limit the distributions of many species. For many species the Strait of Hormuz marks a strong boundary between favourable and inhospitable conditions.

Phytoplankton production and standing stock are greater in the Arabian Gulf than in the Gulf of Oman. This pattern is thought to be caused by the input of nutrients in the Shatt Al-Arab and to a lesser extent, more rapid remineralisation in the shallow Gulf. Studies have not found that zooplankton standing stock follows the pattern of increased phytoplankton standing stock from the Strait to the NW Arabian Gulf. In fact, different studies have reported a variety of patterns of the distribution of zooplankton biomass. All of the studies have found copepods to numerically dominate the zooplankton in this region, ranging from >50% to >90% of all individuals. Michel *et al.* (1986b) measured particularly high abundance of the small copepods *Oithona* spp., *Oncaea* sp. and *Paracalanus* sp. when sampling with a net capable of capturing these species. Other abundant taxonomic groups include cladocerans, chaetognaths, appendicularians, doliolids and ostracods.

The differences observed in the spatial distribution of zooplankton by the various studies can be explained by a strongly patchy distribution of zooplankton in this region. At the mesoscale, the heterogeneity in the zooplankton distribution may be controlled by variability in the physical environment, characterised by a large and biologically significant salinity gradient in the Strait of Hormuz.

2.2 METHODS: R.R.S. *CHARLES DARWIN* CRUISE 104 – COLLECTION OF DATA AND SAMPLES, AND THEIR PROCESSING AND CALIBRATION

A multidisciplinary dataset, comprising hydrography, pelagic biology and meteorology, was collected during leg 1 of R.R.S. *Charles Darwin* cruise 104 (CD 104) between 12th February 1997 and 19th March 1997 (cruise report: Roe *et al.*, 1997). This section describes the sampling techniques, processing and calibration of the various data used in this thesis. Additional information about these datasets can be found in the SOC Research & Consultancy reports (Allen, 1997; Allen and Griffiths, 1997; Mustard, 1997; Smeed, 1997; Smeed *et al.*, 1997; Crisp *et al.*, 1998).

2.2.1 Introduction to the cruise and the sampling strategy

CD 104 included profiling CTD surveys in the Gulf of Oman, the Strait of Hormuz and the Arabian Gulf, SeaSoar surveys in the Strait of Hormuz and the Arabian Gulf, and zooplankton net samples in the Gulf of Oman, the Strait of Hormuz and the Arabian Gulf. Concurrent sampling of the physicochemical environment and the distribution of zooplankton populations is essential for the detailed study of their interrelationship at the mesoscale (Roe *et al.*, 1996). SeaSoar is a suitable for this type of study because it is capable of the appropriate spatial resolution and coverage of mesoscale features within a quasi-synoptic time scale, and can be fitted with a suite of instruments (Pollard, 1986). The main dataset used in this thesis is the SeaSoar survey in the Strait of Hormuz, although other data collected during the cruise is used to understand the situation in the Strait.

A suite of biological instrumentation was deployed synchronously with the SeaSoar, to determine the distribution of plankton populations. These were a fluorimeter, an optical plankton counter (OPC), and a biological sonar, the EK500. Actual filtered samples of plankton, needed for calibration and to provide taxonomic information, were collected by Niskin bottle and from the ship's non-toxic supply for chlorophyll, and by a Longhurst-Hardy plankton recorder (LHPR) for mesozooplankton. In addition, a profiling CTD fitted with a rosette of Niskin bottles was used to determine the hydrography of full depth water column. The profiling CTD can also collect water samples which allow more precise calibrations of salinity, potential density and chlorophyll, as well as variables not measured by SeaSoar, such as the dissolved oxygen concentration. This section describes the methods used to obtain these data.

Additional data (macrozooplankton samples, wind and sea surface temperature) collected with RMT nets and meteorological sensors has been used in minor ways in this thesis but the details of these methods are not presented (for details see Herring *et al.*, 1999; Moat *et al.*, 1997). I had no input to survey design for this cruise (§1.2.3).

2.2.2 Hydrographic measurements made with a SeaSoar

The Strait of Hormuz SeaSoar survey consisted of 6 approximately parallel transects around the Masandam peninsula (**Fig 2.2.2.i**). Each transect was about 280 km long and extended from the NW of the Gulf of Oman into the eastern Arabian Gulf. A mechanical seizure in the drum holding the fared cable resulted in SeaSoar only being deployed on unfaired cable, which limited the maximum profiling depth to 90-100 m. This was adequate in the Strait of Hormuz, where water depth varies between 25 and 120 m. The survey was confined to the southern half of the Strait, in the waters of Oman and the United Arab Emirates, because permission was not obtained to work in Iranian waters.

The SeaSoar (**Fig 2.2.2.ii**) was deployed on 02/03/97 (Jday 61) at 06:50 GMT and recovered at 14:30 GMT on the 07/03/97 (Jday 66). Two breaks occurred in the survey: the first for 3 hours before sunrise on the 04/03/97 (Jday 63) when the SeaSoar was entangled in fishing line. It was redeployed at dawn (02:45 GMT). On the evening of the 05/03/97, the SeaSoar was recovered at 14:45 GMT as a precaution against loss or damage from fishing lines during the night, and it was redeployed at dawn (02:20 GMT) on the 06/03/97.

The position of SeaSoar was determined as the position of the ship 50 seconds previously. The position of the ship was determined using primarily GLONASS satellites. The Russian GLONASS system is similar to GPS, but does not deliberately degrade the position data. This system produced fixes with errors of less than 10 m without the use of a differential correction station.

During this survey the SeaSoar was fitted with the following instruments:

i) Neil Brown / G.O. Mk IIIc CTD Shallow 04
ii) Chelsea Instruments PAR Lightmeter
iii) Chelsea Instruments Mk III Aquatraka Fluorimeter (see §2.2.3)
iv) Focal Technologies Inc. Optical Plankton Counter (see §2.2.4)

The CTD on the SeaSoar measured conductivity, temperature and pressure, from which potential temperature, potential density, salinity and depth were determined.

Figure 2.2.2.i A map showing the positions of the six transects of the SeaSoar survey and the LHPR biological stations in the Strait of Hormuz

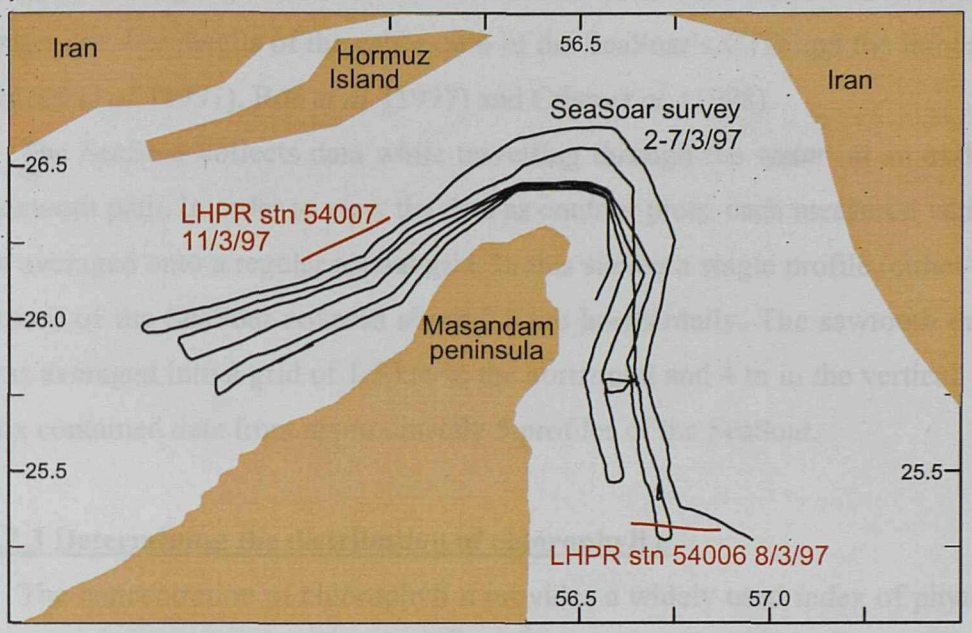

Figure 2.2.2.ii SeaSoar fitted with optical plankton counter (OPC)

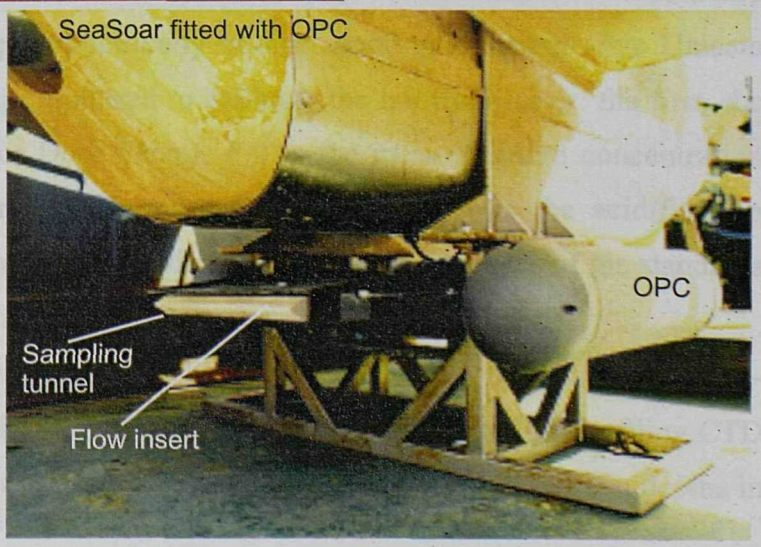

The salinity calibration was verified using hourly surface salinity samples, which were analysed using a Guildline Autosal standardised with IAPSO standard seawater ampoules. For details of the calibration of the SeaSoar's CTD and the light sensor see Smeed *et al.* (1997), Roe *et al.* (1997) and Crisp *et al.* (1998).

The SeaSoar collects data while travelling through the water on an undulating or sawtooth path. In order to view the data as contour plots, each measured variable must be averaged onto a regular spatial grid. In this survey a single profile (either an up or a down) of the SeaSoar covered about 0.3 km horizontally. The sawtooth data stream was averaged into a grid of 1.5 km in the horizontal and 4 m in the vertical. Each grid box contained data from approximately 5 profiles of the SeaSoar.

2.2.3 Determining the distribution of chlorophyll *a*

The concentration of chlorophyll *a* provides a widely used index of phytoplankton biomass in oceanographic studies. The distribution of chlorophyll *a* can be measured automatically with a fluorimeter at the same spatial resolution as the physical data (Lorenzen, 1966). On CD 104 fluorimeters were mounted on both the undulating SeaSoar and the profiling CTD frame. The fluorescence output of the instruments was calibrated to chlorophyll *a* concentration using water samples taken during the surveys.

2.2.3.1 The concentration of chlorophyll a in the water samples

The chlorophyll *a* concentration of the water samples was determined using a laboratory fluorimeter on the ship (Turner Designs, model 10-000R). This fluorimeter was calibrated using dilutions of chlorophyll standard solution, made from a Sigma Chemicals chlorophyll *a* pellet (concentrated from *Anacystis nidulans*) dissolved in 90% acetone (JGOFS protocols, 1994). The chlorophyll concentration of the standard solution was determined photometrically with a spectrophotometer (Pye Unicam SP6–500). Two factors were produced to calibrate the lab fluorimeter: the first, the linear calibration factor, (or Door Factor, F_D) is the mean standard concentration divided by the mean standard fluorescence. The second was the acidification coefficient, *Fm*, which is the average ratio between the fluorescence of the standards before and after acidification.

During the SeaSoar survey chlorophyll samples were taken from the ship's non-toxic seawater supply (intake at 3 m) every two hours, and during the profiling CTD surveys water samples were taken from the Niskin bottles fired at specific depths in

the water column (for more details see Roe *et al.*, 1997). All of the samples were duplicated. The phytoplankton cells were collected by filtering 100 ml aliquots of seawater through Whatman GF/F papers, in the dark at low pressure (<6 mm Hg). The pigments were extracted from the phytoplankton cells into a solution of 20 ml of 90% acetone also in the dark at –20°C for between 20 to 22 hours. The samples were then removed from the freezer and warmed to laboratory temperature (20°C) in a darkened water bath. The laboratory fluorimeter was zeroed with a blank of a 90% acetone solution and the concentration of chlorophyll *a* and phaeopigments were determined by the acid addition method (JGOFS protocols, 1994) as follows:

$$Chla\ (mg\ m^{-3}) = F_D\left(\frac{Fm}{Fm-1}\right)(Fb-Fa)\left(\frac{v}{V}\right) \quad . \quad . \quad . \quad . \quad \text{Eq 2.2.1}$$

$$Phaeopig\ \left(mg\ m^{-3}\right) = F_D\left(\frac{Fm}{Fm-1}\right)(Fm*Fa-Fb)\left(\frac{v}{V}\right) \quad . \quad . \quad . \quad \text{Eq 2.2.2}$$

Where:
F_D = Mean Standard Conc. / Mean Standard Fluorescence before acidification
Fm = Mean Fb/Fa of Standard solutions
Fb, Fa = Fluorescence before and after acidification of the sample
v = volume of 90% acetone used in extraction (20ml)
V = Volume of seawater filtered (100ml)

2.2.3.2 The calibration of the CTD frame and SeaSoar fluorimeters

Calibration functions for the CTD and SeaSoar fluorimeters were determined from the regression between the chlorophyll concentration of the samples and the fluorimeter output (in volts). Both of the fluorimeters were calibrated separately for the Gulf of Oman, the Strait of Hormuz and the Arabian Gulf. This is because changes in the dominant species (known to occur: El Gindy and Dorgham, 1992; Rao and Al-Yamani, 1998) can alter the relationship between chlorophyll concentration and fluorescence (Flemer, 1969). The calibration relationship can also be affected by nutrient availability to cells (Kiefer, 1973; Cullen and Renger, 1979) and other sources of fluorescence such as phaeopigments and chlorophyll derivatives (Herbland, 1988; Strass, 1990).

Before the regressions were performed the data were plotted to examine the impact of quenching (**Fig 2.2.3.i**). Quenching occurs when the relationship between fluorescence and chlorophyll concentration is affected by light. At high light intensities a lower than expected fluorescence is recorded, because the photosynthetic apparatus of the cells changes its photo-adaptive state (Falkowski, 1984).

Figure 2.2.3.i The calibration graph for the CTD fluorimeter in the Gulf of Oman, showing the lack of quenching

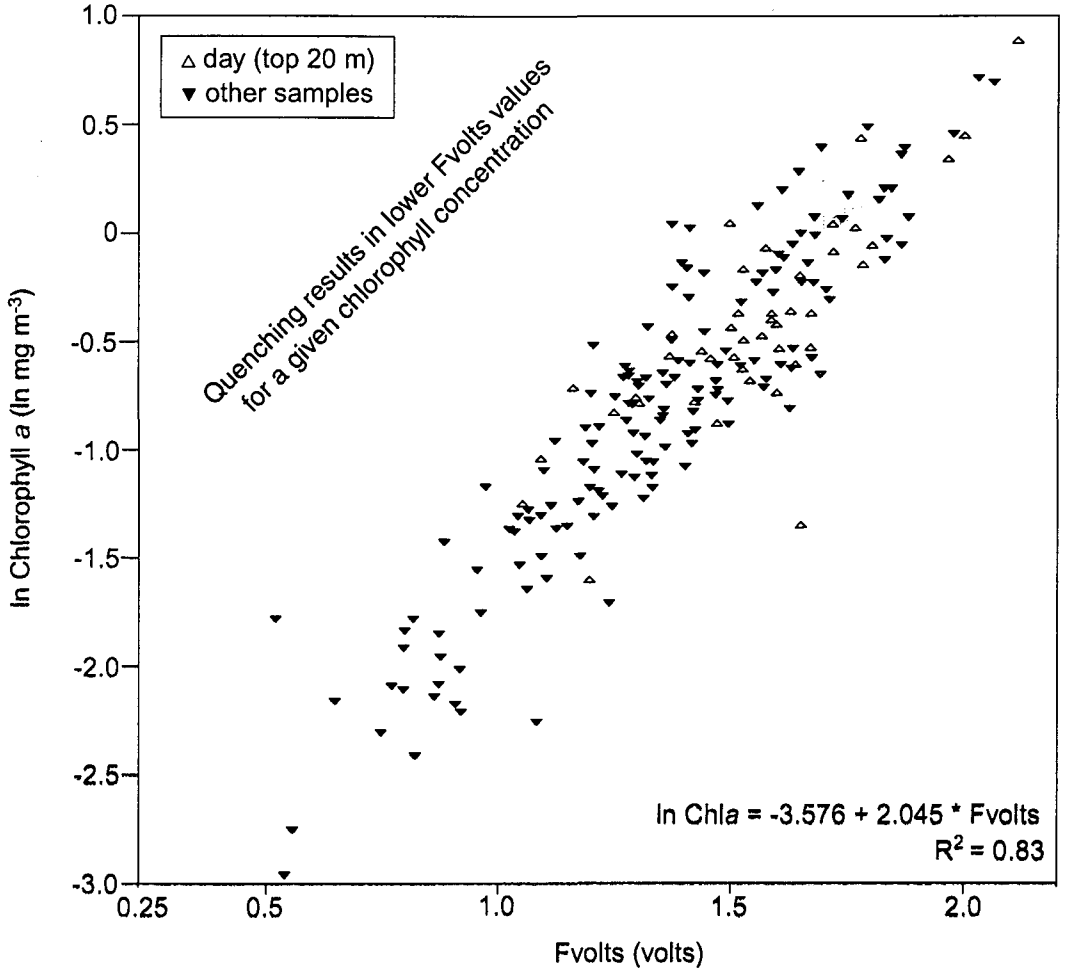

Figure 2.2.4.i Histogram of counts in size classes in the raw OPC data

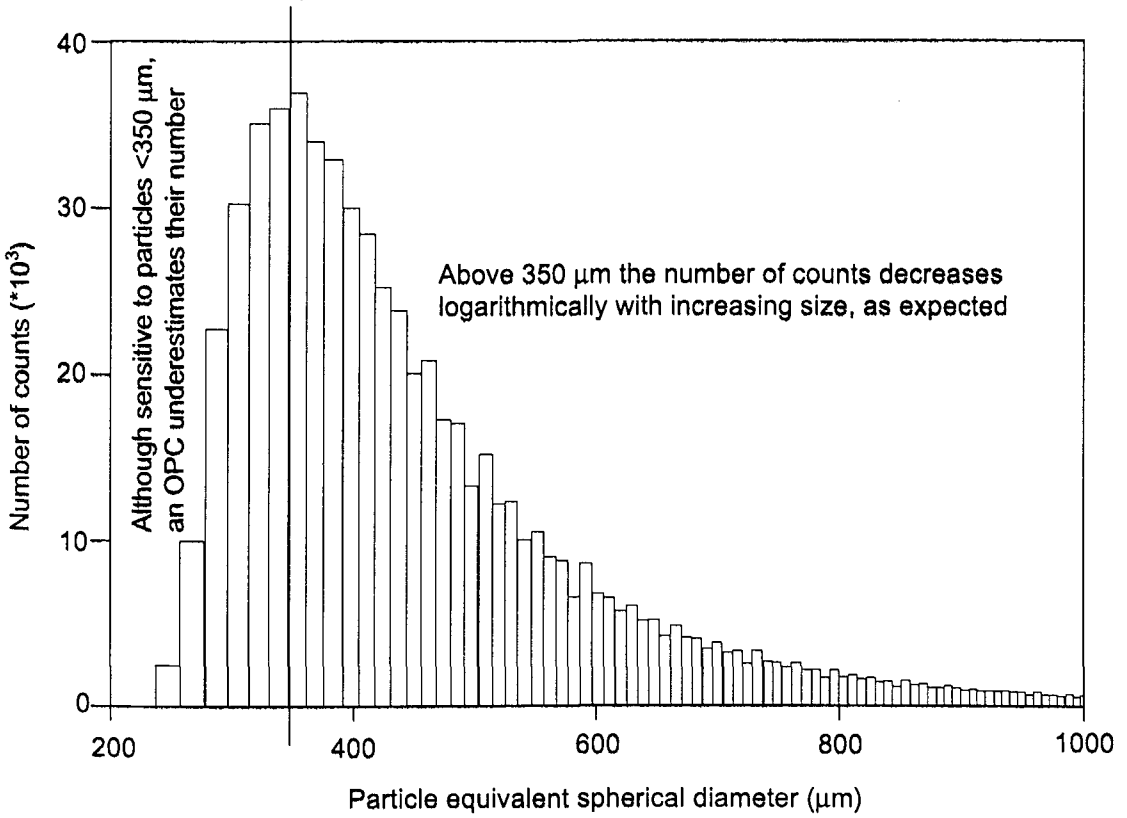

Unexpectedly, there was not a clear quenching affect in the calibration data. **Fig 2.2.3.i** shows the calibration dataset for the CTD fluorimeter in the Gulf of Oman. Fluorimeter measurements made at high light levels (the samples taken in the upper 20 m during the day) showed a similar regression to the unquenched samples. Consequently after inspection, light and dark samples were combined to compute regressions (the graphs for all areas and both fluorimeters are presented in Fig. 2 in Crisp *et al.*, 1998). However, the observations do show a quenching signal (e.g. **Fig 4.1.1.i:** compare 4150 km (night) on leg 3 and at 4275 km (day) on leg 4), which suggests that more calibration samples should have been taken to resolve quenching.

The regressions were calculated between the variables Fvolts, the voltage output of the fluorimeter, and ln Chl*a*, the natural log of the chlorophyll concentration. These variables allow a regression to be determined linearly, using a PEXEC program plreg2. PEXEC is a set of Fortran programs that run on a UNIX operating system (see Alderson, 1997). Clearly anomalous values (>that double or half the expected value) were identified and removed before the regression was calculated, which resulted in a removal of only about 1% of all the measurements. The calibration functions for the CTD and SeaSoar fluorimeters are presented in Table 2.2.3.a:

Table 12.2.3.a The calibration functions for the CTD and SeaSoar fluorimeters in each area

Calibration function	Fluorimeter	Area
ln Chl*a* = -3.5759 + 2.0451 * Fvolts	CTD	Gulf of Oman (CTD stns 1–108)
ln Chl*a* = -4.3452 + 2.7234 * Fvolts	CTD	Strait of Hormuz (CTD stns 109-144)
ln Chl*a* = -2.6600 + 1.4774 * Fvolts	CTD	Arabian Gulf (CTD stns 145 –187)
ln Chl*a* = -4.277 + 2.342 * Fvolts	SeaSoar	Strait of Hormuz (03-08/03/97)

The calibration dataset for the SeaSoar fluorimeter showed greater spread than for the CTD fluorimeter because there were fewer calibration data points and these were all at the surface. However, the calibration coefficients for the SeaSoar fluorimeter in the Strait are similar to those for the CTD fluorimeter in this region, which gives confidence that a reliable calibration has been achieved for the SeaSoar fluorimeter.

2.2.4 Methods for processing Optical Plankton Counter data

An optical plankton counter (OPC) was used to evaluate the distribution of mesozooplankton synchronously with other environmental measurements made by SeaSoar. This offers advantages both scientifically, as both biological and physical data are sampled on the same time and space scales, and economically, as data are gathered without using extra cruise time. The OPC is a relatively new instrument and

data from it is widely used in this thesis. In this section, background information concerning this instrument is presented and the processing is described in detail.

2.2.4.1 The optical plankton counter - background information

Prior to this survey an OPC had never been used in the Arabian Gulf or the Gulf of Oman, and in fact there still remain no reports of its use in the entire Indian Ocean in the literature. The OPC was developed by Alex Herman at the Bedford Institute of Oceanography, Nova Scotia, Canada in conjunction with Focal Technologies Inc. This instrument evolved from the family of sensors based on the Coulter Counter (Coulter, 1957) such as conductivity based counters, (Maddux and Kanwisher, 1965; Boyd and Johnson, 1969; Herman and Dauphine, 1980), the Opto-electronic Plankton Sizer (Cooke *et al.*, 1970) and the Hiac Particle Size Analysis, (Pugh, 1978).

The OPC has been used to describe the spatial distribution of zooplankton from the finescale (Herman *et al.*, 1993) through the mesoscale (Huntley *et al.*, 1995) to basin scales (Gallienne and Robins, 1998). Currie *et al.* (1998) have modified an OPC to study micro-scale patchiness.

The OPC system comes in two forms: a towed instrument, and a laboratory instrument. The towed OPC has been used on a variety platforms ranging from towed profilers and CTDs to net systems (Table 3.1.1.a). This instrument has been deployed in a variety on environments including oceanic (Huntley *et al.*, 1995), coastal (Herman *et al.*, 1993), fjordic (Heath, 1995), and freshwater (Sprules *et al.*, 1998).

Table 3.1.1.a Platforms used for the optical plankton counter

Platform type	References
Batfish (towed profiler)	Herman *et al.*, 1991 & 1993
SeaSoar (towed profiler)	Huntley *et al.*, 1995; Pollard *et al.*, 1996
V-fin (towed profiler)	Sprules *et al.*, 1992 & 1998; Rissik *et al.*, 1997
Seabird-25 (towed profiler)	Currie *et al.*, 1998
VPR (video system)	Ortner, 1993
ARIES (net system)	Backhaus *et al.*, 1994; Heath, 1995
LHPR (net system)	Wieland *et al.*, 1997; Grant *et al.*, 2000
BIONESS (net system)	Herman, 1992
MOCNESS (net system)	Foote, 2000
moored (in a vane)	Herman, 1993

The laboratory benchtop OPC (OPC-1L) pumps zooplankton samples through its sensor. The benchtop OPC has been used to help to calibrate towed version (Wieland *et al.*, 1997; Grant *et al.*, 2000), to analyse preserved samples (Beaulieu *et al.*, 1999), and as an underway survey tool connected to a pumped seawater supply (Gallienne *et al.*, 1996; Checkley *et al.*, 1997; Gallienne and Robins, 1998). Checkley *et al.*

developed the system further with the coupling of a video camera to produce a continuous fish egg sampler (CUFES).

2.2.4.2 The sensing mechanism of a OPC

In this study the towed OPC was used. This instrument consists of a sampling tunnel flanked by pressure cases, which contain transmitting and receiving optics (**Fig 2.2.2.ii**). A light beam, projected across the sampling tunnel, is used to detect zooplankton. The light beam is produced by six high intensity LEDs, focused by a cylinder lens, collimated by a 4mm aperture and contained by highly polished PVC plates above and below it. The resulting beam has dimensions of 220 x 20 x 4 mm and is focused by another cylinder lens onto the photodiode monitor.

As the instrument is towed through the water, a particle is detected and sized (a count) as it partially impedes the light beam. The size of the particle is recorded as the size of the spike (negative) in light level detected by the receiver, which is converted to a digital output in one of 4096 size classes (Herman, 1992). The size of the spike is dependant on the area of the shadow cast, determined by the cross sectional area (CSA) and orientation of the particle in the beam. The size of the particle is then computed from the digital output with the manufacturer's calibration equation (§2.2.4.4), which was determined empirically using spherical nylon beads (Herman, 1992). As a result, the measurement of the particle's CSA (which may be any shape), is converted to the equivalent spherical diameter (ESD) in mm of a sphere which projects the same CSA as the particle. The count is time stamped to the nearest second. An OPC is capable of sizing particles with equivalent spherical diameters (ESDs) between 0.25 mm and 14 mm (Herman, 1992).

An OPC also measures the slow rate of change in light attenuance across the tunnel caused by background variation in seawater turbidity. This is done by monitoring the light level of the beam at the receiver and compensating for changes by increasing or decreasing the intensity of the LED light source. This provides a source of uncalibrated attenuance, and also ensures that particle measurements are not effected by the variations in the background attenuance in the tunnel (Herman, 1992; Focal Technologies, 1995). These measurements are made every half a second.

The remainder of this section describes how these two measurements (counts and attenuance), were processed to produce useful biological information from the counts.

2.2.4.3 OPC data collection

An OPC (OPC-1T) was attached to the underside of the SeaSoar (**Fig 2.2.2.ii**) in the same way as developed on the Antares XIII/2 cruise on F.S. *Polarstern* (Pollard *et al.*, 1996). Because SeaSoar is towed relatively fast (about 4 ms^{-1}) the sampling tunnel of the OPC was fitted with a flow insert, which reduced the intake to 20% of the standard area (from 0.005 to 0.001 m^2). By reducing the volume of water sampled, the insert lessens the chance of coincident counts, which occur when two particles pass through the sampling beam simultaneously, producing a single over sized count. Another benefit of reducing the volume of water sampled is that it maintains the count rate at a level (<200 s^{-1}) which is within the capabilities of the OPC's software (Herman, 1992). During CD 104 the count rate rarely exceeded 100 s^{-1}. Another consequence of decreasing the volume sampled is the reduction in the total number of counts made. This is not a problem with the most numerous smaller species, but larger, less abundant species are not recorded at a high enough rate for their distribution to be determined robustly. On CD 104 this imposed a useful upper limit of size detection of about 5 mm ESD.

The count and attenuance data were transmitted up the fared conducting cable of the SeaSoar, to the OPC deck unit on the ship. The data were logged via the deck unit attached to a PC, which was networked, using PC-NFS, allowing the raw data files to be written directly to a UNIX file system, as a network drive. A new data file was started every 4 hours, so that previous files could be processed. During the SeaSoar survey of the Strait 33 files were written. The 1st, 26th and 28th files were lost as a result of a problem with the software, and therefore there are no OPC data from these four hour segments. The OPC sized 16 million zooplankton and measured attenuance 0.8 million times during the 6 day survey of the Strait.

2.2.4.4 OPC Data Processing

There were three main tasks in the OPC data processing. The first was to calculate useful biological measurements such as zooplankton abundance and biovolume in size classes. The second task was to calibrate as reliably as possible the biological measurements produced by the OPC (this is the subject of Chapter 3). The third was to organise this information on the same space scale as the SeaSoar data so that the zooplankton distribution could be analysed in relation to the environment. The OPC data were processed using PEXEC programs, and these are listed in Appendix 1.

The data were split into two files: one for the zooplankton counts data, and the other for the attenuance data. The counts were given a more precise time stamp by dividing each second by the number counts, and spacing the counts evenly through the second in the order they were sampled (as Pollard *et al.*, 1996). In order to determine the position of each zooplankton count and attenuance measurement, spatial information (depth and distance) and time were merged from the SeaSoar files with the OPC data. Then all the count files and all the attenuance files were joined together, producing two master data files - one for counts and one for attenuance. In this form the data are measurements of zooplankton sizes and attenuance, distributed along the sawtooth track of the SeaSoar. Then both files were averaged into a regular two dimensional spatial grid of 1.5 km in the horizontal and 4 m in the vertical, in the same way as the SeaSoar data. Each grid box or bin contained the data averaged from between 4 and 6 profiles of SeaSoar. The OPC counted approximately 650-800 particles in each bin.

The attenuance data has not been calibrated and is not presented in this thesis, although it is presented by Mustard (1997). The distribution of this variable shows little correlation with either the zooplankton measured by the OPC, the chlorophyll *a* measured by the fluorimeter or the physical structure of the water column. Some studies have shown that attenuance can be related to phytoplankton abundance in the open ocean (Strass *et al.*, submitted). Zhang *et al.* (2000) found that the attenuance could be used to quantify the amount of detritus in the water, that may be counted as zooplankton (as coincidence counts) by an OPC in highly turbid estuarine waters.

The averaging of the counts data from an OPC is unusual because measurements are not made at regular intervals, but whenever a particle happens to pass through the sampling beam. This is contrary to instruments such as the CTD and fluorimeter which typically make 16 measurements each second. The number of particles and the volume they represent was summed for each grid box, and these data were divided by the volume of seawater passing through the OPC to calculate the number of zooplankton per cubic metre (the abundance) and the volume of zooplankton per cubic metre (the biovolume). It was not possible to directly measure the volume of seawater passing through the OPC. Instead the volume was calculated from the inlet area of the OPC multiplied by the distance travelled by the ship. This was scaled by 1.033 to account for the undulating path of SeaSoar (§3.1.2).

The volume of zooplankton was calculated from the sum of the volume of each particle sampled by the OPC. The OPC determines the size of a particle from the area of the shadow it casts in the sampling beam and records it as a digital size (DS_{opc}). The manufacturer's calibration equation (Eq 3.2.1) converts this into an ESD in μm (Herman, 1992; Focal Technologies, 1995). This ESD is the diameter of a sphere (or circle) that has the same CSA as the particle, irrespective of the particle's shape.

This non-linear equation has been widely used in published datasets from the OPC (Huntley *et al.*, 1995; Wieland *et al.*, 1997; Checkley *et al.*, 1997; Sprules *et al.*, 1998; Beaulieu *et al.*, 1999; Zhang *et al.*, 2000). In this study zooplankton biovolume from the OPC was calculated from the DS_{opc} output of the OPC with the calibration equations (and assumptions) listed in §3.2.2. The CSA of the particle was calculated from the ESD, and then the volume was calculated assuming that all the zooplankton were opaque spheroids, with dimensions defined by measurements of zooplankton from the LHPR samples, see §3.2.2 for more details.

The zooplankton abundance and biovolume measurements were divided into size classes of organisms. For contouring 5 size classes were selected, these were defined with reference to the reliable particle size sampling limits of 0.35 and 5 mm ESD (**Fig 2.2.4.i**) and also to fit within the constraints of the biomass size spectra theory (Sheldon *et al.*, 1972; Platt and Denmann, 1978) and are therefore in log2 increments of particle volume; the size classes are shown in **Table 2.2.4.a.**

Table 2.2.4.a OPC zooplankton size classes used for contouring

Log_2 Volume range (mm^3)	Volume range (mm^3) midpoint in brackets	ESD range (mm)	Digital Size range
$2^{-7} - 2^{-5}$	0.0078 – 0.031 (0.016)	0.40 – 0.64	16.5 – 38.5
$2^{-5} - 2^{-3}$	0.031 – 0.125 (0.063)	0.64 – 1.02	38.5 – 90.5
$2^{-3} - 2^{-1}$	0.125 – 0.5 (0.25)	1.02 – 1.61	90.5 – 211.5
$2^{-1} - 2^{1}$	0.5 – 2 (1)	1.61 – 2.56	211.5 – 506.5
$2^{1} - 2^{3}$	2 – 8 (4)	2.56 – 4.07	506.5 – 1230.5

This produced a data file that was averaged into a grid with three dimensions: distance, depth and zooplankton size class. In other words, for each spatial bin there are measurements of abundance and biovolume in each of the 5 size classes.

The OPC data were also split into 12 size classes, at a lower spatial resolution of 16 m by 6 km to ensure enough counts were made in each bin, for looking in detail at size relationships with the environment (see §5.1.3 and Table 5.1.3.a).

2.2.4.5 Calculations of carbon biomass from the OPC measured biovolume

The carbon biomass of the zooplankton was calculated from the biovolume using two conversion methods. The first uses Wiebe's (1988) conversion equation which was determined from empirical zooplankton data collected in a range of environments:

$$Log_{10}(Carbon) = 1.2195 Log_{10}(Volume) + 1.7488 \quad . \quad . \quad . \quad . \quad \text{Eq 2.2.3}$$

The second uses the conversion method of Parsons *et al.* (1977) that was developed to calculate carbon from volume determined from ESD measurements of a Coulter counter. This approach assumes that wet weight is equal to the volume multiplied by the density of the water, dry weight is 10% of wet weight and carbon is 50% of dry weight. These assumptions were modified by substituting the data of Matondkar *et al.* (1995) from the Arabian Sea in March 1992. Matondkar *et al.* determined that the dry weight of copepod dominated mesozooplankton samples was 9.16% of wet weight, and carbon was 44.6% of dry weight. Further details are given in Appendix 4, where the results of these conversions are compared (see p242).

2.2.5 Zooplankton samples collected with a Longhurst-Hardy plankton recorder

A Longhurst Hardy Plankton Recorder - LHPR (Longhurst *et al.*, 1966; Longhurst and Williams, 1976; Williams *et al.*, 1982) was used to take a series of discrete zooplankton samples with concurrent measurements of conductivity, temperature and pressure (§2.2.5). The samples were taken to be used both in the calibration of the OPC and for comparison with OPC data (Chapter 3), and also to describe the distribution of taxonomic groups (§4.2). This section provides some background information about the LHPR and describes the processing of the samples.

2.2.5.1 The LHPR – background information

The LHPR, modifies the Hardy principle of continuous filtration (Hardy, 1936), using a sampling cod-end that filters zooplankton onto a long strip of gauze, which is wound on after a predetermined time periods, producing a series of discrete samples. This allows the distribution of zooplankton to be determined at a high spatial resolution in a single tow. The sampler is fitted to a standard net in place of a simple cod-end bucket, trapping zooplankton on the sampling gauze. Because of the bulk of the net and the cod-end, they are mounted in a metal frame. Although this increases the size of this instrument, the frame provides a platform for a suite of environmental sensors, such as a CTD and flowmeter.

The LHPR has been used widely to study the distribution of zooplankton, in relation to the physical structure of the water column, in both the vertical and the horizontal. This is because it offers a higher spatial resolution than standard nets and makes concurrent physical measurements of the water column structure. Early work included Longhurst (1967), Wiebe (1970), and Fasham *et al.* (1974)

These early studies identified several problems that have led to modifications of the LHPR (Haury, 1973; Haury *et al.*, 1976; Williams *et al.*, 1982). The residence time of zooplankton within the net was the major problem of early LHPRs (Haury, 1973). This can be divided into two processes: stalling and hang-up which result in smearing (Haury *et al.*, 1976). Smearing occurs when two plankton enter the net together, but as a result of their different residence times in the net are smeared into separate sections of the sampling gauze. Stalling results when a zooplankter temporarily stops in the net, either by sticking to the side or as a result of poor water flow through the net. Hang-up is a permanent attachment of zooplankton to the side of the net or sampler. Clogging and periodical washing out of accumulated zooplankton was also noted in early LHPR nets (Haury *et al.*, 1976).

The design of the modern LHPR reduces many of these problems (Williams *et al.*, 1982). This net is able to reduce stalling and smearing because of its reducing cone and large net, which further increase the filtration efficiency (from 58-70% to 87-97%) and the open area ratio (OAR = 9.1). A LHPR incorporating these advances was used in this survey.

2.2.5.2 The collection of zooplankton samples with the LHPR

It is not possible to deploy a LHPR synchronously with a SeaSoar (and in addition no provision was made to mount the OPC on the LHPR) so two stations were occupied with the LHPR on either side of the Strait of Hormuz to collect data to compare with the OPC (**Fig 2.2.2.i**). At both stations the LHPR was towed on a profile from the surface to a maximum depth as close to the sea floor as possible and back to the surface with a stepped ascent. The depths of the steps were selected with reference to the real time uncalibrated EK500 backscatter (§2.2.6). The LHPR was towed at 4.5 knots, with the cod-end winding on and revealing a fresh surface of filtering gauze every two minutes (about every 250 m horizontally). The net had a 333 μm mesh and was fitted with a reducing cone and a flow meter. The gauze in the cod-end had a 280 μm mesh. The LHPR was fitted with a depressor weight, drogue and tail plane to ensure a horizontal orientation. The rolled up filtering gauze was removed from the

cod-end after each tow, and was stored in a 5% formaldehyde solution. The samples were processed when returned to the UK three months after the cruise.

The gauzes were rolled out and each discrete sub-sample was identified and then separated. At all times care was taken to avoid the samples drying out and preserving fluid (Table 2.2.5.a) was added in moderation to keep the catch damp. The zooplankton were then washed off using distilled water supplied under pressure by a hand pump. Each sample was suspended in preserving fluid and transferred into a labelled storage vial. There was some minor damage and fragmentation of individuals during this process, and in some samples it was not always possible remove all of the zooplankton from the gauze. Both of these factors result in an underestimation of biovolume and abundance.

Table 2.2.5.a: The composition of preserving fluid used to store the zooplankton samples

Volume	Chemical
1500 ml	propan-1,2-diol
150 ml	formaldehyde (40% solution)
75 ml	anti bacterial agent 1 phenoxy propan-2-ol
Made up to 10 l	distilled water

2.2.5.3 Size fractionation of the zooplankton samples

The zooplankton samples from the LHPR were split into three size classes to allow a more precise comparison with the OPC data. The three size fractions were the plankton that were retained on a 4.5 mm meshed net, hereafter >4.5 mm size class; the plankton that passed through the 4.5 mm and were retained on a 1.5 mm net, hereafter >1.5 and <4.5 mm size class; and the plankton that passed through the 1.5mm and were retained on a 0.28 mm net, hereafter <1.5 mm size class. The true lower limit of the <1.5 mm class is actually 0.33 mm, which is the mesh size of the LHPR net. This procedure will select size classes in a different way to the sizes measured by the OPC, and will have biases introduced by selectivity for different shapes (see Appendix 5). Only three meshes were used because the total volume of zooplankton in each LHPR sub-sample was too small to allow the samples to be divided into more fractions.

Each sample was introduced at the top of a stack of the three meshes (ordered in decreasing mesh size) and washed through with low pressure fresh water. Each sample was washed for approximately two minutes until there was no obvious further movement of the plankton through the meshes. In general, the largest mesh did not retain many individuals but removed large species, which were too sparsely distributed to be sampled adequately, but greatly elevated the sample's total biovolume. The smallest mesh (0.28 mm) reliably retained even the smallest forms in the samples

because it was smaller that the LHPR's net (0.33 mm), and zooplankton are retained by larger nets once preserved (Vannucci, 1965).

2.2.5.4 Determining the abundance of the major taxonomic groups

The abundance of zooplankton in the major taxonomic groups were determined using a dissection stereo-microscope (6-50 X zoom). Identification to species level was not attempted because many of the individuals collected by the LHPR are compacted or fragmented when it is towed at 4.5 knots, and also as a result of laboratory processing of the samples. This analysis was performed on all three size classes, but only from the down profile of the LHPR at each station, because of the time consuming nature of this type of work. The taxonomic groups identified in these samples were medusae, siphonophores, polychaetes, copepods, euphausiids, decapods, amphipods, ostracods, bracyurans, heteropods, pteropods, other gastropods, cephalopods, ophiuroids, chaetognaths, doliolids, appendicularians and fish.

Animal fragments were only counted as a whole organism when the head was present. This problem frequently affected chaetognaths, and often led to this taxa being under represented in the >1.5 mm classes, and over represented in the <1.5 mm classes. Jelly plankton were also problematic because these organisms were easily broken up during sampling. Scyphozoan medusae were only counted where a whole animal was clearly present, and siphonophores were only counted when the hydrophyllia (or bracts) were present, (although the number of swimming bells (nectophores) was also noted). As a result in some samples there was a considerable amount of amorphous jelly fragments in the residue.

In the <1.5 mm size class the number of zooplankton was too high to count in the majority of the samples, so these samples were split prior to counting. Before splitting some of these samples contained up to 14000 copepods. A Folsom plankton splitter was used to divide these samples so that the number of individuals that were counted was between 300 and 1000.

2.2.5.5 Determining the zooplankton biovolume

Biovolume was determined as displacement volume of the zooplankton, by measuring increase in volume when the zooplankton were added to a liquid filled measuring cylinder. The interstitial fluid surrounding the zooplankton was removed by placing the sample onto absorbent laboratory paper before the volume was measured. The displacement volume of each discrete sample was recorded for the total zooplankton and for each size class. The volume of zooplankton was divided by the

volume of seawater filtered (measured by a flow meter) to determine the biovolume in ml m^{-3}. Biovolume can be a misleading measurement of zooplankton population densities because its relationship with dry weight is variable (Postel *et al.*, 2000). The dry weight of the samples was not determined because the samples were also needed for taxonomic identification.

Newell and Newell (1963), Tranter and Fraser (1968), Omori and Ikeda (1992) and Postel *et al.* (2000) were the main references for the techniques and for identification.

2.2.6 The measurement of bio-acoustic backscatter

The distribution of large meso, macrozooplankton and micronekton can be investigated with sonar, which detects the sound that reverberates from their bodies (e.g. Bary, 1966; Holliday, 1977; Smith *et al.*, 1992). During this study the acoustic backscatter from zooplankton was collected by both an acoustic Doppler current profiler (ADCP) and a multifrequency sonar, the Simrad EK500 biological echosounder (Bodholt *et al.*, 1998). Only the backscatter from the EK500 is presented in this thesis, because the three frequencies measured by the EK500 (38, 120 and 200 kHz) overlap the range of the single 150 kHz frequency of the ADCP (see Crisp *et al.*, 1998) and the ADCP data were not calibrated after the cruise.

The EK500 was deployed throughout the cruise in a separate tow-fish which allowed it to sample concurrently with the SeaSoar, the profiling CTD, the LHPR and the RMT nets. The acoustic backscatter measurements were averaged into bins of 1 m depth by 2 mins for the 120 and 200 kHz frequencies and into bins of 2m by 2 mins for the 38 kHz. Two minute bins represent approximately 0.5 km in distance during the SeaSoar survey, when the ship's speed was about 8 knots. The calibration of the EK500 data was divided into two stages: the first was the calibration the instrument's transducers using known targets, and the second was correcting the backscatter measurements for variations in the sound absorption coefficient of the water.

2.2.6.1 Transducer calibration of the EK500 at sea

The transducer frequency calibration was performed during the overnight break in the SeaSoar survey in the Strait of Hormuz (5^{th} March, Jday 64). Standard Simrad copper calibration spheres were suspended on mono-filament line below the EK500 and the backscatter from these known targets was used to calibrate the split beam transducers (38 and 120 kHz) using the Simrad "LOBE" program. The 200 kHz transducer is single beam and could not be calibrated in this way, consequently the

frequency distribution of the target strength of the sphere in the beam was used. Full details of these calibrations are given in the cruise report (Roe *et al.*, 1997).

2.2.6.2 Sound absorption calibration of the EK500

Backscatter data from the EK500 were corrected for variations in the *in situ* sound absorption coefficient to produce the mean volume backscattering strength, MVBS (Roe *et al.*, 1996). The sound absorption coefficient is determined by the temperature and salinity of the water column, which was measured by the SeaSoar in the Strait of Hormuz. MVBS standardises backscatter for variations in sound absorption, which allows data from different environmental conditions (such as either side of a front) to be quantitatively compared. Further details are given by Crisp *et al.* (1998).

2.2.6.3 Future calibration using scattering group algorithms

MVBS is not always directly related to zooplankton biomass (Kogeler *et al.*, 1987), but the relationship between MVBS and zooplankton biomass can be quantified by comparison with net catches, which enable portions of the MVBS to be attributed to certain groups (Stanton *et al.*, 1996; Wiebe *et al.*, 1996). Algorithms have been computed by these authors for anatomical groups with different scattering characteristics, and by combining these with net samples the sources and population densities of the individuals responsible for the MVBS can be determined. These algorithms have not been used in this study, but could be used in the future help to explain the distribution of MVBS recorded in the Strait of Hormuz.

2.2.7 The data collected by the profiling CTD

In addition to the SeaSoar survey, a profiling CTD frame was deployed 187 times in surveys in the Gulf of Oman, Strait of Hormuz and southern Arabian Gulf. The datasets from this instrument demonstrate the sources and the fates of the water in the Strait. In addition, the CTD allowed other environmental variables, such as dissolved oxygen concentration to be determined.

The instruments fitted to the CTD frame included:

i) General Oceanics Mk. IIIb CTD deep 01 (+ oxygen current)

ii) Chelsea Instruments Alphatracka transmissometer (25cm path length)

iii) Chelsea Instruments Mk. III Aquatracka fluorimeter (§ 2.2.3)

iv) FSI "Sure-fire" 24 position multi-sampler pylon and 12 Niskin bottles (10 l)

Three surveys were made with the profiling CTD during CD 104. The survey in the Gulf of Oman (CTDs 1 – 108) took place between 13/02/97 and 23/02/97; in this

region the CTD was deployed to 500m, or to the sea floor if shallower, except in 9 cases where the CTD made full depth profiles (down to a maximum of 3250m). This survey formed a grid between the coast and the middle of the Gulf of Oman, the boundary with the Iranian water. The survey in the Strait of Hormuz (CTDs 109 – 139) was completed either side of the SeaSoar survey, between 28/02/97 and 11/03/97, and consisted of four lines of stations running perpendicular from the Arabian coast to the centre of the Strait. As a result of the shallow nature of this region all CTDs sampled to the seabed. The survey in the southern Arabian Gulf (CTDs 140 – 187), was made between 11/03/97 and 14/03/97. This consisted of a grid of stations in shallow water (<50m) north of Abu Dhabi.

The sensors were calibrated using similar techniques to those used for the SeaSoar data, with salinity, chlorophyll and oxygen calibrations incorporating data from water samples drawn from the Niskin bottles fired at specific depths. For further details see Roe *et al.* (1997) and Smeed (1997). The oxygen concentration of the samples was measured using the Winkler whole bottle titration method, using amperometric end point detection (Culberson and Huang, 1987; and WOCE manual Culberson, 1991). These samples were then used to correct the profiles measured by the sensor.

CHAPTER 3

The calibration of OPC data into accurate estimates of zooplankton abundance and biovolume in the Strait of Hormuz

3.1 COMPARISON OF OPC ABUNDANCE WITH THE ABUNDANCE ENUMERATED FROM THE LHPR SAMPLES 58
3.2 CALIBRATION OF ZOOPLANKTON BIOVOLUME FROM ESD MEASUREMENTS OF THE OPC . 72
3.3 COMPARISON OF CALIBRATED OPC BIOVOLUME WITH LHPR BIOVOLUME . . 81
3.3 FURTHER EVALUATION OF CALIBRATED OPC BIOVOLUME 85

FIGURES

3.1.2.i Profiles of mean particle concentration derived from OPC data taken during up and down profiles of SeaSoar 64
3.1.3.i Zooplankton abundance from the OPC and the LHPR at stn 54006 . . 68
3.1.3.ii Change in water column between OPC and LHPR samples . . . 68
3.1.3.iii Zooplankton abundance from the OPC and the LHPR at stn 54007 . . 70
3.1.3.iv Change in water column between OPC and LHPR samples . . . 70
3.2.2.i Diagram representing the effect of orientation on the shadow size . . . 76
3.2.2.ii Graph showing the CSA of a spheroid determined by Eq 3.2.3 at various angles . 76
3.2.2.iii CF_{ran} to correct CSA measured by the OPC to the maximum CSA, for spheroids with different values of r 76
3.2.3.i CFvol for spherical model for spheroids with different values of r . . . 76
3.3.1.i Uncalibrated zooplankton biovolume from the OPC and LHPR at stn 54006 . 82
3.3.2.i Calibrated zooplankton biovolume from the OPC and LHPR at stn 54006 . . 82
3.4.2.i A comparison of the OPC biovolume calibration used in the Strait of Hormuz with the calibration factors used in other studies 88
3.4.3.i Comparison of phytoplankton and mesozooplankton carbon biomass in a section of the survey on the west side of the Strait of Hormuz 88

The aim of this chapter is to calibrate the optical plankton counter (OPC) data into accurate estimates of zooplankton biovolume and to check the consistency of the OPC abundance and calibrated biovolume against net samples collected by a Longhurst Hardy plankton recorder (LHPR). The OPC provides two types of information: an enumeration of the number of animals, and their size as an equivalent spherical diameter (ESD) from which abundance, biovolume and biomass can be estimated.

Plankton abundance can be enumerated relatively simply from OPC data, but an OPC cannot distinguish between zooplankton and other particles. Therefore the OPC abundance is compared against the number of animals in the LHPR net samples to investigate if non-zooplankton particles caused additional counts. Calculating zooplankton biovolume from OPC data is problematic, because the volume of each particle must be calculated from the particle size, recorded by the OPC as an ESD. If zooplankton were spherical, biovolume could be calculated directly from the manufacturers equation for ESD ($V=4/3\pi(ESD/2)^3$). However, zooplankton are not typically spherical and so a more sophisticated calibration is presented here which relates biovolume to the ESD measured by the OPC when zooplankton pass through the sampling beam. Therefore biovolume is calibrated using a theoretical spheroid[1] model, a shape which is more representative of the numerically dominant taxa, copepods, in this region (§2.2.2). The length to width ratio of the spheroid required for calibration is determined from measurements of the dimensions of the zooplankton in the LHPR samples. The resulting calibrated biovolume is compared with biovolume measured directly from LHPR samples.

This chapter is divided into four sections: §3.1 comparison of OPC counts with the animals enumerated from the LHPR samples, §3.2 calibration of OPC biovolume using a theoretical spheroid model, §3.3 comparison of calibrated OPC biovolume with biovolume measured directly from LHPR samples, §3.4 additional evaluation of OPC biovolume calibration with independent datasets. In §3.1 the sampling biases (spatial, temporal and size class) of the OPC and LHPR are quantified and corrected to produce comparable datasets. Further corrections are then applied to the OPC data which are required when the OPC is used on SeaSoar. The abundance measured by the OPC and LHPR is then compared, and any differences are discussed. In §3.2 the

[1] A spheroid is a geometric shape formed by the rotation of an ellipse around either its major or minor axis. A spheroid has a circular and an elliptical cross section.

theoretical calibration to convert ESD into volume is presented, which accounts for the shape, dimensions, orientation of the zooplankton in the Strait. In §3.3 the zooplankton biovolume determined from the OPC both before and after calibration is compared with the biovolume measured in the LHPR samples, and differences are discussed. In §3.4 the calibration of the OPC biovolume is further evaluated against independent datasets. First, the OPC abundance and biovolume are compared with net samples from previous studies in the Strait of Hormuz. Second, the OPC biovolume calibration is compared with empirical calibration factors derived in previous OPC studies. Third, OPC biovolume is converted into mesozooplankton biomass and compared with phytoplankton biomass measured concurrently.

3.1 Comparison of OPC abundance with the abundance enumerated from the LHPR samples

Calculating particle abundance from OPC data is relatively straight forward, and is accomplished by dividing the number of counts made by the volume of water sampled. However, an OPC cannot distinguish between zooplankton and other similarly sized particles. Consequently, particles such as aggregated phytoplankton, faecal pellets, marine snow, other detritus and even abiotic particles such as sediment and air bubbles may be counted as zooplankton. Zhang *et al.* (2000) have demonstrated that OPC data can be influenced by the high detrital concentrations in estuaries, but false counts are thought to be less important in oceanic waters, away from terrigenous inputs. In this section the zooplankton abundance measured by the OPC is compared with the zooplankton abundance enumerated from the LHPR samples (which contained only zooplankton). If the OPC is accurately measuring zooplankton abundance then an approximate 1:1 relationship between the instruments is expected.

3.1.1 Correction of the sampling biases of the OPC and LHPR

An LHPR was chosen to collect samples for comparison with the OPC data because it is capable of a higher spatial resolution than most nets (§2.2.5). This allows many discrete samples to be collected by the LHPR in a single deployment. These can then be compared with OPC data averaged over the same depth range. Physical environmental measurements were collected concurrently with the data from both instruments, enabling the comparison to be made with reference to the water column structure. Before the data from the instruments can be compared the sampling biases

associated with each must be quantified. For a valid comparison it is essential that the biases of each instrument are standardised (Skjoldal *et al.*, 2000).

The first, and possibly the largest problem in comparing the OPC and LHPR data from this cruise is that they were not collected concurrently. This occurred because the LHPR and the SeaSoar (fitted with the OPC) can not be towed synchronously, and there was no provision made in this survey to mount the OPC on the LHPR (as Wieland *et al.*, 1997). The SeaSoar was deployed between Jdays 61 and 66 and the LHPR was fished on Jdays 67 and 70. In addition, the LHPR was not fished exactly over the SeaSoar track (**Fig 2.2.2.i**). It is not possible to correct for this error other than to selected the geographically closest OPC data for comparison with the LHPR. Although the spatially detailed data collected by the OPC showed consistent features in areas of the Strait (**Fig 4.1.1.i**) there was also well defined patchiness in the zooplankton distributions on scale of 5 to 50 km. In addition, Roman *et al.* (2000) estimated population doubling rates for mesozooplankton between 4 and 25 days in the Arabian Sea, which become significant over these gaps in the sampling. Therefore the spatial and temporal differences between the OPC and LHPR data do not permit a robust empirical fitting of the OPC data to the net data.

These two instruments measured the distribution of zooplankton at different spatial resolutions, and are standardised to the coarser resolution of the LHPR. Therefore, both datasets are averaged into 4 m depth bins over 15 km horizontally, which is equal to the length of the LHPR tow.

The second problem is the different size range of plankton sampled by each instrument. It is essential to compare the same size range of particles, as different size classes of organisms can show distinct and even inverse distribution patterns (e.g. Folt *et al.*, 1993). Moreover smaller organisms are usually considerably more numerous than larger ones (e.g. Sheldon *et al.*, 1972). Although the size ranges overlap, an OPC samples smaller zooplankton than a LHPR. Therefore the OPC determines the upper limit and the LHPR the lower limit of the overlapping size range for comparison.

It has already been established (§1.4.1.1) that nets do not retain particles slightly larger than their pore size, and even large particles can pass though the silk by active escapement (Saville, 1958; Vannucci, 1965). Barnes and Tranter (1965) determined that an Indian Ocean Standard net, which has the same mesh net as the LHPR used here (333 μm), reliably retained only copepods >1 mm. The LHPR was towed at a high speed (2 ms^{-1}), which reduces net avoidance by larger more motile species

(Omori *et al.*, 1965; Bernard *et al.*, 1973), but at the same time also increases the pressure gradient across the net and forces more small zooplankton through the mesh (Vannucci, 1965). Nichols and Thompson (1991) examined the net retention of a LHPR, deployed at similar towing speeds to this study, and found that 95% of copepods are retained by a mesh size about 75% of their width. For a 333 μm net this is a copepod length of 1.33 mm (assuming a length to width ratio of 3:1). The smallest copepod measured in the LHPR samples was 0.95 mm after preservation (Appendix 3), which is consistent with the recommendation of Barnes and Tranter (1965).

An OPC can detect and size particles between 0.25 and 14 mm (Herman, 1992). When an OPC is configured for towing (§2.2.4) the volume of water that passes through the instrument is greatly reduced. Large zooplankton are less abundant than smaller species and are not encountered regularly enough for their distributions to be robustly determined. This imposes a maximum reliable size limit of about 4 to 6 mm (Herman *et al.*, 1993; Mustard, 1997; Rabe *et al.*, 1998; Pollard *et al.*, submitted) depending on the in situ abundances of zooplankton of this size.

Therefore, for the comparison between the instruments only data between 1 and 4.5 mm have been selected. Large particles were removed from the LHPR data by passing the samples through a 4.5 mm mesh during the size fractionation (§2.2.4). As a result zooplankton between 0.3 and 1 mm are not included in the comparison, although data from this size range are used in this thesis. It has been assumed that errors in the OPC data were consistent throughout the whole range it samples, and any calibrations have been extrapolated for the entire range.

There are several additional errors associated with each method that cannot be corrected, but are worth noting. Any net sample is biased because different species are retained by the net to differing degrees. For example, a species with appendages perpendicular to its body will be retained by a net to a greater extent than a streamlined species of the same size (Saville, 1958). Gelatinous species are usually fragmented by nets, and are often lost through the mesh. Certain groups, such as chaetognaths have been reported to adhere strongly to the LHPR net and the intake tunnel and therefore do not always reach the sampling gauze (Haury *et al.*, 1976).

The OPC has similar biases resulting from different species having different relationships between their true size and the size measured by the OPC. As a result a particle may be counted but incorrectly sized. Differences in the measured CSA of a particle can result from its orientation in the sampling beam, the translucency of the

organism and the number and extent of its appendages. Because particles are assumed to be opaque, translucency will lead to their size being underestimated.

Summary of standardisation of data

The closest (spatial) OPC data to the LHPR stations were selected for the comparison between the datasets. This was believed to be the most reliable choice because the zooplankton distributions had remained relatively constant during the SeaSoar survey. A standardised size range of particles was selected for the comparison. This was where there was an overlap between the instruments: between 1 and 4.5 mm. The data from both instruments was also standardised in terms of spatial resolution and was averaged into 15 km by 4 m bins.

3.1.2 Further corrections required when using an OPC on SeaSoar

During this survey it was not possible to directly measure either the volume passing through the OPC's sampling tunnel or the distance travelled by the SeaSoar. It was only possible to measure the distance travelled by the ship (§2.2.2). As a result, the volume of water passing through the OPC was estimated from the distance travelled by the ship and the mouth area of the sampling tunnel of the OPC.

It is important to accurately estimate the volume of water that passes through the tunnel of an OPC to determine the quantity of zooplankton per m^{-3} of water. In this section the errors that arise in estimating the volume of water sampled by an OPC while undulating on SeaSoar are quantified and corrected.

3.1.2.1 Correction for the distance travelled by SeaSoar

A SeaSoar will pass through more water than a ship, because of the additional distance it travels when it undulates. As a consequence, more water (and particles) than is assumed in the calculation of volume sampled, will pass through the sampling tunnel of the OPC, and the density of particles will be overestimated.

The survey in the Strait of Hormuz was shallow (<100 m), and as a consequence the undulations made by SeaSoar were densely spaced. A single profile of the SeaSoar was completed in about 0.3 km (§2.2.2). The additional distance travelled by the SeaSoar in comparison to the ship can be estimated using Pythagoras' theorem, by assuming that SeaSoar followed an angular sawtooth profile making 10 profiles in every 3 km, to an average depth of 80 m.

Therefore the distance travelled by the SeaSoar in one undulation can be simply estimated from the following equation:

$$(\text{SeaSoar distance})^2 = (\text{profiling depth})^2 + (\text{ship distance})^2 \quad . \quad \text{Eq 3.1.1}$$

$$(\text{SeaSoar distance km})^2 = (0.08\ \text{km})^2 + (0.3\ \text{km})^2$$

$$\text{SeaSoar distance km} = \mathbf{0.31\ km}$$

When the ship travels 3 km the SeaSoar will travel 3.1 km and make 10 profiles. This is only an increase in the volume sampled by the OPC of 3.3%, and therefore an overestimate of zooplankton abundance by 3.3%. The smallest overestimate will occur where there are the smallest number of profiles per km and the depth is shallowest. Taking the lower limit in the data of 8 profiles in 3 km and a profiling depth of 70 m, the overestimate is 2%. The largest overestimate occurs when frequency of undulations is highest and their amplitude is greatest. Taking the upper limit in the data of 12 profiles in 3 km and a profiling depth of 90 m; the largest overestimate is less than 6%.

However, in reality the highest number of profiles per km will be recorded when the SeaSoar dives shallowest. The true value of the correction needed is probably close to the original estimate of 3.3%. The volume of water sampled by the OPC in this survey has been increased by this factor in all the OPC data subsequently presented in this thesis. This error is small and but can be easily corrected.

3.1.2.2 Bias resulting from the changing speed of SeaSoar during towing

The speed of the SeaSoar and therefore the amount of water sampled by the OPC varies independently of ship's speed. SeaSoar is towed on a fixed length cable that is short in comparison to the depth of the undulations. As SeaSoar dives it moves through an arc described by a radius equal to the cable length. At the bottom of the arc the SeaSoar is considerably closer in the horizontal plane to the ship. Therefore, the SeaSoar travels further than the ship as it dives and less distance than the ship as it ascents. This unaccounted horizontal distance is large because SeaSoar is able to pull the cable to a considerable angle from the horizontal: in normal open ocean deployments this angle exceeds 45°. In addition, the effect is exaggerated because the SeaSoar is typically undulated as frequently as possible to increase the spatial density of measurements. As a result this additional horizontal movement of SeaSoar occurs during a relatively short distance travelled by the ship.

The magnitude of the additional distance travelled by the SeaSoar is estimated from the depth of the SeaSoar assuming that the SeaSoar cable remains straight. These calculations are made for the survey in the Strait and also for an open ocean survey in the Mediterranean (which is a more typical SeaSoar survey).

In the Strait of Hormuz, SeaSoar was towed on an undulating path from the surface to a maximum depth of 90 m, at a ship speed of 4 m s^{-1} on 200 m of un-fared cable. An average up profile took 40 seconds (ship distance of 160 m) and a down profile took 43.25 seconds (ship distance of 173 m). Assuming that the cable was straight between the SeaSoar and the ship (and was not bowed out by its own drag) the SeaSoar will be 20 m closer to the ship, in the horizontal plane, at the bottom of the profile than at the surface. As a consequence the SeaSoar will travel 11.5% further than the ship distance corrected for the undulations on the down profile and 13% less than the ship distance corrected for the undulations on the up profile.

In the open ocean example SeaSoar was towed at a ship speed of 4 m s^{-1} on 500 m of fared cable and undulated from the surface to 360 m. An up profile of SeaSoar took 3 minutes (ship distance of 700 m) and a down profile took 4 minutes (ship distance of 1000 m). The SeaSoar will be 153 m closer to the ship, in the horizontal plane, at the bottom of the undulation (360 m) than at the surface. As a result, on the down profile the SeaSoar will travel an additional 153 m, an increase of 15%. Conversely during the up profile the SeaSoar will travel 153 m less than the ship distance corrected for the undulations, which is a decrease of 20%.

If the volume of water sampled by the OPC is determined from the ship distance corrected for the undulations then the zooplankton abundance is overestimated in the Strait by 11.5% on the down profile and underestimated by 13% on the up profile. In the open ocean example these are larger, with an overestimate of 15% on the down profile and underestimate of 20% on the up profile. This results in a 35% difference in estimates of particle concentration between the up and down profiles.

The influence of the changing speed of the SeaSoar on the counts per m^3 can be seen in **Fig 3.1.2.i**. Two graphs are presented, the first (**a**) shows data from this study (CD 104) and the second (**b**) shows data from the full depth SeaSoar survey in the Mediterranean (cruise report: Allen and Guymer *et al.*, 1997). These graphs show the mean up and down profiles of particle concentration measured by the OPC in the Strait of Hormuz (top) and the Mediterranean (bottom). Each profile is an average of 250 profiles and the error bars show the 99% confidence interval of the means. These graphs show a greater difference between the up and down profiles than predicted, of up to 40% in the Strait, and 70% in the Mediterranean, compared with predictions of 25% in the Strait and 35% in the Mediterranean.

Figure 3.1.2.i Profiles of mean particle concentration derived from OPC data from up and down profiles of SeaSoar in the Strait of Hormuz (top) and in the Mediterranean (bottom). Each profile is an average of 250 profiles, error bars show 99% confidence interval of the means. Note different x and y scales.

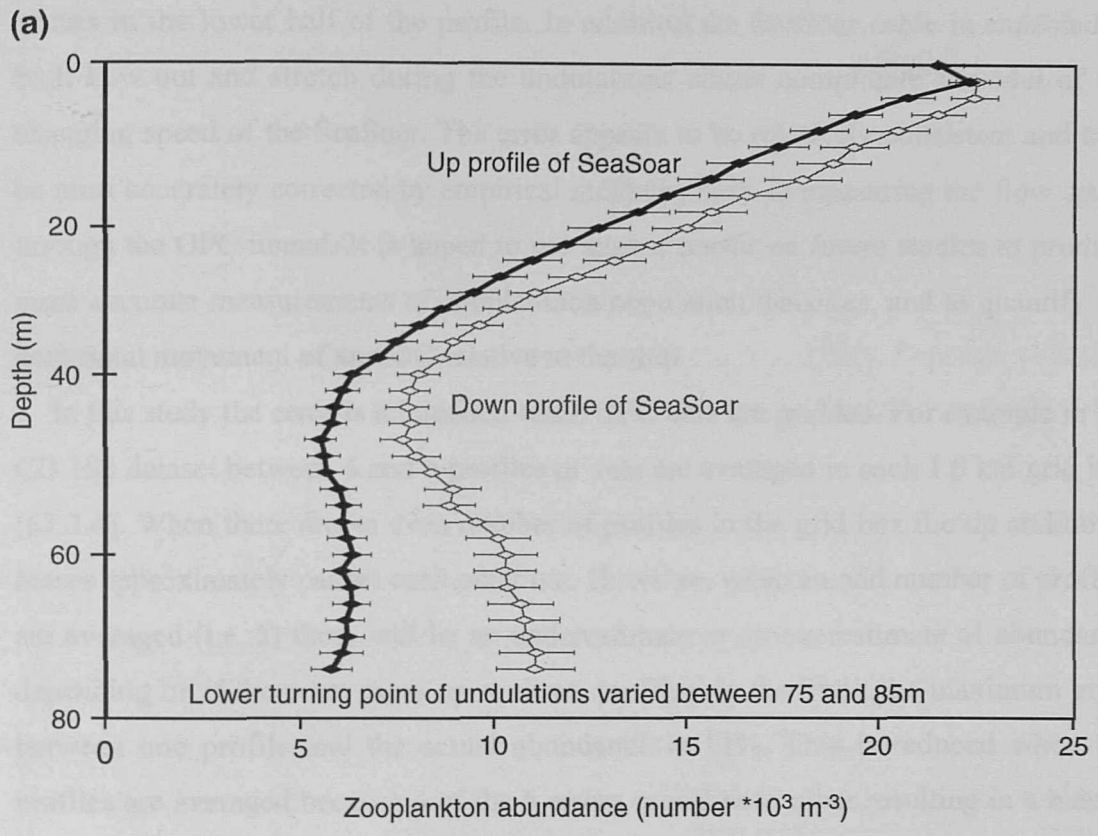

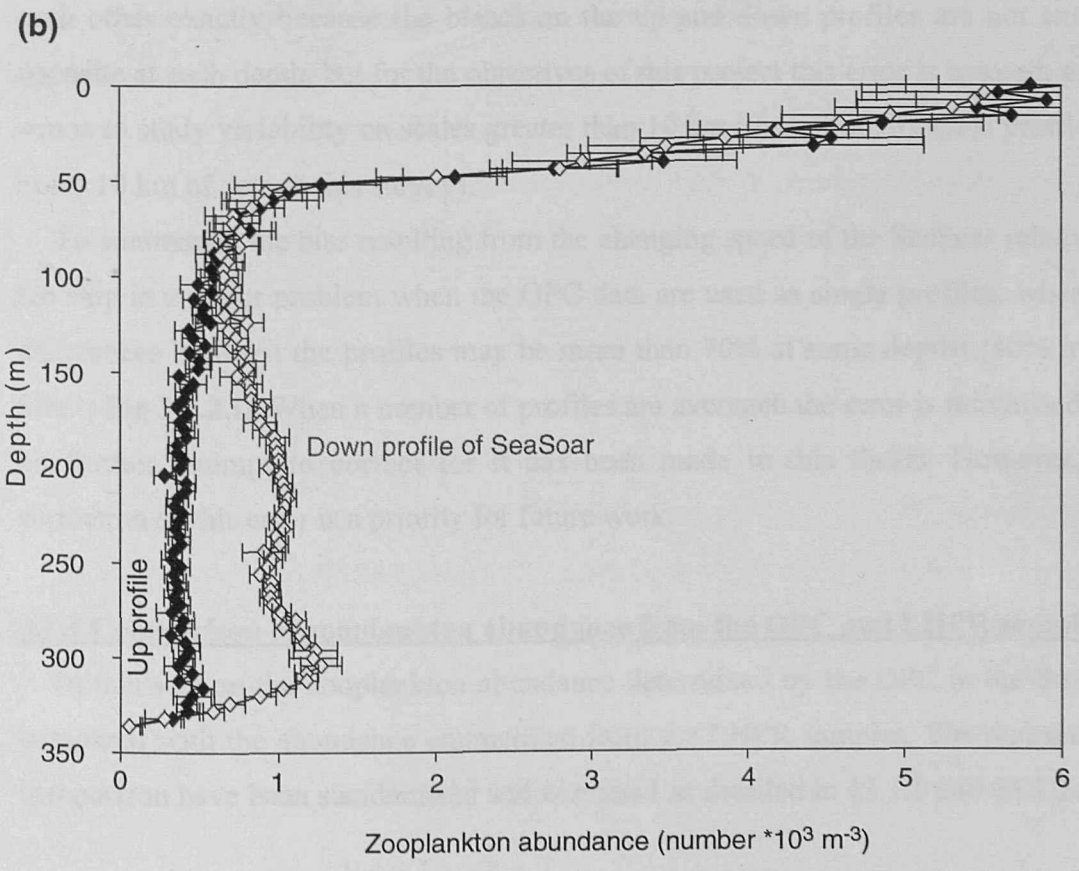

3.1.2.3 Practical considerations of this bias

The error imposed on the OPC data is larger than was predicted from the straight cable calculations because the majority of the horizontal movement of the SeaSoar occurs in the lower half of the profile. In addition the SeaSoar cable is expected to both bow out and stretch during the undulations which complicate a model of the changing speed of the SeaSoar. The error appears to be relatively consistent and may be most accurately corrected by empirical methods, such as measuring the flow speed through the OPC tunnel. It is hoped to use such a sensor on future studies to produce more accurate measurements of zooplankton population densities, and to quantify the horizontal movement of an OPC relative to the ship

In this study the error is minimised when OPC data are gridded. For example in the CD 104 dataset between 4 and 6 profiles of data are averaged in each 1.5 km grid box (§2.2.4). When there are an even number of profiles in the grid box the up and down biases approximately cancel each other out. However, when an odd number of profiles are averaged (i.e. 5) there will be an underestimate or an overestimate of abundance depending on if there are more up or down profiles. In the Strait the maximum error between one profile and the actual abundance is 13%. This is reduced when the profiles are averaged because 4 of the 5 errors cancel each other resulting in a bias of only 2.5%. In fact the situation is more complicated because the errors will not cancel each other exactly because the biases on the up and down profiles are not exactly opposite at each depth, but for the objectives of this project this error is ignored, as the aim is to study variability on scales greater than 10 km (there were 33 OPC profiles in every 10 km of data in this survey).

To summarise the bias resulting from the changing speed of the SeaSoar relative to the ship is a major problem when the OPC data are used as single profiles, when the differences between the profiles may be more than 70% at some depths (40% in the Strait; **Fig 3.1.2.i**). When a number of profiles are averaged the error is minimised and no further attempt to correct for it has been made in this thesis. However, the correction of this error is a priority for future work.

3.1.3 Comparison of zooplankton abundance from the OPC and LHPR samples

In this section the zooplankton abundance determined by the OPC in the Strait is compared with the abundance enumerated from the LHPR samples. The datasets for comparison have been standardised and corrected as detailed in §3.1.1 and §3.1.2. The

OPC data is compared with the vertical profiles of abundance determined by the LHPR at both station 54006 and 54007 in the Strait of Hormuz (§2.2.5).

The OPC has been shown to underestimate net measurements of abundance by Sprules *et al.* (1998) and overestimate by Huntley *et al.* (1995) in previous studies. Grant *et al.* (2000) attribute these differences to a lack of concurrent sampling. By taking LHPR samples concurrently with an OPC, Grant *et al.* (2000) observed "no consistent overestimate or underestimate by the OPC relative to the net". In this study the LHPR and OPC datasets were not concurrent (§3.1.1) so therefore some spread of values about a ratio of 1:1 is expected.

3.1.3.1 Comparison of OPC zooplankton abundance with LHPR Station 54006

The LHPR was towed for 15 km on the east side of the Strait at stn 54006 (**Fig 2.2.2.i**). This biological station was in the inflowing water from the Gulf of Oman, and bisected the SE end of legs 2 and 3 of the SeaSoar survey. Both the LHPR and OPC sampled in this area during daylight, but the LHPR was fished 4 days later.

The OPC data selected for comparison with the LHPR were 3945-3960 km on leg 2 and 3970-3985 km on leg 3 (**Fig 4.1.1.i**). The data between 3961 and 3969 km were not used as these were collected during the turn between legs and the SeaSoar was not flown to full depth. Both the SeaSoar and the LHPR recorded the surface temperature above 23.2°C and the surface salinity above 36.6 in this area, and both platforms measured the range of temperature (throughout the water column) between 22.2 and 23.4°C and salinity between 36.5 and 36.7.

Fig 3.1.3.ia shows the profiles of zooplankton abundance determined by the OPC and the LHPR at stn 54006. The OPC abundance profile represents data averaged from approximately 100 profiles, with the error bars showing the standard deviation of the mean, and the single LHPR profile represents data from the down cast. Both methods measured decreasing abundance with depth. The LHPR measured the highest abundance in all the samples shallower than the thermocline, which was at 40 m (**Fig 3.1.3.iia**). Below 40 m the abundance steadily decreased until 80 m, where the minimum abundances were measured. The OPC also measured the highest abundance at the surface, but this decreased rapidly until 25 m, which was within the thermocline. Below 30 m the abundance continued to decrease gradually to the minimum, measured between 60 m and 80 m.

Fig 3.1.3.ib re-plots the same data as 3.1.3.ia, comparing the OPC measured zooplankton abundance in each depth bin with the LHPR data. In general, the data fall

close to a 1:1 line, and all points were within a factor of two. The OPC abundance was within the same range as that measured by the LHPR, except for the highest abundances which were in the upper 18 m where there were no LHPR samples. The OPC appears to underestimate zooplankton abundance relative to the net in the middle of the water column, however the data are generally with the one standard deviation of the LHPR. This could be attributed to inefficient filtering by the OPC during dives and ascents of the SeaSoar, but this is not consistent with the data from stn 54007 where the OPC overestimates abundance in the middle of the profile. There were not LHPR data from the upper 18 m, where the OPC abundance was highest, but these data would be expected to be above the 1:1 line, correcting the misconception that the OPC underestimated abundance at high zooplankton densities.

The difference between the abundance measurements of each instrument in the upper 40 m can be explained by the change in the water column structure between the deployment of the OPC and LHPR. The LHPR data shows that the thermocline was deeper, and the water above it was cooler than during the SeaSoar survey (**Fig 3.1.3.iia**). This may be a result of advection or the internal waves that were recorded in this part of the Strait (§5.3). Another major problem was a strong Shamal wind blew during the four day gap in sampling (Roe *et al.*, 1997). The data presented in Moat *et al.* (1997) showed that the wind speed increased from 0 to 10 knots when the OPC data were collected to 30 to 40 knots before the LHPR data were collected. The Shamal wind was correlated with a slight cooling of the sea surface temperature. This evidence provides a mechanism to explain the depressed thermocline and deeper extending, but lower surface zooplankton abundance maximum in the LHPR data. The redistribution of zooplankton by wind induced shear has been observed by Haury *et al.* (1990), who showed the wind induced mixing depressing the thermocline and dispersing a near surface zooplankton population over a wider depth range.

Fig 3.1.3.iib compares the abundance measured by the OPC and LHPR in each 0.05°C temperature bin. This plot should correct for some of the bias that results from the redistribution of zooplankton by wind driven mixing. The data in this plot are closer to the 1:1 line, but are still not an exact fit. The data indicate that the OPC overestimated abundance at low levels, and underestimated abundance at higher levels. The data in **Fig 3.1.3.ia** are not consistent with this, as the maximum abundance recorded by the OPC was higher than the LHPR. The OPC data below 80 m do appear to show the OPC overestimating abundance at low abundances.

Figure 3.1.3.i Zooplankton abundance from the OPC and the LHPR at stn 54006

a) Vertical profiles of zooplankton abundance from LHPR stn 54006 and the OPC data from legs 2 & 3, averaged into 4 m depth bins
Error bars show +/- standard deviation of OPC

b) Plot comparing the zooplankton abundance measured at each depth by the OPC and LHPR (same data as Fig 3.2.2.ia)

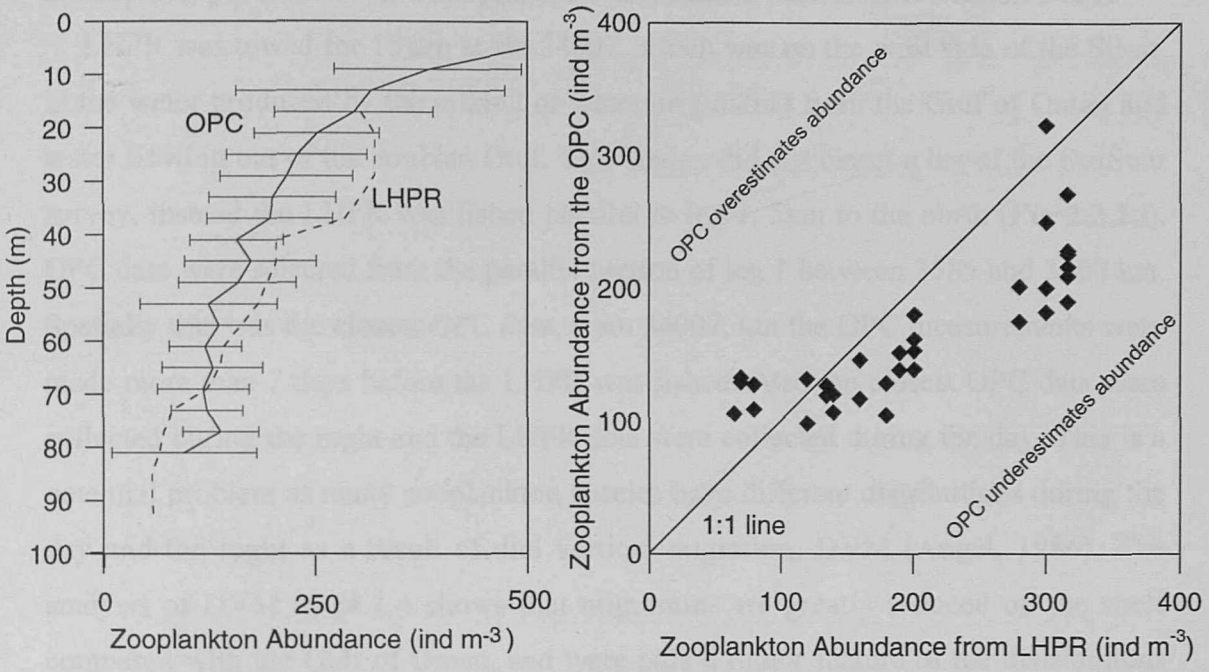

Figure 3.1.3.ii Change in water column structure between OPC and LHPR samples

a) Vertical profiles of temperaure from LHPR stn 54006 and the SeaSoar data from legs 2 & 3

b) Plot comparing the zooplankton abundance measured by the OPC and LHPR in each 0.05°C temperature bin

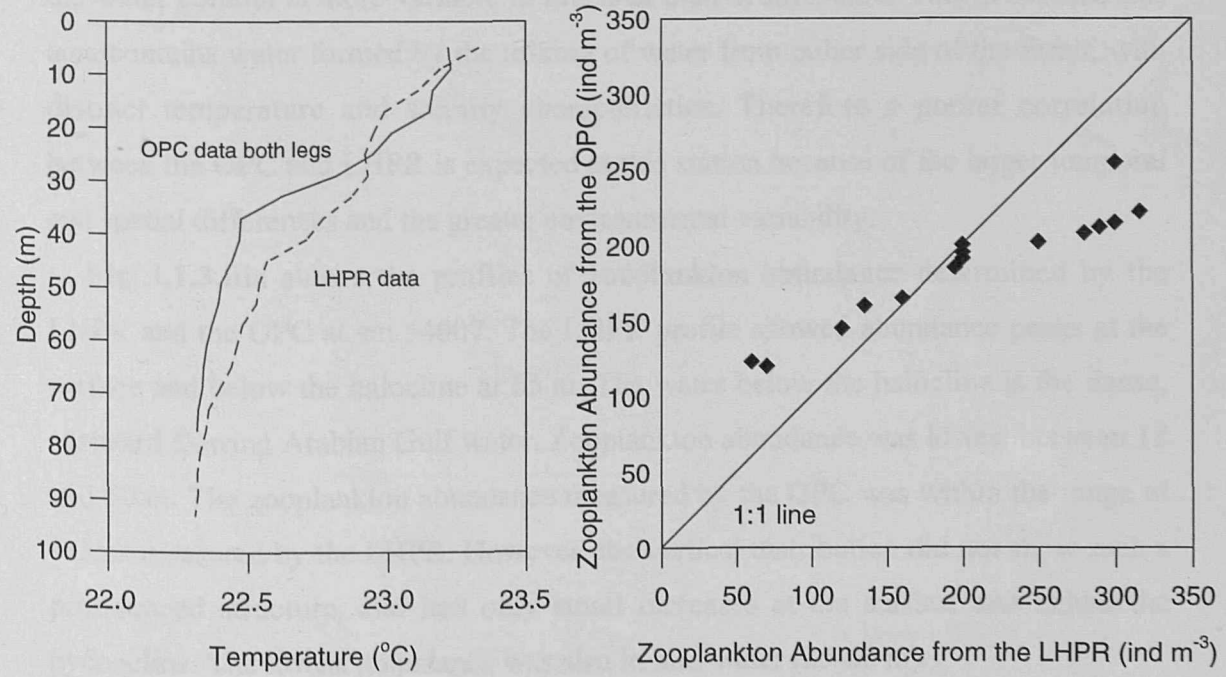

In summary, the OPC produced measurements of zooplankton abundance that were in the same range as the LHPR at stn 54006 when the temporal gap (and associated physical changes) between the collection of each dataset is considered.

3.1.3.2 Comparison of OPC zooplankton abundance with LHPR Station 54007

LHPR was towed for 15 km at stn 54007, which was on the west side of the Strait, in the water produced by the mixing of water originating from the Gulf of Oman and water flowing out of the Arabian Gulf. This station did not bisect a leg of the SeaSoar survey, instead the LHPR was fished parallel to leg 1, 5km to the north (**Fig 2.2.2.i**). OPC data were selected from the parallel section of leg 1 between 3585 and 3600 km. Spatially this was the closest OPC data to stn 54007, but the OPC measurements were made more than 7 days before the LHPR was fished. Also the closest OPC data were collected during the night and the LHPR data were collected during the day. This is a potential problem as many zooplankton species have different distributions during the day and the night as a result of diel vertical migration, DVM (Angel, 1986). The analysis of DVM in §4.1.4 shows that migrations are greatly reduced on the shelf compared with the Gulf of Oman, and were only a minor feature of the distributions measured by the OPC. The abundance measurements of the OPC and LHPR are compared assuming there were no significant diel differences in distributions.

At stn 54007 the dominant physical feature was a sharp pycnocline between 50 and 70 m, where salinity increased from less than 38 to more than 40 (**Fig 3.1.3.iv**). This was observed in both the LHPR and SeaSoar data. However, the physical structure of the water column is more variable in this area than at stn 54006. This is because this area contains water formed by the mixing of water from either side of the Strait, with distinct temperature and salinity characteristics. Therefore a poorer correlation between the OPC and LHPR is expected at this station because of the larger temporal and spatial differences and the greater environmental variability.

Fig 3.1.3.iiia shows the profiles of zooplankton abundance determined by the LHPR and the OPC at stn 54007. The LHPR profile showed abundance peaks at the surface and below the halocline at 65 m. The water below the halocline is the dense, eastward flowing Arabian Gulf water. Zooplankton abundance was lowest between 18 and 60 m. The zooplankton abundance measured by the OPC was within the range of values measured by the LHPR. However, the vertical distribution did not show such a pronounced structure, and had only small increases at the surface and below the pycnocline. The lowest abundance was also in mid-water (25-60 m).

Figure 3.1.3.iii Zooplankton abundance from the OPC and the LHPR at stn 54007

a) Vertical profiles of zooplankton abundance from LHPR stn 54007 and OPC data from leg 1, averaged into 4 m depth bins
The error bars show +/- std. dev of mean OPC

b) Plot comparing the zooplankton abundance measurements at each depth from the LHPR and OPC (same data as Fig 3.2.3.ia

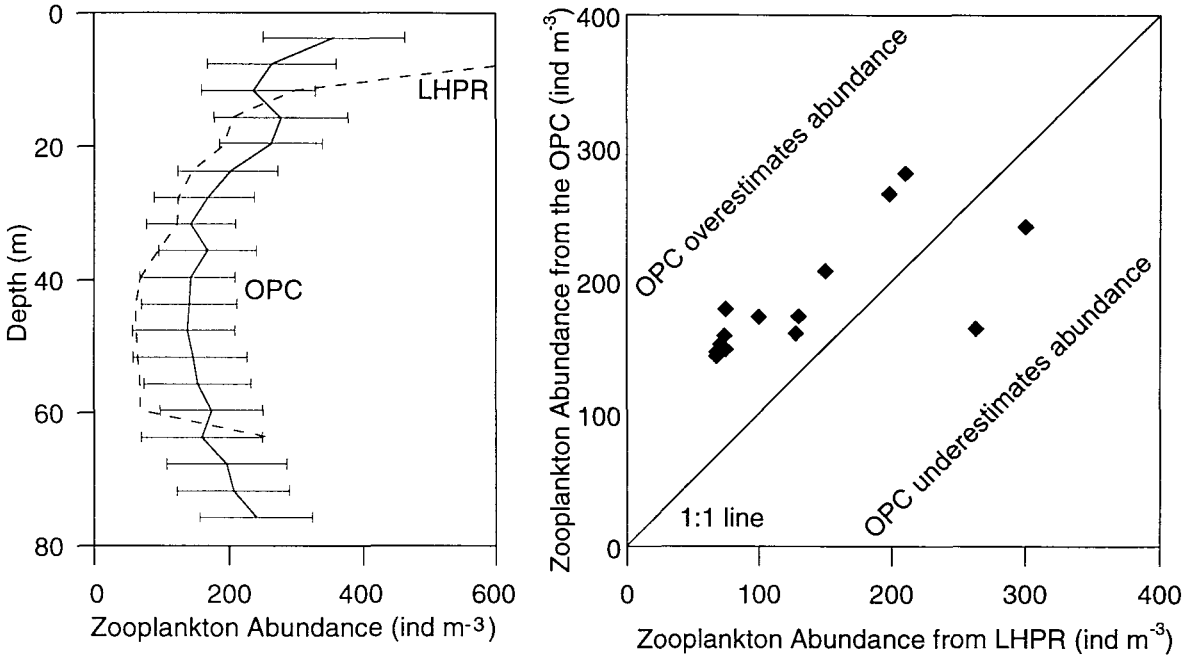

Figure 3.1.3.iv Change in the water column structure between OPC and LHPR samples at stn 54007

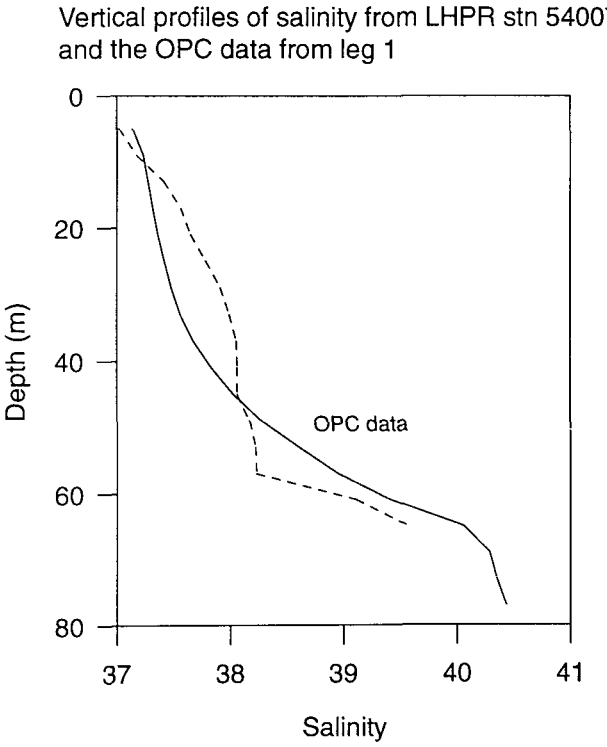

These data are re-plotted in **Fig 3.1.3.iiib** which compares the zooplankton abundance measured by the OPC with that from the LHPR in each depth bin. At stn 54007 there was not as close a fit to the 1:1 line as there was at stn 54006, although the data from the OPC were within a factor of two of the LHPR. These data suggest that the OPC underestimates high abundances, and overestimates at low abundances. However, the expected changes in the environment during 7 days are large, and the data here were insufficient to comment further on the OPC's performance.

Despite the differences in the vertical distribution of zooplankton, the OPC and LHPR produce approximately equivalent total integrated abundances over the top 65 m. The LHPR measured 13000 zooplankton m^{-2} and the OPC measured 15000 m^{-2}., and the OPC data are generally within 1 standard deviation of the LHPR. Although there are differences, the observations suggests that the two methods produced comparable measurements of abundance.

3.1.3.3 Evaluation of the zooplankton abundance measurements from the OPC

The temporal and spatial differences between the collection of the LHPR and OPC data significantly influences their comparison. It is likely that the vertical distribution of zooplankton at each station was different when each instrument was deployed. However, at both stations the OPC enumerated abundance in the same order as were present in the LHPR samples. The evidence indicates that the OPC reliably enumerated zooplankton abundance, and the influence of non-zooplankton particles was small. Zhang *et al.* (2000) have demonstrated that OPC data can be influenced by the high detrital concentrations in estuaries, but non-zooplankton counts are thought not to be problematic in oceanic waters, away from terrigenous inputs. In addition, Herman (pers. comm., 1998) reported that there was no statistical difference in particle counts from an OPC when a mesh, designed to break up marine snow, was fitted over the intake.

The differences between the OPC and the LHPR have been largely related to changes in the water column structure, and would be expected to be more closely correlated with the LHPR samples if concurrent samples were taken. These observations make a strong case for concurrent comparative datasets in future studies to evaluate the performance of the OPC.

The OPC abundance measurements have been accepted as being realistic values of zooplankton density in the Strait, suitable for studying the relationship between zooplankton and mesoscale environment in the Strait.

3.2 Calibration of Zooplankton Biovolume from ESD measurements made by the OPC

This section presents a theoretical calibration equation for determining zooplankton biovolume from the particle size measured by the OPC. The calibration is determined from theoretical considerations of how an OPC measures the size of a zooplankter and how particle volume is computed from this. The size of a zooplankter measured by an OPC is influenced by its shape, orientation, appendages and translucency (Herman, 1992; Beaulieu *et al.*, 1999).

The calibrated OPC biovolume is compared with the biovolume measured by the LHPR at stn 54006 in §3.3. In §3.4 the calibration is evaluated against net samples from previous studies in the Strait, OPC calibration factors derived by other authors and phytoplankton biomass computed from concurrent fluorimetric measurements.

Zooplankton abundance is a useful measurement, but it is predominantly determined by the more numerous, smaller sized species (Sheldon *et al.*, 1972). Measurements of biovolume and biomass allow more meaningful comparisons to be made between size classes and trophic levels when studying an ecosystem. Biovolume has been chosen as the product of this calibration because it can be determined more directly (with fewer assumptions) from the OPC data. Biomass in weight requires additional conversion factors (e.g. Wiebe, 1988; Postel, 1990). In addition, biomass can only be determined from the LHPR samples by incineration, which prohibits subsequent taxonomic sorting. Therefore, biovolume is more suitable for comparisons between the datasets in §3.3.

An OPC does not measure zooplankton biovolume directly so this must be computed from the sizes of particles measured by the instrument. Several authors have produced empirical calibrations of biovolume or biomass from OPC data (see §3.2.1), but these methodologies are not followed exactly in this study. This is because the LHPR data were not considered to be reliable enough for an empirical calibration. As discussed in §3.1, the spatial, temporal and size differences between the datasets reduce the validity of such a calibration. Grant *et al.* (2000) suggest that these factors can explain the discrepancies in comparisons between OPC and net data in many studies. Second, a theoretical framework needs to be developed for calibrating the OPC in this and future studies. In this study, empirical data is only used to tune the calibration, for determining the dominant taxa and providing dimensions of

zooplankton. These factors are expected to be less changeable than biovolume during the gap between the OPC and LHPR data being collected.

3.2.1 Previous calibrations of biovolume and biomass from the OPC

The manufacturer's calibration equation (Eq 3.2.1) has been widely accepted and used to calculate the ESD size of zooplankton passing through the OPC (e.g. Huntley *et al.*, 1995; Heath, 1995; Wieland *et al.*, 1997; Sprules *et al.*, 1998; Beaulieu *et al.*, 1999). Grant *et al.* (2000) provide an exception, as they re-calibrated the OPC output directly into cross sectional area, CSA, and then presented zooplankton abundance in CSA size classes.

As discussed above, zooplankton biovolume is a more useful measurement than abundance, and therefore biovolume has been estimated by most OPC users. Biovolume can be determined most easily from the ESD using a spherical model where the volume is $4/3\pi(ESD/2)^3$ (e.g. Heath, 1995; Gallienne, *et al.*, 1995; Beaulieu *et al.*, 1999; Zhang *et al.*, 2000). Several authors have shown that this spherical model overestimates zooplankton biovolume (Sprules *et al.*, 1998; Beaulieu *et al.*, 1999; Pollard *et al.*, submitted). Mesozooplankton are not typically spherical, and a spheroid is a more realistic representation of copepods (Herman, 1992).

Stockwell and Sprules (1995) and Sprules *et al.* (1998) calculated the volume of the particle as the volume of a spheroid, where the major axis was equal to the ESD and the minor axis was the ESD divided by 1.6 and 1.33, respectively. The dimensions of their spheroids were derived as those that produced the best fit between the total wet weight calculated from the OPC data and that measured in their nets. Sprules *et al.* (1998) state that their 1998 calibration was an improvement on their 1995 study, and show a relationship that is statistically indistinguishable from 1:1 with net samples, although the spread of data around the regression line is quite broad.

Huntley *et al.* (1995) used a different method: the ESD was converted into particle length using a width to length ratio from unpublished data from the survey area and was then converted to carbon biomass (after Rodriguez and Mullin, 1986). Potential problems with this technique occur in converting ESD into length, and also in the length into weight, as both relationships are variable in natural communities. This procedure produces much higher biomass values than other calibrations which have been adopted in more recent papers by other authors.

All the published surveys report that it is possible to get comparable estimates of biovolume or biomass from a calibrated OPC and a net. These studies conclude that with adequate calibration the OPC can be used to accurately measure zooplankton distributions in a variety of environments (e.g. Herman, 1992; Gallienne *et al.*, 1996; Sprules *et al.*, 1998; Beaulieu *et al.*, 1999).

3.2.2 Calibration equations for determining zooplankton biovolume with an OPC

In this section a set of calibration equations for determining biovolume from the OPC are presented. This calibration does not attempt to fit OPC data to net data, but instead biovolume is calculated by quantifying the factors that control the size of a zooplankter measured by the OPC, and then the resulting biovolume was compared with the LHPR samples. The OPC measures the size of the shadow cast by a zooplankter (its projected CSA), as it passes through the sampling beam, as a digital voltage DS_{opc} (an integer between 1 and 4096). The manufacturer's calibration equation converts the DS_{opc} to the ESD that would be cast by a sphere to give the shadow area represented by the DS_{opc}. This calibration was determined empirically using spherical beads. ESD_{man}:

$$ESD_{man}(\mu m) = \left(2088.76 + \left(10879(e^{\sqrt{3.65-(DS_{opc}/1000)^2}})\right)^{1.923} + 85.85 * \sqrt{DS_{opc}}\right) * \left(1 - e^{(-0.0465*\sqrt{DS_{opc}} + 0.0000803*DS_{opc})}\right) \quad \text{Eq 3.2.1}$$

The area of the shadow corresponding to the ESD_{man} (i.e. the shadow actually cast by the particle), CSA_{opc}, is therefore the area of a circle:

$$CSA_{opc}(\mu m^2) = \pi\left(\frac{ESD_{man}}{2}\right)^2 \quad \text{Eq 3.2.2}$$

The numerically dominant mesozooplankton in the Strait of Hormuz are copepods: the LHPR samples collected in the Strait are composed of more than 90% copepods (§4.2) and all of the studies of mesozooplankton in the Strait of Hormuz and eastern Arabian Gulf have found that copepods were the numerically dominant taxa (Yamazi, 1974; Jacob *et al.*, 1980; Gibson *et al.*, 1980; Michel *et al.*, 1986b). Copepods are not typically spherical. A more realistic representation of a copepod is a prolate spheroid (Herman, 1992), where the radius of the major axis is a, and the radius of the minor axis is b (**Fig 3.2.2.i**). In this calibration the volume of each zooplankter is determined

assuming that they are all spheroids. It is possible to calculate the volume of a spheroid of know CSA if its dimensions are known.

The shadow cast by an opaque spheroid depends on *a* and *b* and its orientation relative to the beam. The dimensions (*a* and *b*) of the model spheroid for the copepods in the Strait were quantified by microscopic measurements of the lengths and widths of 75 copepods in the LHPR samples. The ratio, *r*, of *a*:*b* was determined from these measurements as r_{cop} = 2.72 (see Appendix 2 for data) and this average ratio was applied to all particles measured by the OPC.

The orientation of a non spherical particle relative to the beam will influence the size of the shadow measured by the OPC. The angle of the spheroid relative to the beam can be specified by θ, so that when the major axis of the spheroid (*a*) is perpendicular to the beam θ=0° and when major axis is parallel to the beam θ=90°. Therefore the maximum CSA of the particle is recorded when θ=0° and the minimum CSA is recorded when θ=90° (**Fig 3.2.2.i**). Each particle passing through the OPC will have its own angle θ, the CSA cast by the spheroid for any given θ, CSA_{opc}, is then:

$$CSA_{opc}(\mu m^2) = \pi b\sqrt{a^2\cos^2\theta + b^2\sin^2\theta} \quad . \quad . \quad . \quad . \quad . \quad \text{Eq 3.2.3}$$

The influence of θ on the projected CSA_{opc} of an average spheroid (r_{cop} = 2.72:1) with a length of 1600 μm (*a* = 800) and a width of 588 μm (*b* = 294) is shown in **Fig 3.2.2.ii**. The maximum CSA of this spheroid is 0.74 mm^2 (θ=0°), and the minimum CSA is 0.27 mm^2 (θ=90°). This graph shows that the actual CSA is close to the maximum until the rotation is greater than about 60°. When θ is between 0 and 35° the CSA projected is between 95 and 100% of the maximum, and is above 80% of the maximum even when θ is 58°. At θs greater than 60° the projected CSA is reduced rapidly to <40% of the maximum CSA at 90°.

It is not possible to measure θ for each particle, therefore the calibration must take into account the total angular distribution of particles relative to the beam. If the angular distribution of the particles relative to the beam is random then not all θs are equally probable (Kirk, 1976). This is because the particle is rotated in three dimensions. By using equation 5 given by Kirk (1976) and Eq 3.2.3, it is possible to calculate the mean CSA_{opc} for a randomly orientated particle:

$$\overline{CSA}_{opc}(\mu m^2) = \int_0^{\pi/2} \pi b\left(\sqrt{a^2\cos^2\theta + b^2\sin^2\theta}\right)\cos\theta d\theta \quad . \quad . \quad . \quad \text{Eq 3.2.4}$$

Figure 3.2.2.i Diagram representing the effect of orientation on the shadow size

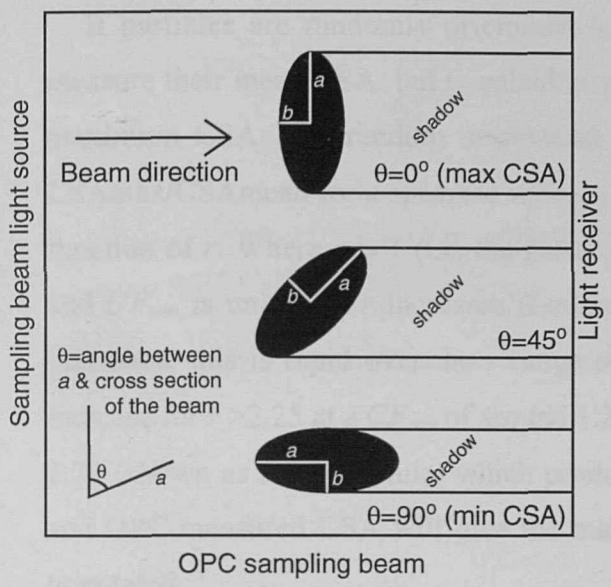

Figure 3.2.2.ii Graph showing the CSA of a spheroid from Eq 3.2.3 at various angles (where a = 800 μm, b = 294 μm)

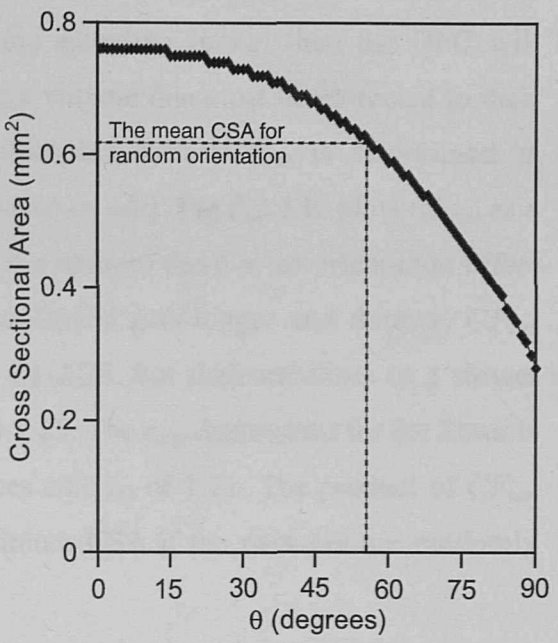

Figure 3.2.2.iii CF_{ran} to correct the measured CSA to the maximum CSA (θ = 0°) for spheroids with different values of r (=a/b). Dashed line shows r_{cop}

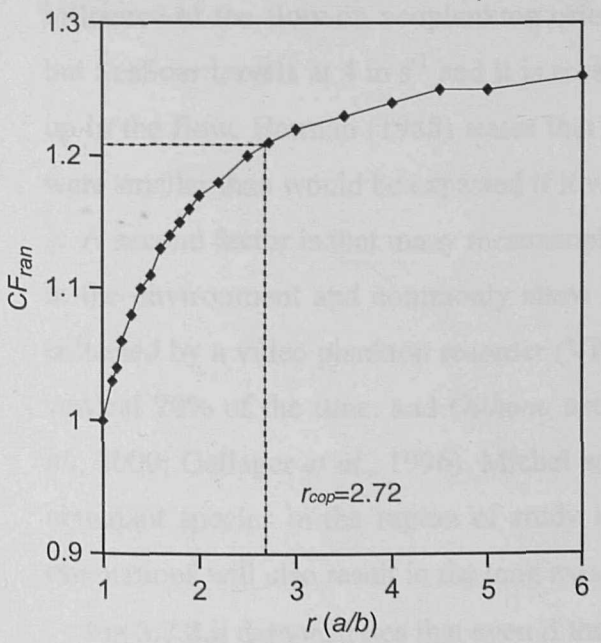

Figure 3.2.3.i CF_{vol} for spherical model for spheroids with different values of r (=a/b). Dashed line shows r_{cop}

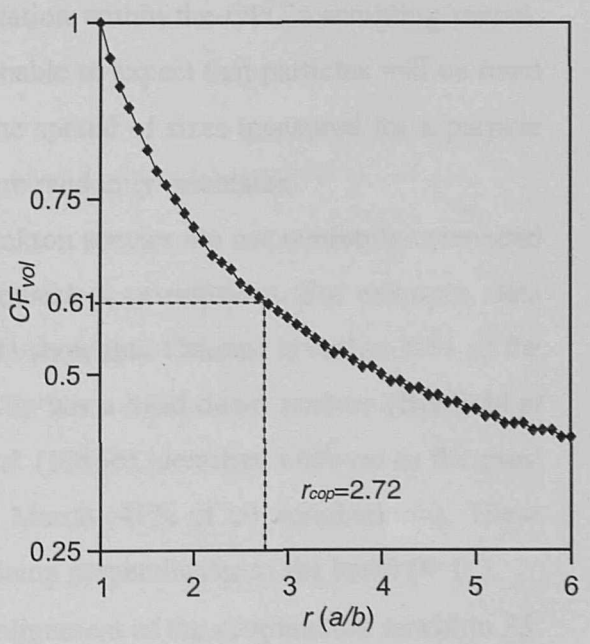

Using the average spheroid (r_{cop} = 2.72:1, a = 800 μm, b = 294 μm) the mean CSA_{opc} of randomly orientated particles is 0.61 mm^2, which is 82% of the maximum CSA (shown as dotted line on **Fig 3.2.2.ii**).

If particles are randomly orientated in the sampling tunnel then the OPC will measure their mean CSA, but to calculate their volume this must be corrected to their maximum CSA. The random orientation correction factor CF_{ran} is determined as CSAmax/CSAmean for a spheroid with a given r (= a/b). **Fig 3.2.2.iii** plots CF_{ran} as a function of r. Where r is 1 (i.e. the particle is a sphere) there is no orientation effect and CF_{ran} is unity. As r increases (i.e. the spheroid gets longer and thinner) CF_{ran} increases, this is rapid over the r range of 1.1-2.25, but then stabilises to a slower increase for r >2.25 at a CF_{ran} of around 1.20-1.25. The r_{cop} determined for the Strait is 2.72 (shown as a dashed line) which produces a CF_{ran} of 1.21. The product of CF_{ran} and OPC measured CSA will give the maximum CSA if the particles are randomly orientated.

However, the assumption that particles are randomly orientated when passing through the sampling beam of the OPC is not justified. First, the flow of water through the tunnel is expected to align the major axis (a) of particles with the flow, thus making it perpendicular to the beam (so θ tends to 0°). Bernstein and Shapiro (1994) observed that in laminar flows cylindrical particles become increasing lined up as the flow speed increased. To date, no measurements have been made of the influence of the flow on zooplankton orientation within the OPC's sampling tunnel, but SeaSoar travels at 4 m s^{-1} and it is reasonable to expect that particles will be lined up in the flow. Herman (1988) states that the spread of sizes measured for a particle were smaller than would be expected if it were randomly orientated.

A second factor is that many mesozooplankton species are not randomly orientated in the environment and commonly show consistent orientations. For example, data collected by a video plankton recorder (VPR) show that *Calanus* is within 30% of the vertical 70% of the time, and *Oithona* usually has a head down posture (Benfield *et al.*, 2000; Gallager *et al.*, 1996). Michel *et al.* (1986b) identified *Oithona* as the most abundant species in the region of study in March (41% of all zooplankton). These orientations will also result in the long axis being perpendicular to the beam (θ=0°).

Fig 3.2.2.ii demonstrates that even if the alignment of the zooplankton is within 35° of perpendicular with the beam (θ<35°) the measured CSA is >95% of the maximum.

Therefore, in this calibration of the OPC on SeaSoar, it is assumed that the OPC sees the maximum CSA of each particle. By assuming that θ=0° Eq 3.2.3 can be simplified:

$$CSA_{opc}(\mu m^2) = \pi ba \quad \text{Eq 3.2.5}$$

It is known that $a = b\, r_{cop}$, so:

$$CSA_{opc}(\mu m^2) = \pi (b)^2 r_{cop} \quad \text{Eq 3.2.6}$$

It is now possible to calculate the magnitude of b for any particle of unknown size but known CSA by rearranging Eq 3.2.6:

$$b_{opc}(\mu m) = \sqrt{\frac{CSA_{opc}}{\pi * r_{cop}}} \quad \text{Eq 3.2.7}$$

The volume of a spheroid is:

$$V(\mu m^3) = \frac{4}{3}\pi b^2 a \quad \text{Eq 3.2.8}$$

Therefore, the volume of the particle measured by the OPC, V_{opc}, is then:

$$V_{opc}(\mu m^3) = \frac{4}{3}\pi b_{opc}^3 r_{cop} \quad \text{Eq 3.2.9}$$

Eq 3.2.9 can be re-written in terms of CSA_{opc}

$$V_{opc}(\mu m^3) = \frac{4}{3}\pi r_{cop}\left(\frac{CSA_{opc}}{\pi r_{cop}}\right)^{3/2} \quad \text{Eq 3.2.10}$$

And can also be re-written in terms of ESD_{man} if it is assumed that θ=0°:

$$V_{opc}(\mu m^3) = \frac{4}{3}\pi r_{cop}\left(\sqrt{\frac{\left(ESD_{man}/2\right)^2}{r_{cop}}}\right)^3 \quad \text{Eq 3.2.11}$$

Eq 3.2.11 is the calibration equation for determining the volume of a zooplankter by the OPC, assuming that it is opaque spheroid, with dimensions defined by r_{cop} and θ=0°. If it is assumed that the orientation of the particles are random then the volume of each zooplankter is calculated from Eq 3.2.9, with the CSA_{opc} in Eq 3.2.7 corrected by CF_{ran} for that particular r_{cop} (**Fig 3.2.2.iii**).

3.2.3 Evaluation of errors associated with the calibration

In this section the errors associated with the assumptions made in the calibration are quantified and discussed. The first assumption was to represent zooplankters by an opaque geometric shape. Herman (1992) comments that translucent zooplankton do not block the light from the sampling beam effectively, and as a result their CSA is underestimated. This problem occurs with gelatinous species such as medusae, and translucent items such as fish eggs (Beaulieu *et al.*, 1999; Wieland *et al.*, 1997; Checkley *et al.*, 1997). Beaulieu *et al.* (1999) have determined that transparency of these groups usually causes an underestimate of the ESD by between 3 and 25% but this can be up to 40%. In the Strait the vast majority of zooplankton were crustaceans, which are typically opaque and block the light beam reliably (Herman, 1992). Therefore the assumption that the zooplankton were opaque is considered reasonable in this study. The second problem is that zooplankters were represented by a geometric shape (a spheroid) and it is clear that many species are not exactly spheroids. Also, the CSA of a smooth spheroid may differ from that of an actual animal of the same volume because the CSA of the zooplankter is increased by appendages. This effect is assumed to be negligible in this study, but it has not been quantified here, and is an important investigation of future studies.

It is useful to compare the volume calculated using spherical and spheroidal models because it permits the calibration derived here to be compared with others in the literature (§3.4.2). Moreover the variation in particle volume for different values of r can also be calculated. The volume calculated using a spheroidal model relative to that calculated using a spherical model, CF_{vol}, can be determined for a given CSA_{opc} by dividing the solution of Eq 3.2.10 for the given r by the solution with $r = 1$ (i.e. a sphere). **Fig 3.2.3.i** shows CF_{vol} as a function of different values of r. The r_{cop} used in this study was determined as 2.72 (see Appendix 2 for data), which produces an CF_{vol} of 0.61. This indicates that the spherical model overestimates biovolume by 40% in comparison to the spheroid model.

Representing copepods as a spheroid is certainly an improvement on a spherical model. In this study r_{cop} was determined by measuring the lengths and widths of only 75 copepods, and the standard deviation of r_{cop} was 0.4, which produces a range of CF_{vol} of 0.57-0.66 (mean=0.61). In addition the size range caught by the LHPR did not contain any species smaller than 1 mm, and the r_{cop} was extrapolated to the full size range of zooplankton counted by the OPC. It is recommended that in future studies

more individuals are measured, and their sizes should cover the complete range of OPC data. The data in **Fig Appen.i** (see appendix 2) show that r showed more variation in larger size classes, and future calibrations might be improved by using different values of r_{cop} for different size classes.

The second assumption was that the particles were orientated so that their major axis was with 35° of being perpendicular to the sampling beam (so that the CSA was within 5% of the maximum, and could be assumed to be maximum). This assumption is expected to be true for the SeaSoar, which is towed at 4 m s^{-1}, but when the OPC is mounted on slower towed platforms, such as nets, the particles may be more randomly orientated. Therefore the maximum CSA should be calculated from the CF_{ran} and the OPC measured CSA. A random orientation of particles is also expected for the laboratory bench top OPC (especially when used with preserved samples).

Future studies should attempt to quantify experimentally these assumptions. For example simple laboratory experiments passing spheroids through the OPC in a tank simulating SeaSoar towing conditions would show if particles are randomly or consistently orientated (future work is discussed in more detail in §6.1).

Summary: The OPC calibration equation used to determine biovolume

In this study zooplankton biovolume from the OPC was calculated from the DS_{opc} output of the OPC with the calibration equations (and assumptions) listed in §3.2.2. By assuming that the all the zooplankton were opaque spheroids, with dimensions defined by r_{cop} and θ=0°, then Eq 3.2.9 was used to determine their volume:

$$V_{opc}(\mu m^3) = \frac{4}{3}\pi b_{opc}^3 r_{cop} \quad \text{Eq 3.2.9}$$

where b_{opc} is the length (μm) of the radius of the minor axis of the spheroid
and r_{cop} is the ratio of the major axis/minor axis of the spheroid (in this study = 2.72)

This calibration is now compared with the biovolume measured in the LHPR samples (§3.3) and with the biovolume measured by previous zooplankton studies in the Strait, with CF_{vol} factors from other studies, and with phytoplankton biomass in the Strait (§3.4).

3.3 Comparison of calibrated OPC biovolume with LHPR biovolume

In this section the biovolume measured by the OPC is compared with the zooplankton biovolume measured in the LHPR samples. Despite the problems in comparing the LHPR with the OPC data (as outlined in §3.1), the LHPR still provides the most reliable dataset available to evaluate the OPC calibration. The comparison is only made between the OPC data and the data from LHPR stn 54006 because at stn 54007 the temporal and spatial difference between collection of the datasets produced much larger discrepancies in the profile shapes (§3.1.3). For these reasons a poorer correlation would be expected at stn 54007, and no comparison is made here.

3.3.1 Comparison of OPC and LHPR biovolume before calibration

Fig 3.3.1.i shows the uncalibrated zooplankton biovolume profiles from the OPC and the LHPR at stn 54006. The OPC biovolume in this graph has been determined using a spherical model, where the volume of each particle is determined assuming each particle is spherical. No error bars are presented for the OPC profile, but are a similar extent as for the abundance (§3.1.3.1). **Fig 3.3.1.i** shows the biovolume for the same data that was compared in terms of abundance in **Fig 3.1.3.i**. Despite these instruments producing equivalent measurements of zooplankton abundance, the estimate of zooplankton biovolume from the OPC data was consistently larger than from the LHPR samples.

The difference between the biovolume measurements of the two instruments is caused by the way in which zooplankton volume is determined for the OPC relative to the LHPR. The OPC biovolume calibration (Eq 3.2.9) is expected to produce a more accurate calibration. The displacement volume of zooplankton measured in the LHPR samples must also be corrected for the affect of shrinkage caused by preservation. The LHPR filters zooplankton into a sandwich of sampling silk and as a result the samples are not easily accessible at sea. In this study, the biovolume could only be measured after the ship had returned to the UK, when the samples had already spent several months in a 5% buffered formaldehyde solution (§2.2.5). It is well established that the preservation of zooplankton in formaldehyde solutions can result in the substantial shrinkage of zooplankton biovolume, with shrinkage typically ranging from 5 to 40% (Beers, 1976; Omori and Ikeda, 1992; Beaulieu *et al.*, 1999). The biovolume of the LHPR samples could not be measured before preservation and so shrinkage could not be avoided or directly quantified.

Figure 3.3.1.i Uncalibrated zooplankton biovolume determined from the OPC and the LHPR at stn 54006

a) Biovolume profiles of LHPR and OPC measurements averaged into 4 m depth bins

b) Plot comparing biovolume measured at each depth by the LHPR and the OPC (same data as Fig 3.3.1.ia)

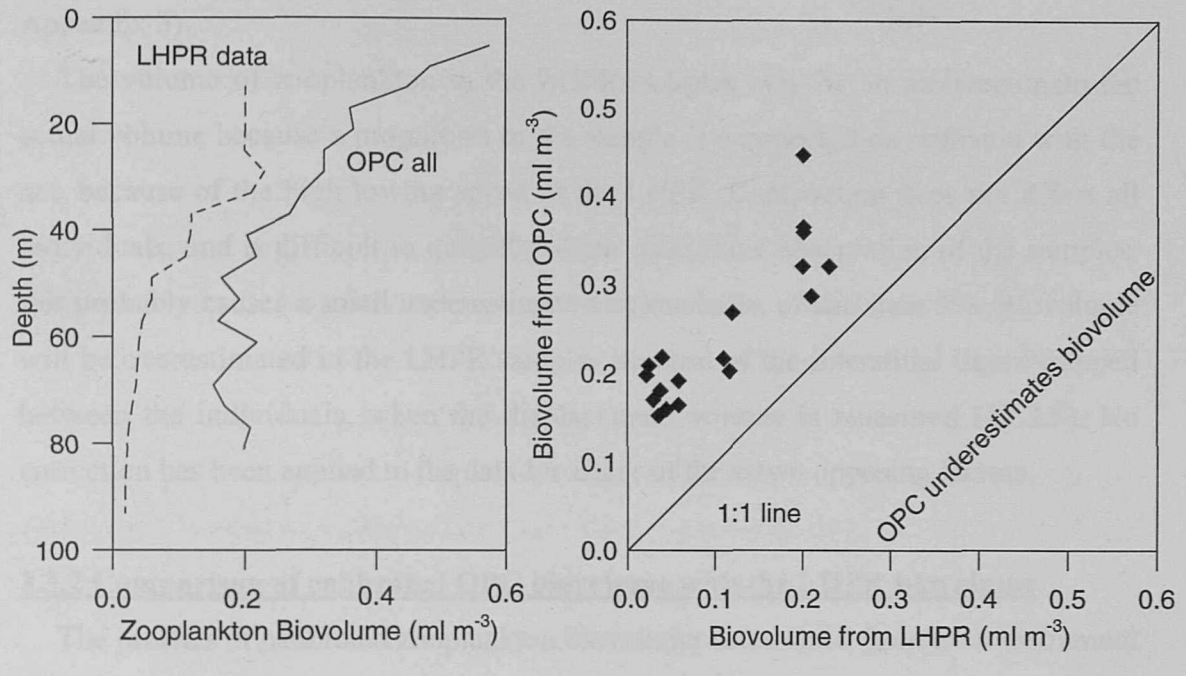

Figure 3.3.2.i Calibrated zooplankton biovolume determined from the OPC and the LHPR at stn 54006

a) Biovolume profiles of LHPR and OPC measurements averaged into 4 m depth bins

b) Plot comparing biovolume measured at each depth by the LHPR and the OPC before and after calibration

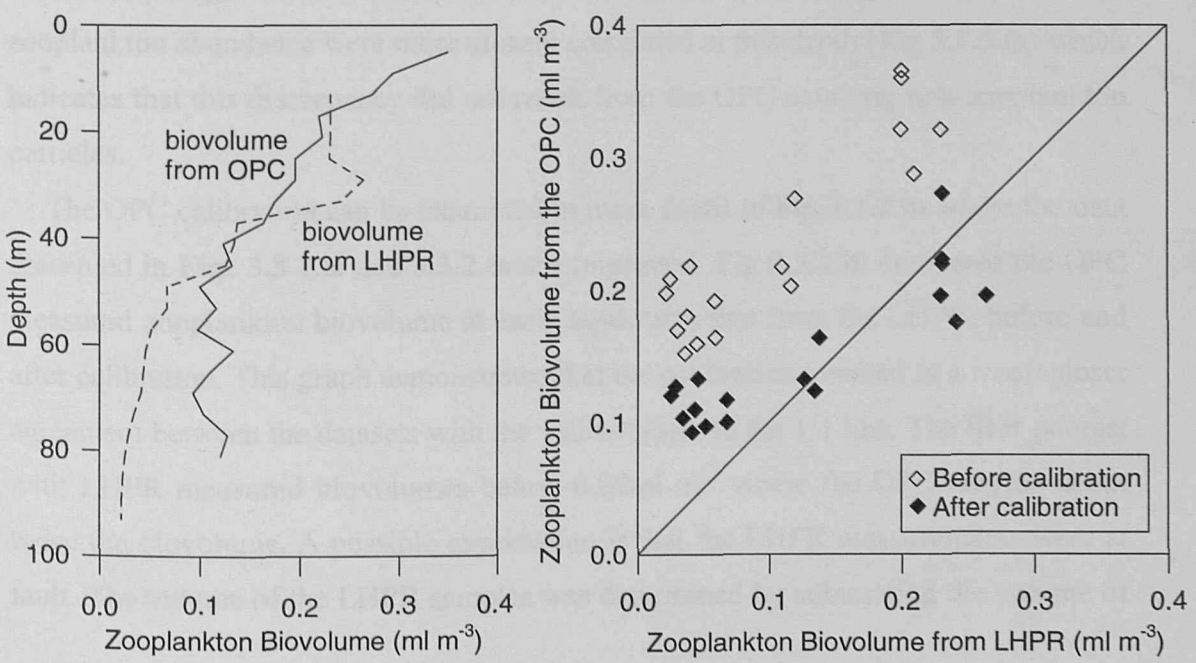

The shrinkage has been estimated using the RMT samples collected during the cruise, the volumes of which were measured before and after preservation (Herring *et al.*, 1997). The shrinkage of these samples was between 12 and 23% of the volume. As a result the LHPR biovolume has been increased by 15% to correct for shrinkage (see Appendix 3).

The volume of zooplankton in the LHPR samples may be an underestimate the actual volume because a proportion of the sample is compacted on collision with the net, because of the high towing speed of the LHPR. Compaction does not affect all individuals, and is difficult to quantify. From qualitative observation of the samples, this probably causes a small underestimate of biovolume, of less than 5%. Biovolume will be overestimated in the LHPR samples because of the interstitial liquid trapped between the individuals, when the displacement volume is measured (§2.2.5). No correction has been applied to the data for either of these two opposing factors.

3.3.2 Comparison of calibrated OPC biovolume with the LHPR biovolume

The profiles of calibrated zooplankton biovolume determined from each instrument at stn 54006 are shown in **Fig 3.3.2.ia**. In the upper 50 m the OPC produced consistent and equivalent measurements of the mesozooplankton biovolume with that of the LHPR. The difference in the shapes of the profiles at this depth range result from the same factors that were discussed for the difference in the abundance profiles in §3.1.3.1 (wind mixing, internal waves and advection). Below 50 m where the zooplankton were at lower concentrations, the biovolume determined by the OPC was consistently larger than the biovolume measured in the LHPR samples. The profiles of zooplankton abundance were more closely correlated at this depth (**Fig 3.1.3.ia**) which indicates that this discrepancy did not result from the OPC counting non-zooplankton particles.

The OPC calibration can be examined in more detail in **Fig 3.3.2.ib** where the data presented in **Figs 3.3.1.ia** and **3.3.2.ia** are re-plotted. **Fig 3.3.2.ib** compares the OPC measured zooplankton biovolume at each depth with that from the LHPR, before and after calibration. This graph demonstrates that the calibration resulted in a much closer agreement between the datasets with the values closer to the 1:1 line. The fit is poorest with LHPR measured biovolumes below 0.05ml m^{-3} where the OPC records about twice the biovolume. A possible explanation is that the LHPR measurements were at fault. The volume of the LHPR samples was determined by subtracting the volume of

the particles retained on the 4.5 mm mesh from the total sample volume. Because the total sample volumes were small at these depths the volumes of both the total sample and the >4.5 mm fraction were close to the precision of the method (§2.2.5) and similar values were recorded for each. When the volume of the >4.5 mm fraction was subtracted from the total the resulting volume close to zero. The difference can also be expected to be the fault of the OPC calibration: it is possible that their was a change in the species so that the spheroid calibration was not representative. Future work is needed to more accurately quantify the performance of the OPC in these conditions.

The calibration of the biovolume from the OPC data, by the procedure detailed in §3.2.2, has resulted in data that are in agreement more closely with the LHPR net samples than the spherical model. The calibration provides a similar spread of estimates around the 1:1 line as determined between abundance measurements, therefore within the limits expected when spatial and temporal differences are considered. Further evaluation of the calibration is presented in §3.4.

3.4 Further evaluation of calibrated OPC Biovolume

In this section the reliability of the calibration of zooplankton biovolume (and abundance) from the OPC and in the Strait of Hormuz is assessed by comparison with other datasets. First the calibrated OPC data are compared with zooplankton net samples from previous surveys the Strait of Hormuz (§2.1.3). The OPC calibration is also compared with other published OPC calibration factors. Finally, the mesozooplankton biomass determined with the OPC is compared with the phytoplankton standing stock biomass determined from concurrent calibrated fluorimetric measurements (§2.2.3). This final assessment of the OPC calibration has several possible errors and is probably the least persuasive evidence.

3.4.1 Comparison with previous studies in the region

There have only been a few surveys of zooplankton standing stock in the Strait of Hormuz, and all have been made using standard zooplankton nets. These provide an independent source of information to compare with the calibrated OPC data.

The study of RV *Atlantis* from Woods Hole Oceanographic Institute, 20 years to the month before the CD 104 survey (Gibson *et al.*, 1980), is the most suitable for comparison. First, both the surveys of RV *Atlantis* and R.R.S. *Charles Darwin* were made at the same time of year (March), which is an important consideration in a monsoon region (§2.1, Halim, 1984; Burkill, 1999). Secondly the RV *Atlantis* survey collected zooplankton net samples from several stations throughout the Strait.

3.4.1.1 Comparison of zooplankton abundance

Gibson *et al.* (1980) used a 243 μm mesh net, which was towed obliquely through the upper 60 m of the water column (or from the seabed, when shallower). Zooplankton abundance was determined between 416 to 2159 m^{-3}. This net and the OPC do not sample exactly the same size range of zooplankton, and the range must be standardised before a meaningful comparison can be made between the datasets (§3.1.3). Interpolating the findings of Barnes and Tranter (1965) a plankton mesh of 243 μm should reliably retain zooplankton larger than about 0.7 mm. OPC data were standardised to match Gibson *et al.*'s samples by selecting the data between than 0.7 and 4.5 mm and averaging over the upper 60 m of the water column. When averaged in this way the OPC abundance was between 860 and 1561 m^{-3} which was within the range measured by Gibson *et al.* (1980). Before being averaged over the upper 60 m

OPC abundance ranged from 152 and 5155 m^{-3} which encompassed the range measured by Gibson *et al.*

3.4.1.2 Comparison of zooplankton biovolume

Gibson *et al.*'s data also provide an opportunity to evaluate the calibrated biovolume from the OPC. Gibson *et al.* (1980) recorded zooplankton biovolume in the Strait between 0.11 and 2.27 ml m^{-3}, although the majority of samples were between 0.3 and 1.0 ml m^{-3}. The calibrated OPC biovolume (standardised as above to match the biases of Gibson *et al.*'s net) ranged between 0.29 and 0.55 ml m^{-3}. Before being averaged over the upper 60 m, the biovolume ranged from 0.04 and 2.3 ml m^{-3}.

The calibrated OPC biovolume values are within the range of biovolume in the net samples. However the abundance data from the OPC and the net were more closely matched than the biovolume data. The OPC underestimate biovolume in comparison with the net, although the data were still in the same range.

Gibson *et al.* (1980) determined biovolume by measuring the amount of water that drained by gravity from a concentrated zooplankton sample, in a solution of know volume. This methodology can leave a large amount of interstitial water within the zooplankton sample: Frolander (1957) determined that vacuum suction removes 1.5 times more fluid than gravity draining. As a result the volume of Gibson *et al.*'s samples might be overestimated, which may be the cause of the discrepancy with the OPC samples. In addition, no upper size limit was placed on the net samples (while OPC data larger than 4.5 mm was excluded) and as a result a few larger species might have been present, significantly increasing the biovolume.

Table 3.4.1a Comparison of zooplankton densities measured by the OPC during CD 104 and the net of Gibson *et al.* (1980) twenty years earlier in the Strait of Hormuz

Sampling Method	Abundance (nos m^{-3})	Biovolume (ml m^{-3})
0.243 mm net (Gibson *et al.*, 1980)	416 – 2159	0.11 – 2.27 (most 0.3 – 1.0)
OPC (standardised to net)	860 – 1561	0.29 – 0.55

In summary, the abundance and biovolume determined from the OPC were within the range measured by Gibson *et al.* (1980) with a plankton net in the Strait of Hormuz 20 years earlier. This provides additional evidence that the spheroidally calibrated OPC measurements were realistic and reliable.

3.4.2 Comparison with existing OPC calibration factors

The first published datasets from the OPC determined zooplankton biovolume from the measurements of particle ESD using a spherical model. However, this method can

overestimate the zooplankton volume in comparison to net samples. Consequently, more recent work has used empirical data to calibrate the OPC biovolume (Sprules *et al.*, 1998; Pollard *et al.*, submitted). The OPC biovolume calibration applied in this study is compared with biovolume calibration factors from other OPC studies.

3.4.2.1 Details of other biovolume calibration factors used for OPC data

Stockwell and Sprules (1995) and Sprules *et al.* (1998) used spheroid models determined from empirical biovolume calibrations to estimate biovolume from OPC data in freshwater. Volume was computed assuming that the major axis was equal to the ESD and the minor axis was the ESD/1.6 and ESD/1.33, respectively in the two studies. The size of the minor axis was derived to produce the best fit with the biovolume in net samples taken periodically within the OPC survey. These calibrations are proportional to the spherical model, and it is possible to calculate the scaling factor, CF_{vol} (§3.2.3), of the spherical model each represents. For Stockwell and Sprules (1995) the CF_{vol} is 0.39, and for Sprules *et al.* (1998) the CF_{vol} is 0.57. Pollard *et al.* (submitted) calibrated OPC biomass in the Southern Ocean by a CF_{vol} of 0.6. This scaling factor was determined by comparing OPC data with the biomass of zooplankton in net samples. The OPC biovolume calibration determined in this study is equivalent to a CF_{vol} of 0.61.

3.4.2.2 Comparing the calibration factors with the OPC data in the Strait

Fig 3.4.2.i shows the profiles of the OPC biovolume (as used **Fig 3.3.2.ia**) computed using the spherical model, and the calibrations determined by Stockwell and Sprules (1995), Sprules *et al.* (1998) and Pollard *et al.* (submitted). Also presented for comparison are the OPC biovolume determined in this study and the LHPR measured biovolume from stn 54006. The calibrations of Sprules *et al.* and Pollard *et al.* are almost identical to the calibration determined in this study, and produce an equally good a fit with the LHPR data as the calibration. The calibration of Stockwell and Sprules (1995) does not compare as closely with the other factors, and in comparison underestimates zooplankton biovolume, although is still within the range of the LHPR

3.4.3 Comparison between zooplankton and phytoplankton carbon biomass

A further way to evaluate the reliability of the zooplankton biovolume produced by the OPC is by comparison with the phytoplankton standing stock, in the form of a biomass pyramid.

Figure 3.4.2.i A comparison of the OPC biovolume calibration used in the Strait of Hormuz with the calibration factors used in other studies. (The brackets show the CF_{vol})

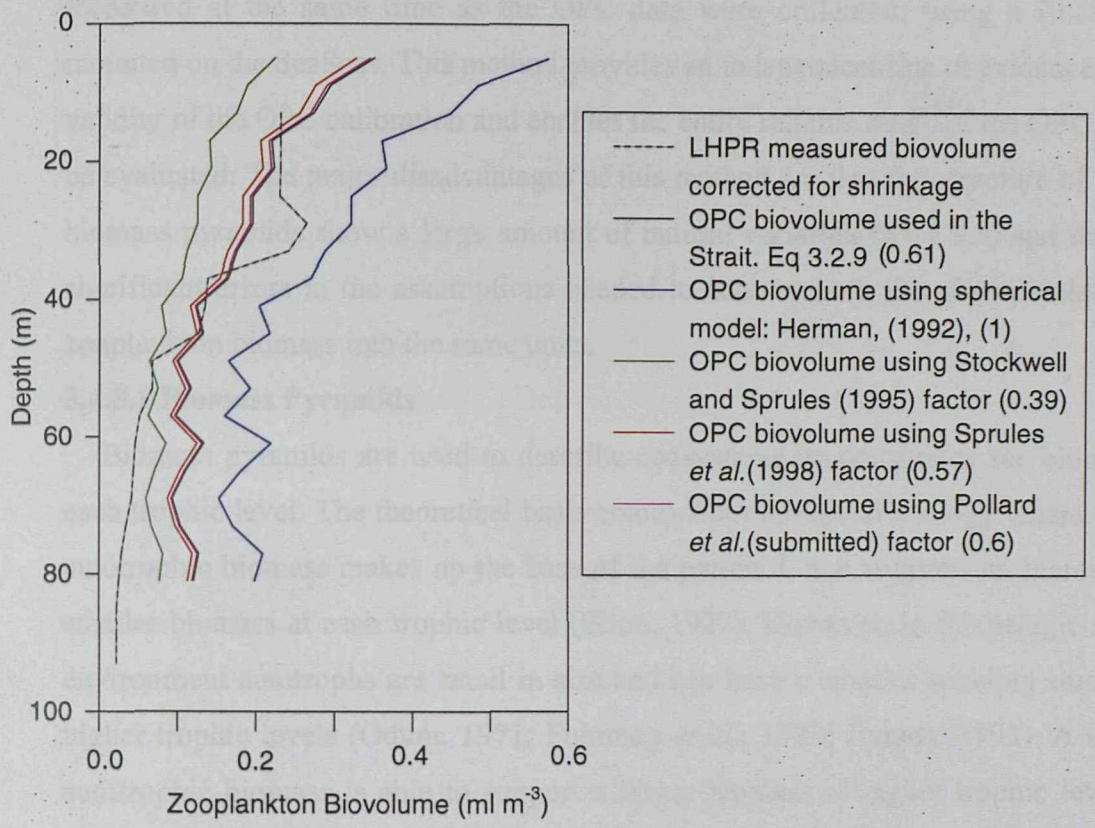

Figure 3.4.3.i Comparison of phytoplankton and mesozooplankton carbon biomass (0.3-4 5mm ESD) in a section of the survey on the west side of the Strait of Hormuz Carbon biomass averaged over the upper 25m plotted as a function of salinity

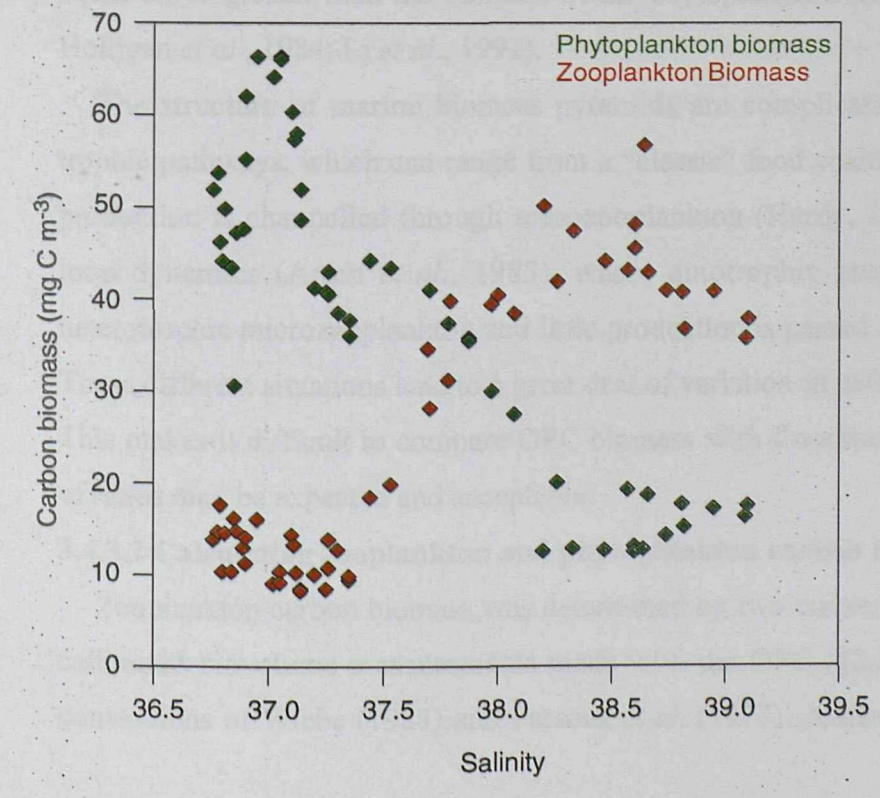

This method is advantageous because the OPC calibrated biovolume is compared against a concurrent dataset. The phytoplankton chlorophyll concentration was measured at the same time as the OPC data were collected, using a fluorimeter mounted on the SeaSoar. This method provides an independent line of evidence for the validity of the OPC calibration and enables the entire reliable range of the OPC data to be evaluated. The major disadvantages of this method are that the structure of marine biomass pyramids show a large amount of natural variation (§3.4.3.1) and there are significant errors in the assumptions needed to convert both the phytoplankton and zooplankton biomass into the same units.

3.4.3.1 Biomass Pyramids

Biomass pyramids are used to describe ecosystems by comparing the biomass at each trophic level. The theoretical basis comes from terrestrial ecology where a large autotrophic biomass makes up the base of the pyramid, and supports an increasingly smaller biomass at each trophic level (Elton, 1927). However, in the pelagic marine environment autotrophs are small in size and can have a smaller standing stock than higher trophic levels (Odum, 1971; Fuhrman *et al.*, 1989; Jumars, 1993). A smaller autotrophic biomass is able to support a larger biomass at higher trophic levels by having a greater production than higher levels because of a faster turnover time of the population (O'Neill and DeAngelis, 1981; Gasol *et al.*, 1997). Many studies of planktic communities have demonstrated that the biomass of mesozooplankton can be equal to, or greater than the biomass of the phytoplankton (e.g. Eppley *et al.*, 1977; Holligan *et al.*, 1984; Li *et al.*, 1992).

The structure of marine biomass pyramids are complicated further by different trophic pathways, which can range from a "classic" food chain, where phytoplankton production is channelled through mesozooplankton (Hardy, 1924), to the microbial loop dynamics (Azam *et al.*, 1983), where autotrophic production is utilised by heterotrophic microzooplankton and little production is passed on to larger organisms. These different situations lead to a great deal of variation in pelagic biomass pyramids. This makes it difficult to compare OPC biomass with fluorimeter biomass as a range of ratios may be expected and acceptable.

3.4.3.2 Calculating zooplankton and phytoplankton carbon biomass

Zooplankton carbon biomass was determined by two conversion methods from the calibrated biovolume measurements made with the OPC (§2.2.4.4). These were the conversions of Wiebe (1988) and Parsons *et al.* (1977). A size range of zooplankton

covering 0.3 and 5.5 mm ESD was selected to approximately cover the traditional mesozooplankton herbivores. There are more details and a comparison of these two calibrations in Appendix 4.

The carbon weight of phytoplankton was determined from measurements of chlorophyll in the Strait using a "standard" carbon-to-chlorophyll *a* ratio of 50. A value of 50 was used because no measurements of the ratio were made during this survey and no regional data could be found in the literature. Numerous experiments have showed that this ratio can be variable, with factors including regional, latitudinal, depth and seasonal (irradiance and photoperiod) differences (e.g. Banse, 1977; Taylor *et al.*, 1997) taxonomic and growth rate differences (Chan, 1980) and nutrient availability (Riemann *et al.*, 1988; Geider *et al.*, 1998). Taylor *et al.* (1997) recorded variation in cultures of this ratio between 12 and >200. Other recent work has indicated that a value of 100 may be more realistic for the open ocean, doubling the carbon concentration calculated here (Welschmeyer and Lorenzen, 1984; Hewes *et al.*, 1990). Moreover, in some oligotrophic areas the ratio may be as high as 200 (Buck *et al.*, 1996).

3.4.3.3 Comparing zooplankton and phytoplankton biomass

Fig 3.4.3.i shows phytoplankton and mesozooplankton (using the Parsons *et al.* method) carbon biomass averaged over the upper 25m plotted as function of salinity, in a section of the survey from the Strait of Hormuz. This section was chosen as a wide range of values were present in a short distance, and it was surveyed during the night, so that the chlorophyll concentration was not influenced by quenching.

Fig 3.4.3.i shows that there was a large variation in the standing stock biomass of both the phytoplankton and zooplankton. At low salinities (36.5-38.0) phytoplankton biomass was about 3 times larger than mesozooplankton biomass, but at high salinities (38.0-39.5) mesozooplankton biomass was twice that of phytoplankton. These values suggest that zooplankton carbon biomass, derived from the calibrated OPC biovolume, are within an acceptable range when compared with phytoplankton carbon biomass. Although a wide range of shapes of biomass pyramids may be expected, this is further evidence for the reliability of the OPC calibration.

3.4.4 Summary of the evaluation of the calibrated OPC biovolume

In summary: the OPC measured biovolume and abundance were within the range of those measured in previous studies in the Strait. The biovolume calibration factor,

based on a spheroidal model, was almost identical to empirical calibrations derived by Sprules *et al.* (1998) and Pollard *et al.* (submitted). When the zooplankton carbon biomass was estimated from the calibrated zooplankton biovolume it was found to be within a realistic range when compared with phytoplankton biomass. These three lines of independent evidence indicate that the OPC calibration used in the Strait produces a realistic estimate of zooplankton biovolume.

As a result of the comparison with the LHPR and these three additional lines of evidence, the measurements of zooplankton abundance and biovolume calculated from the OPC data are accepted as being accurate for the study the relationship between zooplankton and their physico-chemical environment in the Strait of Hormuz.

Qualitative assessment of the species responsible for the OPC counts

In this study size is used to determine different functional groups of mesozooplankton because current technology does not allow the distribution of species to be determined at the mesoscale. By making accurate length and width measurements of zooplankton from net samples it is possible to attribute the peaks in the particle size spectra produced by an OPC to species or even the different life stages in regions of low zooplankton diversity (Herman, 1992; Herman *et al.*, 1993; Rissik *et al.*, 1997; Beaulieu, *et al.*, 1999). In high diversity communities it is not possible to resolve clear taxonomic information from the OPC (Wieland *et al.*, 1997) because factors such as the orientation in the sampling beam result in a wide range of measured sizes for a species that overlap those of other species. Determining species is not a main aim of this study, so this is only a brief qualitative assessment of the dominant species.

The LHPR catch and previous zooplankton surveys in the region have been used to identify the groups of plankton that are likely to be represented by the counts made by the OPC. The LHPR samples demonstrated that copepods are the most abundant mesozooplankton in the Strait, where this taxa accounted for between 80 and 95% of all individuals (§4.2.3). Previous studies in this region have also shown the numerical dominance of this group. Michel *et al.*, (1986b) used 110 μm nets to sample in the Strait in March 1980, and their dataset is probably the best available to represent the OPC in terms of size. Michel *et al.* (1986a) state that a 333 μm net (such as a LHPR) will underestimated copepod density in this region, as many of the numerically dominant smaller copepods, such as *Oithona* spp., *Oncaea conifera* and *Paracalanus*

spp. would pass through the mesh. These species would be recorded: an OPC was used by Rissik *et al.* (1997) to measured *Oithona* spp. between 0.5 and 0.6 mm ESD and *Oncaea* spp. between 0.4 and 0.6 mm ESD. Michel *et al.*'s (1986b) samples were also dominated by copepods (90% of the total), with 10 species accounting for 80% of all the zooplankton caught. From that dataset the following species are likely to account for the majority of the OPC counts: the cyclopoids *Oithona* spp. and *Oncaea conifera*, and the calanoids *Paracalanus crassirostis* and *P. aculeatus*. Other groups may be locally important, such as the appendicularians *Oikopleura* spp. and the cladocerans *Penilia avirostris* and *Evadne* sp., but it is not possible to resolve these from the copepods in the OPC dataset. The peaks at larger sizes will still be dominated by copepods, although other groups will become increasingly important, such as chaetognaths (probably *Sagitta enflata* and *S. neglecta*), euphausiids (various stages of *Pseudeuphausia latifrons*) and molluscan veligers (see also Appendix 5).

Summary of the OPC Calibration in the Strait of Hormuz

The reliability and accuracy of the OPC's measurements of zooplankton population density were evaluated by comparison with LHPR samples. For a valid comparison the data were standardised in terms of spatial resolution and size class to remove biases. The closest OPC data to the LHPR stations were used, and abundance was compared in each depth bin between the two instruments. The data from each instrument were comparable to within a factor of two, and were equally spread about a 1:1 relationship. The vertical profiles from the two instruments showed different structures, which was mainly attributed to temporal gap between the collection of the datasets and associated environmental and advective changes. The consistency of the OPC abundance with the LHPR indicates that it was not significantly increased by counts of non-zooplankton particles. This is consistent with expectations in clear subtropical waters. Coincidence counts were also not thought to be a problem, as the counts made each second were less than 100, which much lower than theoretical maximum of 167 s^{-1} (Sprules *et al.*, 1998).

The biovolume from the OPC was calibrated with a spheroidal model tuned with dimensional measurements of zooplankton in the LHPR samples. The LHPR samples were corrected for shrinkage due to preservation (increased by 1.15). The zooplankton biovolume calculated from the OPC data with both a spherical and spheroidal model were compared with the LHPR biovolume. The spherical model overestimated the

biovolume in the LHPR samples, but the spheroidal model produced an improved fit, close to the 1:1 line. The spheroidal model appeared to overestimate biovolume in comparison to the net in the deepest samples where the biovolume was lowest.

The abundance and biovolume calibrated from the OPC were within the ranges measured by Gibson *et al.* (1980) with net samples taken in the Strait in March 1977. In addition, the calibration factor, CF_{vol}, was almost identical to empirical calibrations derived by Sprules *et al.* (1998) and Pollard *et al.* (submitted) for the OPC.

The OPC measurements of abundance and calibrated biovolume have been accepted as accurate for describing the spatial distribution of mesozooplankton size classes in the Strait, and to study their relationship with the physico-chemical environment (Chapters 4 and 5).

CHAPTER 4

Description of the physico chemical environment and distribution of plankton in the Strait of Hormuz in March 1997

4.1 DATA COLLECTED WITH A SEASOAR AND A CTD IN THE STRAIT OF HORMUZ . . 95
4.2 DATA COLLECTED WITH A LONGHURST HARDY PLANKTON RECORDER IN THE STRAIT OF HORMUZ 127

FIGURES

4.1.1.i Contour plots of legs through the Strait of Hormuz 98-113
4.1.1.ii Maps of the distribution of surface salinity, temperature, chlorophyll a, OPC measured zooplankton abundance and biovolume, and MVBS at 120 kHz from EK500 . 114
4.1.1.iii Contoured CTD sections from the Strait of Hormuz 115
4.1.1.iv Full depth data from CTD line D 116
4.1.2.i Temperature as a function of salinity for the water sampled by the CTD in the Gulf of Oman and the Arabian Gulf, and by SeaSoar in the Strait of Hormuz . . 116
4.1.4.i Diel vertical migration of MVBS at 38kHz in the Gulf of Oman and the Strait . 123
4.1.4.ii The vertical distribution of MVBS at 38 kHz over 24 hours in the Gulf of Oman . 123
4.1.4.iii Day and night profiles of zooplankton biovolume in four OPC size classes . 124
4.1.4.iv Mesozooplankton biovolume in each size class in the upper 30 m in the GOS . 124
4.2.1.i The distribution of zooplankton biovolume with depth at Stn 54006 . . 129
4.2.1.ii The vertical distribution of zooplankton biovolume at Stn 54007 . . . 129
4.2.1.iii The percentage of zooplankton abundance of each taxonomic group at 54006 . 130
4.2.1.iv The percentage of zooplankton abundance of each taxonomic group at 54007 . 131
4.2.1.v Abundance profiles of dominant zooplankton groups at stn 54006 . . . 132
4.2.1.vi Abundance profiles of dominant zooplankton groups >1.5 mm at stn 54006 . 133
4.2.1.vii Abundance profiles of dominant zooplankton groups at stn 54007 . . 134
4.2.1.viii Abundance profiles of dominant zooplankton groups >1.5 mm at stn 54007 . 135
4.2.4.i Acoustic backscatter at 120 kHz at stn 54007 142
4.2.4.ii Bars showing zooplankton biovolume in each LHPR sample at stn 54007 . . 142
4.2.4.iii Vertical profiles of biovolume, salinity and backscatter from stn 54007 . . 142

The aim of this chapter is to describe the physical, chemical and biological environment sampled in the Strait during the CD 104 survey, in March 1997. To meet this objective, measurements of the physical environmental variables and the spatial distribution of the pelagic community (phytoplankton, mesozooplankton, macrozooplankton and micronekton) are presented graphically and summarised in the text. The major physical features in the Strait are also introduced and their biophysical interaction with the plankton is discussed. These relationships will be analysed in more detail in chapter 5 and discussed in chapter 6. The majority of the data are from the Strait of Hormuz, but additional measurements from the Arabian Gulf and Gulf of Oman are presented to help interpret the conditions in the Strait.

R.R.S. *Charles Darwin* Cruise 104 was the first multidisciplinary survey of the Strait of Hormuz made with an undulating sampler (Roe *et al.*, 1997). Previous studies have been limited to fixed CTD stations and vertical net samples (e.g. Leveau and Szekielda, 1968; Brewer and Dyrssen, 1985; Reynolds, 1993), which showed the inflow and outflow through the Strait but were inadequate to resolve mesoscale and sub-mesoscale variability in both the physical environment and the planktic community. The data presented in this chapter represent the most spatially explicit survey of the Strait of Hormuz made to date, and the first time the distribution of plankton in the Strait has been described other than at fixed stations.

This chapter is divided into two sections: the first presents physical and biological measurements made with a SeaSoar and CTD, and the second describes net samples and concurrent temperature and salinity measurements made with a Longhurst Hardy plankton recorder.

4.1 Data Collected with SeaSoar and CTD in the Strait of Hormuz

This section presents the data collected by the SeaSoar, EK500 echosounder and the CTD in the Strait of Hormuz, during March 1997. The data are presented in contour plots in §4.1.1. A hydrographic interpretation of the data is then made in §4.1.2, an examination of the plankton distributions in §4.1.3, the diurnal migration of zooplankton is evaluated in §4.1.4 and the findings are summarised in §4.1.5.

4.1.1 Presentation of SeaSoar and CTD data

The SeaSoar survey data are illustrated as contour plots in **Fig 4.1.1.i**, representing transects through the Strait of Hormuz (with the position of each transect or leg

highlighted in red on the map). Each variable is contoured as a function of depth and distance travelled by the ship, (except the acoustic data which has been plotted as a function of depth and time (§2.2.6), although the time axis corresponds spatially with the distance in the other plots). There are 16 variables contoured for each leg, with each plotted from west to east (from the Arabian Gulf AG to the Gulf of Oman GO), irrespective of the direction of travel of the ship. At the top of each page there are equivalent axes of time (Jday and hours GMT) and longitude (in degrees).

Only the first four (northern most) legs of the SeaSoar survey are presented in the figure because the final two legs, closest to the Masandam coast, were shallow (<40m) on the west side of the Strait, and OPC and SeaSoar data were disrupted when SeaSoar was fouled with fishing line and when OPC data files were lost (§2.2.4). All six transects are presented by Smeed *et al.*, (1997) for the SeaSoar data, by Mustard (1997) for the OPC data and by Crisp *et al.*, (1998) for the acoustic backscatter.

The following variables are contoured for each leg in **Fig 4.1.1.i**: salinity, potential temperature, density, light, zooplankton biovolume in 5 size classes, total zooplankton biovolume for all these classes, total zooplankton abundance for all these size classes, chlorophyll *a* concentration, mean volume backscattering strength (MVBS) measured at three frequencies by an EK500, and the Brunt Vaisala Frequency of stratification. The approximate positions of the three water types (defined in §4.1.2) are indicated on the density plot.

The near surface SeaSoar data (averaged between 7 and 11 m depth) are also presented as maps of the Strait of Hormuz (**Fig 4.1.1.ii**). These data are not contoured to produce a complete spatial coverage because the quasi-synoptic nature of the data would lead to unacceptable biases during interpolation. Instead, coloured points are plotted representing the values of each variable in each spatial bin (1.5 km) gridded from the raw data. The variables displayed are salinity, potential temperature, chlorophyll *a* concentration, total zooplankton abundance and total zooplankton biovolume for particles between 0.4-4.0 mm ESD. Acoustic backscatter at 20 m (the shallowest reliable data) is also displayed, which is the MVBS at 120 kHz.

Four lines of CTD stations were made in the Strait of Hormuz, each line consisting of between 5 and 7 stations. Variables have been contoured along each line and are presented in **Fig 4.1.1.iii** as contour plots on the same spatial scales as the SeaSoar data in **Fig 4.1.1.i**. The sections are labelled A to D, and their positions relative to the SeaSoar survey are shown on the map in **Fig 4.1.1.iii**. The contour plots represent

these sections from the Masandam coast out to the centre of the Strait, irrespective of the direction in which they were surveyed. The following variables are contoured: salinity, potential temperature, oxygen concentration and chlorophyll *a* concentration. The same colour scales are used as in **Fig 4.1.1.i**.

Fig 4.1.1.iv presents the full depth data from the Line D, which illustrates the low oxygen intermediate water in the northern Gulf of Oman. The spatial and colour scales used are the same as in **Figs 4.1.1.i** and **iii**.

4.1.2 Hydrographic conditions in the Strait of Hormuz

4.1.2.1 Two layered exchange in the Strait of Hormuz

The contour plots of the SeaSoar survey (**Figs 4.1.1.i**) show the two layered exchange, whereby warmer (>22.6°C) and fresher (<36.8) water from the Gulf of Oman flows westward at the surface overlying cooler (<21.7°C) and more saline (>38.0) water flowing eastward from the Arabian Gulf. The same two layered structure was described by Leveau and Szekielda (1968). The CTD sections also show the same hydrographic structure (**Fig 4.1.1.iii**; note these are perpendicular to the SeaSoar transects), which demonstrate that the AGO travels adjacent to the Masandam coast, and the GOS near the centre of the channel. The *Mt Mitchell* expedition (1992) survey, which had lines of 5 CTD stations crossing the whole Strait, demonstrated that the inflow was even stronger closer to the Iranian coast (Reynolds, 1993). Sultan and Elghribi (1996) have attributed the horizontal distribution of the inflow and outflow to the effect of Coriolis force. Evaporation in the Arabian Gulf is four times greater than freshwater inputs (Reynolds, 1993), and to balance this deficit water is drawn into the Arabian Gulf through the Strait from the Gulf of Oman. The high evaporation also forms the high salinity outflow, which forms a density driven flow back out eastwards through the Strait.

The surface inflow from the Gulf of Oman (GOS), and the high salinity outflow from the Arabian Gulf (AGO) are mixed together in the Strait, to form a distinct water type the Strait transition water (STW). The STW represents a frontal region between the two flows formed by mixing at the mesoscale. **Fig 4.1.2.i** is a temperature-salinity plot for the water sampled by the CTD in the Gulf of Oman (red) and Arabian Gulf (green) and by the SeaSoar in the Strait of Hormuz (blue). The plot shows that the STW was only found in the Strait and is characterised by a temperature between 21.7 and 22.6°C, and a salinity between 36.8 and 38.0.

Figure 4.1.1.ia Contour plots of legs through the Strait of Hormuz

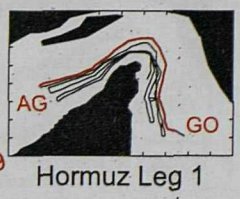

Hormuz Leg 1

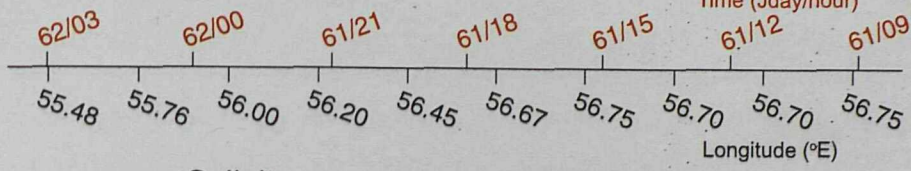

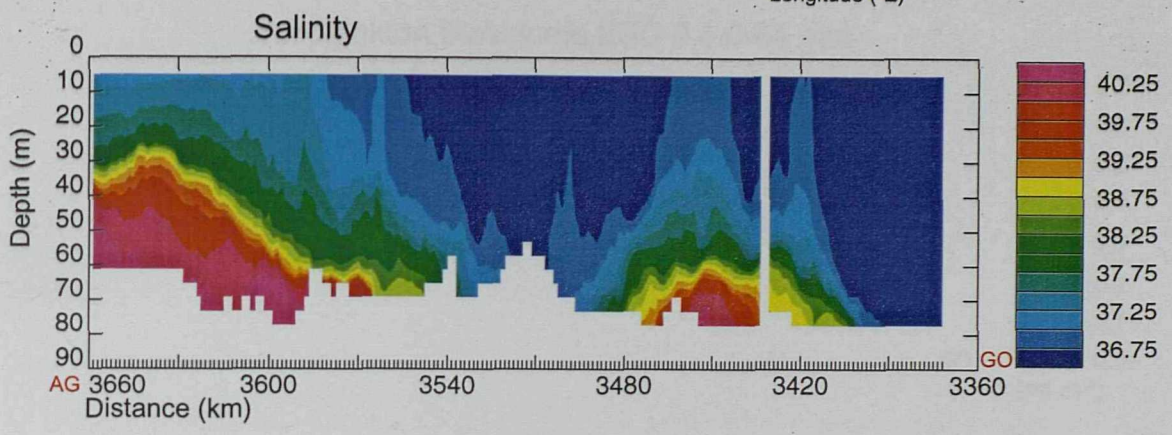

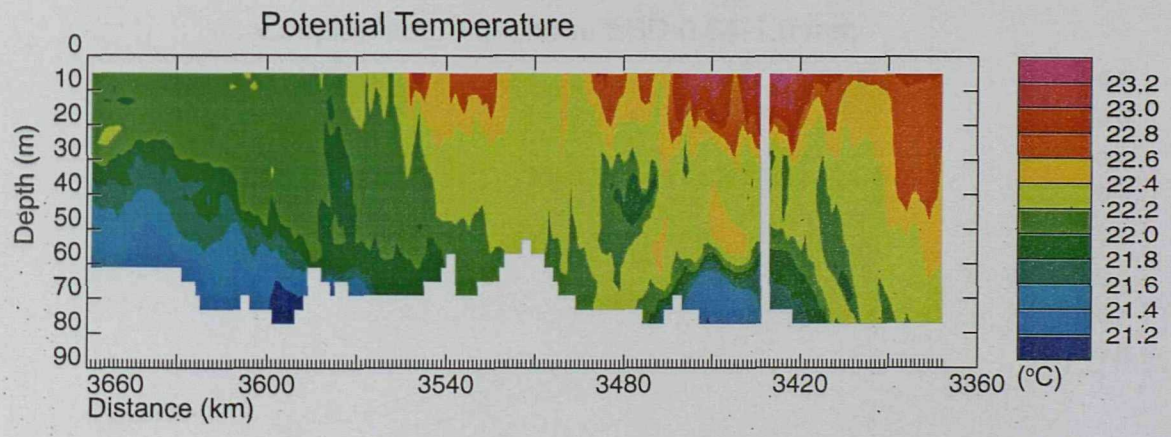

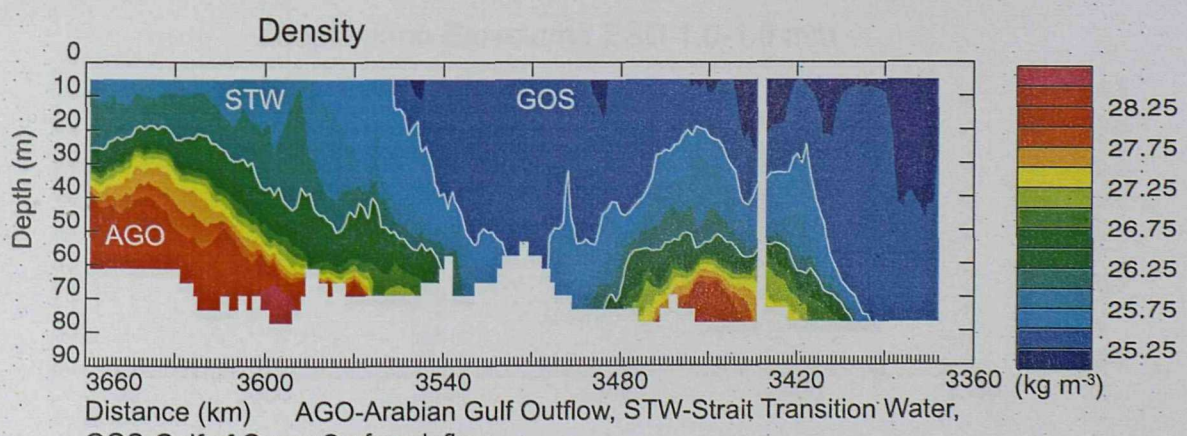

Distance (km) AGO-Arabian Gulf Outflow, STW-Strait Transition Water, GOS-Gulf of Oman Surface inflow

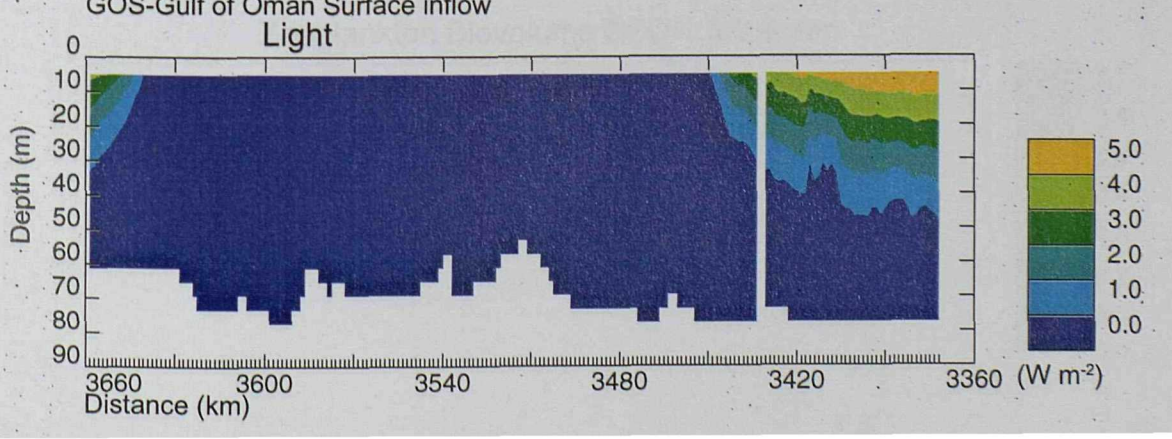

Figure 4.1.1.ib Contour plots of legs through the Strait of Hormuz

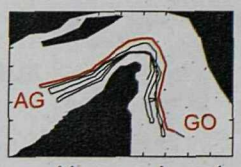

Hormuz Leg 1

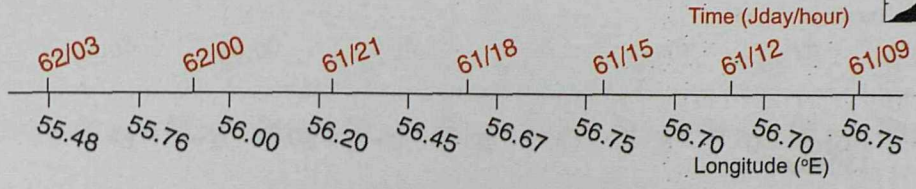

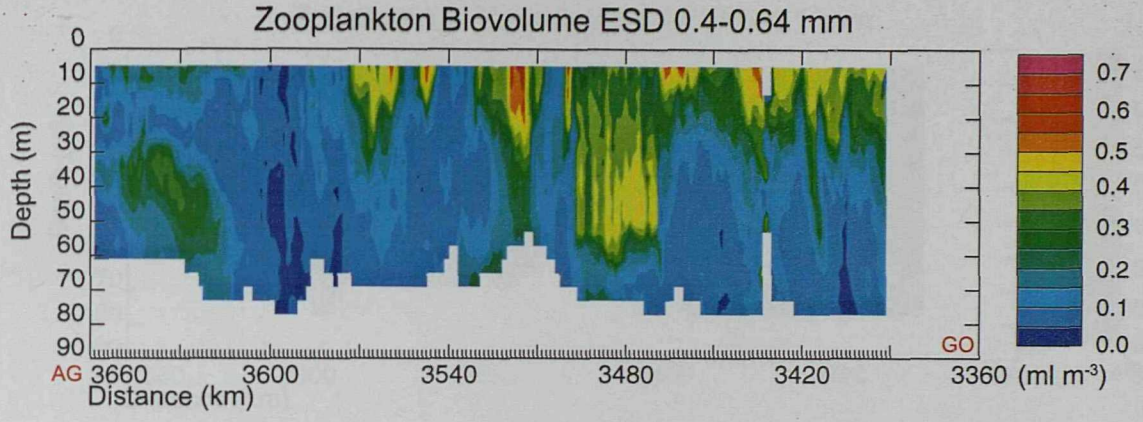

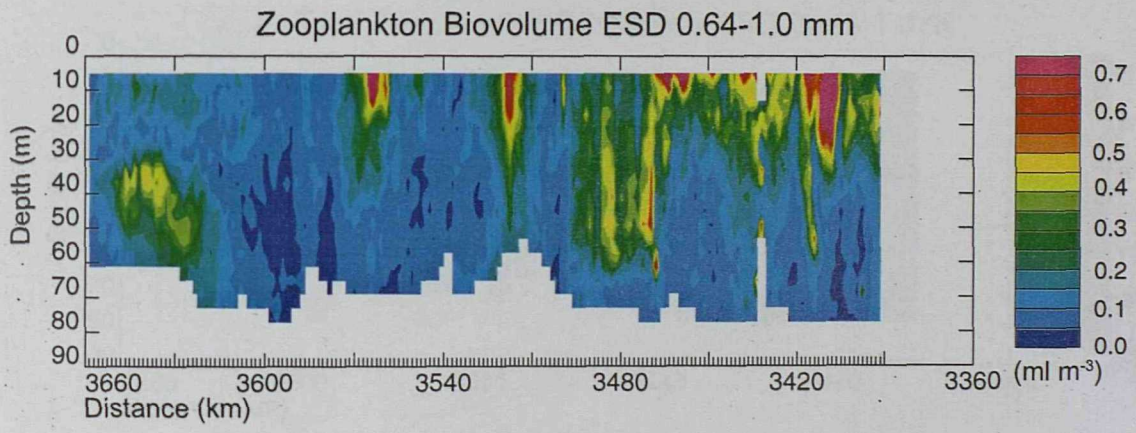

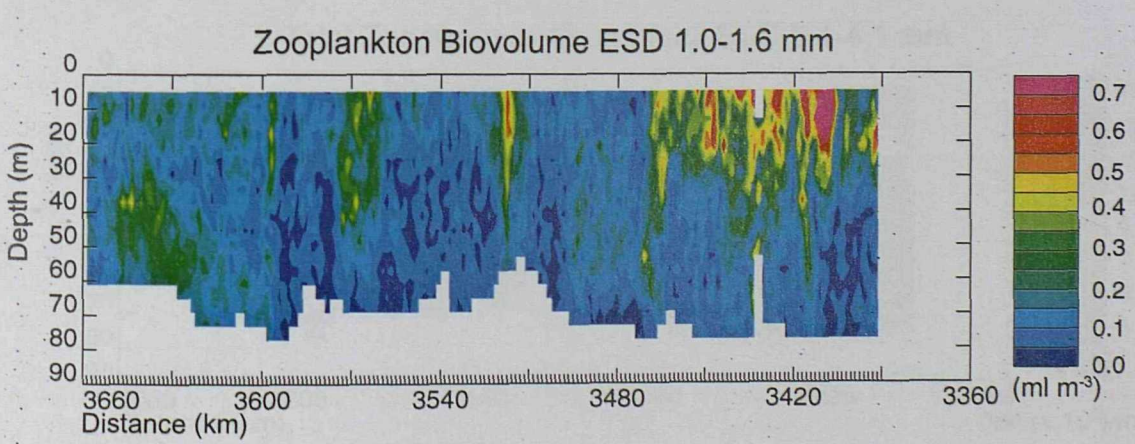

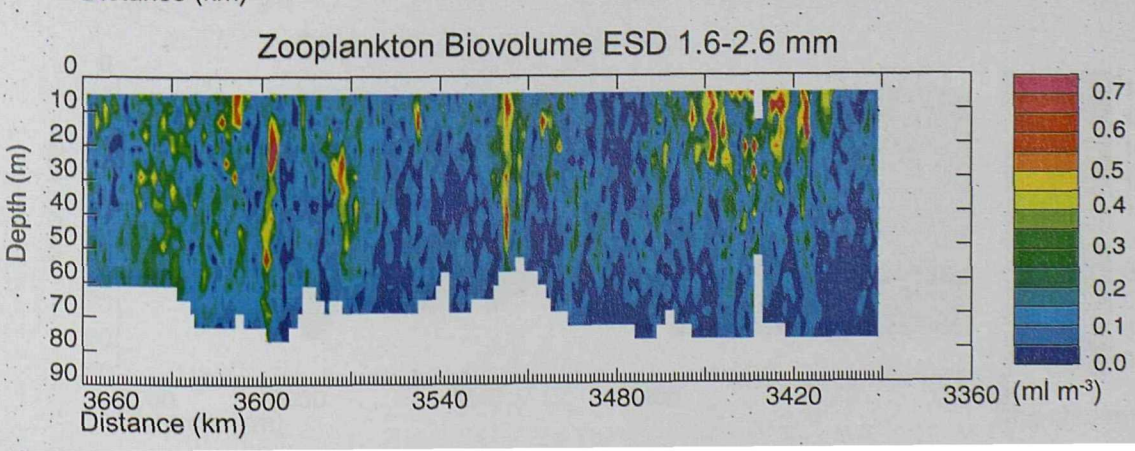

Figure 4.1.1.ic Contour plots of legs through the Strait of Hormuz

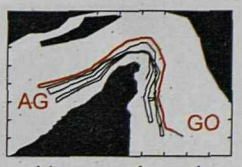

Hormuz Leg 1

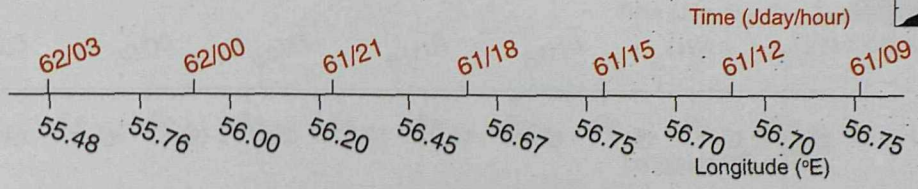

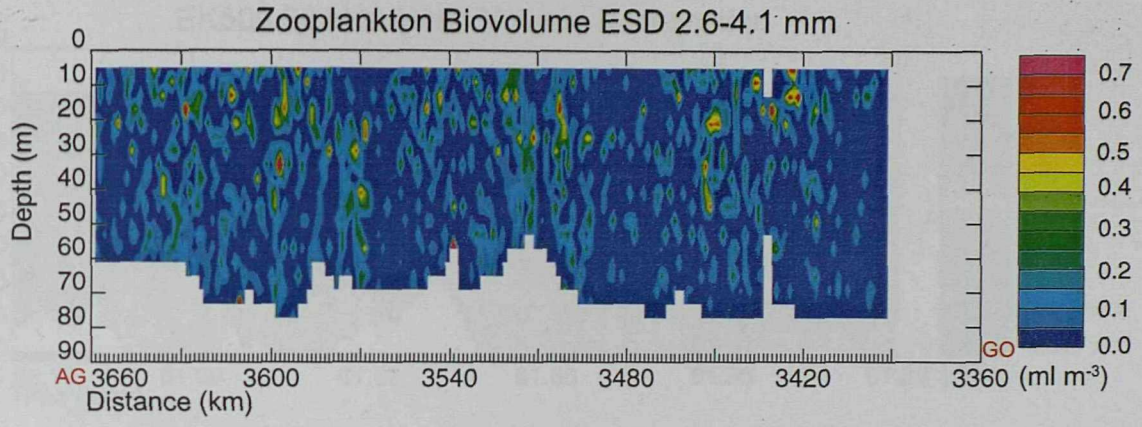

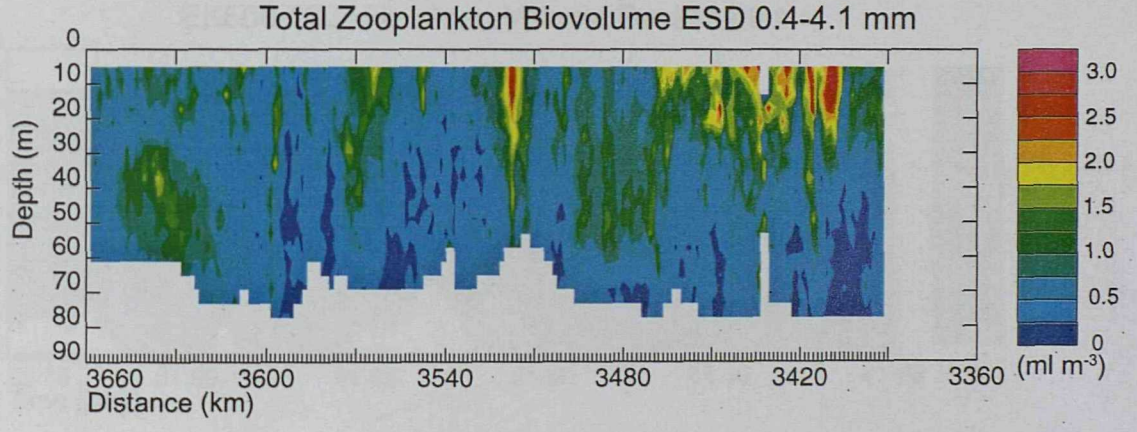

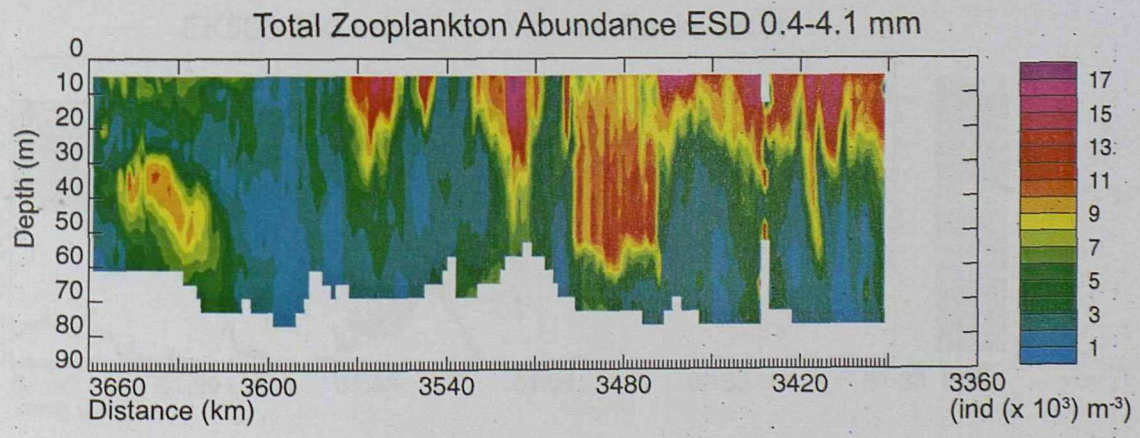

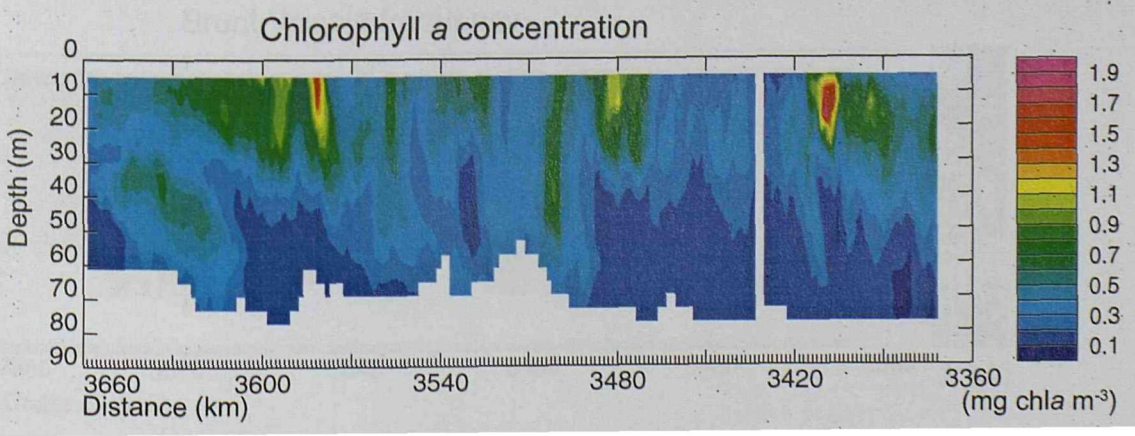

Figure 4.1.1.id Contour plots of legs through the Strait of Hormuz

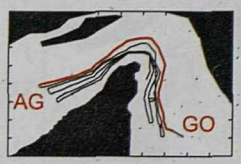

Hormuz Leg 1

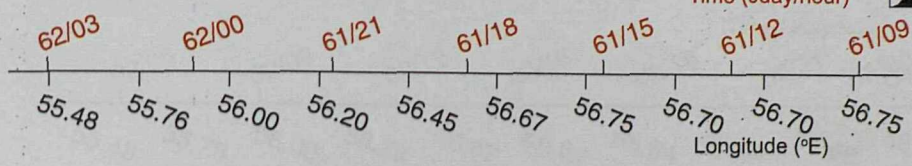

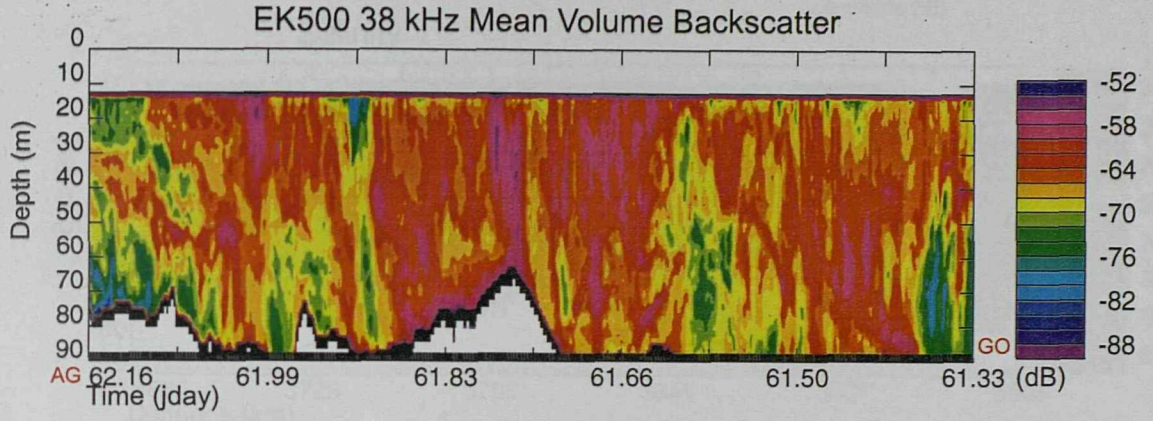

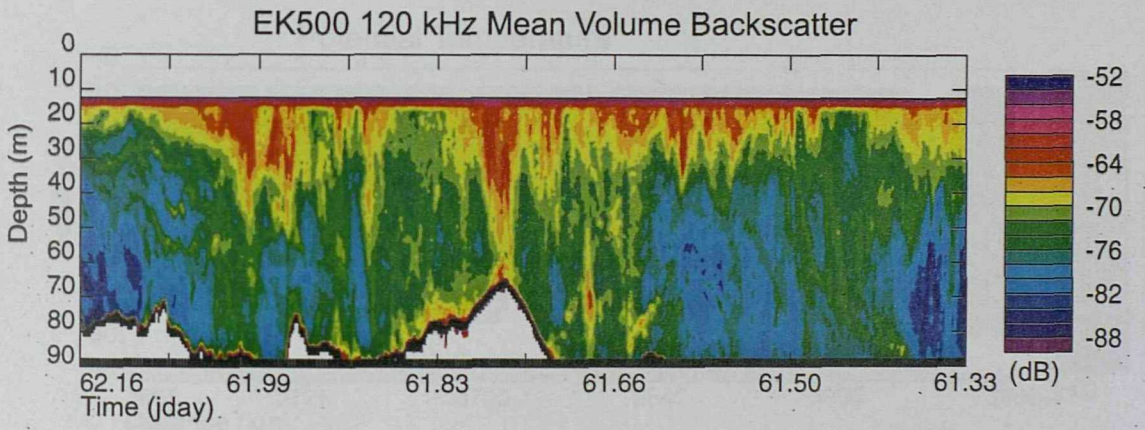

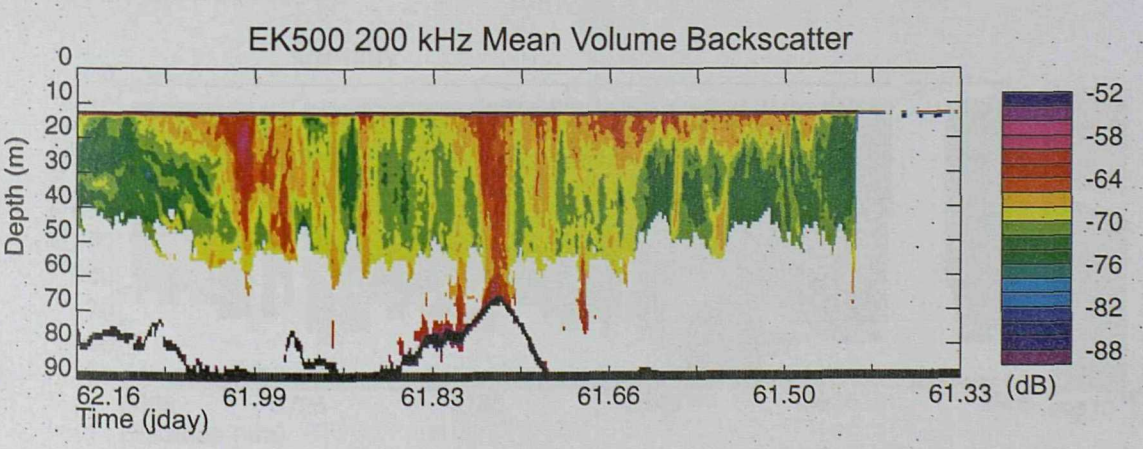

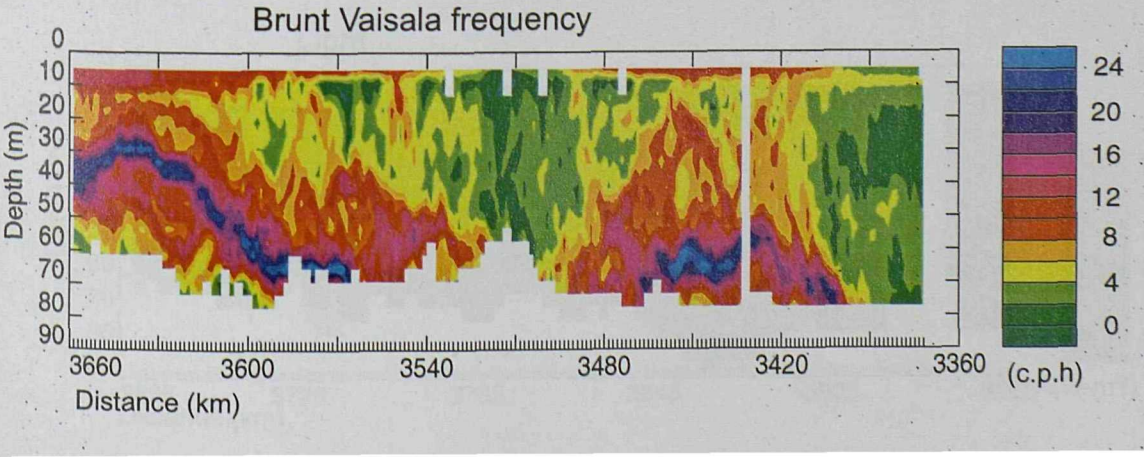

Figure 4.1.1.ie Contour plots of legs through the Strait of Hormuz

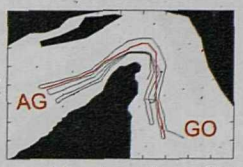

Hormuz Leg 2

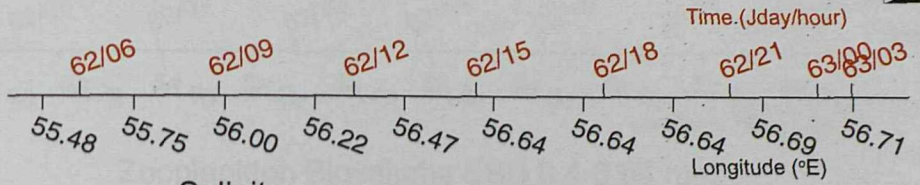

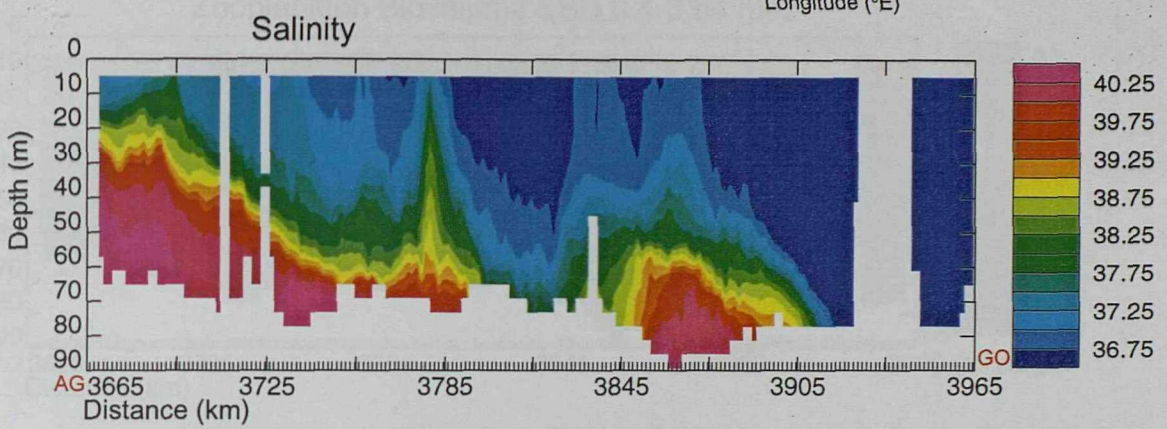

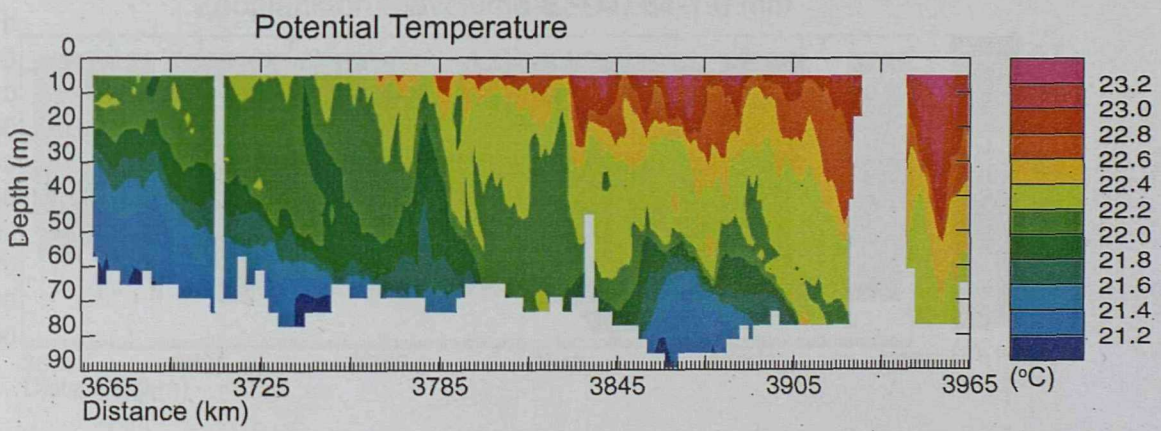

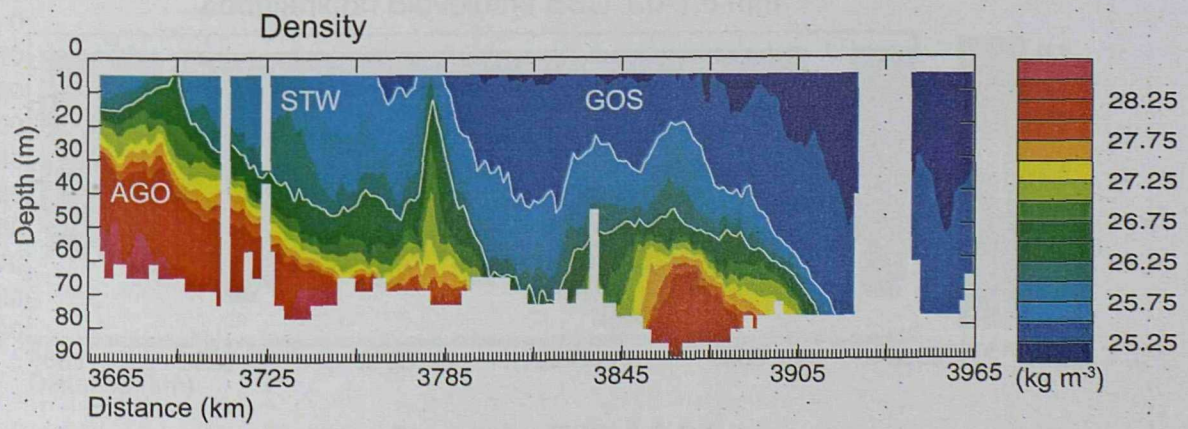

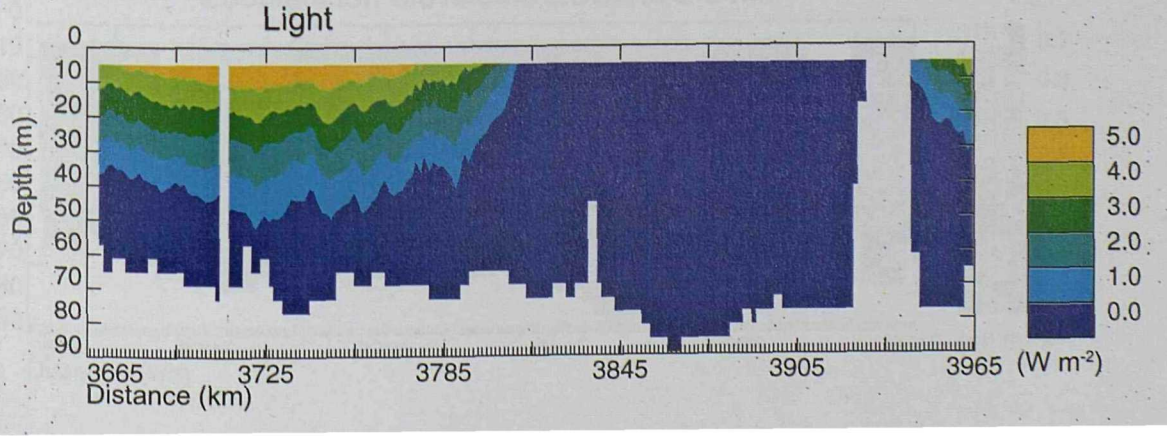

Figure 4.1.1.if Contour plots of legs through the Strait of Hormuz

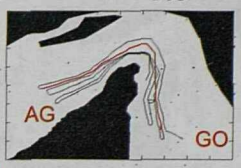

Hormuz Leg 2

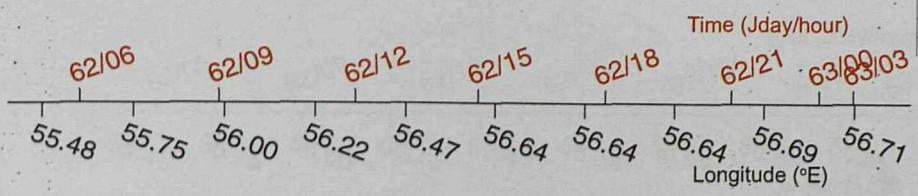

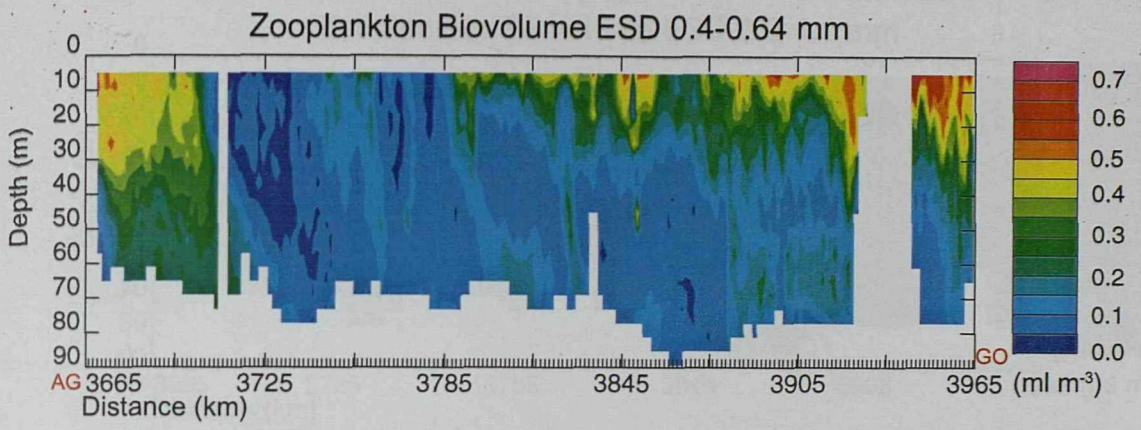

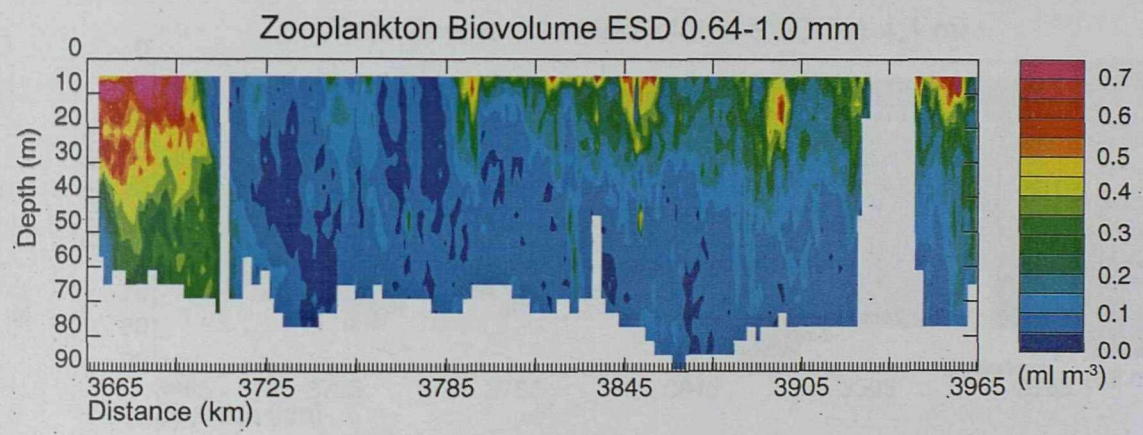

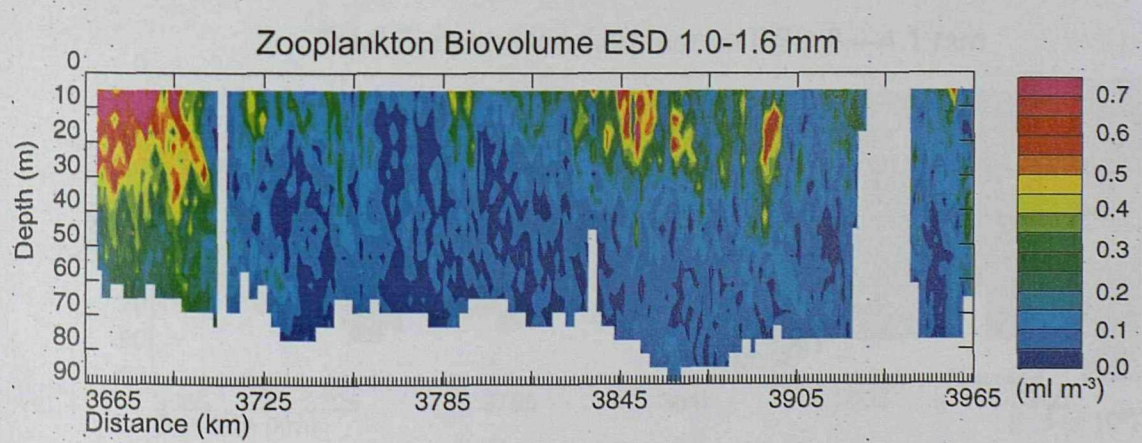

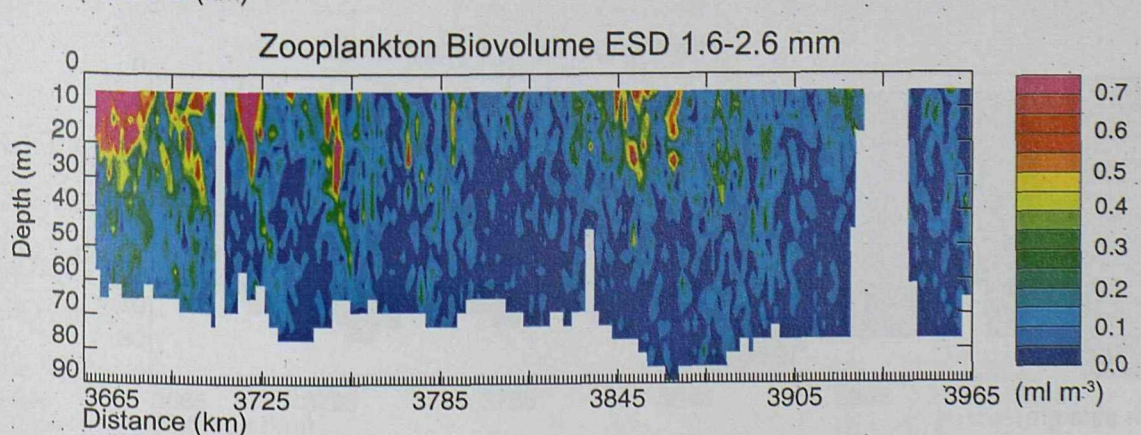

Figure 4.1.1.ig Contour plots of legs through the Strait of Hormuz

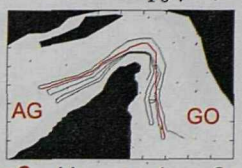

Hormuz Leg 2

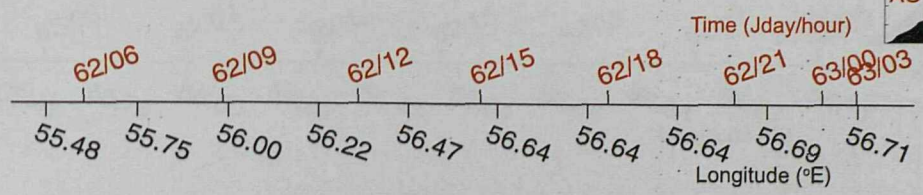

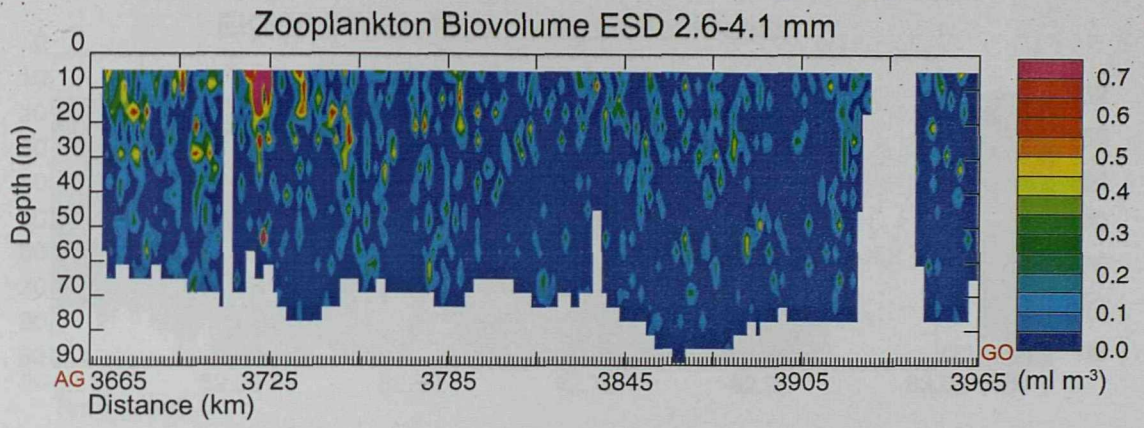

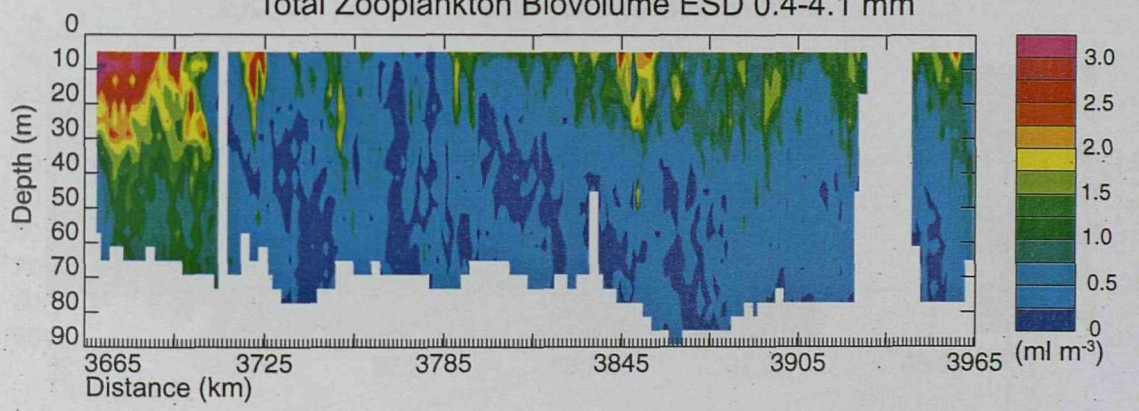

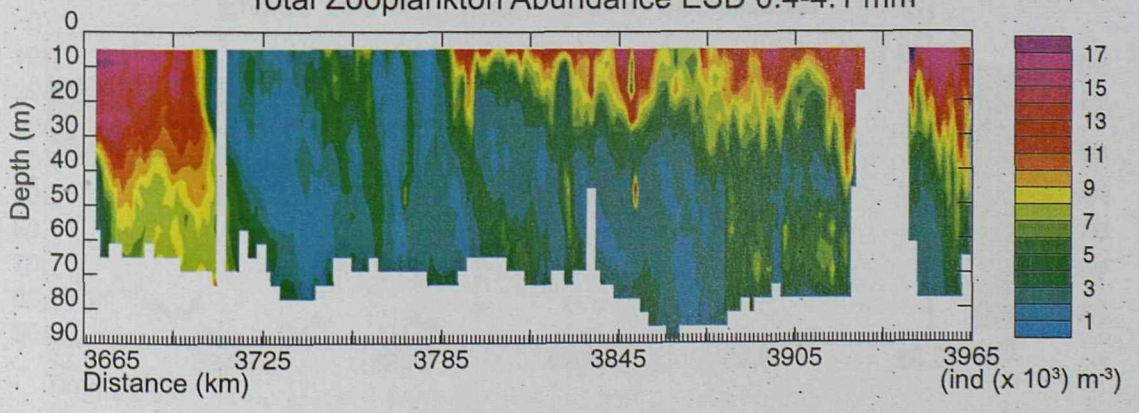

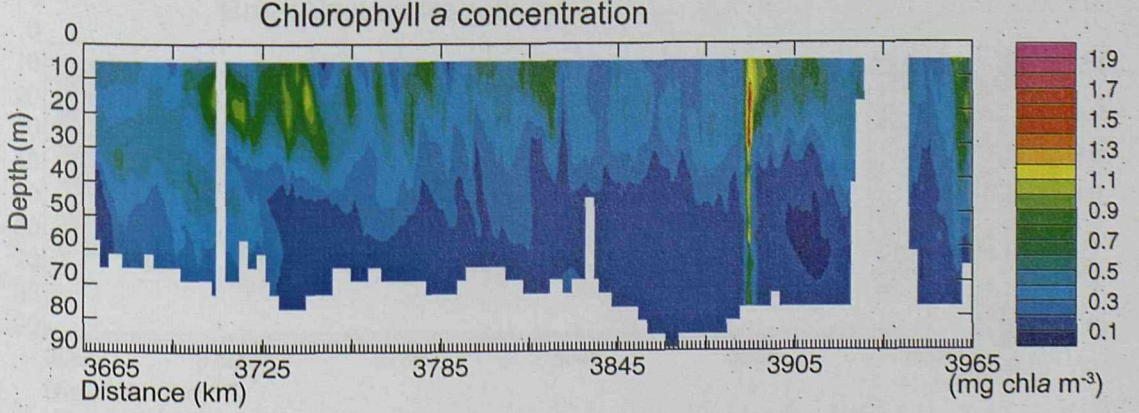

Figure 4.1.1.ih Contour plots of legs through the Strait of Hormuz

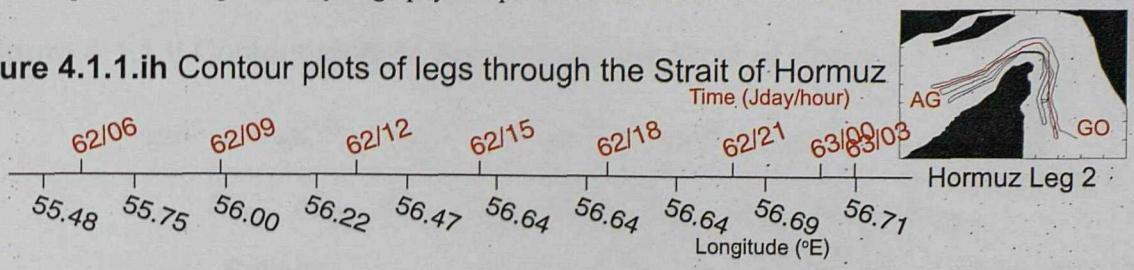

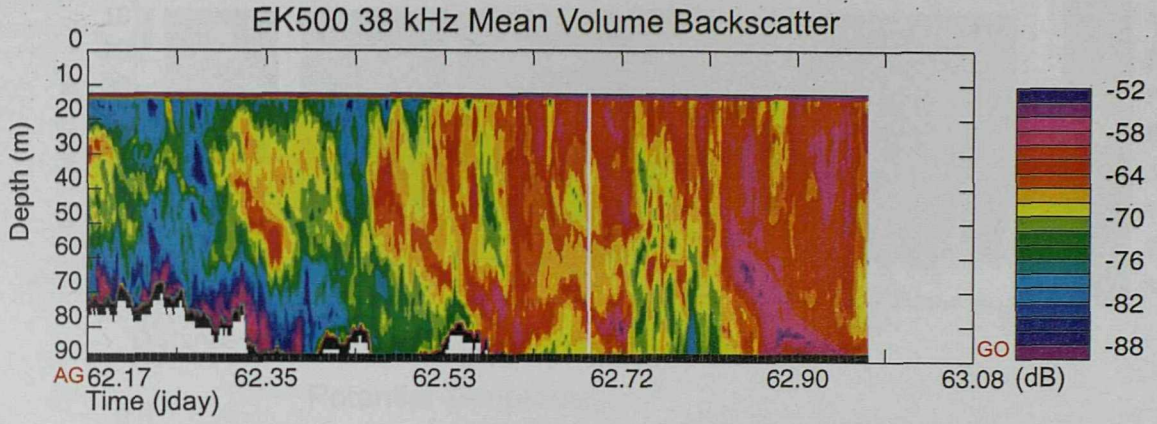

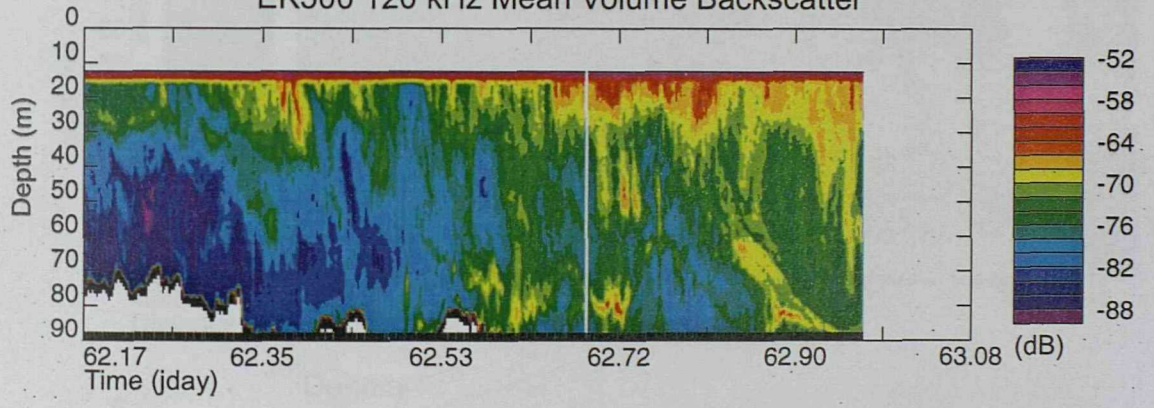

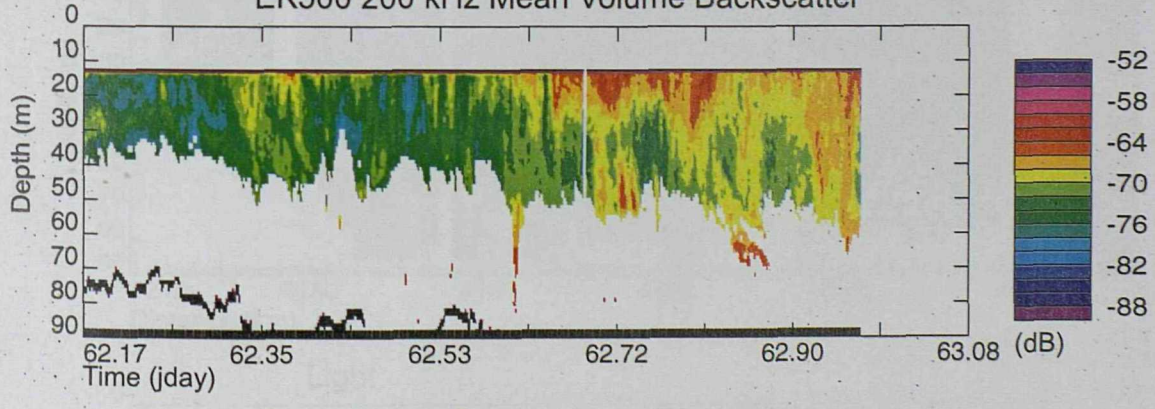

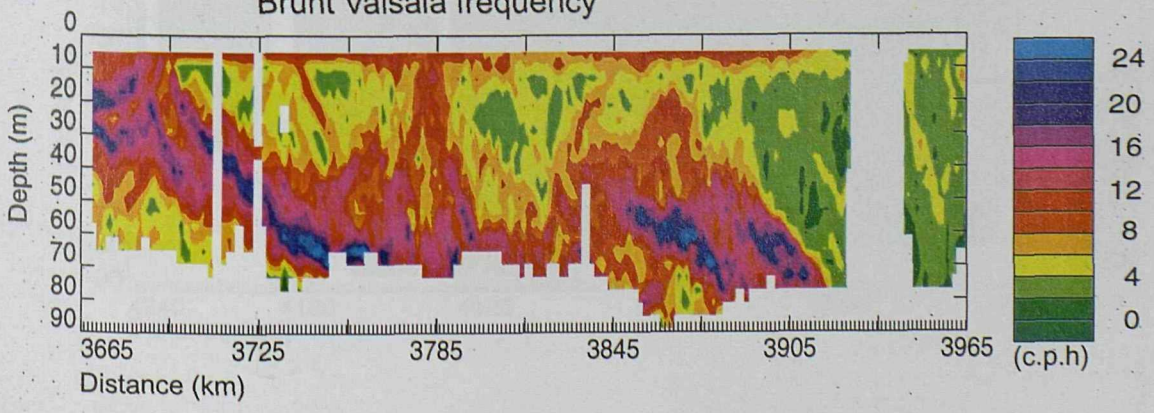

Figure 4.1.1.ij Contour plots of legs through the Strait of Hormuz

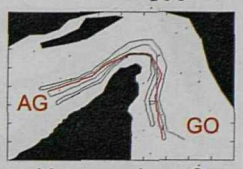

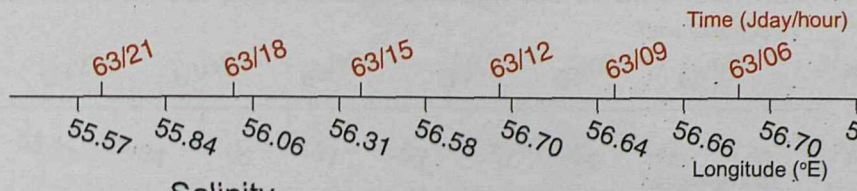

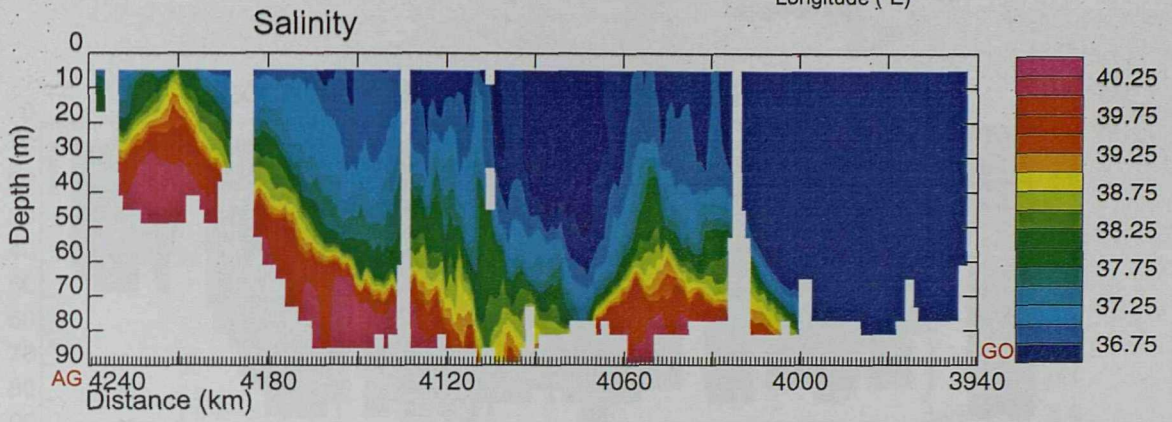

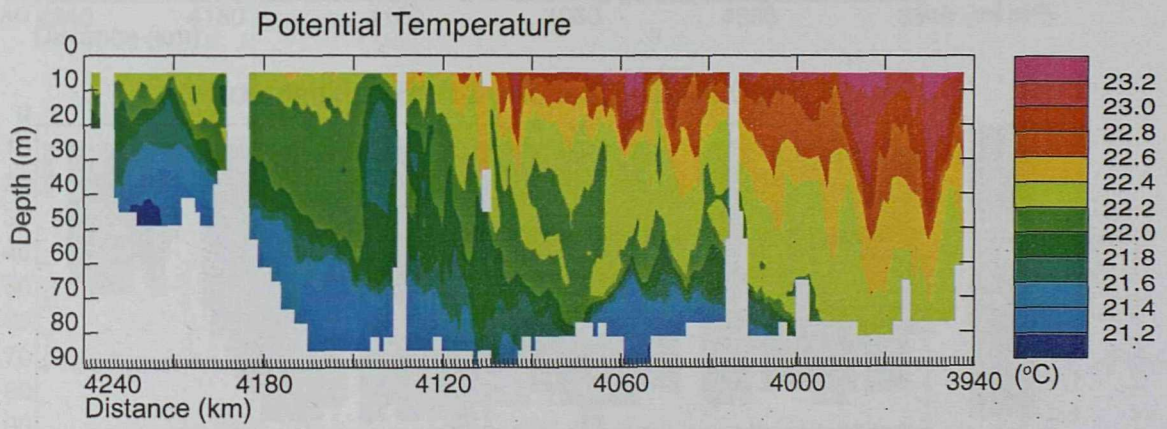

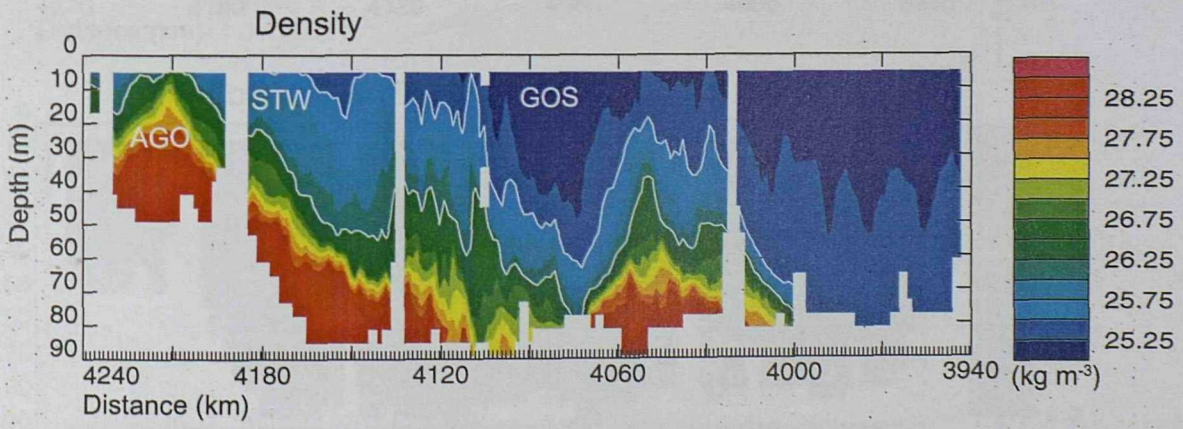

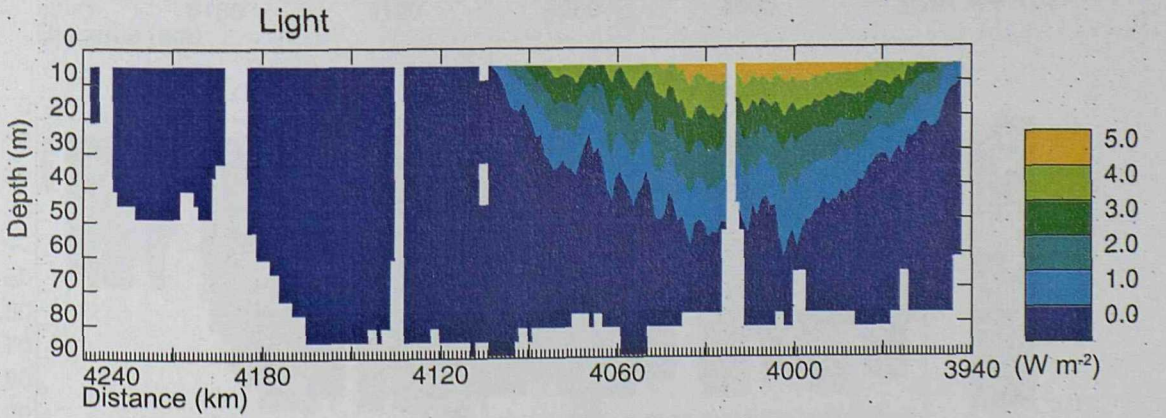

Figure 4.1.1.ik Contour plots of legs through the Strait of Hormuz

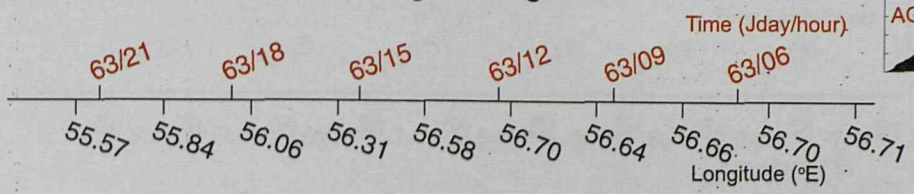

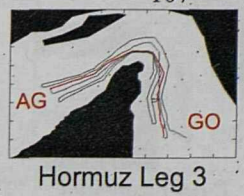

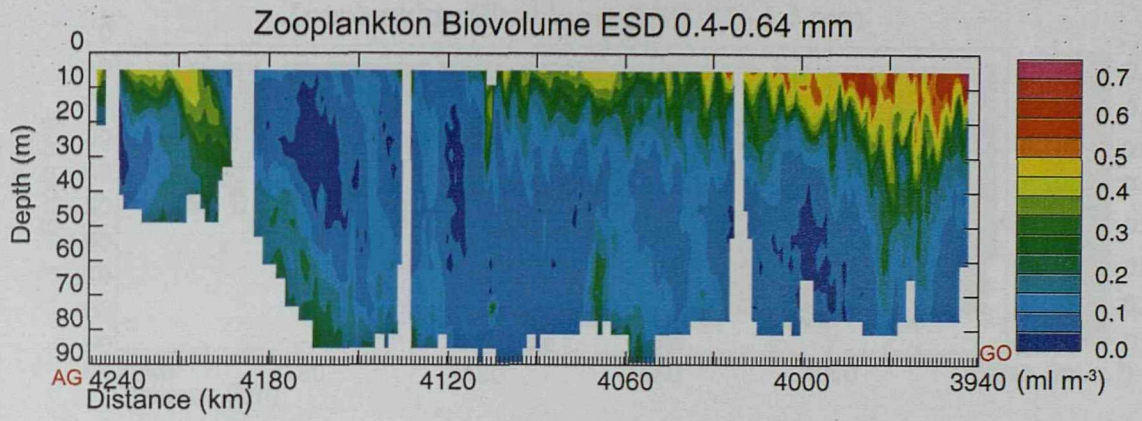

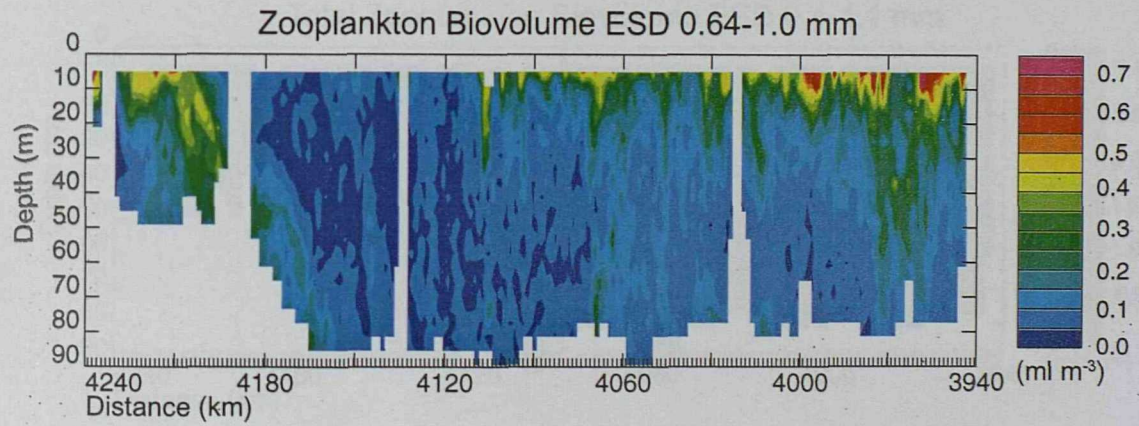

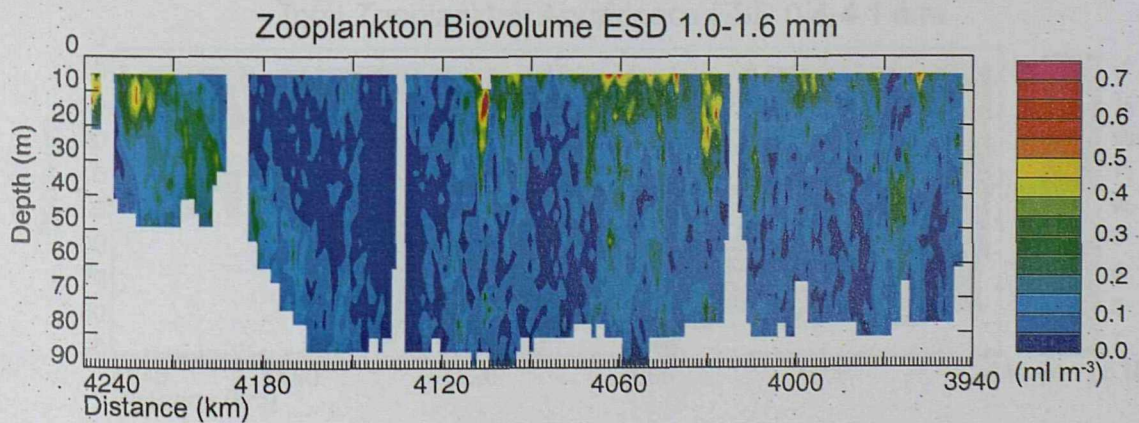

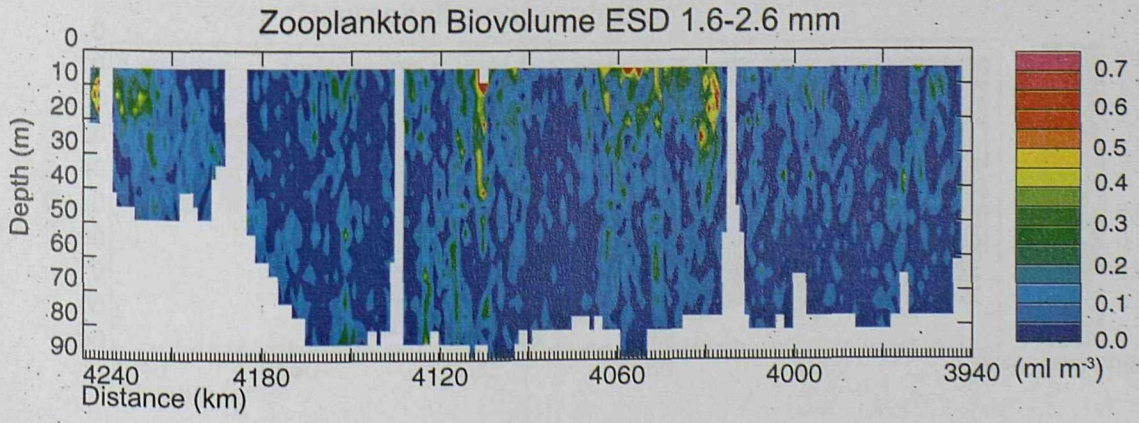

Figure 4.1.1.il Contour plots of legs through the Strait of Hormuz

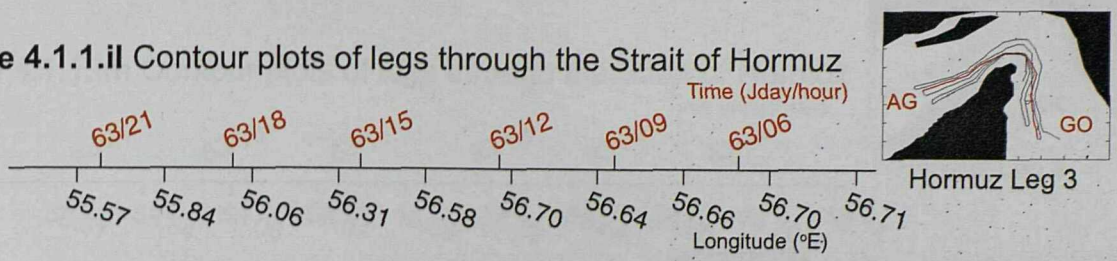

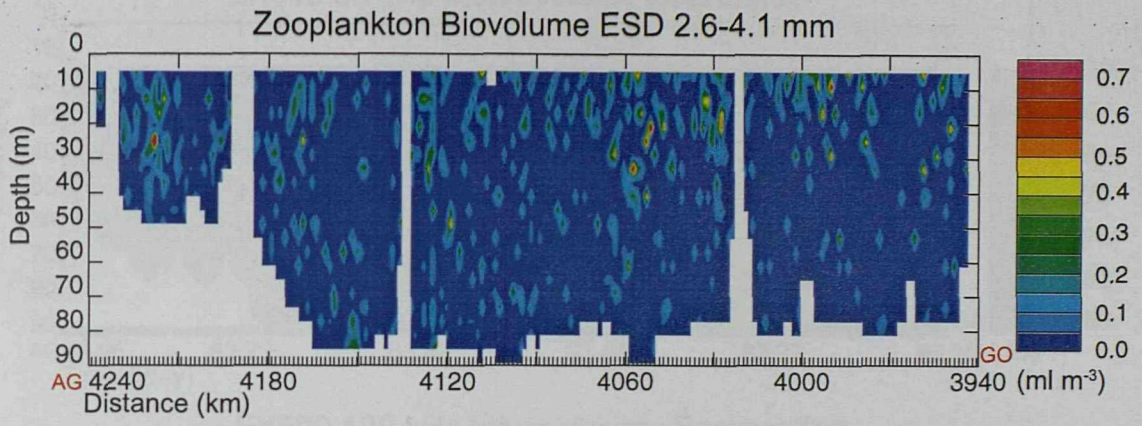

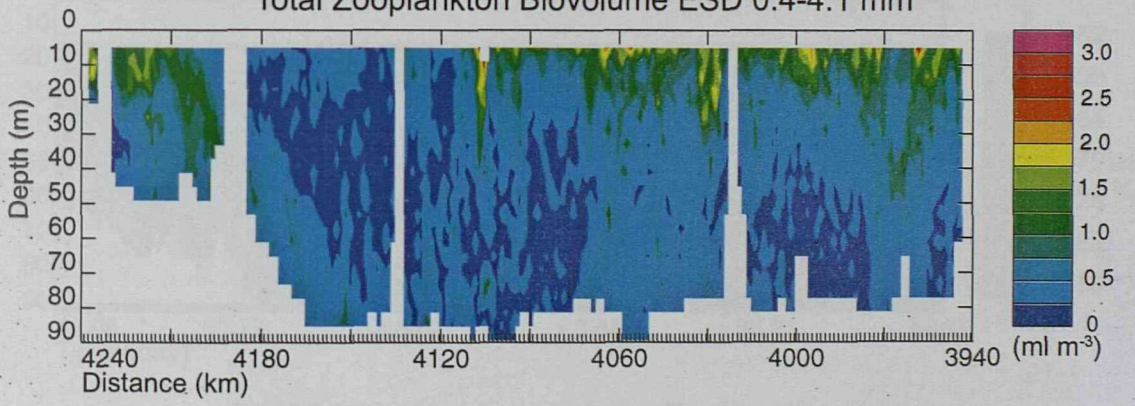

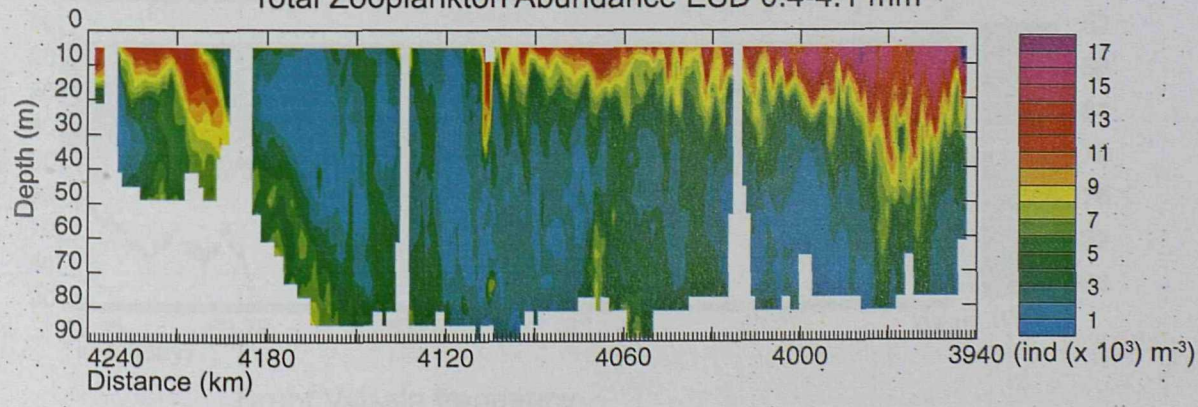

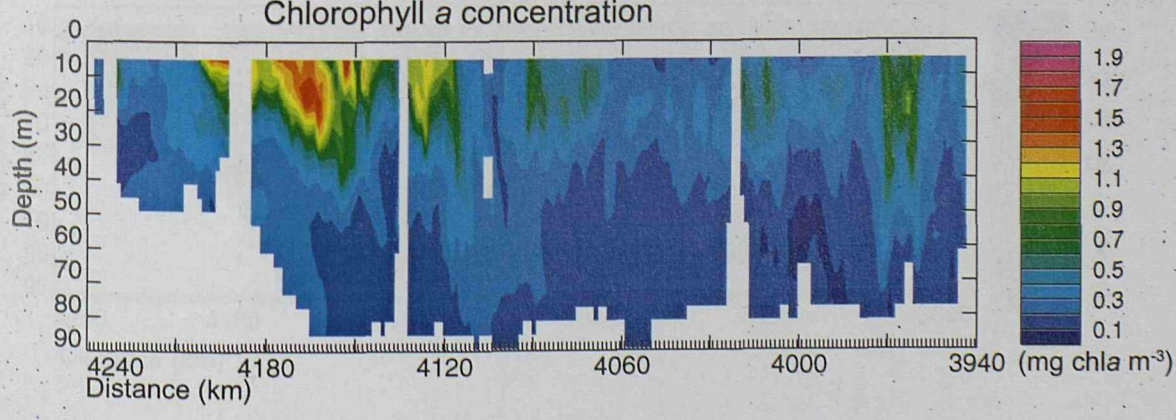

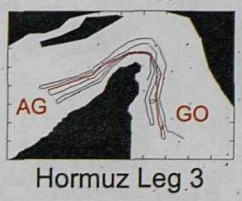

Figure 4.1.1.im Contour plots of legs through the Strait of Hormuz

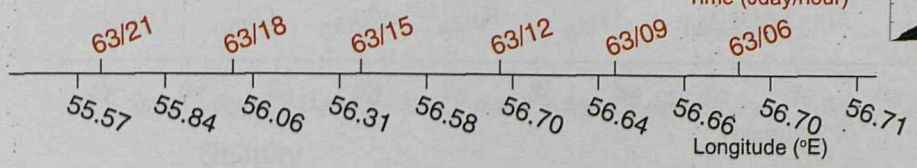

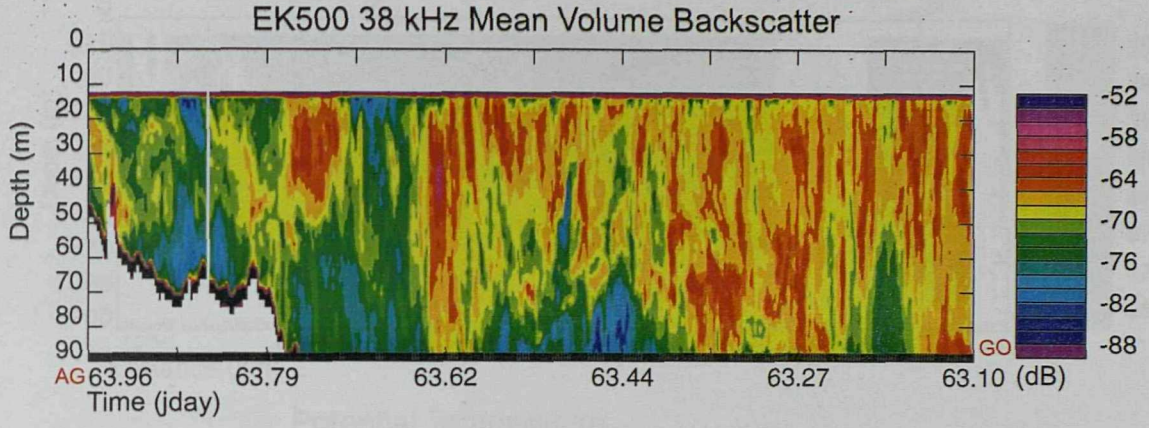

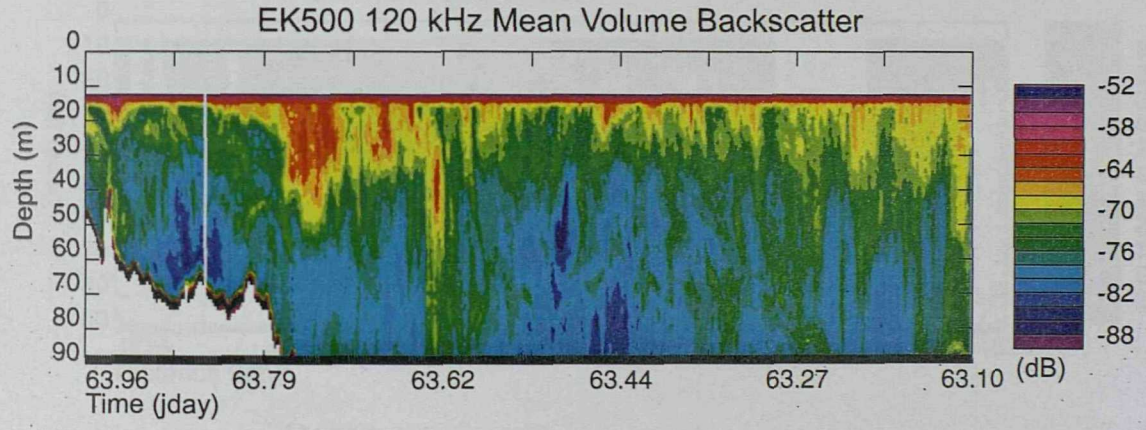

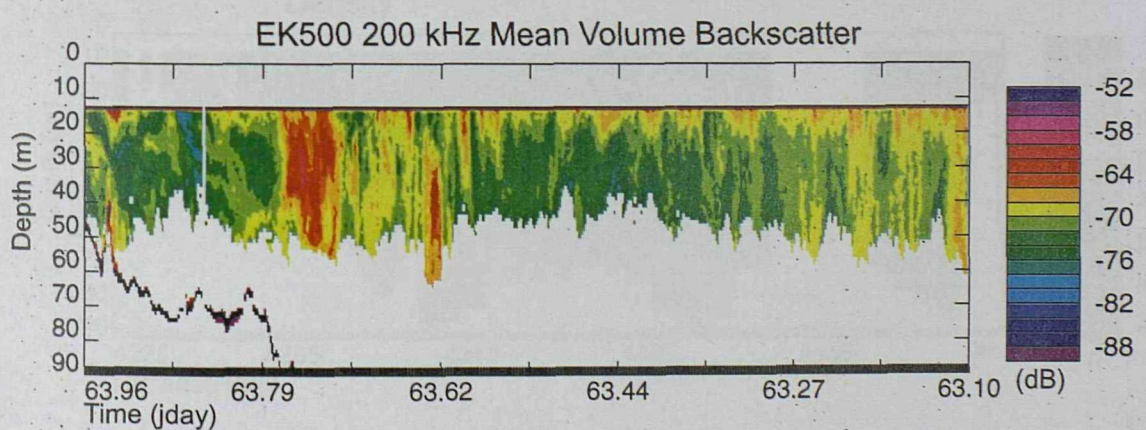

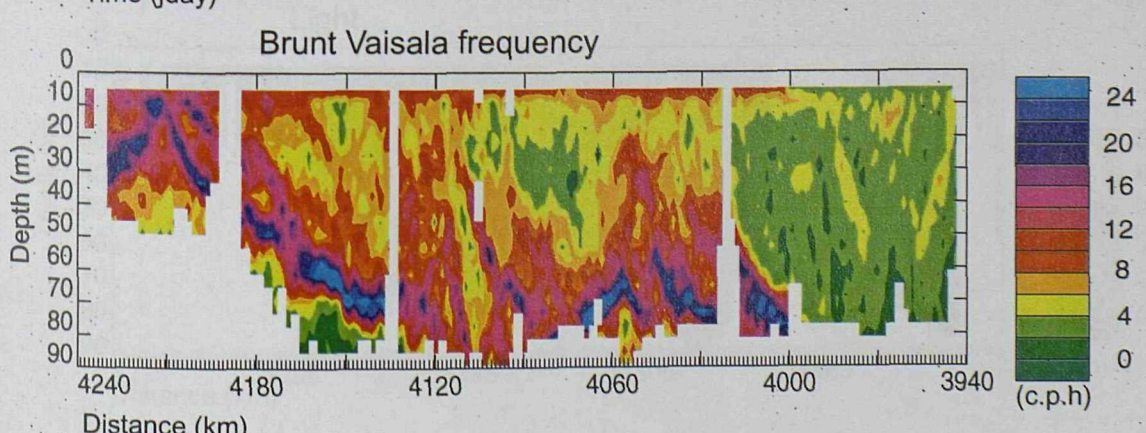

Figure 4.1.1.in Contour plots of legs through the Strait of Hormuz

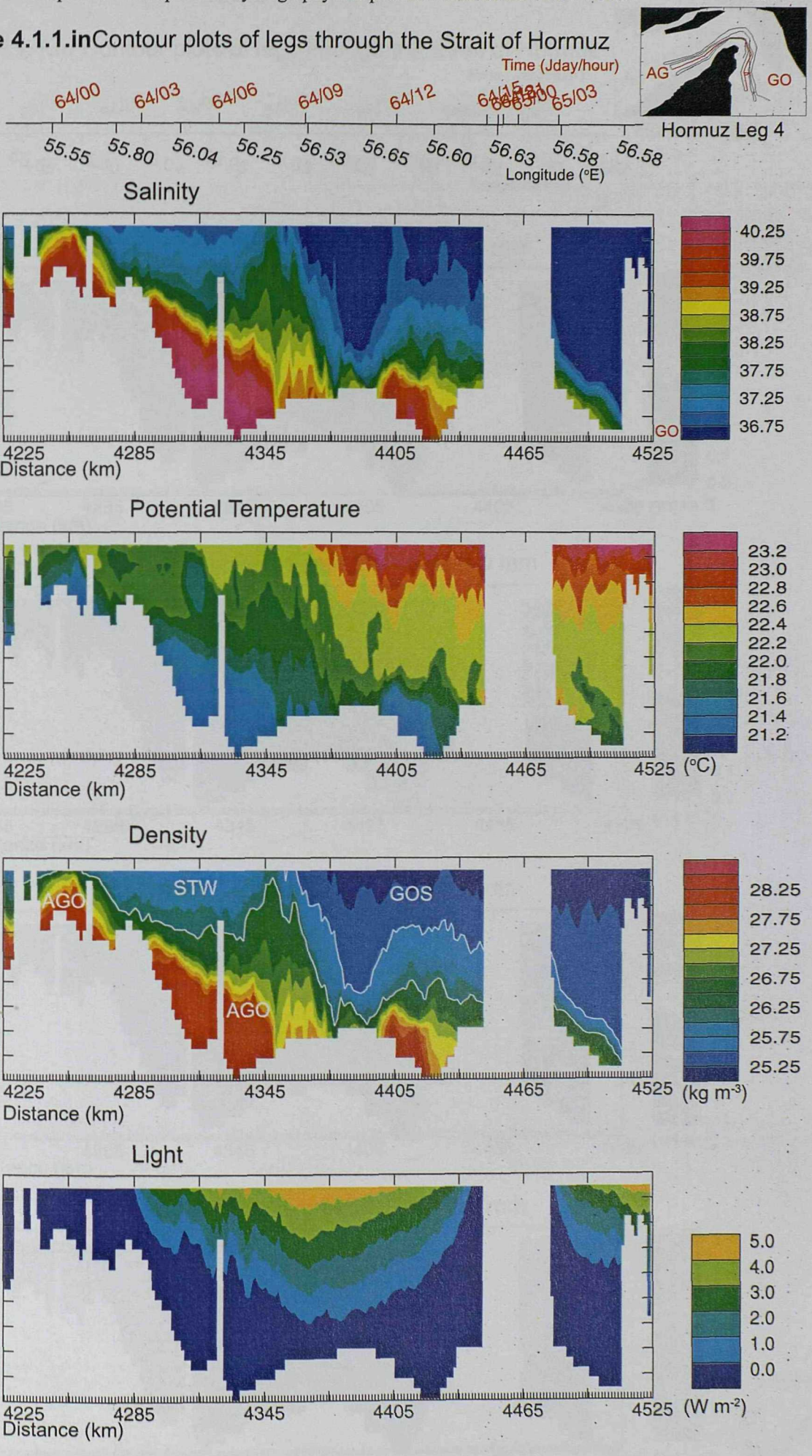

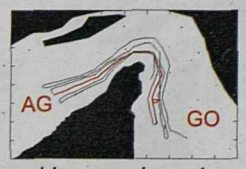

Hormuz Leg 4

Figure 4.1.1.io Contour plots of legs through the Strait of Hormuz

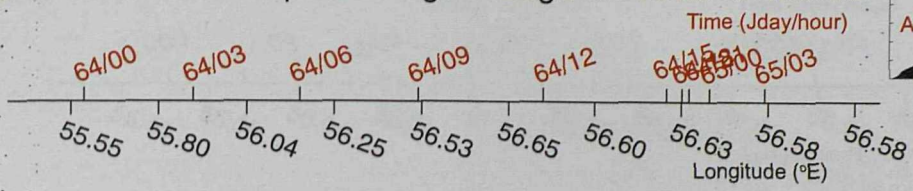

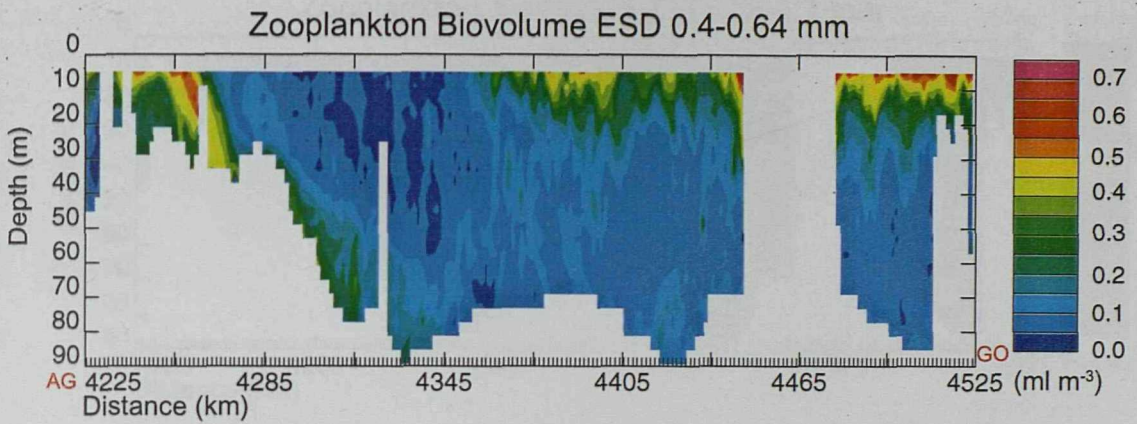

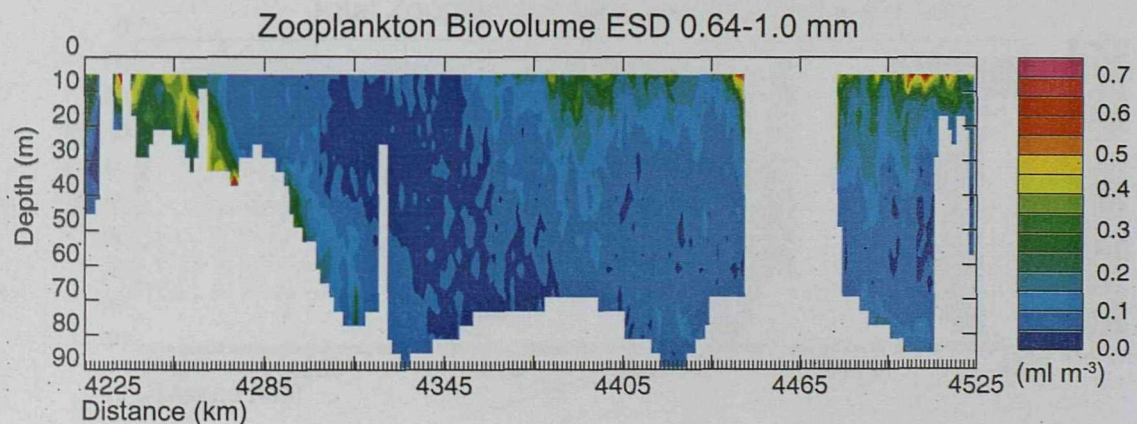

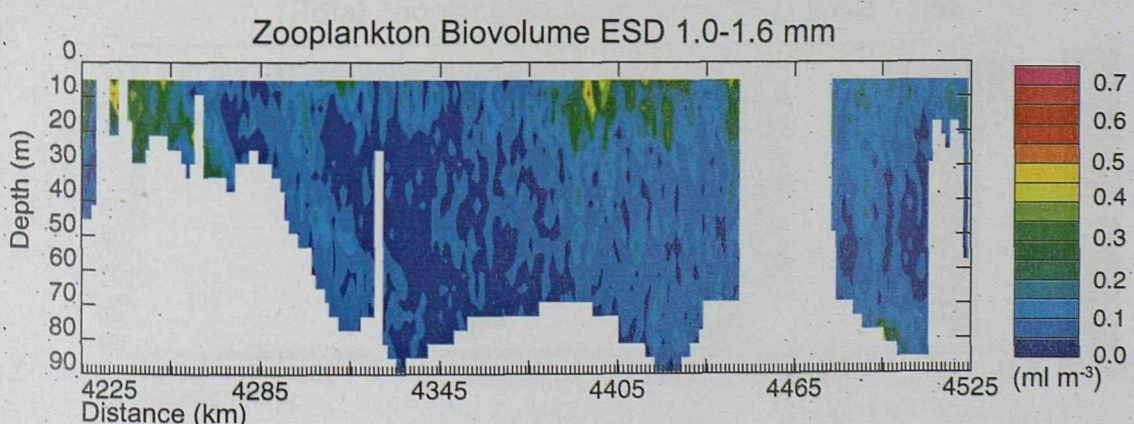

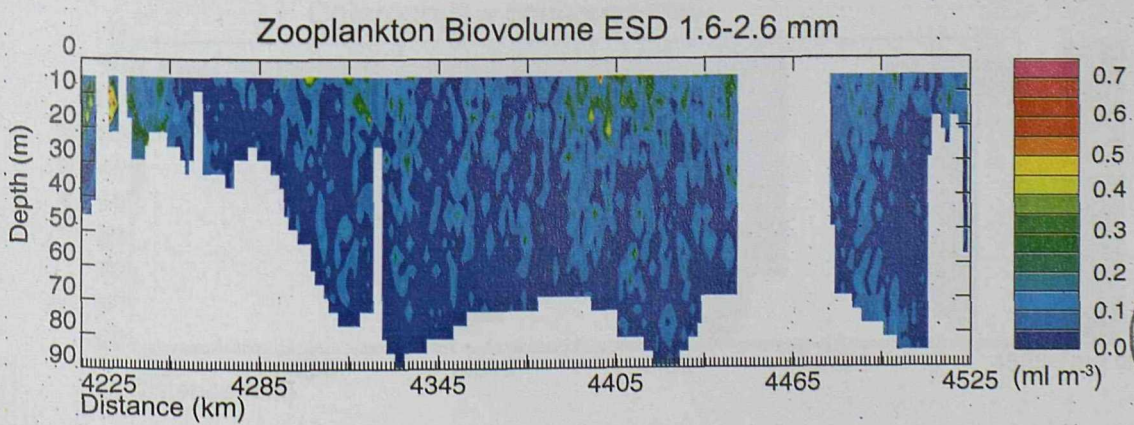

Figure 4.1.1.ip Contour plots of legs through the Strait of Hormuz

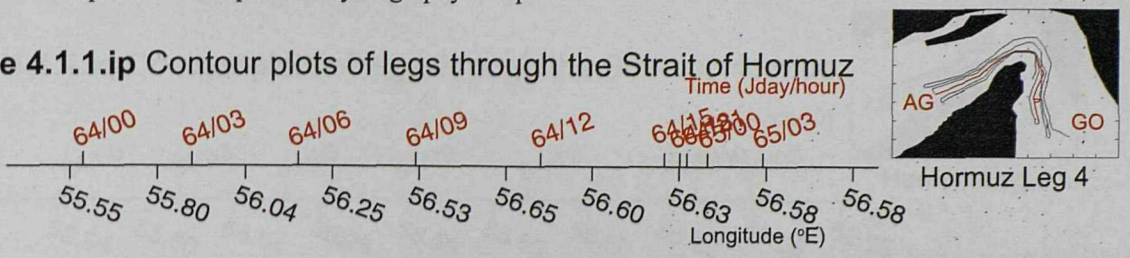

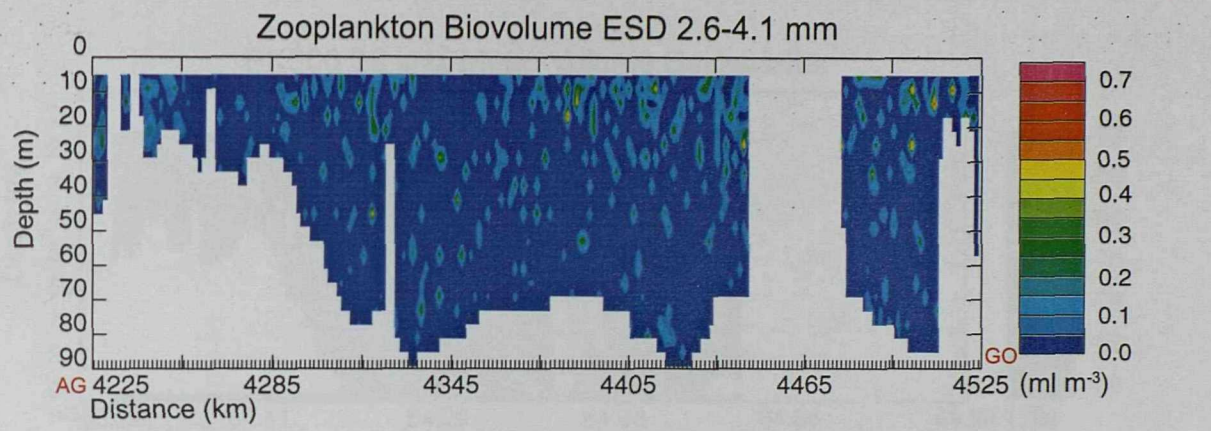

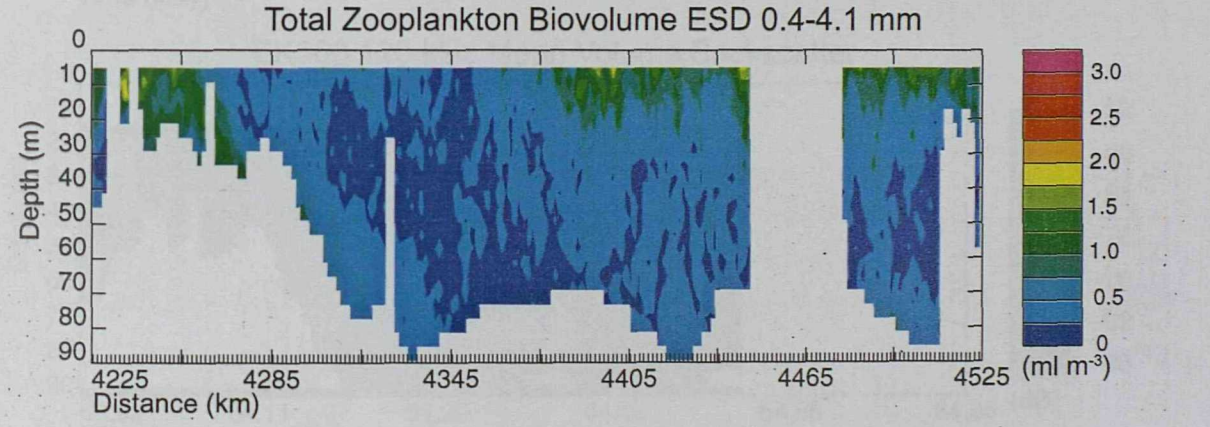

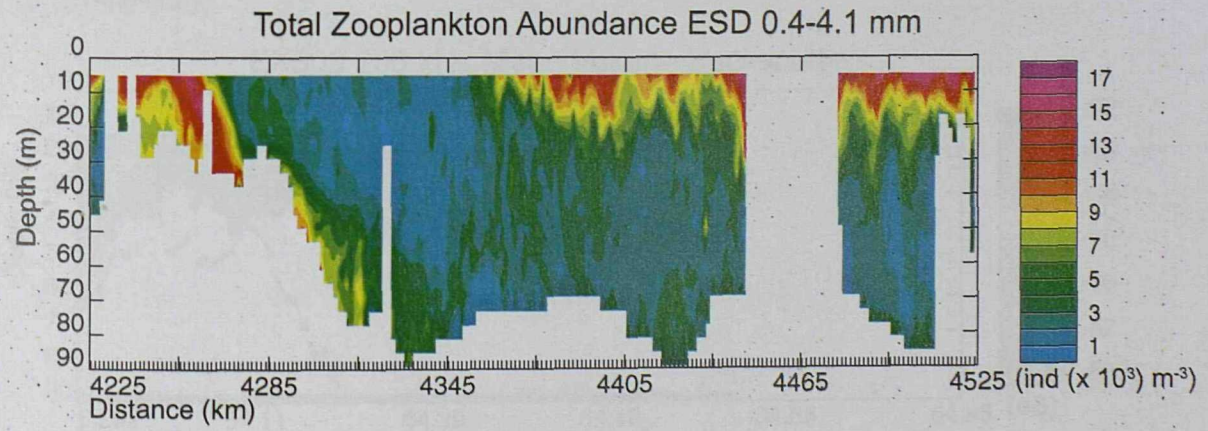

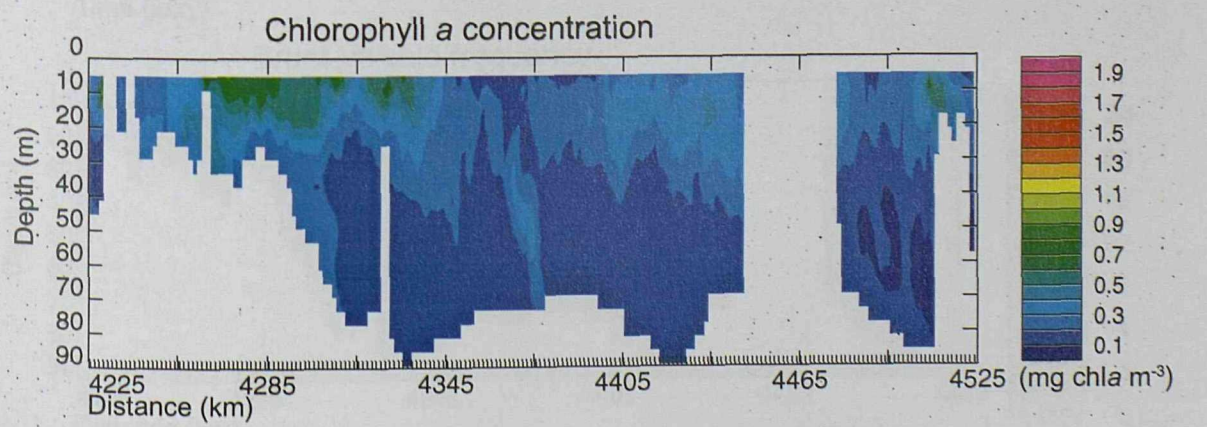

Figure 4.1.1.iq Contour plots of legs through the Strait of Hormuz

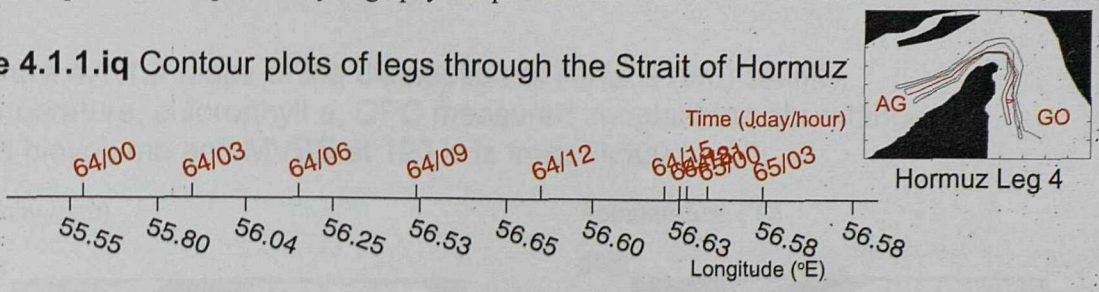

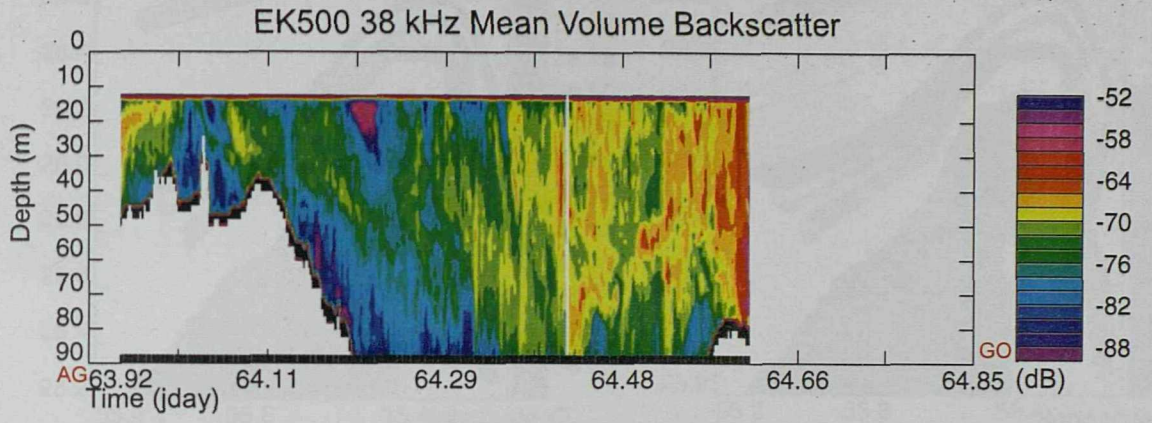

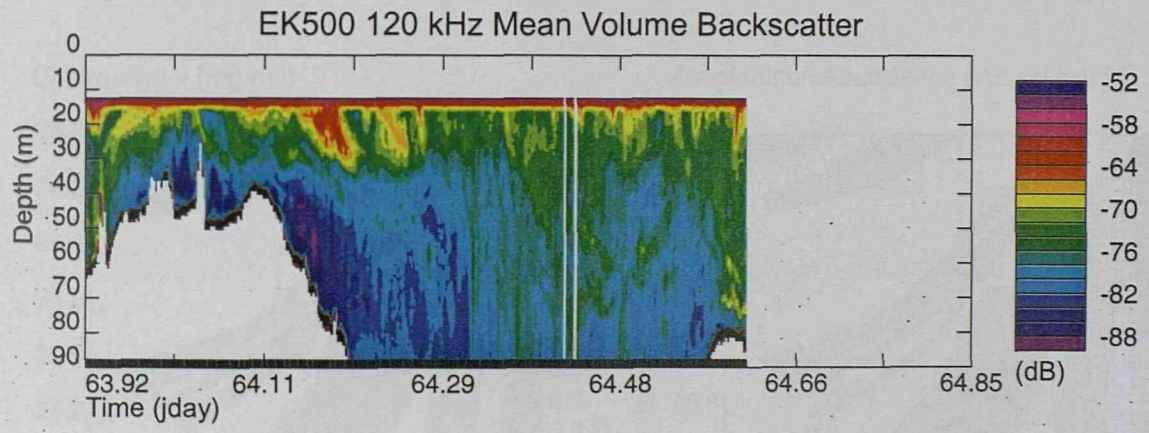

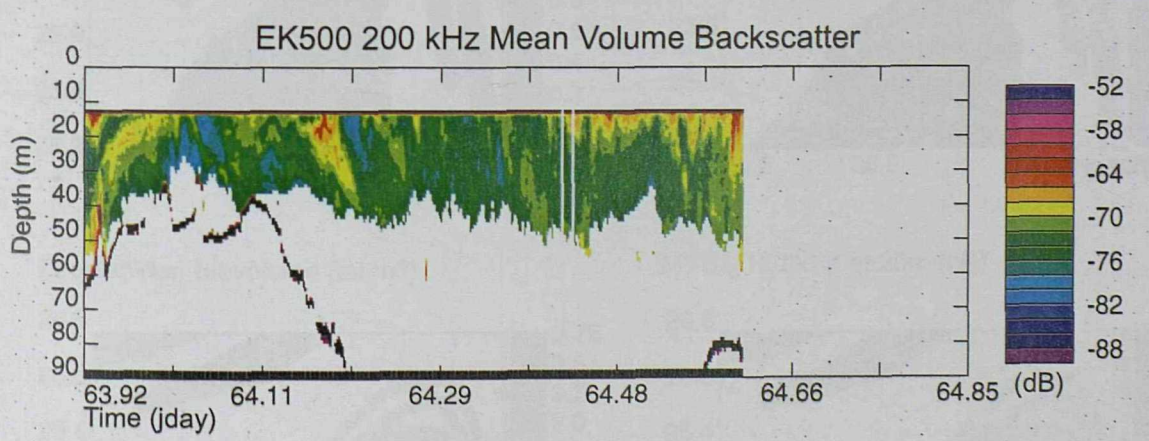

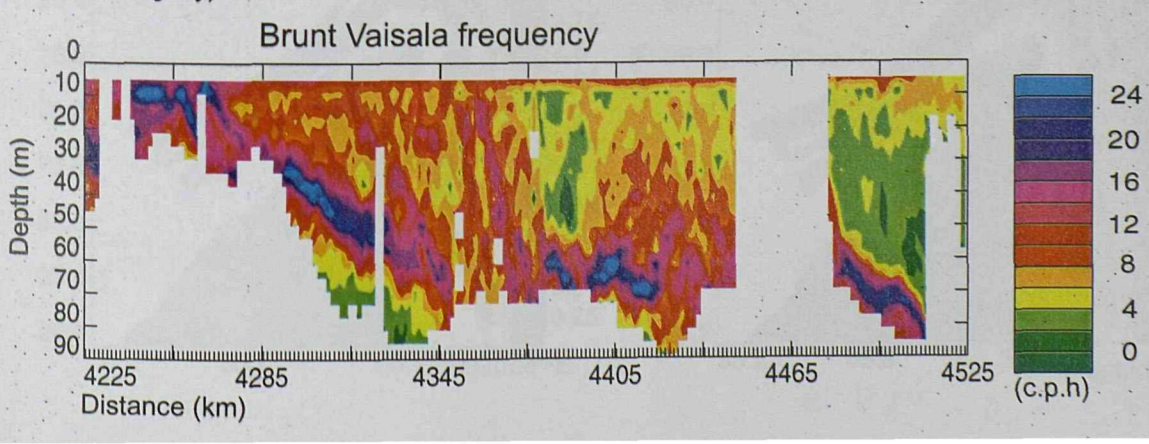

Figure 4.1.1.ii Maps of the distribution of surface (9m) salinity, temperature, chlorophyll *a*, OPC measured zooplankton abundance and biovolume and MVBS at 120 kHz from Ek500

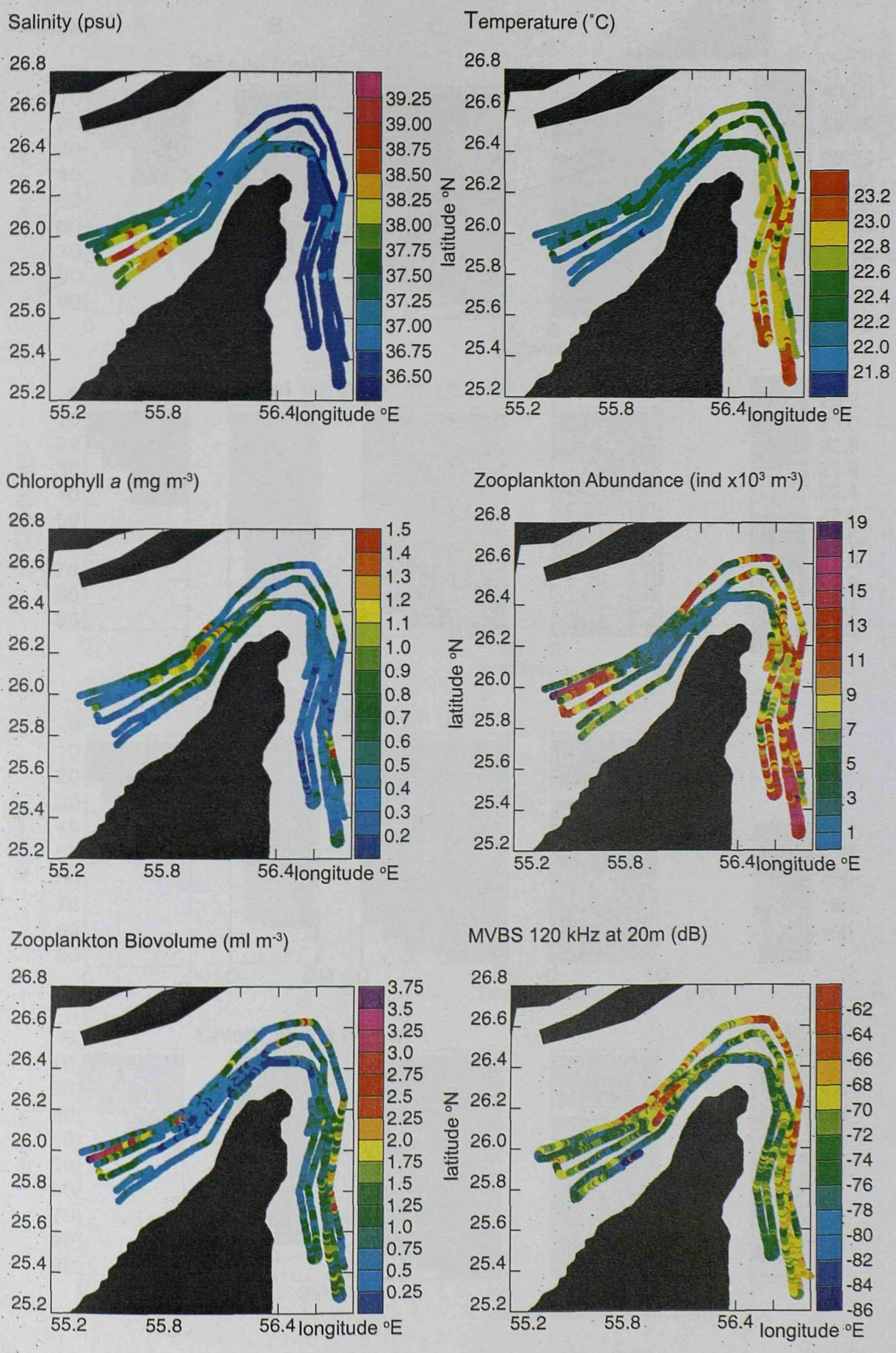

Figure 4.1.1.iii Contoured CTD sections from the Strait Variables: salinity, temperature,oxygen and chlorophyll *a*. Sections run from the coast into the centre of the Strait Line A 6 Stns, Line B 7 Stns, Line C 7 Stns, Line D 5 Stns

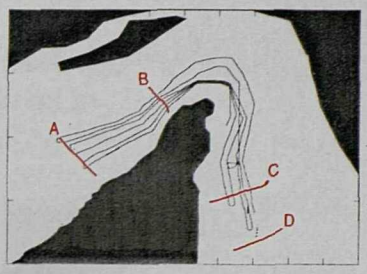

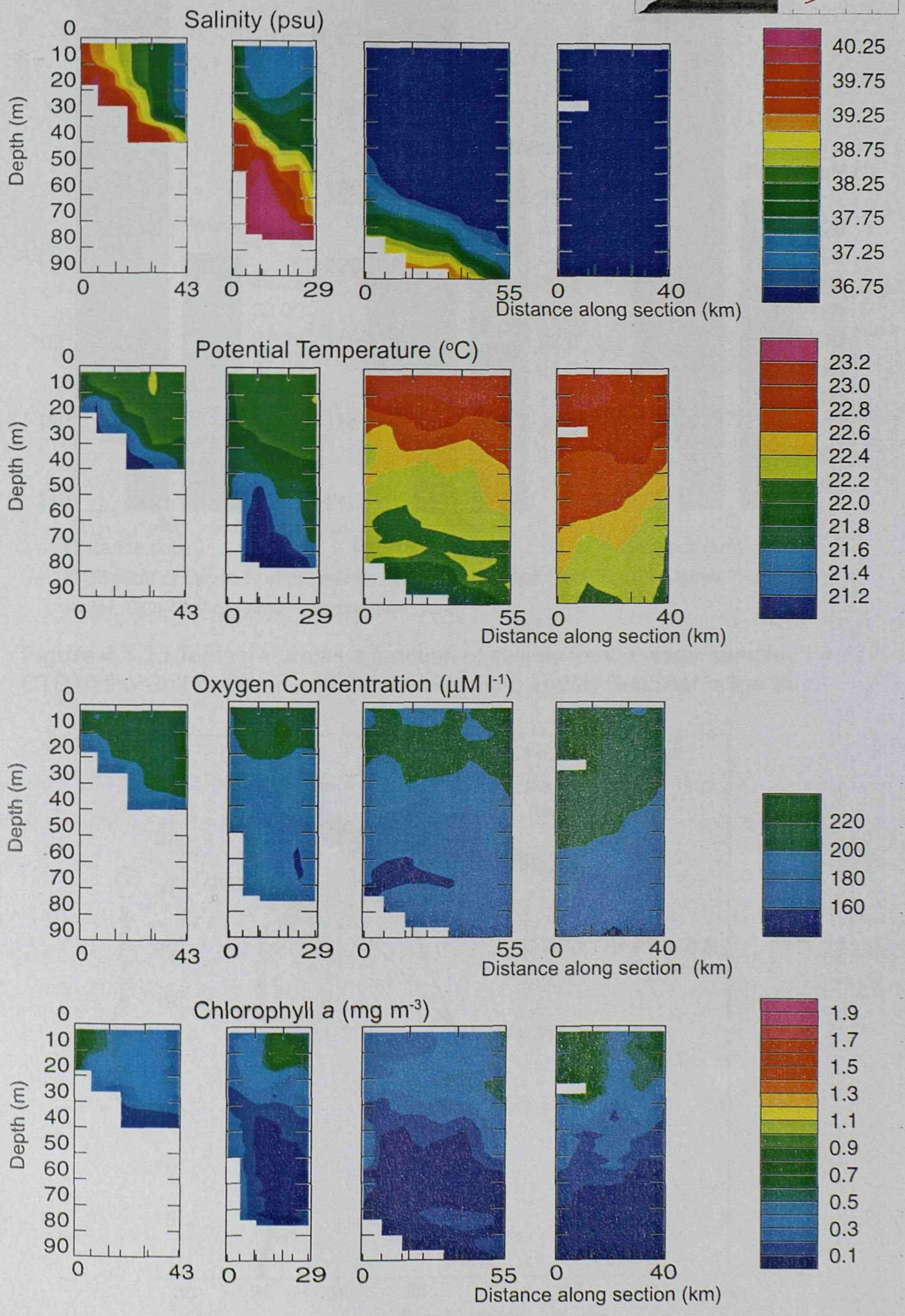

Figure 4.1.1.iv Full depth CTD data from Line D: profiles of salinity, temperature and dissolved oxygen. This is the same section as in Fig 4.1.1.iii, but contoured to the full depth of the sea floor

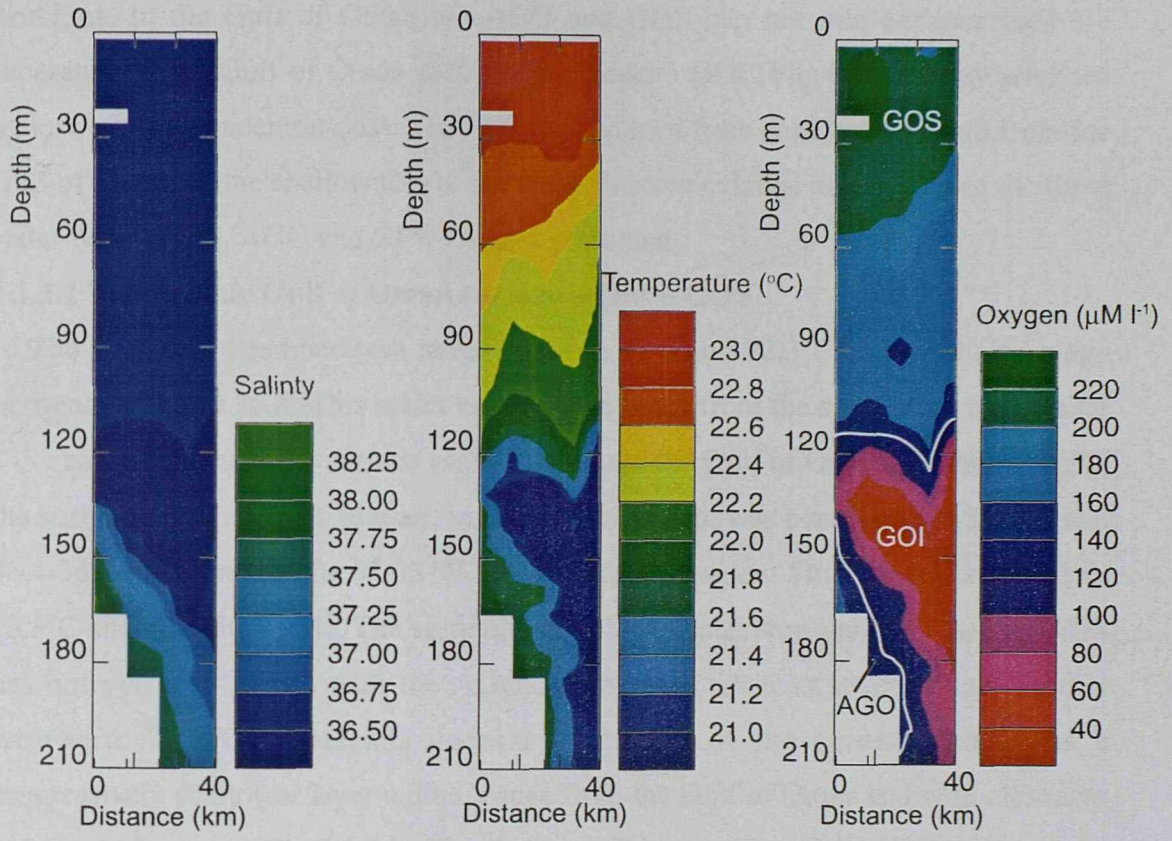

GOS-Gulf of Oman Surface inflow, AGO-Arabian Gulf Outflow, STW-Strait Transition water, GOI-Gulf of Oman Intermediate water

Figure 4.1.2.i Temperature as a function of salinity for the water sampled by CTD in the Gulf of Oman and the Arabian Gulf, and by SeaSoar in the Strait

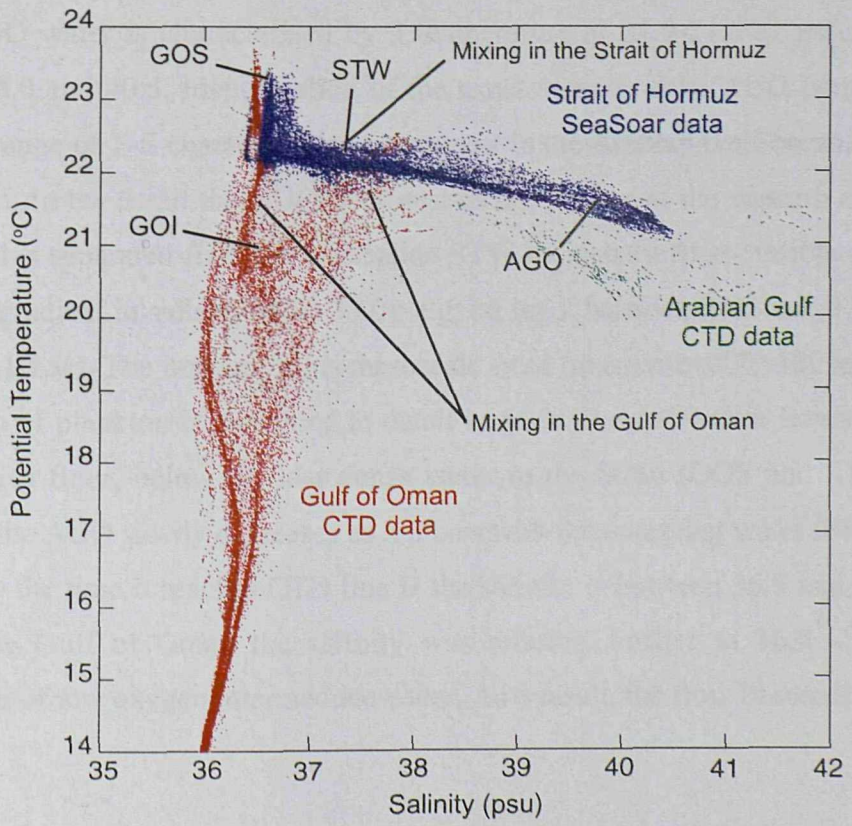

This water is only formed on the Strait because the AGO and GOS are only able to mix there, where the shallow seafloor forces them together, despite their different densities. In the Gulf of Oman the AGO and GOS can not mix because they are separated by the Gulf of Oman intermediate water - GOI (**Fig 4.1.1.iv**: characterised by low oxygen concentrations). The GOI is prevented from entering the Strait from the Gulf of Oman by the shallowness of the shelf. A more detailed description of the three water types (GOS, AGO and STW) is now presented.

4.1.2.2 The oceanic Gulf of Oman surface inflow – GOS

The GOS has a temperature range between 22.6 and 22.3°C and a salinity range between 36.4 and 36.8. This water entering the Strait from the south east, has similar T-S characteristics to the surface water throughout the Gulf of Oman. On the 21/02/97 the surface water north of Muscat, in the Gulf of Oman, was between 23.0-23.5°C and 36.4-36.6 PSU, and on the 03/03/97 the water in the eastern Strait was between 23.0-23.3°C and 36.4-36.7 PSU. The similarity in T-S characteristics indicates that the GOS has not yet been mixed with the AGO, which does occur as it propagates further westward. The GOS extends deepest in the SE of the survey, and forms a progressively shallower layer with distance from the Gulf of Oman and with closeness to Masandam coast (**Fig 4.1.1.i**). The thermo-haline structure of the GOS water on the east side of the Strait shows variability on scales between 5 and 50 km which resulted from the presence of internal waves.

4.1.2.3 The high salinity Arabian Gulf outflow – AGO

The AGO water is characterised by a temperature of 21.0-21.7°C and a salinity between 38.0 and 40.5. Identification of the exact source of the AGO is not simple because a range of T-S characteristics are present in the Arabian Gulf because of high evaporation. In the Strait the AGO is closest to the surface at the western end of the survey, and is separated from the less saline STW by a sharp front (visible as a large horizontal gradient in salinity (40.0-37.0): e.g. on leg 2 between 3695 and 3725 km at 25m **Fig 4.1.1.ie**). The impact of this mesoscale front (at a scale of 20-100 km) on the distribution of plankton is examined in detail in §5.2. The AGO then flows eastward along the sea floor, below the less dense water in the Strait (GOS and STW). The salinity of the AGO slowly decreases as it mixes with the overlying water (**Fig 4.1.1.iii** and **iv**). By the time it reaches CTD line D the salinity is between 36.5 and 38.0, and once in the Gulf of Oman the salinity was reduced further to 36.4 – 37.4, by entrainment of low oxygen intermediate water. As a result, the flow becomes neutrally

buoyant on the slope at about 250 m and leaves the seabed (this occurs outside the area represented in **Fig 4.1.1.i**, in the Gulf of Oman).

4.1.2.4 The water formed by mixing in the Strait – STW

The STW is formed by mixing between the AGO and GOS and is characterised by a temperature of 21.7-22.6°C and a salinity of 36.8-38.0. This water is distributed along the boundary between the AGO and GOS and represents a mesoscale frontal region between them. The sharp front between the STW and the AGO is a part of this frontal region. The STW is present in the upper 40m of the water column to the west of the tip of the Masandam Peninsular (**Figs 4.1.1.ii** and **5.1.1.i**). Although the STW has the characteristic intermediate T and S properties which would be expected to result from the mixing of the GOS and AGO, the biological features in this water are much more complex. The biological differences between the water types is examined in detail in §5.1.

4.1.2.5 Dissolved oxygen concentrations in the Strait

Brettschneider *et al.* (1970) measured oxygen deplete, phosphate rich water penetrating onto the shelf in the south east Strait of Hormuz at a depth as shallow as 20 m. The presence of low oxygen water in Strait would be expected to affect the distribution of zooplankton, as it does in the Gulf of Oman (e.g. Herring *et al.*, 1997). CTD data from the Strait showed that the anoxic intermediate water in the Gulf of Oman was below 120 m, and during the survey did not penetrate onto the shelf (**Figs 4.1.1.iii** and **iv**). A temperature/salinity analysis of the SeaSoar data demonstrated that water with the T and S characteristics of the low oxygen water was also absent in the Strait. The lowest oxygen values recorded in the Strait were 140-160 $\mu M\ l^{-1}$, compared with surface concentrations of 180-160 $\mu M\ l^{-1}$, and an oxygen minimum of 0 $\mu M\ l^{-1}$ in the Gulf of Oman. From this analysis it is assumed that at the time of this survey, low oxygen water did not influence zooplankton in the Strait.

4.1.3 Distribution of plankton in the Strait of Hormuz

The distribution of components of the plankton community was determined using a fluorimeter, an optical plankton counter, and an EK500 echosounder. The distribution of plankton measured by each of these instruments is described in this section.

4.1.3.1 Distribution of phytoplankton standing stock (sampled by fluorimeter)

The distribution of chlorophyll *a* was measured with a fluorimeter mounted on SeaSoar (§2.2.3). These data have not been corrected for the effect of quenching,

which is manifested as lower than expected chlorophyll concentrations during daylight, near to the surface (**Fig 4.1.1.i**: compare day data at 3700-3760 km on leg 2, with corresponding night data at 4120-4200 km on leg 3).

Chlorophyll *a,* measured by the SeaSoar fluorimeter, ranged from 0 to 1.7 mg m^{-3} in the Strait when averaged into 1.5 km by 4 m grid boxes. The mean concentration in the upper 30 m, at night (unquenched), was 0.57 mg m^{-3} (std. dev. 0.27). These values indicate that at the time of the survey the phytoplankton standing stock was relatively high. In general, the highest chlorophyll concentrations were in the upper 30 m, with much lower concentrations below this depth. Although on the east side of the Strait, where the thermocline was depressed locally and stratification maximum (quantified as the Brunt Vaisala Frequency) was deepest, the concentration was greater than 0.5 mg m^{-3} down to 50 m in places (e.g. Leg 3 at 3960-3970 km; **Fig 4.1.1.i**).

The highest concentrations of chlorophyll *a* (up to 1.5 mg m^{-3} in the upper 30 m) were west of the tip of the Masandam Peninsular (see Leg 3, **Fig 4.1.1.i**) with lower values in other areas. The concentration of chlorophyll was correlated with the water types (§5.1). On the east side of the Strait the concentration of chlorophyll was lower and was markedly patchy over 5-50 km space scales: characterised by patches >0.7 mg m^{-3} interspersed with lower values (<0.3 mg m^{-3}). These patches appear to predominantly correlate with the physical variability resulting from internal waves (**Fig 4.1.1.i**). This correlation is examined in detail §5.3.

4.1.3.2 Distribution of mesozooplankton (sampled by optical plankton counter)

An optical plankton counter (OPC) was used to enumerate and size zooplankton between 0.4 to 4.1 mm ESD. This instrument was attached to SeaSoar for the entire survey (§2.2.4). The OPC data have been calibrated as detailed in Chapter 3. These data show that mesozooplankton (0.4-4.1 mm ESD) abundance varied between <1000 and 17000 m^{-3} and biovolume ranged between 0.01 and 3.0 ml m^{-3}.

The distribution of mesozooplankton show clear vertical gradients in the Strait: their maximum concentration was in the upper 40 m where their abundance varied between 2000 and 15000 m^{-3} and biovolume between 0.1 and 2.5 ml m^{-3} (**Fig 4.1.1.i** and **ii**). The vertical structure of zooplankton distributions has not been resolved by previous studies in this region (Gibson *et al.*, 1980; Michel *et al.*, 1986b). In the horizontal, mesozooplankton are most abundant (>10000 m^{-3}) at the western end of the survey, where the AGO is at the surface, and also on the eastern side of the Strait in the GOS. In the area to the west of the Peninsular the zooplankton abundance was

halved (<5000 m^{-3}) which correlated with the frontal region between the flows represented by the STW.

On the east side of the Strait the total mesozooplankton abundance was reduced with distance westward from the Gulf of Oman (**Fig 4.1.1.i**). In addition, the distribution of zooplankton was patchy on scales of 5-50 km and appears to correlate with variability in the thermo-haline structure resulting from internal waves (§5.3).

The AGO contained the highest mesozooplankton biovolume in the survey region. The spatial extent of the high biovolume correlates with the sharp front between the AGO and STW. However the distribution of zooplankton around this front was different on each leg of the survey (**Fig 4.1.1.i**). On leg 2, high salinity (>38.25) water is in the upper 20m, and the zooplankton maximum extends from the surface down to 60m. On legs 3 and 4, the highest zooplankton abundance and biovolume was concentrated within the top 20m west of where the 38.25 isohaline was at the surface. East of this point, on both legs, the patch of high zooplankton abundance extended away from the surface, following the isohalines in the front. On leg 3 this maximum extended to 35 m and on leg 4 to 55 m. On leg 1, which is furthest from the Masandam coast and therefore had the weakest influence of the AGO, the 38.25 isohaline was much deeper at around 25-35 m. The zooplankton maximum was also deeper between 30 and 55 m. On legs 3 and 4 the biovolume of the smaller size classes (0.4 to 1.6 mm ESD) was elevated in the AGO as it flowed deeper away from the surface maximum (**Fig 4.1.1.i**), but the biovolume of larger species was reduced rapidly with depth.

The patches of high biovolume of the larger size classes were less spatially extensive than the patches of the smaller species throughout the Strait (**Fig 4.1.1.i**). This may indicate a greater influence of behavioural aggregation in larger species. This pattern of less extensive patches does not extend to the distributions of MVBS of larger macrozooplankton described by the EK500, and may represent shortcomings in the OPC's ability to sample large mesozooplankton.

4.1.3.3 Distribution of macrozooplankton and micronekton (sampled by EK500)

A Simrad EK500 echosounder was used describe the distribution of MVBS of macrozooplankton and micronekton (§2.2.6). The instrument measures backscatter at three frequencies, which have approximate minimum detection limits of 7.5 mm for the 200 kHz, 1cm for the 120 kHz and 4 cm for the 38 kHz, (Griffiths *et al.*, 1996). The acoustic return from zooplankton is also influenced by body structure and population density: Brierley *et al.* (1998) show that the EK500 can detect aggregations

of smaller species, such as *Rhincalanus gigas* (>5 mm). Therefore it is not possible to define precise size detection limits, but it is clear that the EK500 observes considerably larger zooplankton than an OPC, and there is a gap (≈4.5-7.5 mm) that is not resolved by either.

The MVBS at all three frequencies was lower in the Strait of Hormuz than in the adjacent Gulf of Oman (data in Crisp *et al.*, 1998). In general, the MVBS in the Strait, decreased with distance from the Gulf of Oman, although there were clear patches within this gradient, some of which correlated with changes in seafloor topography, such as in the centre of the Strait on leg 1. The lowest MVBS was at the western end of the survey in the AGO. Within the Strait the MVBS at 38 kHz was greater than at the other two frequencies, and was distributed more evenly through the water column (**Fig 4.1.1.i**). The peaks in MVBS at 120 and 200 kHz were generally in the upper 30 m. In a number of places the MVBS maximum is above (for 120/200 kHz) or within (for 38 kHz) the strongest stratification. For example the MVBS at 38 kHz was correlated with the maximum Brunt Vaisala Frequency on leg 2 around 3725 km and 3905 km.

4.1.4 Diel vertical migration of zooplankton in the Strait and Gulf of Oman

Diel vertical migrations (DVM) are a fundamental feature of zooplankton biomass distributions (e.g. Russell 1927; Roe 1974; Angel 1986). In the first part of this section the DVM of the macrozooplankton (measured with an EK500) is quantified and contrasted between the oceanic Gulf of Oman and the shallow Strait. The DVM of these species is expected to be reduced on the shelf (in the Strait) because the sea floor stops these species to reaching their usual day time depths. In the second part of this section the DVM of the mesozooplankton (measured with an OPC: §2.2.4) in the Strait is quantified in each size class. Larger mesozooplankton (2-20 mm) often perform DVM, while smaller species (0.2-2 mm) do not migrate as much (e.g. Morales *et al.*, 1991). Previous studies are ambiguous as to whether an OPC can determine DVM in the size range it senses. For example Pollard *et al.* (submitted) report a weak migration signal in their largest size class (>4.0 mm ESD), while Huntley *et al.* (1995) note that diel migration was undetectable.

4.1.4.1 DVM in acoustic backscatter measured by the EK500 and RMT samples

Extensive, diel vertical migrations of backscatter have been widely reported as a conspicuous feature of bioacoustic datasets from a variety of regions (e.g.

Plueddemann and Pinkel, 1989; Roe and Griffiths, 1993). During CD 104, the MVBS at 38, 120 and 200 kHz (representing the macrozooplankton and micronekton) was characterised by a clear DVM signal in the Gulf of Oman. **Fig 4.1.4.ia** presents the day and night vertical profiles of MVBS at 38 kHz, averaged for Julian days 47 to 51 (1997). The data have not been split into the hydrographic regimes of the Gulf of Oman, and it has been assumed that each regime was sampled equally during the day and the night. The data from the 2 hours covering sunset and sunrise have been excluded as this was the time when the species were moving. **Fig 4.1.4.ii** shows the vertical distribution of MVBS at 38 kHz over a 24 hour period on Julian day 50.

Both figures show clear DVM of the mesopelagic scatterers in the Gulf of Oman. During the day the MVBS maximum was between 250 and 350 m, and at this depth was 10 to 15 dB greater than during the night. At night the peak in MVBS was between 25 and 100 m, and was up to 20 dB greater than during the day. The 120 and 200 kHz frequencies did not show these patterns as clearly, because these frequencies do not penetrate deep enough to sample the daytime MVBS peak at 300 m.

RMT[1] net samples were taken to identify the species that dominated the migrating biomass in the Gulf of Oman. The large organisms caught by the RMT8 showed a clear DVM pattern, but DVM was not clear enough to be quantified for the smaller species captured by the RMT1 (Herring *et al.*, 1998 and 1999). In the Gulf of Oman the largest biovolume was between 300 and 400 m during the day, but at night the biovolume was reduced by more than 50% at this depth. During the night between 50 and 150 m the biovolume was 4 times larger than during the day (data from Herring *et al.*, 1998). The migrating biovolume in the nets was dominated by the myctophid fish *Diaphus arabicus*, *D. thiollieri*, *Benthosema pterotum* and photoichthyid fish *Vinciguerria nimbaria* (28-42 mm), and the decapods *Pasiphaea marisrubri*, *Plesionika persica* and *Sergestes semissis* (12-30 mm), (Herring *et al.*, 1999).

Fig 4.1.4.ib shows the day and night profiles of MVBS at 38 kHz, averaged in the GOS in the Strait. The graph shows the entire 100 m of the water column, unlike the previous figure where the water depth is more than 2000 m. The data from **Fig 4.1.4.ia** are re-plotted for comparison. There is no obvious evidence for DVM in the Strait, since both the day and night profiles of MVBS are uniform with depth.

[1] The rectangular midwater trawl, RMT system consists of 2 sets of opening and closing nets: the RMT8 has an 8 m^2 mouth area and 4.5 mm filtering mesh, and the RMT1 has a 1m^2 mouth area and 333μm filtering mesh.

Figure 4.1.4.i Diel vertical migration of MVBS at 38 kHz
a) Day and night vertical profiles of MVBS at 38 kHz from the Gulf of Oman
b) Day and night vertical profiles of MVBS at 38 kHz from the GOS (in the Strait) overlayed on the data from **a** - (note different scales)

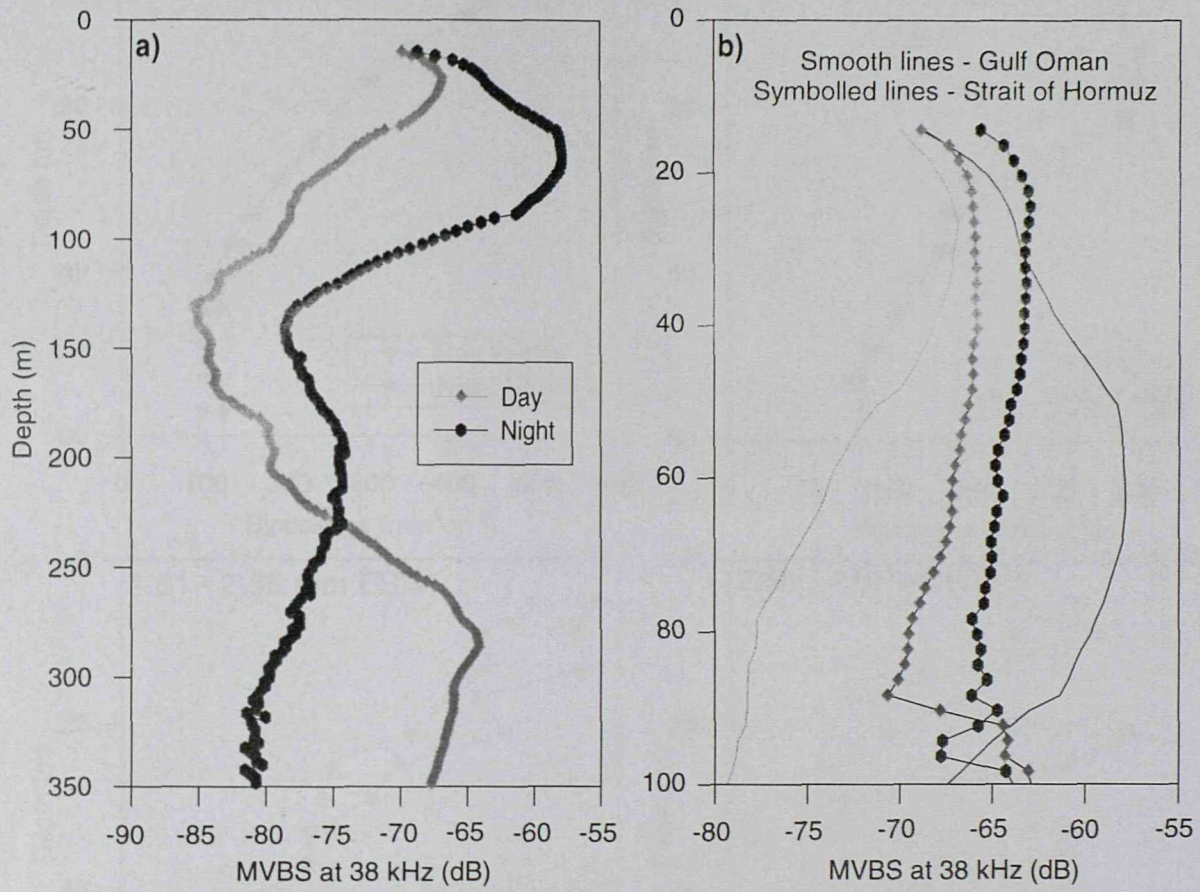

Figure 4.1.4.ii The vertical distribution of MVBS at 38 kHz over 24 hours in the Gulf of Oman

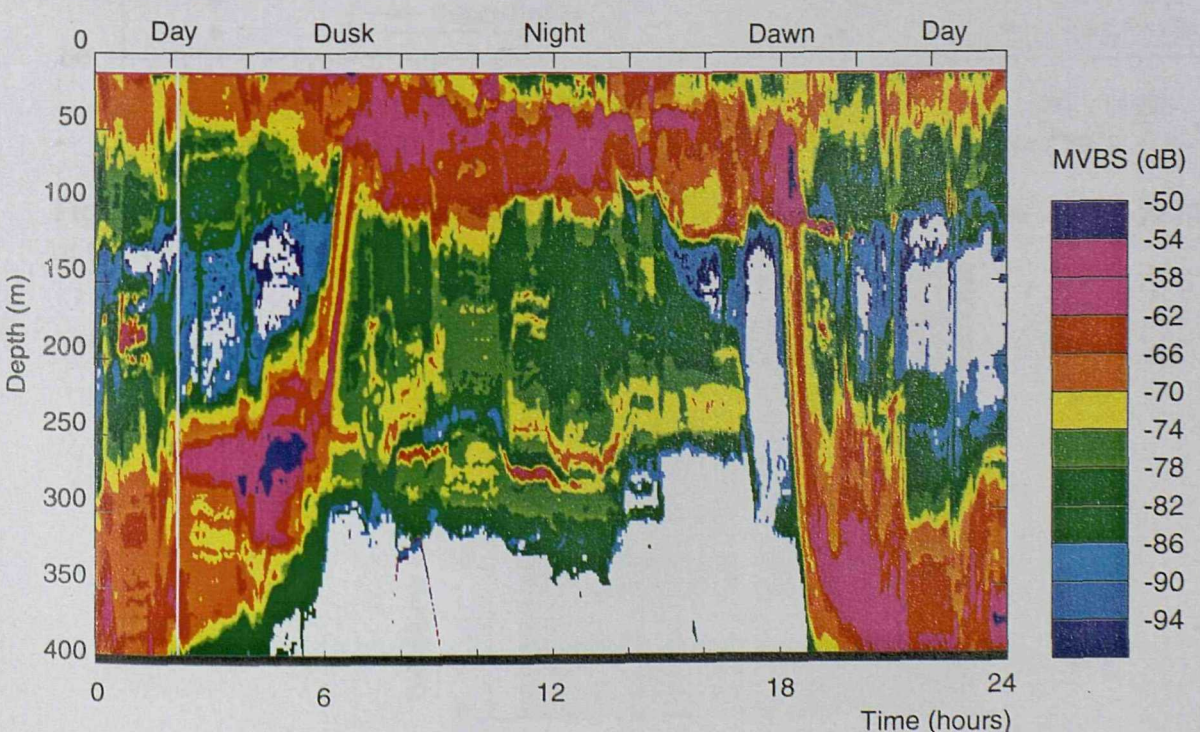

Figure 4.1.4.iii Day and night profiles of zooplankton biovolume in four OPC size classes in the GOS

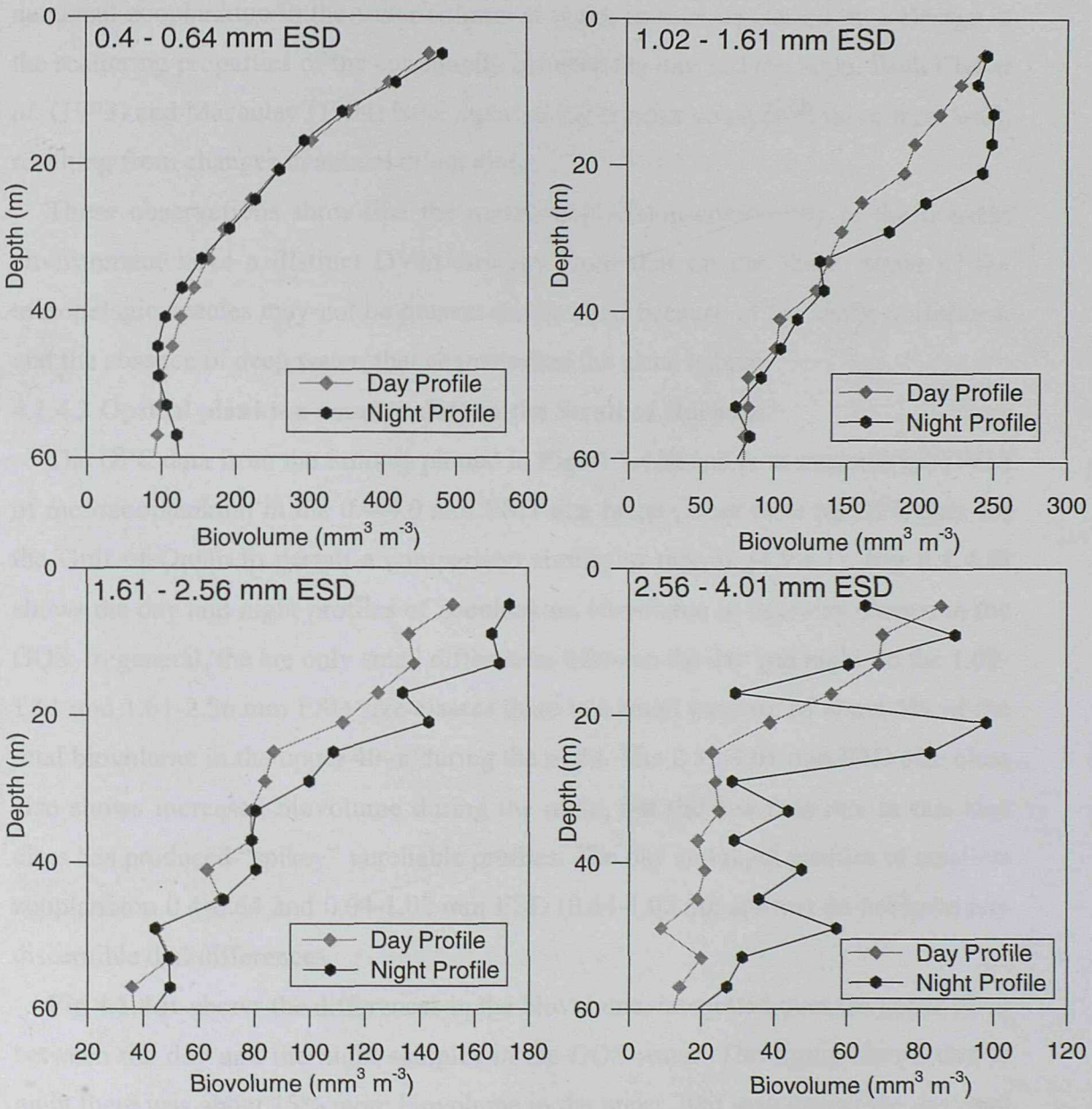

Figure 4.1.4.iv Mesozooplankton biovolume in each size class in the upper 30 m of the GOS

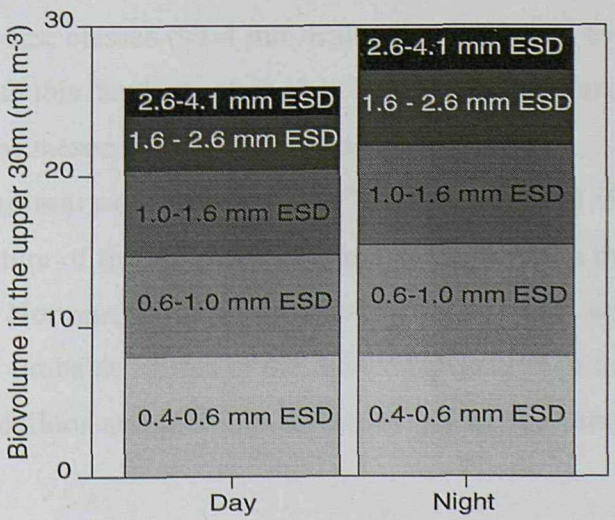

Curiously, the MVBS during the night was 2-4 dB larger than during the day, throughout the water column. This increase of MVBS may result from the presence demersal zooplankton in the water column at night, or may be caused by a change in the scattering properties of the community between the day and the night. Both Chu *et al.* (1993) and Macaulay (1994) have reported backscatter changes of more than 5 dB, resulting from changes in animal orientation.

These observations show that the macrozooplankton community in the oceanic environment have a distinct DVM strategy from that on the shelf. Some of the mesopelagic species may not be present on the shelf because of the shallow seafloor, and the absence of deep water, that characterises the usual habitat.

4.1.4.2 Optical plankton counter data in the Strait of Hormuz

The OPC data from the Strait is plotted in **Figs 4.1.4.iii** and **iv** to examine the DVM of mesozooplankton in the 0.4-4.0 mm ESD size range (there were no OPC data for the Gulf of Oman to permit a comparison similar to that in §4.1.4.1). **Fig 4.1.4.iii** shows the day and night profiles of zooplankton biovolume in four size classes in the GOS. In general, the are only small differences between the day and night. In the 1.02-1.61 and 1.61-2.56 mm ESD size classes there is a small increase of about 5% of the total biovolume in the upper 40 m during the night. The 2.56-4.01 mm ESD size class also shows increased biovolume during the night, but the low data rate in this size class has produced "spikey" unreliable profiles. The day and night profiles of smallest zooplankton 0.4-0.64 and 0.64-1.02 mm ESD (0.64-1.02 not shown) do not have any discernible diel differences.

Fig 4.1.4.iv shows the differences in the biovolume, integrated over the upper 30m, between the day and the night samples in the GOS water. The figure shows that at night there was about 15% more biovolume in the upper 30m than during the day, and that the increase was not equal in all the size classes. The biovolume increase was limited to the three largest size classes (≈1-4 mm ESD). This provides evidence that there was a migration up into this depth range at night by the larger mesozooplankton, resulting in this change in the mesozooplankton size spectra.

4.1.4.3 Conclusions and summary of patterns in DVM in the Strait of Hormuz

DVM is not a major feature of the distribution of macrozooplankton measured by the EK500 in the Strait of Hormuz, which is a notable contrast to the water further south in the Gulf of Oman. Probable causes of the reduced migration in the Strait are the shallow depth of the seafloor and possibly the sharp halocline. Lampert (1993)

hypothesised that a driving force for DVM in zooplankton is the avoidance of visual predators during the day. In the clear, well lit, shallow shelf water there may be no selective advantage for DVM, because the efficiency of predators is not significantly reduced from the surface to the seabed. A change in species also appears to be correlated with the change in community behaviour. The shallow depths of the Strait also mark the limit of the distributions of many migratory mesopelagic species: Herring *et al.* (1999) recorded 8 species of myctophid fish in RMT8 samples from the Gulf of Oman, and only 3 species in samples taken above the continental slope.

The observations of the DVM of mesozooplankton made with an OPC show no migration in the smaller species (<1 mm ESD) and weak migration signals in the larger species (1-4 mm ESD). Smaller species are less mobile than larger zooplankton, and may be less able to migrate. For example the small copepod *Oithona* (<1 mm ESD: Rissik *et al.*, 1997) is well documented not to undertake diel migrations (e.g Haury *et al.*, 1990). In addition, Head *et al.* (1999) report no diel differences in zooplankton biomass between 0.2-1 mm, but consistent (but not significant) diel differences in the 1-2 mm species in the North Atlantic. However other studies have resolved DVM. In conclusion, DVM should not be expected to be a prominent feature of OPC datasets because of the small size of zooplankton detected, although a DVM signal may be detected in the larger size classes (>1 mm ESD).

4.1.5 Summary of hydrographic and biological observations made with SeaSoar

The SeaSoar and CTD datasets (presented in §4.1) show a two layer, reverse estuarine exchange between the surface inflow from the Gulf of Oman (the GOS) and the high salinity outflow from the Arabian Gulf (the AGO) through the Strait of Hormuz. In addition to these two end members a third water type the STW is defined which is formed by the mixing of the GOS and AGO. This mixing occurs at the mesoscale, and the STW represents a frontal region between the GOS and AGO. Although the STW shows the characteristic intermediate T-S properties which would be expected as the GOS and AGO mix, the biological features in this water are much more complex (the effect of the formation of the STW on the planktic community is examined in §5.1).

At the western boundary of the STW, the gradient of change in salinity increases forming a sharp front between the AGO and STW. This front is investigated as a separate mesoscale feature in §5.2, because it is correlated with clear changes in the

distribution of plankton. On the eastern side of the Strait, the water column structure is influenced by sub-mesoscale variability resulting from internal waves. The effect of the internal waves on the distribution of plankton is examined in §5.3.

The populations of phytoplankton, meso- and macrozooplankton were most densely concentrated in the upper 30m of the water column. However, the larger, more mobile micronekton were more evenly distributed through the water column. The stocks of plankton in the waters entering the Strait on either side of the Strait (the AGO and GOS) were quite similar to each other in terms of quantity. Both waters contain dense stocks of mesozooplankton (with the biovolume dominated by small <1 mm ESD species), and moderate concentrations of chlorophyll. Within the Strait, the frontal water (STW) was at the surface to the west of the tip of the Peninsular. The stocks in this area were distinct and this water contained twice the concentration of chlorophyll *a*, but half the biovolume of mesozooplankton than the end members. The MVBS of macrozooplankton showed a gradient through the Strait, with the highest backscatter in east and lowest in the west. There was not a strong diel vertical migration signal in the distribution of mesoplankton (<4.0 mm) or macrozooplankton MVBS in the Strait. In the Gulf of Oman the MVBS of macrozooplankton did show strong migration signals. The interrelationships between the physical environment and the biology measured during this survey are examined further in Chapter 5.

4.2 Data Collected with a Longhurst Hardy Plankton Recorder

The processing of the zooplankton samples collected with a Longhurst Hardy plankton recorder (LHPR) was described in §2.2.5. In chapter 3 the measurements of abundance and biovolume from the LHPR were used in the calibration of the abundance and biovolume computed from OPC data (§3.2 and §3.3). In this section the LHPR samples are used to describe the vertical distribution of zooplankton taxonomic groups and size classes in the Strait. The distributions are related to the water column structure, and the water types. This information complements the data described in §4.1, and is useful in determining the factors influencing the distribution of plankton in the Strait.

Two LHPR stations were fished in the Strait of Hormuz (map: **Fig 2.1.1.i**). Stn 54006 was located at the south east end of the SeaSoar survey, and was characterised by GOS water at all depths sampled. Stn 54007 was in the centre of the channel to the west of the Masandam peninsular, and was characterised by STW above 60m, and

AGO below 65m. The zooplankton samples were split into 3 size classes: these were plankton that were retained on a 4.5 mm meshed net, hereafter >4.5 mm size class; the plankton that passed through the 4.5 mm and were retained on a 1.5 mm net, hereafter >1.5 and <4.5 mm size class; and the plankton that passed through the 1.5mm and were retained on a 0.28 mm net, hereafter <1.5 mm size class[2] (see also Appendix 5). Biovolume was measured for each size class for both the up and down profiles of the instrument, but abundance was only enumerated for the down profiles at each station.

4.2.1 Presentation of the data collected by the LHPR

This section presents the graphs of data produced by the analysis of the LHPR samples. **Fig 4.2.1.i** shows zooplankton biovolume as a function of depth, determined from the LHPR zooplankton samples at stn 54006 (08/03/97). Unlike the data used in chapter 3 these measurements have not been gridded, and the width of the bars represents the actual depth range of each two minute sub-sample. The bars are divided into the three size classes: the <1.5mm, the >1.5 and <4.5mm, and >4.5mm. The temperature and salinity profiles from the down profile are also presented. **Fig 4.2.1.ii** shows the same variables at stn 54007 (11/03/97). Note that the x axes have different scales to **Fig 4.2.1.i**.

Figs 4.2.1.iii and **iv** show the percentage of total zooplankton abundance of each major taxonomic group as a function of depth at stations 54006 and 54007. The four plots are **a)** the total zooplankton, **b)** zooplankton >4.5 mm, **c)** >1.5 and <4.5 mm, and **d)** <1.5 mm. Note that numerically, most zooplankton are in the <1.5 mm size class, and therefore the plot for this size class is similar to that for the total zooplankton.

Figs 4.2.1.v and **vi** present the abundance profiles of all zooplankton and the numerically dominant taxonomic groups at stn 54006. These groups are copepods, chaetognaths, euphausiids and ostracods in the <1.5 mm class (**Fig 4.2.1.v**) and copepods, chaetognaths, euphausiids and siphonophores in the >1.5 and <4.5 mm class (**Fig 4.2.1.vi**). **Fig 4.2.1.v** shows abundance profiles for the whole sample and the <1.5mm size class, and **Fig 4.2.1.vi** shows the >1.5 and <4.5mm size class. **Figs 4.2.1.vii** and **viii** are in the same format as the previous two figures, but for the data from stn 54007. The groups are copepods, chaetognaths, euphausiids and ostracods in the <1.5 mm class (**Fig 4.2.1.v**) and copepods, chaetognaths, euphausiids and the dinoflagellate *Noctiluca* sp. in the >1.5 and <4.5 mm class (**Fig 4.2.1.vi**).

[2] Note that the LHPR net was 0.33 mm, which is the true lower limit of the <1.5 mm size class

Figure 4.2.1.i The distribution of zooplankton biovolume with depth at Station 54006: biovolume divided into size classes - profiles of salinity and temperature of the down profile also displayed

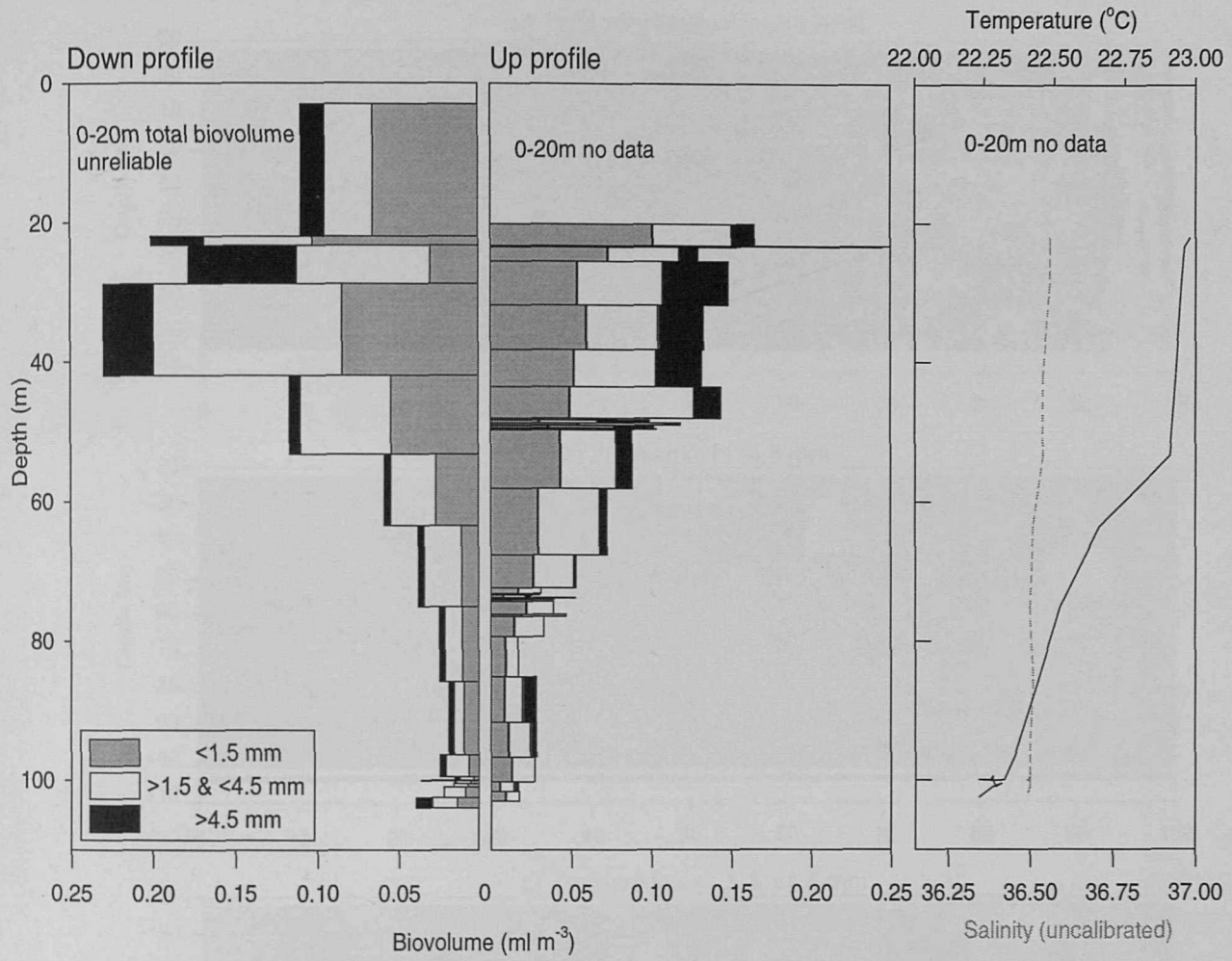

Figure 4.2.1.ii The vertical distribution of zooplankton biovolume at Station 54007: biovolume divided into size classes - profiles of salinity and temperature of the down profile also presented

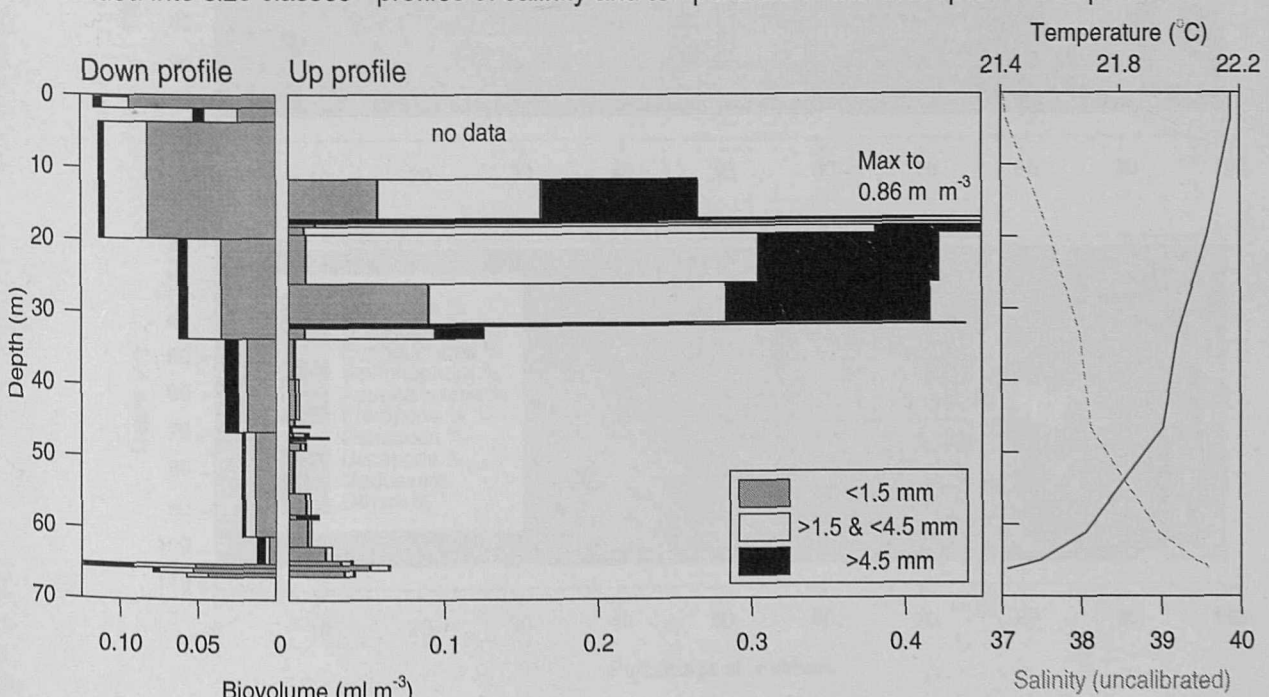

Figure 4.2.1.iii The percentage of zooplankton abundance represented by each taxonomic group on the down profile at Station 54006 (08/03/97) - note that there was no reliable data between 0 and 20 m

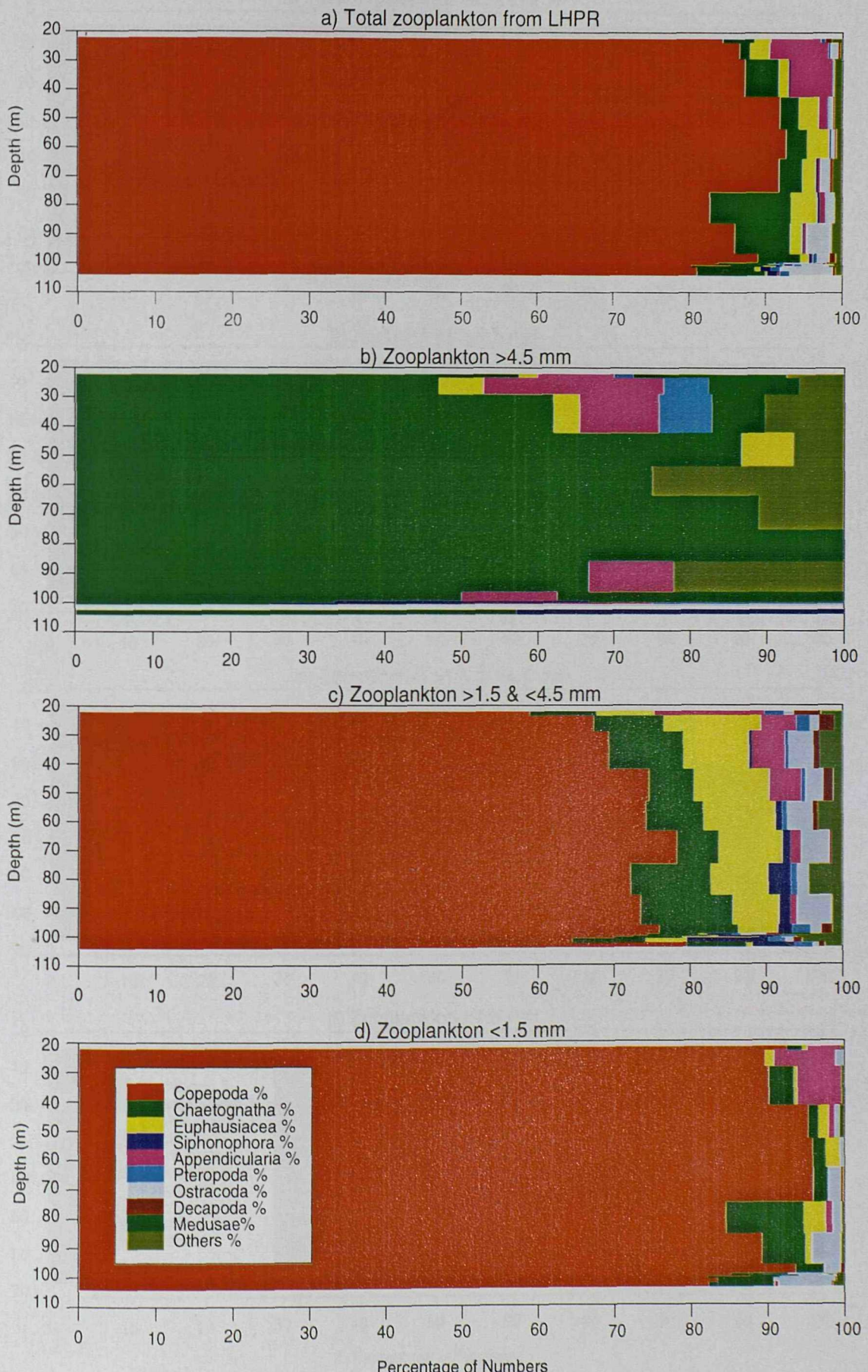

Figure 4.2.1.iv The percentage of zooplankton abundance represented by each taxonomic group on the down profile at Station 54007 (11/03/97)

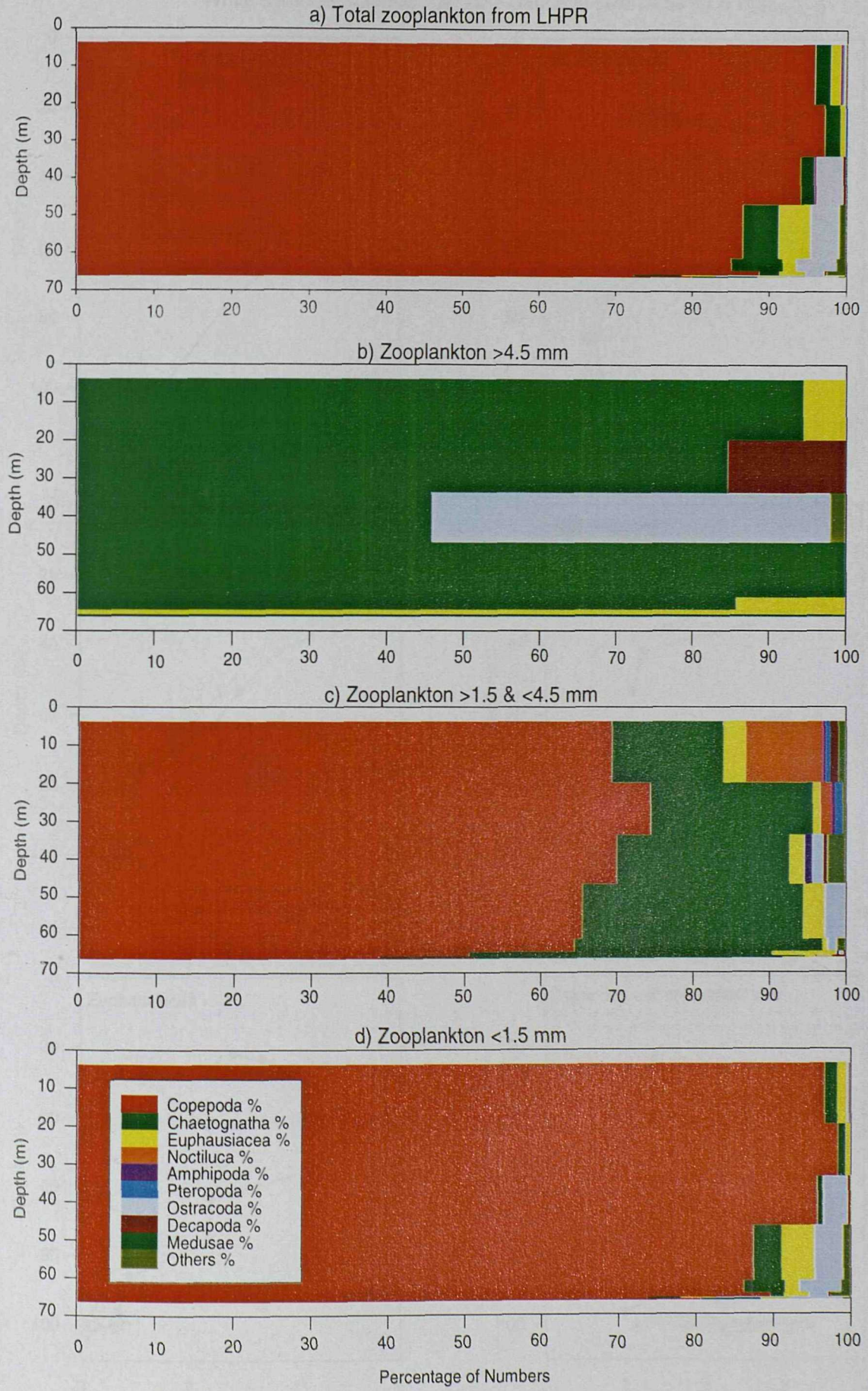

Figure 4.2.1.v Abundance profiles of dominant zooplankton groups at Station 54006 (07/03/97)
Black symbols, solid line: total zooplankton abundance
White symbols, dashed line: abundance in size class <1.5 mm

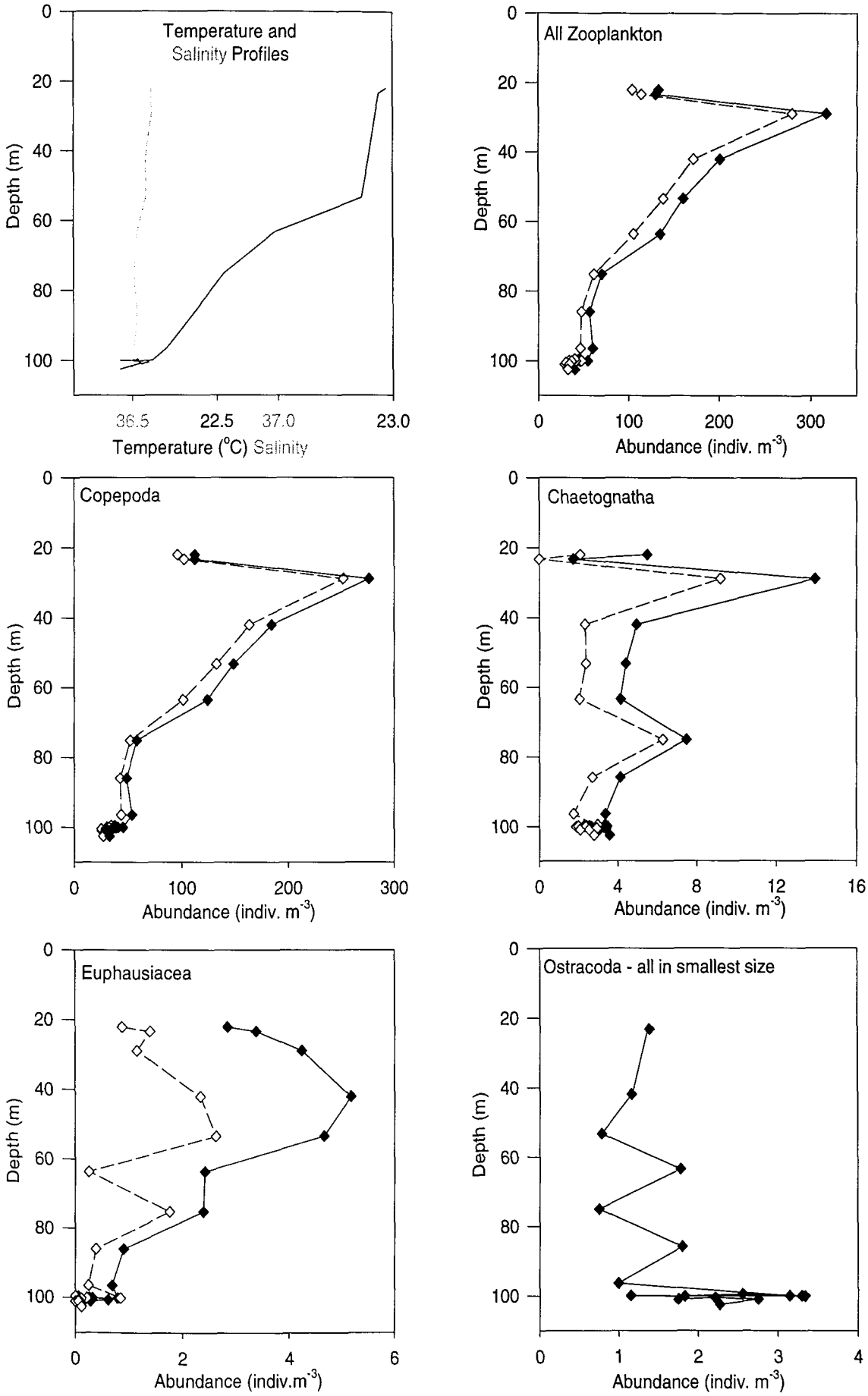

Figure 4.2.1.vi Abundance profiles of dominant zooplankton groups at Station 54006 (07/03/97) For the <4.5 and >1.5 mm size class - note different x axis scales to Figure 4.2.1.v.

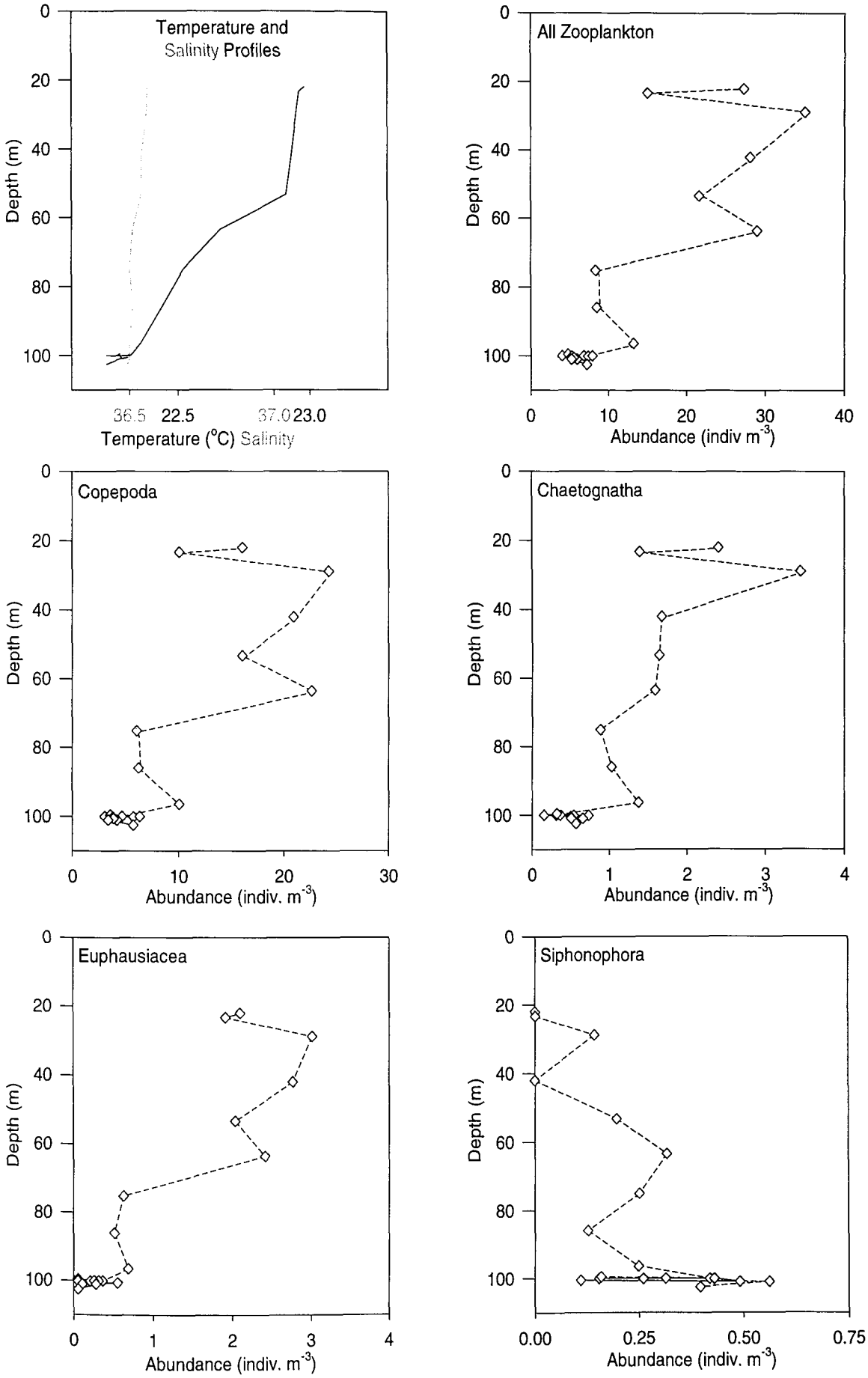

Figure 4.2.1.vii Abundance profiles of the dominant Zooplankton groups at Station 54007 (11/03/97)
Black symbols, solid line: total zooplankton abundance
White symbols, dashed line: abundance in size fraction <1.5 mm

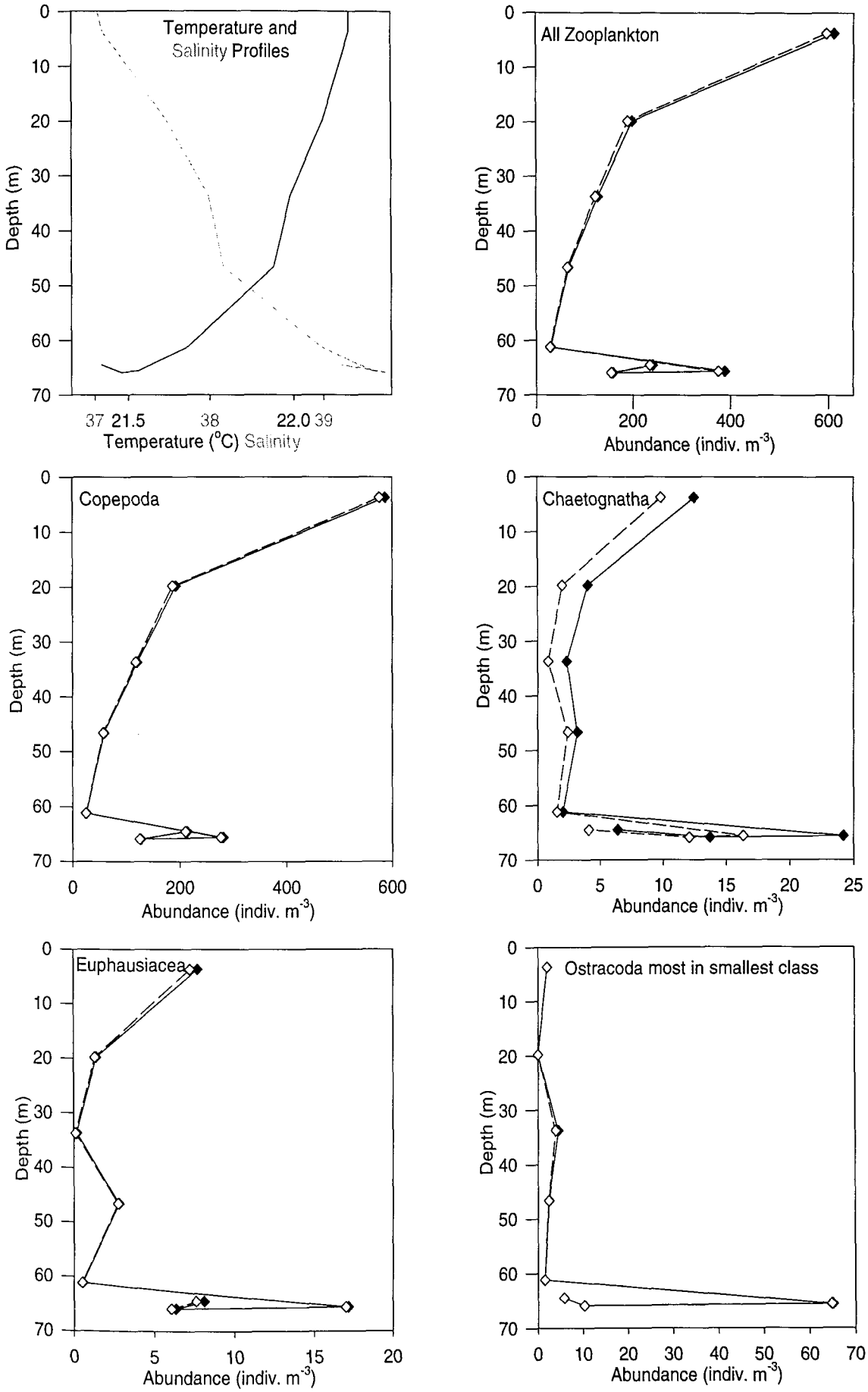

Figure 4.2.1.viii Abundance profiles of dominant zooplankton groups at Station 54007 (11/03/97) For the <4.5 and >1.5 mm size class - note different x axis scales to Figure 4.2.1.vii.

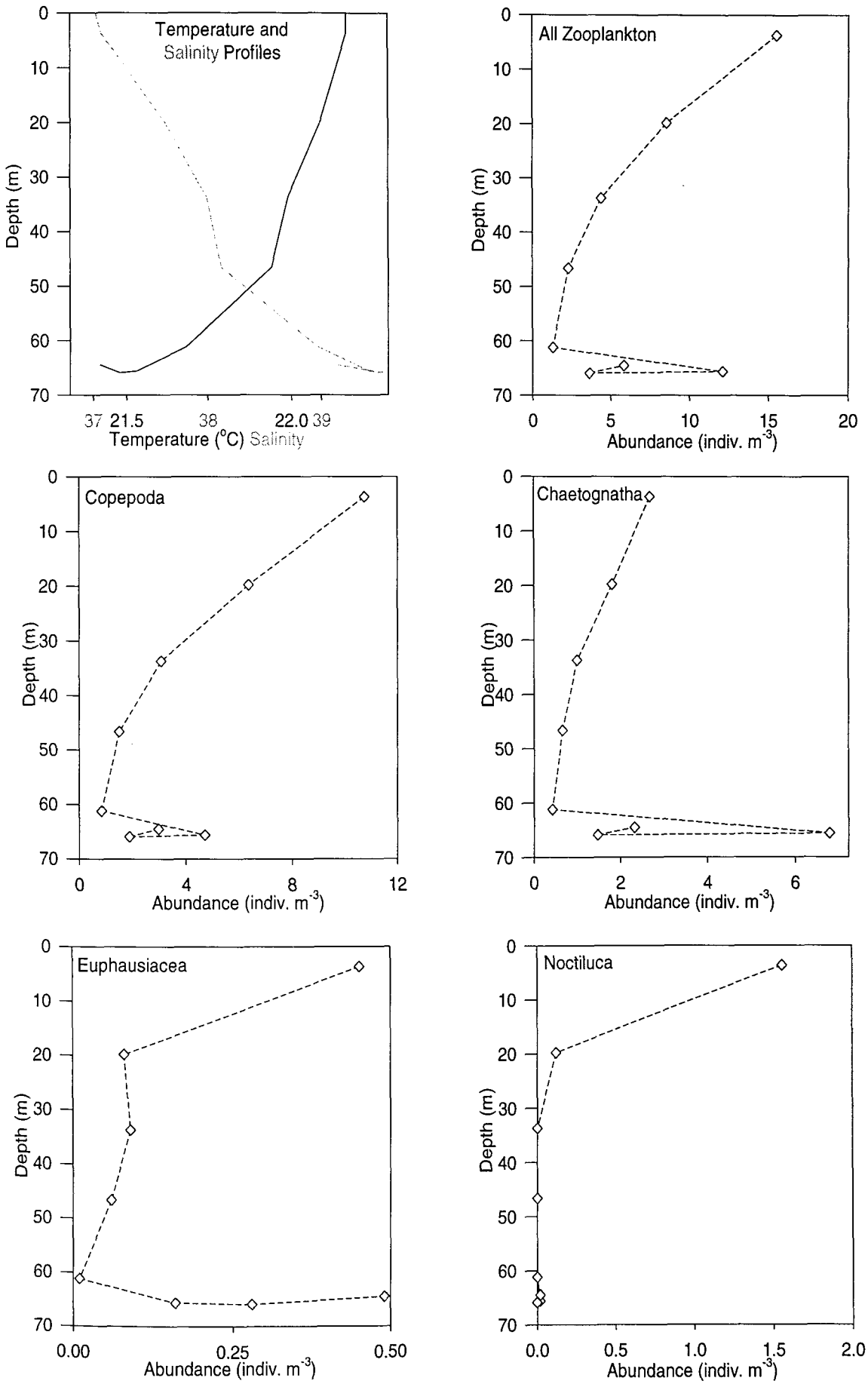

4.2.2 Hydrographic conditions at both LHPR stations

This section briefly describes the water column structure measured at stns 54006 and 54007. Station 54006, at the south eastern end of the SeaSoar survey, is characterised by GOS throughout the water column. At this station the water column structure remained consistent during the down and up profiles of the instrument (data not shown). Salinity was generally homogeneous in the upper 90 m of the water column with values between 36.5 and 36.6. The CTD data from line D (**Fig 4.1.1.iv**) showed that the high salinity AGO was present at about 130 m, but unfortunately the LHPR was not fished close enough to the seabed to sample this water. Above this depth temperature dominated the density field: with a relatively homogeneous surface mixed layer (SML) that extended to about 50 m, beneath which is the thermocline which is sharpest between 50 and 60 m, and persists to 100 m (**Fig 4.2.1.i**). During the SeaSoar survey (4 days previous) the depth of the SML was between 35-40 m. This change in the depth of the SML is probably due to an increase in wind driven mixing resulting from a shamal wind (wind speeds increased from 0-10 knots when the SeaSoar was deployed to 30-40 knots before the LHPR was fished; Moat *et al.*, 1997).

Station 54007, located to the west of the Masandam peninsular, is characterised by the STW in the upper 60m and the AGO below 60 m. The LHPR travelled sufficiently far (10 km) during the tow that the water column structure was different on the down and up profiles (data not shown). The water column on the down profile was stratified with a consistent gradient in both salinity and temperature down to 50 m (**Fig 4.2.1.ii**). Below this depth, the gradient increased significantly, and below 65 m the T and S characteristics indicated the presence of AGO. The up profile also sampled the AGO below 65 m, and there was a strong halocline and thermocline between 40 and 65 m, with a salinity gradient of 0.15 m^{-1}. Above 40 m the salinity showed little variability indicating a better mixed water column (data not shown). The SeaSoar data in the STW also showed both these structures. The water column structure was notably variable in this area during the SeaSoar survey, and therefore it is not possible to determine a clear effect of the shamal wind at this station.

4.2.3 Distribution of zooplankton measured by the LHPR

A detailed examination of the distribution of zooplankton at both stations is now undertaken. The distributions are discussed with reference to the depth, the physical structure of the water column and the water type present.

4.2.3.1 Distribution of zooplankton biovolume at LHPR stn 54006

The vertical distribution of zooplankton biovolume at stn 54006 was relatively similar on the down and up profiles (**Fig 4.2.1.i**). The zooplankton biovolume maximum (>0.1 ml m^{-3}) was in the surface mixed layer above the thermocline at 50 m. In the mixed layer, zooplankton biovolume was relatively consistent in all the samples from the up profile (≈0.18 ml m^{-3}), and the proportion in each size class was also equal. The quantity zooplankton biovolume in the mixed layer from the downcast was less consistent, but had a similar mean biovolume and ranges from 0.13 to 0.23 ml m^{-3}. Deeper in the water column biovolume was considerably lower (<0.1 ml m^{-3} between 50 and 80 m and <0.05 ml m^{-3} below 80 m). In general, the biovolume was split evenly between the <1.5 mm, and >1.5 and <4.5 mm size classes (41% and 48%, **Fig 4.2.1.i**), with a much smaller proportion in the >4.5 mm class (11%). All fractions contained more biovolume in the mixed layer than within and below the thermocline, and there was no clear relationship between size and depth.

4.2.3.2 Distribution of zooplankton abundance at LHPR stn 54006

At stn 54006 (down profile), the zooplankton abundance was also highest in the mixed layer, peaking at 35m. Abundance decreased from >200 m^{-3} in the upper 50 m (**Fig 4.2.1.v**) to <100 m^{-3} below 80m. Copepods accounted for 80 to >90% of all zooplankton caught (**Fig 4.2.1.iiia**); in the <1.5 mm size class copepods account for 90 to 95% between 20 and 80m, and 80 to 95% below 80 m (**Fig 4.2.1.iiid**). In the >1.5 and <4.5 mm class, copepods account for between 60 and 80% (**Fig 4.2.1.iiic**). Total copepod abundance was not evenly distributed through the mixed layer, and peaked between 30 and 40 m, (**Fig 4.2.1.v**). The >1.5 and <4.5mm copepods had a different vertical distribution, with peaks in the mixed layer at 35 m and within the thermocline at 65 m (**Fig 4.2.1.vi**).

At stn 54006, in the <1.5mm size class (**Fig 4.2.1.iiid**) chaetognaths[2] were the second most abundant group (up to 14 m^{-3}). The percentage of total zooplankton that was accounted for by chaetognaths increased with depth from 5% to more than 10% below 80 m. Chaetognath abundance was highest between 30 and 40 m, which correlates with the copepod maximum. There was also a second smaller peak at 80 m (**Fig 4.2.1.v**). Euphausiids and ostracods were also present (<6 m^{-3}) with each group accounting for about 5% of the total (**Fig 4.2.1.iiid**). Euphausiids were most abundant at the base of the surface mixed layer, just above the thermocline, and ostracods in the deepest samples below 100 m (**Fig 4.2.1.v**). Appendicularians were most abundant in

the mixed layer where they accounted for 5% of the zooplankton, but were almost absent below the surface mixed layer (45 m) (**Fig 4.2.1.iiid**).

As stated above, in the >1.5 and <4.5 mm class copepods dominated numerically but accounted for a smaller percentage of the abundance (70%), with the remainder divided approximately evenly between chaetognaths (~10%), euphausiids (~10%) and all the other groups (~10%). The distribution of chaetognaths[3] had a clear abundance maximum at 35 m within the mixed layer, that was correlated with the <1.5 mm copepods. Euphausiids were again most abundant at the base of the mixed layer but these larger individuals remain abundant deeper to 70 m. Siphonophores are most numerous below 100 m where they account for 5% of the total abundance.

There were too few individuals in the >4.5 mm size class to allow robust profiles to be determined. This size class was dominated by chaetognaths, with less than 1.5 animals m^{-3}. Other taxa present in the samples include decapods, fish, polychaetes, amphipods, heteropods, pteropods and doliolids.

4.2.3.3 Distribution of zooplankton biovolume at LHPR stn 54007

The vertical distribution of zooplankton biovolume at stn 54007 was different on both the down and up profiles (**Fig 4.2.1.ii**). The up and down profiles differed in terms of abundance, biovolume, size and taxonomic composition and this change correlated with a change in the physical structure (§4.2.2).

On the down profile, the highest biovolume (>0.1 ml m^{-3}) was in the upper 20 m, and decreased constantly with depth to 65 m; the lowest biovolume was between 50 and 65 m at 0.025 ml m^{-3} (**Fig 4.2.1.ii**). Below 65 m the biovolume was larger (0.05-0.1 ml m^{-3}) and this change correlates with the presence of AGO water. Biovolume was also high in the AGO on the up profile (0.05-0.08 ml m^{-3}). Biovolume was low in the overlying water between 36 and 65 m, with values ranging from 0.01-0.03 ml m^{-3}, which is lower than at the corresponding depths on the down profile (0.025-0.04 ml m^{-3}). Above 36 m depth the biovolume increased by more than an order of magnitude from 0.01 ml m^{-3} at 36 m to >0.4 ml m^{-3} at 32 m. The biovolume was even higher in all of the samples between 32 and 20m, and ranged from 0.42 to 0.86 ml m^{-3}. Biovolume was slightly lower (0.3 ml m^{-3}) in the shallowest sample taken between 15 and 20m.

[3] Chaetognaths are often only contained in the <1.5 mm fraction because their heads became detached during capture. Many individuals should be placed in the >1.5 & <4.5 mm class, where they would then account for 40% of the total zooplankton abundance.

In the samples from the down profile the <1.5 mm size class contained the most biovolume which averaged 65% of the total. This is also the case for the up profile at depths between 36 and 67 m. In the samples from the up profile between 15 and 33 m the biovolume was dominated by organisms in the >1.5 and <4.5 mm and the >4.5 mm size classes. Between 18 and 27 m these size classes accounted for up to 94% of the total, with just 6% in the <1.5 mm class. These high biovolume samples (between 15 and 32 during the up profile) consisted almost entirely of a single euphausiid species, *Pseudeuphausia* cf. *latifrons*[4] (Sars, 1883). The samples contained both adult males and gravid females, between 14 and 18 mm total length, swarming at densities up to 70 individuals m^{-3}. This species was so dominant that an almost mono-specific zooplankton community existed at these depths. The structure of this aggregation of euphausiids is examined in more detail §4.2.4

4.2.3.4 Distribution of zooplankton abundance at LHPR stn 54007

At stn 54007 the zooplankton abundance was highest (600 m^{-3}) in the shallowest samples (<20 m), and was considerably lower in the samples between 20 and 63 m, where it was between 50 and 200 m^{-3} (**Fig 4.2.1.vii**). Below 65 m the zooplankton abundance increased to between 150 and 400 m^{-3}, again correlated with the presence of the AGO (N.B. only the down profile was analysed). Copepods numerically dominated the zooplankton at this station (**Fig 4.2.1.iva**), and accounted for 85 to 95% of the total. Unsurprisingly the vertical distribution of copepods mirrored that of the total community (**Fig 4.2.1.vii**).

The <1.5 mm size class consisted almost entirely of copepods, with more than 95% in the top 45 m, 87% between 45 and 65 m, and less than 80% below 65 m (**Fig 4.2.1.ivd**). In this size class the remainder of the abundance is accounted for by chaetognaths and juvenile euphausiids, and below 35 m by a third group, the ostracods (**Fig 4.2.1.ivd**). The highest proportion of abundance of each group is below 65 m in the AGO. Their increase in abundance was proportionally larger than for copepods.

In the >1.5 and <4.5 mm class copepods accounted for 65-75% of the numbers in the STW, but below 65 m, in the AGO, copepods accounted for only 50% of all

[4] Identification to species level was not straight forward as the spine on the first segment of the antennule, which is used to distinguish *P. latifrons* from *P. sinica*, was not observed in these specimens (Mauchline and Fisher, 1969; Mauchline, 1980; Brinton, 1975; Baker *et al.*, 1990). However, *P. sinica*, as the name suggests has a distribution limited to the coastal areas of the East China Sea, (Wang and Chen, 1963) and is thought by some to be a junior synonym of *P. latifrons* (Lomakina, 1978). Only *P. latifrons* has been reported in this area before and shows morphological differences to the same species in other areas (Weigmann, 1971). Hereafter, these euphausiids are assumed to be *P. latifrons*.

species (**Fig 4.2.1.ivc**). The copepods in this size class showed a similar vertical distributions to the <1.5 mm copepods (**Fig 4.2.1.viii** and **vii**). Chaetognaths were again the second most abundant group, accounting for 15% of organisms at the surface, which increased to a maximum of 40% in the AGO. If the chaetognaths in the <1.5 mm class were added to the >1.5 and <4.5 mm size class (see footnote 3) then they would account for 50% of individuals at the surface and a maximum of 80% of zooplankton in the AGO. The chaetognath abundance was also higher in the AGO than in the STW (**Fig 4.2.1.viii**). In the >1.5 and <4.5 mm size class, the euphausiids account for less than 5% of the abundance in the STW, but more than 10% in the AGO. The euphausiids were most abundant at the surface in the STW and below 65 m in the AGO. The dinoflagellate *Noctiluca scintillans* was responsible for widespread red tides observed during this cruise (Herring, 1997), and accounted for 10% of the abundance at the surface, but were almost absent below the surface samples.

Chaetognaths were the dominant taxa in the >4.5 mm size class, but there were too few organisms of this size in the samples for analysis to be robust. Other taxa present include decapods, fish, amphipods, heteropods, pteropods and dolliolids.

4.2.4 The distribution of euphausiids at stn 54007

At certain depths in the STW the euphausiid *Pseudeuphausia latifrons*[4] existed as a high density, almost mono-specific community. The euphausiids were only captured in such numbers on the up profile at stn 54007 between 20 and 34 m, where they represent a biovolume between 0.15 and 0.86ml m^{-3} and an abundance up to 70 m^{-3}. In the water directly below the euphausiids the total zooplankton biovolume was an order of magnitude smaller between 0.01 and 0.03 ml m^{-3}, and was numerically dominated by calanoid copepods. In this section concurrent measurements from a LHPR and an EK500 are used to describe the distribution of *P. latifrons*. Biological and physical mechanisms that can account for observed distribution are discussed.

4.2.4.1 A comparison of LHPR and EK500 data at stn 54007

At stn 54007, a LHPR was used to collect a series of discrete two minute samples using a 0.33 mm meshed net (for details see §2.2.5). This net has an approximate minimum retention size of 1 mm (Barnes and Tranter, 1965), but this system caught high densities of adult *P. latifrons*, which are between 14-18 mm long. An EK500 was deployed simultaneously and measured backscatter at 3 frequencies: 38, 120 and 200 kHz (see §2.2.6). The 120 kHz frequency has a minimum size detection limit of

10 mm and was expected to be useful in determining the distribution of *P. latifrons*, as acoustic methods are most reliable on communities dominated by a single species (Foote and Stanton, 2000). The 200 kHz frequency has a minimum detection size of 7.5 mm and was also expected to detect *P. latifrons*. The backscatter presented is not calibrated because the LHPR's sensors were not reliable enough in the large gradients.

Fig 4.2.4.i shows acoustic backscatter at 120 kHz contoured as a function of time and depth. Overlaid on this plot is the sampling path of the LHPR. The bars in **Fig 4.2.4.ii** represent the biovolume in each two minute LHPR at stn 54007, **Fig 4.2.4.i** shows the depth of the LHPR. Overlaid on the bar chart are line graphs showing the acoustic backscatter at 120 and 200 kHz averaged over the depth range sampled by the LHPR in that two minutes. The data have been corrected for the time lag of the LHPR behind the ship (which varies with the amount of towing cable that is deployed). The x axes of both of these plots represent about 15 km. **Fig 4.2.4.iii** shows data from the up profile of the LHPR at stn 54007 averaged into 5 m bins. Zooplankton biovolume is represented by the bars, divided into species smaller and larger than 1.5 mm. The vertical profiles of temperature and acoustic backscatter at 120 kHz are also shown.

It is clear from **Figs 4.2.4.ii** and **iii** that there is not an exact relationship between zooplankton biovolume and acoustic backscatter, especially during the first 80 minutes. A closer relationship is observed between 95 to 115 mins, where the samples were dominated by euphausiids. **Fig 4.2.4.iii** shows differences in the vertical distributions, with the backscatter increasing dramatically between 40 and 50 m and the biovolume increasing shallower as a result of euphausiids between 25 and 35 m.

The discrepancy between the instruments may result from a number of factors. First, an exact relationship is not expected because acoustic backscatter is not determined by abundance, but the sum of the scattering characteristics of the animals present. A closer correlation may be obtained in the future by calculating the predicted backscatter from the LHPR samples and comparing this with the EK500 (Wiebe *et al.*, 1996). Second, the LHPR may not have reliably sampled the spatial distribution of the euphausiids because of the low water volume sampled compared with the acoustics, clogging of the sampling gauze and smearing between the 2 minute samples. The distribution of euphausiids cannot be determined exactly from the acoustic data and as a result more weight will be attached to the LHPR data in the following interpretation. Future use of acoustic models may help to determine the dominant scatterers, enabling the acoustic data to be used to describe the euphausiid distributions in this area.

Figure 4.2.4.i Acoustic backscatter at 120 kHz contoured against time and depth at stn 54007

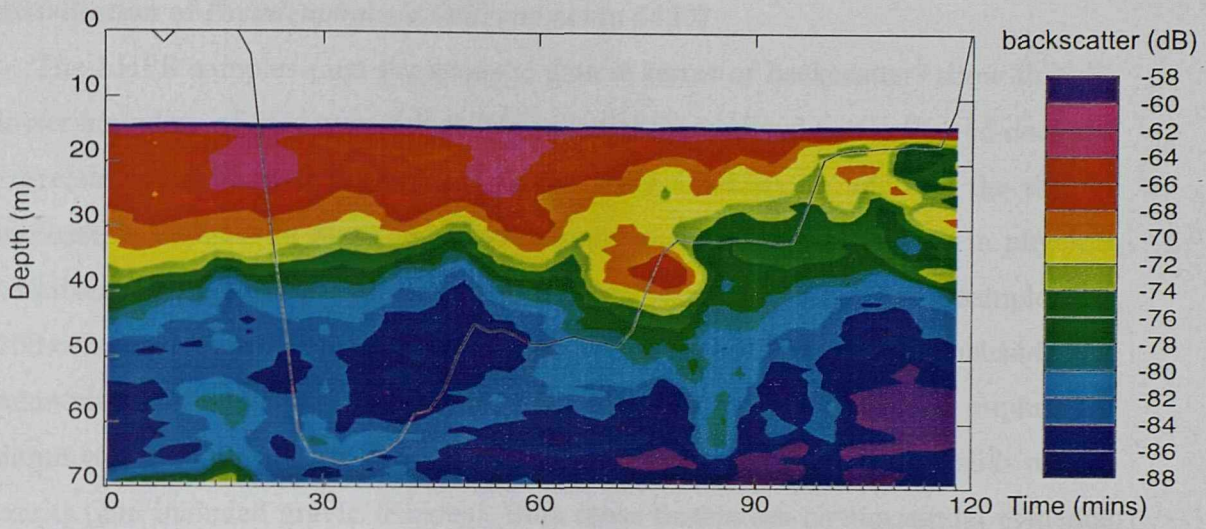

Figure 4.2.4.ii Bars showing zooplankton biovolume in each two minute sample from the LHPR and lines showing concurrent acoustic backscatter for the depth range at 120 and 200 kHz

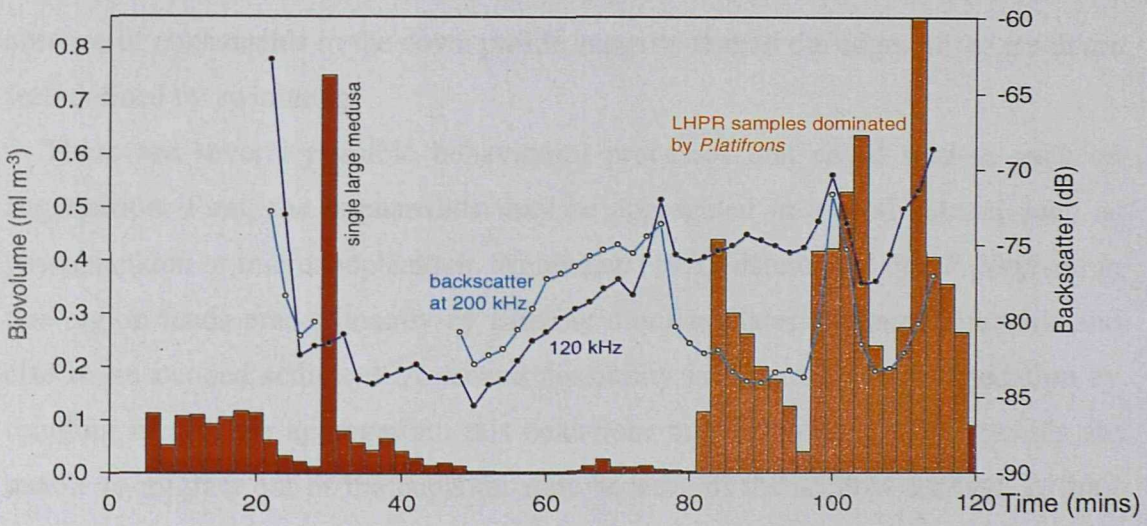

Figure 4.2.4.iii Vertical profiles from the upcast at stn 54007: bars represent zooplankton biovolume, lines represent salinity and acoustic backscatter at 120 kHz

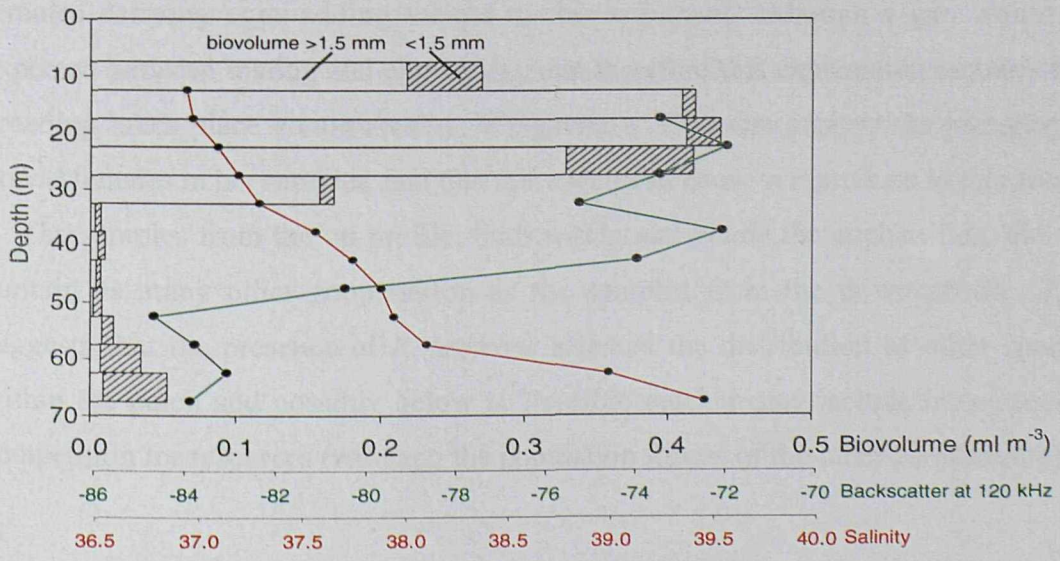

4.2.4.2 Evidence for biological and physical mechanisms in determining the distribution of *Pseudeuphausia latifrons* at stn 54007

The LHPR samples (and the acoustic data in terms of backscatter) show that the lower boundary of the layer of *P. latifrons* is tightly confined vertically and does not correlate precisely with a physical gradient (**Fig 4.2.4.iii**). In addition the rate of increase in euphausiid numbers is much larger than the rate of change in physical variables (LHPR samples from minutes 60-80 contained <0.05 m^{-3}, while samples 80-100 contained >5 m^{-3}). This evidence suggests the base of the layer of euphausiids was maintained by swimming behaviour rather than mixing processes. The euphausiid dominated samples do not contain many other species, and the euphausiids are all adults (and included gravid females). Both these factors are circumstantial evidence that biological mechanisms dominated in determining the patch structure. It is not possible to identify the boundaries and the spatial extent of this aggregation from the acoustic backscatter data. However, the sharp gradient at the base of the layer, and the absence of euphausiids in the down profile suggests that all the edges of the patch are well defined by swimming.

There are several possible behavioural processes that could lead to such an aggregation. First, the euphausiids may be aggregated in a food source, such as phytoplankton or microzooplankton. Weigmann (1970) determined that *P. latifrons* in this region feeds predominantly by filtering dinoflagellates, diatoms, tintinnids and also re–suspended sediment. A second possibility is the avoidance of predation by refuging in a dense aggregation, this behaviour may occur as the euphausiids are unable to migrate out of the euphotic zone because of the shallow sea bed. A third explanation is a breeding swarm; where aggregation increases the chances of mate encounters in a usually sparsely distributed population. The samples did contain females carrying eggs adding weight to this argument, although a gap would be expected between mating and egg laying, and therefore this explanation requires that breeding takes place continuouslys. Weigmann (1971) also reports the presence of gravid females in her samples, and that this species in know to reproduce in this area.

The samples from the up profile, both within and below the euphausiids, did not contain as many other zooplankton as the samples from the down profile. This suggests that the presence of *P. latifrons* affected the distribution of other species within the patch and possibly below it. Possible mechanisms include inter-specific competition for resources (reducing the population fitness of the other zooplankton) or

predation by the euphausiids (reducing directly zooplankton numbers). Weigmann (1970) states that larger specimens (<12 mm) of *P. latifrons* contained significant quantities of copepods in their stomachs, which were actively caught, as they were too large to be caught in the filter feeding apparatus. Similar mechanisms of predation and competition are suggested by Atkinson *et al.* (1999) to explain inverse correlations between *Euphausia superba* and copepods in the Southern Ocean.

4.2.4.3 The ontogenetic distribution of *Pseudeuphausia latifrons*

Adult euphausiids are absent from the down profile samples at stn 54007, although juvenile stages are present at a low density. Juvenile abundance is lower in the STW (0-60 m) where there are between 0.1 and 2.8 m^{-3}, than in the AGO (60-65 m) where there are between 6.3 and 17.2 m^{-3}. The juveniles have not been identified to species, but Weigmann (1971) states that *P. latifrons* is the only species of euphausiid in the Arabian Gulf. If these juvenile euphausiids are *P. latifrons* then this species shows ontogenetic spatial separation in the samples at this station. This would reduce competition between adults and juveniles and minimise possible cannibalism. From these limited observations, and the limited information available on the life cycle of this species in the literature robust conclusions are untenable. It may be speculated that the positioning of reproducing adults in the westward flow (STW) and juveniles in the eastward flow (AGO) would act as a mechanism for the maintenance in the Strait.

4.2.4.4 Discussion of the distribution of euphausiids at stn 54007

The lack of correlation between the sharp boundaries of the euphausiid patch and physical gradients suggests that behavioural aggregation was dominant in the formation of this patch. The physical environment interacts with this forcing by determining conditions that are favourable for the development of the aggregation. For example, both the temperature and salinity must be favourable for *P. latifrons*, and the vertical mixing shear must not exceed their swimming ability.

Weigmann (1970 and 1971) commented on the high abundance of this species in the Arabian Gulf, and measured up to 15 m^{-3} (the LHPR samples contained up to 70 m^{-3}). Weigmann's samples were integrated over the entire water column, and therefore it not possible to know if *P. latifrons* was aggregated at certain depths in her samples as it was here. Krill, *Euphausia superba,* are well known to swarm possibly to reduce the risk of predation, reproduce or migrate (Hamner *et al.*, 1983).

4.2.5 Factors influencing the distribution of zooplankton at each LHPR station

The findings presented in §4.2.3 show that many different sizes and taxonomic groups of zooplankton have distinct distributions in the water column. In this section there is a discussion of the influence of depth, water column structure and water type on the zooplankton present at the two LHPR stations in the Strait.

At both stations the highest abundance and biovolume of zooplankton was concentrated close to the surface. The same distribution pattern was also seen in the data from the OPC and the EK500 (at 120 and 200 kHz) in the Strait (§4.1.3). The degree of stratification of the water column correlates with the vertical extent of these surface zooplankton maxima. At stn 54006, where the SeaSoar showed that the Brünt Vaisala Frequency maximum was deepest (**Fig 4.1.1.i**), the surface mixed layer extended to 50m, and the biovolume maximum was distributed from the surface to this depth, with a sharp decrease at the thermocline. At stn 54007, where the Brünt Vaisala Frequency maximum was shallow (**Fig 4.1.1.i**), the water column was stratified on the down profile and zooplankton abundance and biovolume were reduced consistently with depth, from a maximum at 10 m to a minimum at 60 m. The thermocline and the halocline also act a barrier to some taxonomic groups. For example at stn 54006, appendicularians were more than an order of magnitude more abundant above the thermocline than below.

The distribution of taxonomic groups and size classes is also influenced by the water type present. However, the measurements made at the two LHPR stations cannot be assumed to represent the conditions throughout each water type. This is because of the unreliability of sampling typically patchy zooplankton distributions at a single locality. Both the OPC and EK500 data demonstrate that there was substantial variability in the distribution of plankton within each water type, which was also shown by the differences between the down and up profiles at stn 54007.

The impact on the zooplankton community of a change in water type is clearest when both the AGO and STW are sampled at stn 54007. The AGO contained more than 4 times more zooplankton abundance and twice the biovolume than the overlying STW (between 20 and 60 m). The AGO also contained a lower proportion of copepods (although greater abundance), which result from an even larger increase in the abundance of chaetognaths, euphausiids and ostracods. The GOS is more similar to the STW, although this may be a result of both being at the surface at each station. Zooplankton abundance and biovolume were higher in the GOS than in the STW,

except for the shallowest samples where they were greater in the STW. The GOS contained a lower proportion of copepods in the upper 50 m, as a result of the presence of other taxa, particularly appendicularians which are absent at stn 54007. The down profiles in the GOS and STW contained similar proportions of euphausiids and chaetognaths. The up profile in the STW was dominated entirely by euphausiids, and contained very few copepods and other groups.

The distribution of many groups did not always correlate with obvious physical environmental variables, such as water types or water column structure. This suggests that the behaviour and mobility of the zooplankton are important in determining their distributions. For example, ostracods increased in abundance with depth at both stations, as did siphonophores at stn 54006. Also at stn 54006, >1.5 and <4.5 mm copepods and euphausiids were most abundant at the base of the mixed layer (around 40 m) and in the thermocline between 50 and 70 m. Another example comes from the up profile at stn 54007, where the euphausiids *P. latifrons* are concentrated within a homogeneous layer, but are not evenly distributed from the surface to the base of the layer. These observations indicate that the distributions of many groups are also influenced by active behavioural mechanisms (driven by swimming). These aggregations may have been related to variables that were not measured by the LHPR, such as food availability (e.g. chlorophyll or microzooplankton), the avoidance of predators or may have been part of diel migration cycle (both stations were fished in daylight).

4.2.6 Summary of findings from LHPR data

The LHPR samples demonstrate that zooplankton biovolume and abundance were highest near to the surface at both stations. The vertical extent of the surface maximum correlates with the water column structure and stratification. At stn 54007 (down profile) the maximum is confined to the upper 18 m of the stratified water column, but at stn 54006 it is distributed through the mixed layer to the thermocline at 50 m. Not all taxonomic groups had their highest densities near the surface: for example ostracods and siphonophores had the reverse distribution with their highest abundance at depth. Also, the presence of AGO water at stn 54007 correlated with higher abundance and biovolume below 60 m than in the STW between 20 and 60 m.

Copepods were the most abundant taxonomic group at both stations, accounting for more than 80% of all zooplankton. Chaetognaths were the next most abundant group,

accounting for about 10% of the total zooplankton. This percentage increased to as much as 40% in the >1.4 and <4.5 mm class, and was often more than 80% in the >4.5 mm class. Euphausiids were the next most abundant group, usually accounting for about 5% of the total, and ostracods were abundant in the lower half of the water column at both stations, also accounting for a maximum of about 5%. Other taxa that were present include pteropods, siphonophores, amphipods, decapods, appendicularians (stn 54006) and the dinoflagellate *Noctiluca* (stn 54007).

At stn 54007 the LHPR tow crossed a horizontal physical boundary that divided distinct zooplankton communities, on one side dominated by copepods in the 0.2-1.5 mm size range, and the other by a single species of euphausiid, *Pseudeuphausia latifrons*, 14-16 mm long.

CHAPTER 5

Analysis of the interrelationship between physical, chemical and biological environment and behavioural processes in determining the distribution of zooplankton in the Strait

5.1 THE INFLUENCE OF THE FORMATION OF THE STW ON THE DISTRIBUTION OF DIFFERENT SIZED PLANKTON IN THE STRAIT OF HORMUZ 149

5.2 THE DISTRIBUTION OF PLANKTON AROUND THE FRONT BETWEEN THE AGO AND THE STW IN THE WESTERN STRAIT 157

5.3 THE AFFECT OF VARIABILITY CAUSED BY INTERNAL WAVES AT THE BOUNDARY BETWEEN THE GOS AND THE STW ON THE PLANKTON 169

FIGURES

5.1.1.i The surface positions of the water types defined for the Strait of Hormuz . . 151

5.1.1.ii Biological characteristics of the three types of water identified in the Strait . 152

5.1.3.i Biomass size spectra for the upper 25 m in the GOS, STW and AGO . . 153

5.2.1.i The distribution of chlorophyll *a*, zooplankton abundance and MVBS at the front between the AGO and STW on legs 2 and 3 158

5.2.2.i Zooplankton biovolume, in each size class and chlorophyll *a* integrated over the top 25 m, plotted as a function of the average salinity in the top 25m 162

5.2.3.i The relationship between salinity and the ratio of phytoplankton carbon to zooplankton carbon in the upper 25m in the front between the AGO and STW . . . 163

5.2.3.ii The relationship between salinity and the ratio of phaeopigments to chlorophyll *a* . 163

5.3.1.i Variability in thermal structure and zooplankton abundance . . . 171

5.3.1.ii Zooplankton abundance (size range 0.4-4.1 mm ESD) plotted as a function of potential temperature. Data from east side of the Strait of Hormuz 171

5.3.2.i Variability in the depth of the 22.5°C isotherm and the zooplankton abundance, integrated over the upper 50m of the water column in the GOS 174

5.3.2.ii Zooplankton abundance as a function of the depth of the 22.5°C isotherm . . 174

5.3.2.iii The PCC between abundance and isotherm depth, as a function of size . . 175

5.3.3.i Power spectra of the spatial variability in the depth of the 22.5°C isotherm, chlorophyll and zooplankton abundance (in size classes) in the GOS 179

5.3.4.i The relationship between phytoplankton and temperature in the GOS . . 175

The aim of this chapter is to examine the interrelationship between the physical, chemical and biological environment and behavioural processes in determining the distribution of different size zooplankton in the Strait of Hormuz. In the previous chapter the distribution of zooplankton in relation to certain physical features and the geography of the Strait was described. In this chapter these distributions are analysed objectively to determine correlations that indicate the environmental and behavioural mechanisms that impact on the zooplankton community. Specifically, the impact of three hydrographic features on the distribution of zooplankton is examined covering horizontal scales ranging from the mesoscale to the sub-mesoscale: >100 km to <10 km. First, the conditions in the three water types identified in the Strait are compared: these are the end members, the AGO and GOS, and the STW, a water that represents a mesoscale frontal region between them. Second the front between the AGO and the STW is examined. This feature is part of the frontal region represented by the STW and is at the lower size range of the mesoscale. This front is investigated as a separate feature in this chapter because it is correlated with abrupt changes in the distribution of plankton. Third there is an examination of the spatial variability of the inflow from Gulf of Oman and its influence on plankton distributions. This mesoscale and sub-mesoscale variability resulted from internal waves and possibly also meanders and eddies in the inflow.

5.1 The influence of the formation of the STW on the distribution of different sized plankton in the Strait of Hormuz

In the previous chapter (§4.1.2) three water types were identified in the Strait of Hormuz. These were the oceanic surface inflow from Gulf of Oman (GOS), the high salinity water flowing out of the Arabian Gulf (AGO) and a water formed when they mix, named the Strait transition water (STW). The temperature and salinity characteristics of these water types are listed in Table 5.1.1.a, and their distributions at the surface are plotted in **Fig 5.1.1.i**. The STW is an intermediate between the AGO and GOS, and is formed when these waters mix in the Strait, representing a frontal region between them at the mesoscale.

The object of this section is to quantitatively compare the biological characteristics of the STW with the waters that mix to produce it (the GOS and AGO). In order to allow biological variables to be compared between water types without bias occurring due to different vertical distributions, data are averaged over the upper 25m. Most of

the mesozooplankton were present above this depth horizon. All three water types contained strong vertical gradients in biological variables, which were clear in the data from the fluorimeter, OPC, EK500 and LHPR (§4.1.3 and §4.2.3). This analysis does not consider any differences in the vertical distributions of plankton in each water.

The following biological parameters, that were measured concurrently with the physical data from the SeaSoar, are plotted in **Fig 5.1.1.ii**: chlorophyll *a* concentration, OPC measured zooplankton abundance and biovolume, and mean volume acoustic backscattering strength (MVBS) from an EK500 at 38 kHz, 120 kHz and 200 kHz frequencies. The 95% confidence limits of the means are shown as error bars, which were calculated as mean ± t * Standard Error, where t is Student's statistic defined by the degrees of freedom (Parker, 1983; Fowler and Cohen, 1990). The mean and confidence limits of the acoustic backscatter were calculated after the MVBS data had been converted to a linear scale. The data were then converted back to the typical logarithmic scale and presented in **Fig 5.1.3.i**. **Fig 5.1.3.i** presents the size spectra of mesozooplankton in each water type. Each water type had a clear biological signal in the majority of parameters.

5.1.1 The concentration of chlorophyll *a* in each water type

The chlorophyll *a* data presented in **Fig 5.1.1.ii.a** only represents the measurements made at night, as no reliable correction for quenching has been determined (§2.2.3.2). The two end member water types had similar mean chlorophyll *a* concentrations: of 0.5 mg Chl*a* m^{-3} for the GOS and 0.4 mg Chl*a* m^{-3} in the AGO. The STW, which is produced by the mixing of the AGO and GOS, had a much larger mean chlorophyll *a* concentration of 0.75 mg Chl*a* m^{-3}. A Kruskal-Wallis one way ANOVA on ranks was used to evaluate statistically significant differences between these average concentrations (Howell, 1995). A significant difference ($p<0.05$) existed between, not only, the mean in the STW and others waters, but also between the means in the AGO and the GOS (multiple comparisons made with Dunn's Method). This is consistent with the non-overlapping 95% confidence limits shown on the graph.

5.1.2 Mesozooplankton abundance and biovolume measured by the OPC

The mesozooplankton abundance (**Fig 5.1.1.ii.b**), measured by an OPC for particles between 0.4 and 4.1 mm, was approximately equal in both GOS and AGO: there were on average 9700 m^{-3} in the GOS and 10000 individuals m^{-3} in the AGO. Using the same statistical method as above, no significant statistical difference was found between the mean zooplankton abundance in the AGO and GOS.

Figure 5.1.1.i The surface (9m) positions of the water types defined for the Strait of Hormuz

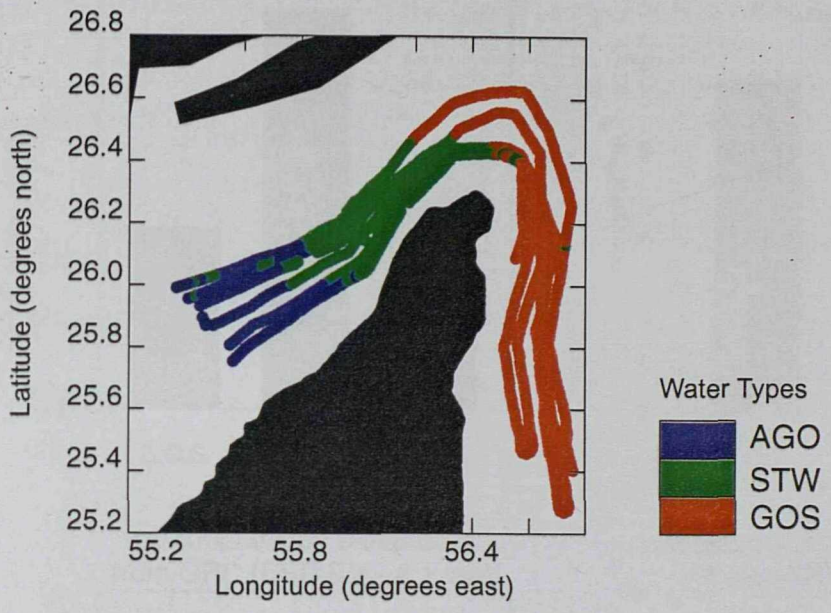

Table 5.1.1a Temperature and salinity characteristics of water types in the Strait

Water Type	Temperature (°C)	Salinity
Gulf of Oman Surface inflow - GOS	22.6 - 23.3	36.4 - 36.8
Strait Transition Water - STW	21.7 - 22.6	36.8 - 38.0
Arabian Gulf Outflow - AGO	21.0 - 21.7	38.0 - 40.5

Table 5.1.3a The size classes of zooplankton used in the size spectra (Figure 5.1.3.i)

Log Volume range (mm^3)	Volume range (mm^3) midpoint in brackets	ESD range (mm)	Digital Output Size range
$2^{-7.5}$ - $2^{-6.5}$	0.0055 - 0.011 (0.008)	0.36 - 0.45	13.5 - 19.5
$2^{-6.5}$ - $2^{-5.5}$	0.011 - 0.022 (0.016)	0.45 - 0.57	19.5 - 30.5
$2^{-5.5}$ - $2^{-4.5}$	0.022 - 0.044 (0.031)	0.57 - 0.72	30.5 - 47.5
$2^{-4.5}$ - $2^{-3.5}$	0.044 - 0.088 (0.063)	0.72 - 0.91	47.5 - 72.5
$2^{-3.5}$ - $2^{-2.5}$	0.088 - 0.177 (0.125)	0.91 - 1.14	72.5 - 110.5
$2^{-2.5}$ - $2^{-1.5}$	0.177 - 0.35 (0.25)	1.14 - 1.44	110.5 - 172.5
$2^{-1.5}$ - $2^{-0.5}$	0.35 - 0.71 (0.5)	1.44 - 1.81	172.5 - 262.5
$2^{-0.5}$ - $2^{+0.5}$	0.71 - 1.41 (1)	1.81 - 2.28	262.5 - 406.5
$2^{+0.5}$ - $2^{+1.5}$	1.41 - 2.83 (2)	2.28 - 2.88	406.5 - 634.5
$2^{+1.5}$ - $2^{+2.5}$	2.83 - 5.65 (4)	2.88 - 3.62	634.5 - 985.5
$2^{+2.5}$ - $2^{+3.5}$	5.65 - 11.3 (8)	3.62 - 4.57	985.5 - 1519.5
$2^{+3.5}$ - $2^{+4.5}$	11.3 - 22.6 (16)	4.57 - 5.75	1519.5 - 2152.5

Figure 5.1.1.ii Biological characteristics of the three types of water identified in the Strait Means (in the upper 25m) and error bars of 95% confidence limits of variables

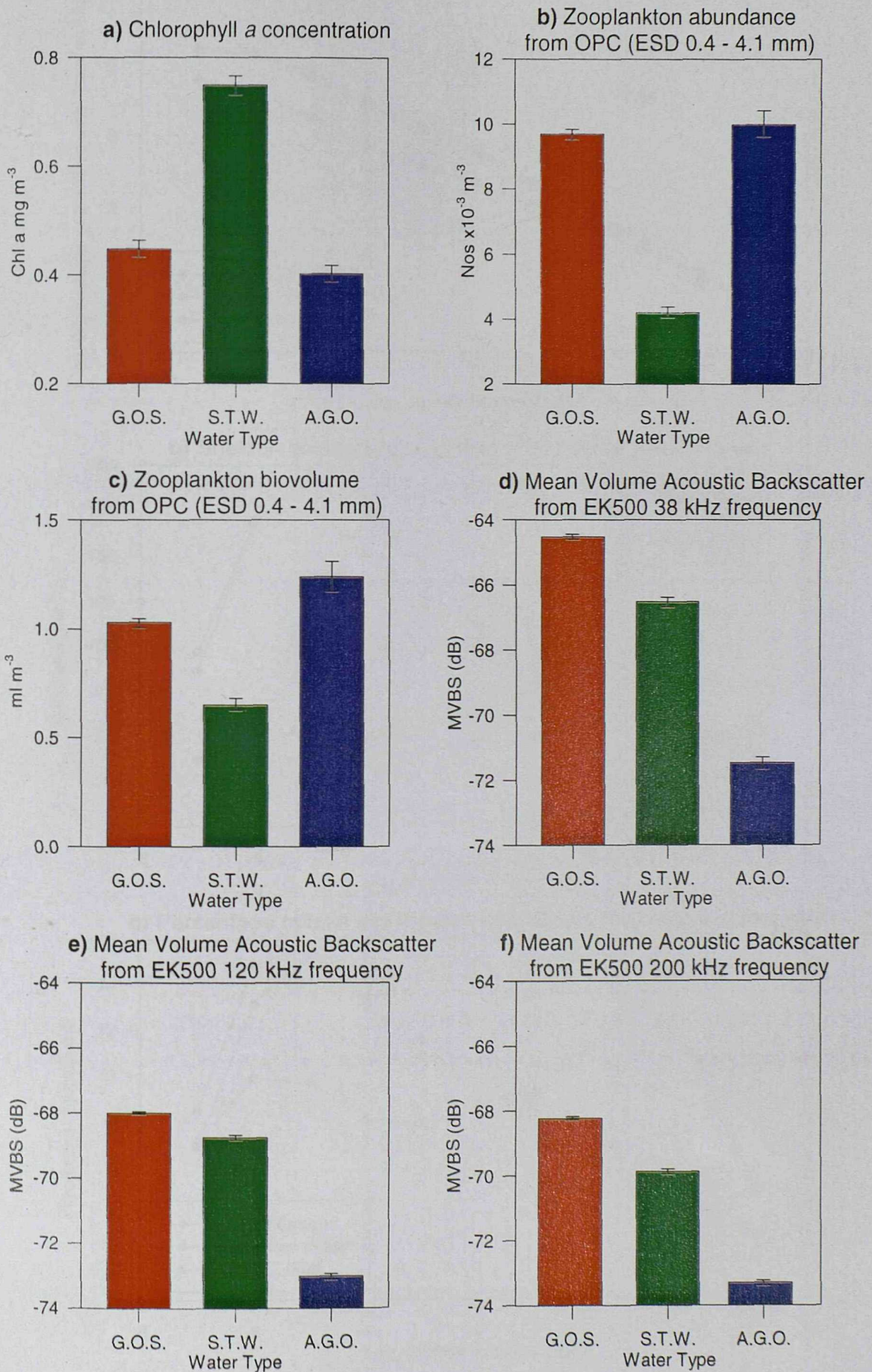

Figure 5.1.3.i Biomass size spectra for the upper 25m in the GOS, STW and AGO

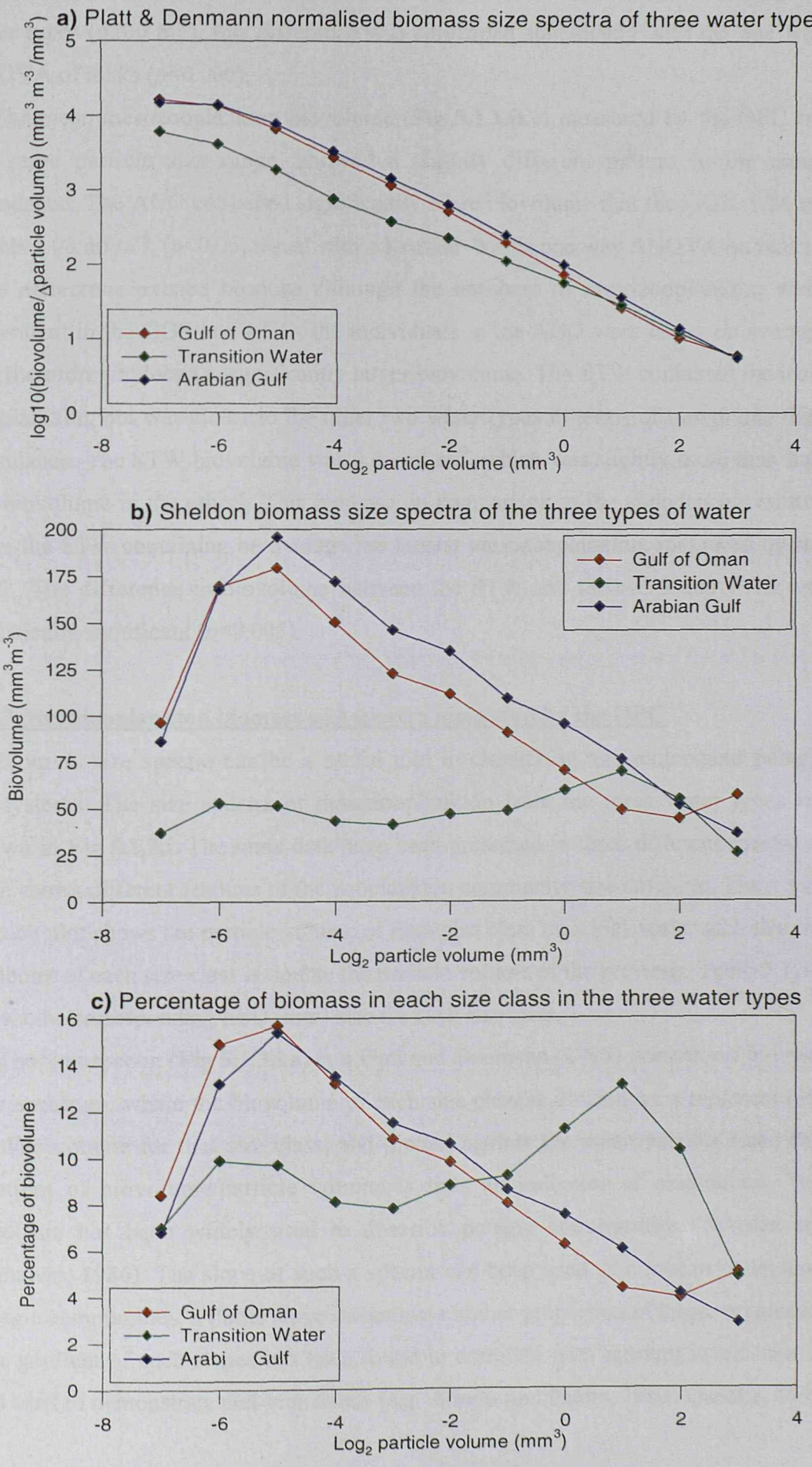

The mean zooplankton abundance in the STW was less than half that in the other water types (4200 m^{-3}), this difference was confirmed statistically with the one way ANOVA of ranks ($p<0.005$).

The mean mesozooplankton biovolume (**Fig 5.1.1.ii.c**) measured by the OPC for the same particle size range, showed a slightly different pattern to the mean abundance. The AGO contained significantly more biovolume that the GOS: 1.24 ml versus 1.03 ml m^{-3}, ($p<0.05$, tested with a Kruskal-Wallis one way ANOVA on ranks). This difference existed because although the numbers of mesozooplankton were equivalent in the GOS and AGO, the individuals in the AGO were larger on average and therefore produced a significantly larger biovolume. The STW contained the least zooplankton, but was closer to the other two water types in terms of biovolume than abundance. The STW biovolume was 0.65 ml m^{-3}, which was slightly more than half the biovolume in the others. This increase, in comparison to the abundance, resulted from the STW containing on average the largest mesozooplankton, measured by the OPC. The difference in biovolume between the STW and the AGO and GOS was statistically significant ($p<0.005$).

5.1.3 Mesozooplankton biomass size spectra measured by the OPC

Biomass size spectra can be a useful tool in classifying and understand pelagic ecosystems. The size spectra of mesozooplankton from the three water types are shown in **Fig 5.1.3.i**. The same data have been presented in three different spectra as each shows different features of the zooplankton community size structure. The x axis of each plot shows the particle volume of each size class on a $\log_2$ scale, such that the midpoint of each size class is double the particle volume of the previous. Table 5.1.3.a shows the corresponding ESD (mm) size for each size class.

The first spectra (**Fig 5.1.3.i.a**) is a Platt and Denmann (1978) normalised biomass size spectrum, where the biovolume of each size class is divided by a representative particle volume for that size class, and plotted against the mean particle size. This quotient of biovolume/particle volume is thus an indicator of abundance. This spectrum has been widely used to describe pelagic communities (Sprules and Munawar, 1986). The slope of such a spectra can been used as a tool to understand pelagic communities: a flatter slope indicating a higher proportion of larger organisms. The gradient of such slopes has been found to correlate with nutrient levels, season and used to demonstrate diel migrations (e.g. Ahrens and Peters, 1991; Gaedke, 1992;

Rodriguez and Mullin, 1986). The three water types identified in the Strait had different gradients of normalised biomass size spectra (**Fig 5.1.3.i.a**) of –0.48 in the GOS, –0.51 in the AGO and –0.31 in the STW. The first point in each spectra was not used to calculate the gradients as the data suggest that the OPC under sampled the abundance of these particles (see §2.2.4). The slope of the STW line indicates a greater proportion of large individuals than in the other water types. An ANOVA test showed a significant statistical difference ($p<0.05$) between the mean gradient of the STW and the other spectra. The slopes for the GOS and AGO were similar and the mean slopes were not statistically different.

The second spectra (**Fig 5.1.3.i.b**) is much simpler: in this Sheldon type spectra the biovolume is plotted against the mean particle size in each class (Sheldon *et al.*, 1972). This is the most commonly used spectrum. The size spectra of zooplankton biovolume in the GOS and the AGO were similar, with the highest biovolume in the 0.72-0.91 mm ESD size class and a steady decrease at larger sizes. The AGO contained slightly more biovolume than the GOS in size range 0.72-4.57 mm ESD. The size spectrum for the STW (**Fig 5.1.3.i.b**) was very different: the total biovolume was lower, with the maximum biovolume in the 2.28-2.88 mm ESD size class. In the small size classes (0.36-0.91mm ESD) the STW contained only about a quarter of the biovolume that was in the AGO and STW, but above 2.28 mm ESD the biovolume in the STW was equal to the AGO and was larger than the GOS.

The final spectrum (**Fig 5.1.3.i.c**) is a modification of the Sheldon spectra, which has been normalised for the total biovolume in each water type. This allows the size class structure to be viewed independently of the biovolume differences between the water types. The spectra for the AGO and GOS were very similar, with the highest percentage of biovolume in the range 0.45-0.91 mm ESD. The spectra for the STW was distinct and had the highest percentage of biovolume in the 2.28-4.57 mm ESD size class.

The spectra indicate that the mesozooplankton community structure in the AGO and GOS were similar, but the STW, which was formed by the mixing of the AGO and GOS, supported a completely different mesozooplankton community as defined by abundance, biovolume and size structure. The biovolume in the AGO and GOS were dominated by small (<1.0 mm ESD) species, while in the STW these species were 4 time less abundant, but the larger species (2.28-4.57 mm ESD) accounted for a higher proportion, although this was within the range in end members.

5.1.4 Acoustic Backscatter from EK500

The mean volume backscattering strength (MVBS), measured at three frequencies (38, 120 and 200 kHz) by an EK500, shows a different pattern to the other biological variables (**Fig 5.1.1.ii**). At all three frequencies there was a gradient from the GOS with the largest to the AGO with the lowest MVBS. Therefore, in terms of MVBS the STW is an intermediate between the AGO and GOS, as it is for physical variables. However, this does not necessarily mean the this water was intermediate in terms of species present, or indeed abundance and biovolume.

5.1.5 Summary and discussion of the influence of the formation of the STW on the distribution of plankton in the Strait

Although mixing between the GOS and the AGO formed the STW, the phytoplankton and mesozooplankton standing stocks did not show a conservative gradient between the end members (GOS and AGO). The STW, when averaged over the upper 25m, contained twice the standing stock of chlorophyll but only half the mesozooplankton abundance of the AGO and GOS. In addition, the size spectrum of mesozooplankton biovolume was different in the STW compared with AGO and GOS. In the GOS and AGO small zooplankton (0.36-0.91 mm ESD) dominated, with up to four times more biovolume than in the STW in the same size range. In the STW larger species (2.28-5.75 mm ESD) account for the highest percentage of the biovolume. The amount of mesozooplankton biovolume in each water type was inversely correlated with the phytoplankton standing stock relative to the others. The temporal development of these observations is discussed in §6.2.2.2.

The majority of mesozooplankton in the 0.36-0.91 mm ESD size range were probably small cyclopoid and calanoid copepods, such as *Oithona*, *Paracalanus* and *Oncaea* which numerically dominate this size range in this region (Michel *et al.*, 1986b). Rissik *et al.* (1997) measured with an OPC the ESD ranges of *Oithona* between 0.48 and 0.61 mm and *Oncaea* between 0.54 and 0.88 mm. The dominant group in the 2.28-5.75 mm size class are still expected to be copepods but the LHPR samples (§4.2.2) indicate that chaetognaths may account for up to 40%.

The macrozooplankton, in terms of MVBS, were intermediate in the STW compared with the GOS and AGO. However, unlike the larger mesozooplankton, the MVBS decreased from the GOS to the AGO. These larger longer lived species were probably influenced by other environmental factors rather than the shorter term

processes associated with the formation of the STW. Leveau and Szekielda (1968) suggest that the shallowing of the seafloor in the Strait reduces the number of species of macrozooplankton, and Kimor (1973) states that the increasing salinity limits the distributions of many species (§2.1.3.3). These factors may explain the reduction of MVBS from the Gulf of Oman side of the Strait to the Arabian Gulf. These findings are discussed further in §6.2.2.

5.2 The Distribution of Plankton around the Front between the AGO and the STW in the Western Strait

This section examines the interaction between the phytoplankton, zooplankton and physical environment in the front between AGO and STW. A front is a region of larger-than-average horizontal gradients of water properties such as temperature, salinity, density, turbidity or colour (Joyce, 1983). This front is at the western extreme of the Strait of Hormuz SeaSoar survey and is characterised by the high salinity AGO being subducted below the STW. The front is in fact part of the frontal region represented by the STW, but is differentiated by an increased horizontal salinity gradient, and is correlated with changes in the distribution of plankton. Therefore the front between the STW and AGO is investigated as a distinct mesoscale feature.

This section is divided into four parts: first there is a description of the front and the associated distribution of plankton in the water either side and within the front. Second these data are analysed to determine the correlations between the zooplankton and their physico-chemical and biological environment across and either side of the front. Third an estimate is made of the importance of herbivory by mesozooplankton in this area, and fourth the top-down predatory control on mesozooplankton is investigated.

5.2.1 Description of the front and the associated plankton distributions

Fig 5.2.1.i presents contour plots of salinity, chlorophyll *a* and mesozooplankton abundance as a function of the depth and distance travelled by the ship, and MVBS at 38 kHz as a function of depth and time (which is equivalent to the distance axis of the other variables). The plots show the data from two parallel legs (5 km apart) through the front: on the left Leg 2, surveyed during daylight on 03/03/97, and on the right Leg 3, surveyed 36 hours later during darkness on 04/03/97. The x axis of each plot represents 80 km (about 5 hours and 270 SeaSoar profiles) with the west on the left and the east on the right. The other legs and variables can be seen in **Fig 4.1.1.i**.

Figure 5.2.1.i The distribution of chlorophyll *a*, zooplankton abundance and mean volume acoustic backscatter at the front between AGO and STW on Legs 2 and 3

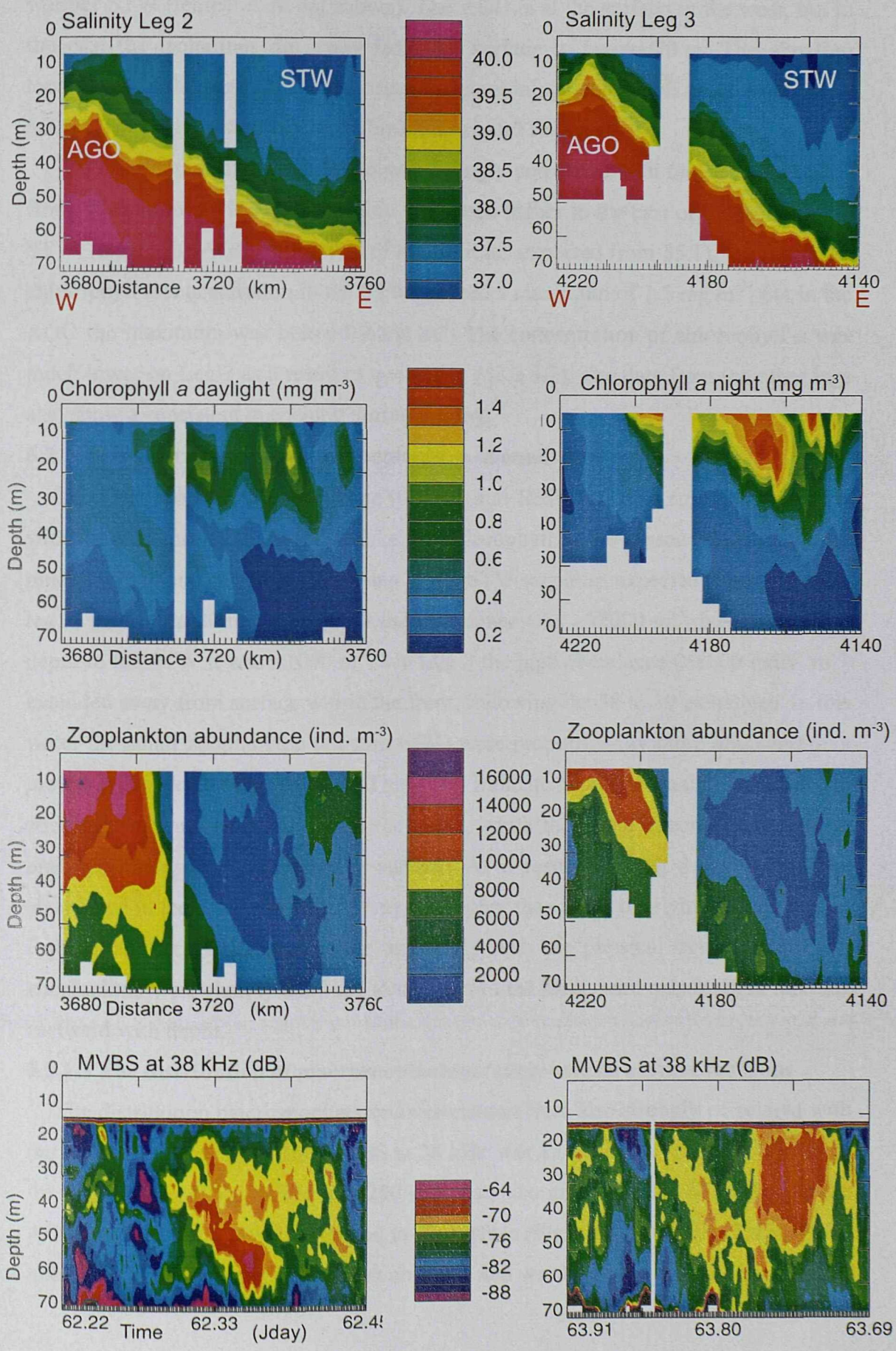

The plots (**Fig 5.2.1.i**) show the front which divides the high salinity, lower temperature AGO, which flows eastward and is subducted beneath the less saline, warmer STW (temperature not shown). The AGO is at the surface in the west, but to the east the isohalines dip away from the surface to below 70 m. The shoaling topography in the west may be important in determining the position of the front.

5.2.1.1 The distribution of phytoplankton around the front

The distribution of chlorophyll *a* was strongly correlated with the structure of the front. The chlorophyll *a* concentration was much higher to the east of the front, in the STW, than in the AGO to the west of the front (as expected from §5.1). On Leg 3 the chlorophyll a concentration in the STW reached a maximum of 1.5 mg m^{-3}, but in the AGO the maximum was below 0.4 mg m^{-3}. The concentration of chlorophyll *a* was much lower on Leg 2 as a result of quenching (§2.2.3.2). The data from the other legs also show a consistent quenching during the day.

5.2.1.2 The distribution of mesozooplankton around the front

The mesozooplankton abundance (0.4-4.1 mm ESD) was also strongly correlated with the structure of the front. Unlike the chlorophyll *a*, the mesozooplankton were much more abundant in the AGO than in the STW (again as expected from §5.1). On leg 2, in the top 20 m of the AGO the abundance was >12000 m^{-3}, but at the same depth in the STW it was ≈1000 m^{-3}. On Leg 3 the high abundance (>8000 indiv. m^{-3}) extended away from surface within the front, following the 38 to 39 isohalines. In this water the small zooplankton (>1 mm ESD) were proportionally more abundant than the larger species (**Fig 4.1.1.i**). This may indicate that the smaller, less motile zooplankton were subducted with the AGO, while the larger species were able to maintain their positions near the surface. As a result, on Leg 3 and Leg 4 the abundance in the AGO (down to 70 m) was higher than in the overlying STW. On Leg 2 the abundance did not correlate as closely with the physical structure, and the zooplankton were sharply confined to the west of the front, with only a slight increase eastward with depth.

5.2.1.3 The distribution of macrozooplankton/micronekton around the front

The distribution macrozooplankton/micronekton were also strongly correlated with the structure of the front. The MVBS at 38 kHz was 15 dB larger in the STW than in the AGO. The MVBS at 120 and 200 kHz was also greater in the STW than in the AGO, but was more closely confined to the surface (**Fig 4.1.1.i**). On Leg 2 the MVBS maximum at 38 kHz was deeper than on Leg 3 and was highest within the halocline of

the front, and was also high in the front on Leg 3. The changes between legs may result from DVM of the dominant scatters, but the data from the other legs were inconclusive in this respect. This change may result from other factors such as advection or the shallower sea floor on Leg 3.

5.2.2 The influence of the physical processes at the front on the plankton

In this section the data are analysed to resolve the details of these correlations, in order to identify the importance of direct physical forcing mechanisms associated with the front on phytoplankton and different sized zooplankton.

The front between the AGO and the STW is determined by a salinity gradient of 36.5-40. Mesozooplankton biovolume in each of the 5 size classes (from legs 1-4) and chlorophyll concentration are plotted as a function of salinity across the front in **Fig 5.2.2.i**. Salinity is used instead of distance to examine if the plankton distributions were conservative with mixing and so that the data from legs 2-4 could be combined. The biovolume has been integrated over the top 25 m to remove any vertical patterns in the data and is plotted against the salinity, averaged over the same range. (Note that in **Figs 5.2.2.i**, **5.2.3.i** & **ii** low salinity is on the left of the graphs, as opposed to the contour plots, **Fig 5.2.1.i**, where the low salinity water is on the right of the plot).

The 0.40-0.64, 0.64-1.02 and the 1.02-1.61 mm ESD size classes all showed a positive correlation with salinity, with the biovolume increasing from the STW to the AGO. These approximately linear relationships (**Fig 5.2.2.i**) demonstrate that the distribution of small (0.4-1.6 mm ESD) mesozooplankton was generally conservative with mixing across the front. The correlations of these size classes with salinity can be quantified by Pearson correlation coefficients - PCCs (Ludwig and Reynolds, 1988) of 0.89, 0.91 and 0.78. The distribution of phytoplankton was less clear because the graph contains quenched measurements but still appeared to be mainly conservative with the mixing.

The largest two size classes of zooplankton (1.61-2.56 and 2.56-4.10 mm ESD) did not show a simple correlation with salinity, resulting in low PCCs of 0.12 and –0.02. The biovolume of these zooplankton (1.6-4.1 mm ESD) was high on either side of the front, but lower within the front. However it should be noted that there are only a few data points within the front. This distribution suggests that salinities between 37.5 and 38.25 were not favourable to species acclimatised to the conditions on each side of the front, and these larger species avoided this water by swimming. The horizontal

distances are too large for zooplankton swimming to be important, but vertical swimming could maintain zooplankton in favoured conditions as vertical gradients of salinity were of the order of 0.1 m^{-1}. Therefore, zooplankton would only have to swim <5-10 metres to avoid unfavourable conditions. The macrozooplankton distributions measured by the EK500 also show non-conservative gradients with mixing across the front (line graphs not shown, see **Fig 5.2.1.i**). For example on Legs 2 and 3 MVBS was high within the front. These non-conservative distributions are expected for the typically greater swimming ability of these larger species.

This analysis has demonstrated that different sized zooplankton have different distributions in relation to physical forcing. The observations were consistent with a hypothesis that larger species were more capable swimmers, and more able to determine their own distributions in the face of mixing. The smaller mesozooplankton (0.4-1.6 mm ESD) behaved as passive tracers with the mixing between the STW and AGO. Larger mesozooplankton (1.6-4.1 mm ESD) did not appear behave as passive tracers, and the data suggest that the species adapted to the STW and AGO apparently avoided intermediate salinity in the front. It should be noted that there are only a few data points for the intermediate salinity water such that the statistical significance of this finding is open to question.

5.2.3 The interrelationship between mesozooplankton and phytoplankton

On either side of the front, there was a negative spatial correlation between the phytoplankton and mesozooplankton in the size range 0.4-1.6 mm ESD (**Fig 4.1.1.i**). A plausible mechanism to explain these observations is that herbivorous grazing by mesozooplankton had a significant impact on phytoplankton standing stock, and that grazing will be greatest in the areas of the highest mesozooplankton biovolume. Any analysis must attempt to disentangle correlation from causation by estimating the importance the biological mechanism: mesozooplankton hebivory. The findings in this section are relevant in understanding the difference between the STW and both end members, as both contained similar zooplankton standing stocks.

In the front there was no significant correlation between phytoplankton and the 1.6-4.1 mm ESD zooplankton (**Fig 5.2.2.i**) suggesting that the <1.6 mm ESD zooplankton had the largest impact as herbivores. This is consistent with what might be expected from the LHPR samples (§4.2.3.4) that showed that carnivorous chaetognaths were abundant in the >1.5 mm size class accounting for between 40-80% of abundance.

Figure 5.2.2.i Zooplankton biovolume, in each size class, and chlorophyll *a* integrated over the top 25m, plotted as a function of the average salinity in the top 25m. The Pearson Correlation Coefficient calculated for each relationship is also shown

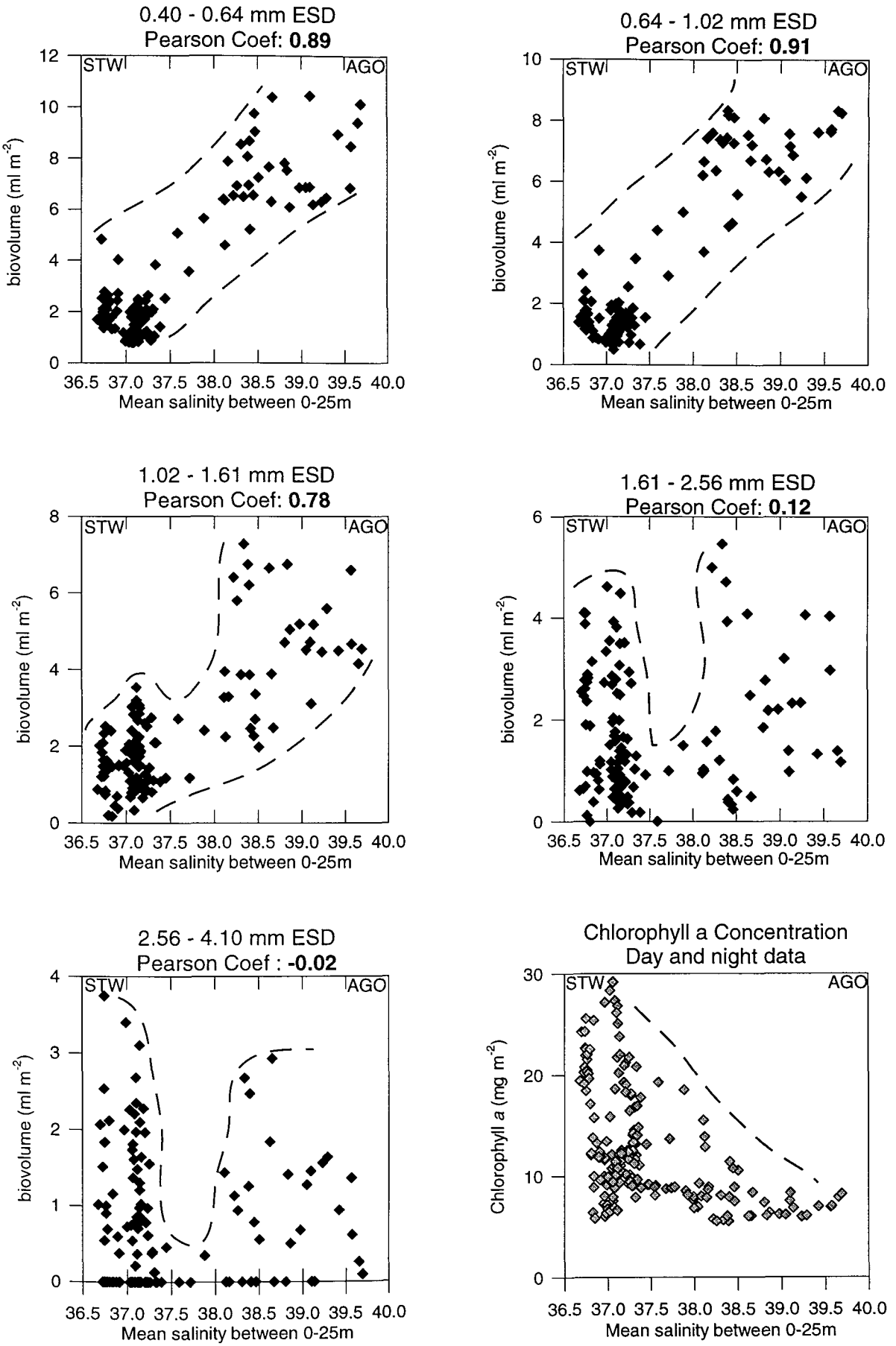

Note that dashed lined are added by hand to aid the descrimination of patterns

Figure 5.2.3.i The relationship between salinity and the ratio of phytoplankton carbon to zooplankton carbon in the upper 25m in the front between the AGO and STW

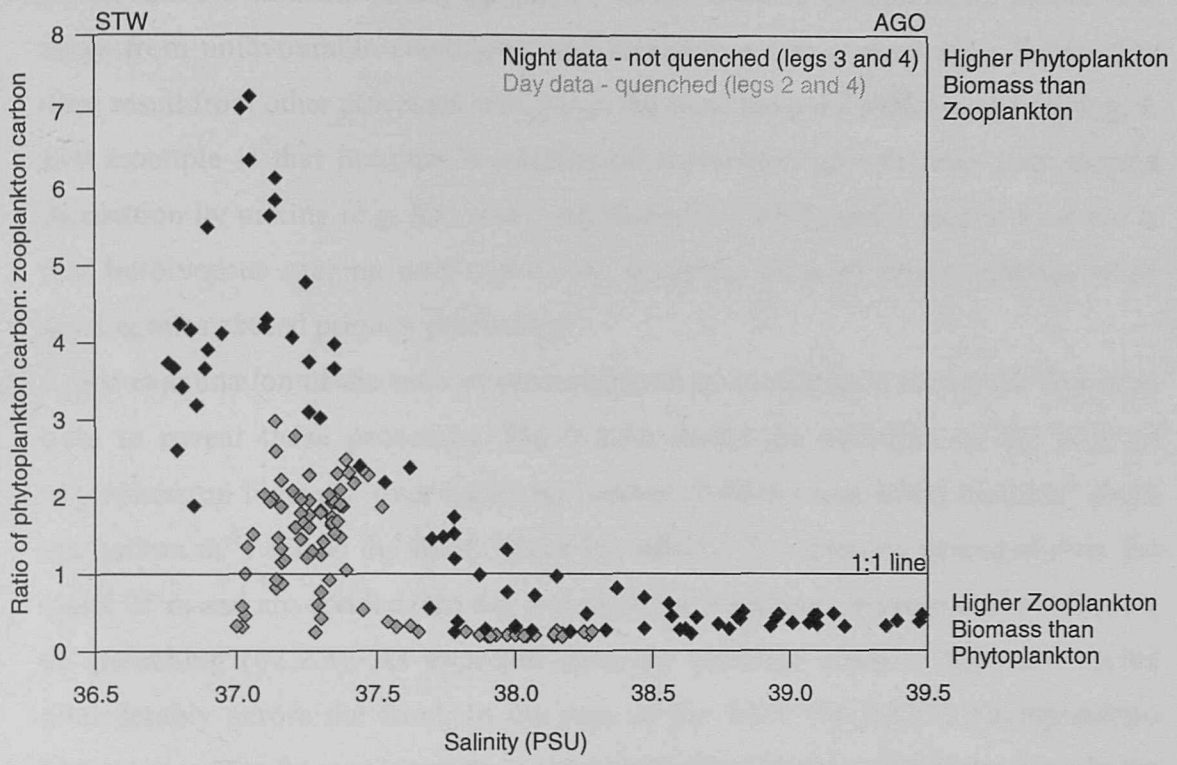

Figure 5.2.3.ii The relationship between salinity and the ratio of phaeopigments to chlorophyll a, in surface samples taken concurrently to those above (additional data from legs 5 & 6)

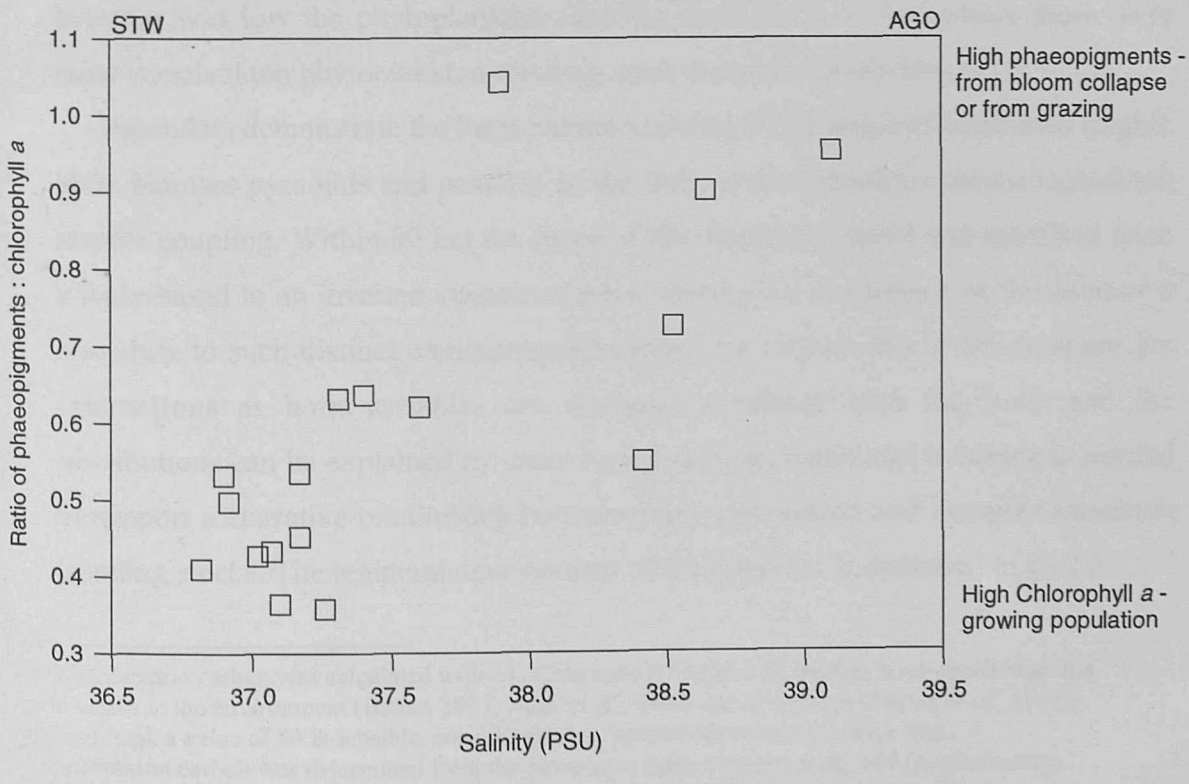

5.2.3.1 The ratio of phytoplankton to mesozooplankton across the front

It was not clear in §5.2.2 whether the distribution of chlorophyll was wholly conservative with salinity. Phytoplankton are not capable of significant locomotion away from unfavourable conditions, and therefore a non-conservative distribution must result from other processes acting over the same temporal scales as the mixing. A first example is that in some conditions phytoplankton growth rates may exceed dissipation by mixing (e.g. Kierstead and Slobodkin, 1953) and a second example is that herbivorous grazing may reduce the standing stock of phytoplankton when grazing rates exceed primary production.

An examination of the ratio of phytoplankton to zooplankton across the front can help to reveal these processes. **Fig 5.2.3.i** shows the variation of the ratio of phytoplankton biomass[1] over mesozooplankton (0.40-4.1 mm ESD) biomass[2] (both mg carbon m^{-3}) across the front, traced by salinity. The data are averaged over the upper 25 m and are divided into day and night measurements because of the influence of quenching (§2.2.3). As expected from the previous analysis the ratio varied considerably across the front. In the east, in the STW (36.5-37.5) phytoplankton biomass was 2 to 8 times larger than mesozooplankton biomass, but in the west, in the AGO (38.5-39.5) mesozooplankton biomass was about 2 times larger than the phytoplankton biomass. The shape of this graph shows that where zooplankton biomass was low the phytoplankton standing stock built up, but where there were more zooplankton phytoplankton standing stock was consistently low.

These data demonstrate the large natural variation in the shape of traditional trophic level biomass pyramids and possibly in the level of phytoplankton mesozooplankton trophic coupling. Within 80 km the shape of the biomass pyramid was modified from a wide-based to an inverted structure, demonstrating the importance of the front as a boundary to such distinct community structures. On its own this is not evidence for interactions as both variables are strongly correlated with the front and the distributions can be explained by cross frontal mixing. Additional evidence is needed to support a causative relationship between high zooplankton and low phytoplankton standing stocks. The temporal development of this situation is discussed in §6.2.3.

---

[1] Phytoplankton carbon was calculated with a C:Chl*a* ratio = 50 (§3.4.3). Studies have shown that this ratio varies in the environment (Banse, 1977; Buck *et al.*, 1996) and in cultures (Taylor *et al.*, 1997), and although a value of 50 is sensible, considerable environmental variation is expected.

[2] Zooplankton carbon was determined from the biovolume (after Parsons *et al.*, 1977), substituting corresponding regional and seasonal empirical data from Matondakar *et al.* (1995) see §3.4.3.

5.2.3.2 Evidence for herbivorous grazing influencing phytoplankton biomass

The circumstantial evidence presented above implies that phytoplankton standing stock was significantly reduced by mesozooplankton herbivorous grazing in the AGO compared with the STW. Direct evidence, in the form of grazing rate measurements of the mesozooplankton sampled by the OPC, was not collected during the cruise. In addition, no measurements of nutrient concentrations were taken, which would identify if the lack of nutrients was limiting the phytoplankton in the AGO. Historical data (§2.1.2) indicate that this is unlikely, as greater concentrations of nutrients are typically present in the Arabian Gulf water (El-Gindy and Dorgham, 1996).

There are other sources that can add to the weight of circumstantial evidence for the different grazing pressure exerted on the phytoplankton in the AGO and STW. Two lines of evidence are investigated: first an analysis of the phaeopigment concentration in relation to chlorophyll, and second an estimation herbivorous consumption from the measured population abundance and grazing rates from the literature.

5.2.3.3 The ratio of phaeopigments to chlorophyll *a*

The ratio of phaeopigments (phaeo) to chlorophyll *a* (Chl*a*) can be used as an index of phytoplankton health. A proportionally low concentration of phaeo to Chl*a* (ratio <0.5) is characteristic of a growing phytoplankton population, and a high proportion (ratio >0.7) can be caused by herbivorous grazing or by a bloom collapsing (Barlow *et al.*, 1993; Head *et al.*, 1994). Zooplankton grazing is considered a major source of phaeopigments in the ocean (Lorenzen, 1967; Daley, 1973; Barlow *et al.*, 1993) and an increased concentration of phaeopigments associated with copepod grazing is well documented (Shuman and Lorenzen, 1975; Carpenter and Berguist, 1985; Roy *et al.*, 1989; Penry and Frost, 1991). However, phaeopigments are not conservative in seawater and are influenced by both biotic and abiotic processes.

Fig 5.2.3.ii shows the ratio of phaeopigments over chlorophyll *a* concentration, in surface water samples taken on either side of the front between the AGO and STW during the SeaSoar survey, plotted as a function of salinity. The data from the front on Legs 5 and 6 are also presented in **Fig 5.2.3.ii** in order to obtain values for a more complete range of salinity across the front. These data are limited to surface samples (5 m) and may not be representative of the upper 25 m when compared with **Fig 5.2.3.i**. The ratio of phaeopigments to chlorophyll *a* was determined by the acid addition technique for evaluating chlorophyll *a* in seawater, (see §2.2.4; JGOFS protocols, 1994). High pressure liquid chromatography (HPLC) pigment analysis has

shown that the acid addition method overestimates the concentration of phaeopigments (Herbland, 1988), but will not affect qualitative comparisons of the ratio at different salinities because the method used in this study was consistent. **Fig 5.2.3.ii** suggests that the phytoplankton in the STW were growing population, but in comparison, the phytoplankton standing stock in the AGO had been reduced from a previously higher level, resulting in higher proportion of phaeopigments. This is not conclusive evidence for grazing, because phaeopigments

5.2.3.4 Estimating the consumption of phytoplankton by mesozooplankton

Ideally, herbivorous consumption[3] (HC) must be compared with primary production and phytoplankton standing stock to determine whether mesozooplankton grazing is an important influence on phytoplankton populations. During CD 104 only measurements of phytoplankton and zooplankton standing stocks were made, meaning that HC had to be approximated from published grazing rates from the region and the zooplankton abundance, and could only be compared with phytoplankton standing stock. The main problem with this method is that it is not possible to determine that all the particles counted by the OPC were feeding on phytoplankton within the range of grazing rates that are used in the calculations.

Goes *et al.* (1999) determined chlorophyll ingestion rates for the copepod *Acrocalanus* spp. and cladoceran *Evadne tergestina* of 1.21-4.28 ng Chl*a* animal^{-1} h^{-1}. These two species of mesozooplankton are known for their predominance in the northern Arabian Sea, and the distributions of both these species extend into the Arabian Gulf (Michel *et al.*, 1986b). Smith (1982) measured both ingestion and filtration rates for copepods assemblages in the NW Indian Ocean and determined an ingestion rate of between 2 and 6 ng Chl*a* animal^{-1} h^{-1} (converted here, assuming a C:Chl*a* ratio = 50). Edwards *et al.* (1999) used Smith's measurements to determine HC from zooplankton biomass in the Arabian Sea.

Herbivorous consumption can be estimated from the chlorophyll ingestion rate and the *in situ* abundance of mesozooplankton (Beers and Stewart, 1970 & 1971):

$$HC = I_{24} * a$$

I_{24} = Ingestion rate per animal per 24 hrs: 1-6 ng Chl*a* animal^{-1} h^{-1} * 24
I_{24} = 24 to 144 ng Chl*a* animal^{-1} day^{-1}
a = zooplankton abundance (per m^{-3})

[3] Herbivorous consumption – HC (Chl*a* m^{-3} day^{-1}) is defined here as the product of pigment ingestion rate per animal (Chl*a* animal^{-1} day^{-1}) and herbivore abundance per cubic metre (animals m^{-3}).

Zooplankton abundance (0.4 to 4.1mm ESD) was 10000 m^{-3} in the AGO, but only 4000 m^{-3} in the STW (**Fig 5.1.1.ii**).

HC in AGO = **0.2** to **1.4** mg Chl*a* m^{-3} day^{-1}

In the AGO the mean concentration of chlorophyll was 0.4 mg Chl*a* m^{-3} (**Fig 5.1.1.ii**) and *HC* was 0.2-1.4 mg Chl*a* m^{-3} day^{-1}. This demonstrates that mesozooplankton grazing in the AGO was 50 to >200% of the phytoplankton standing stock per day. In the STW zooplankton abundance was 4000 m^{-3} and therefore the same calculation indicates that *HC* ranges from (<0.01-0.5 mg Chl*a* m^{-3} day^{-1}), giving a range of <1 to 6% of the phytoplankton standing stock per day. These calculations suggest that mesozooplankton grazing would not significantly reduce standing stock in the STW. (The GOS contained similar mesozooplankton abundance and chlorophyll concentrations to the AGO, and grazing is expected to be equally important in the GOS as in the AGO.)

The ingestion rates from Goes *et al.* (1999) may overestimate *HC* because their study animals differed from the most numerous species counted by the OPC. In addition there may be clear discrepancies between the laboratory determined rates and the situation in the Strait. These rates vary significantly with temperature (Dam and Peterson, 1988), zooplankton size (Morales *et al.*, 1991), species (Gowen *et al.*, 1999), food availability (Parsons *et al.*, 1967) and species, and also over hourly (Goes *et al.*, 1999), diel (Mackas and Bohrer, 1976) and seasonal cycles (Pakhomov *et al.*, 1997).

It is not possible to fully quantify the impact of grazing on the phytoplankton standing stock as no measurements were made of primary production. Primary production can greatly exceed the standing stock, and phytoplankton growth rates can be as high as several population doublings in a day. *HC* will only impact on the distribution of phytoplankton when it is significant in comparison to both the standing stock and the growth rate of the phytoplankton population. However, these calculations also do not consider the role of microzooplankton herbivores, which are typically more important grazers than mesozooplankton. If grazing by microzooplankton removes the majority of the primary production then changes in mesozooplankton grazing may be more important relative the primary production.

Published studies show that the proportion of phytoplankton standing stock removed by mesozooplankton grazing is variable. For example, Head *et al.* (1999) present a table comparing studies in the North East Atlantic, which have determined HC ranging from <1% (e.g. Harris *et al.*, 1998) to 45% (Lenz *et al.*, 1993) of

phytoplankton standing stock. The observations in the CD 104 study have determined a wider range of *HC* as a percentage of phytoplankton standing stock within an area of 100 km (<1%->100%). The data presented in this study indicate that the importance of mesozooplankton grazing is highly variable in space. This variability is only resolved in the spatially explicit data from modern zooplankton sampling technologies, which may explain the smaller range resolved by net samples, which fail to resolve spatial variability and the localised importance of grazing. However, the data the OPC produces does not demonstrate that all the zooplankton were feeding on phytoplankton at the measured rate. It is unlikely that all particles were herbivores, suggesting *HC* is overestimated here. These findings are discussed further in §6.2.1.

5.2.4 The relationship between meso- and macrozooplankton

Fig 5.2.1.i shows that the highest mesozooplankton abundance and the greatest density of scattering macrozooplankton and micronekton were on opposite sides of the front. Spatially inverse correlations existed between MVBS at 38 kHz and mesozooplankton biovolume in the 0.40-0.64, 0.64-1.02 and 1.02-1.61 mm ESD size classes, with PCCs of -0.62, -0.59 and -0.54, respectively. There was a weak inverse correlation in the 1.61-2.56 mm size class (PCC: -0.28), but no correlation was detected in the 2.56-4.10 mm size class. These distributions may indicate a top-down mechanism driven by predation from the macrozooplankton.

From the available data it is not possible to identify the species dominating the backscatter at 38 kHz. In the Gulf of Oman, zooplanktivorous myctophid fish and decapod shrimps dominate the backscatter, but many of these mesopelagic species are not found on the shelf (§5.2.1). The most abundant large (>1 cm) species in the LHPR samples in the STW is the euphausiid *Pseudeuphausia latifrons* (§4.2), but it is smaller than 2 cm and it is not clear if the dense swarms (up to 70 m^{-3}) would dominate the backscatter at 38 kHz. Although the dominant scatterer cannot be identified, it is a reasonable assumption from the size and the species present in the Gulf of Oman, that the dominant scatterer was able to feed on mesozooplankton.

5.2.5 Summary and discussion of observations and findings

The distribution of plankton was relatively consistent in relation to the front, remaining relatively stable for the 6 day duration of the SeaSoar survey. Chlorophyll *a* was highest (1.5 mg m^{-3}) in the upper 30 m of the STW, but was much lower

(0.4 mg m^{-3}) in the same depth range in the AGO. Mesozooplankton abundance was highest (8000 m^{-3}) in the upper 30 m of the AGO, and was much lower in the STW at this depth (1000 m^{-3}). This indicates that the front formed a boundary between distinct communities on a scale of ≈50 km.

5.2.5.1 The distribution of zooplankton across the front

Although the front separated distinct communities the structure of the biological gradients across the front varied with the size of the zooplankton. Small zooplankton (0.4-1.6 mm ESD) behaved as predominantly as passive tracers showing a gradient that was conservative with mixing across the front. The distribution of larger zooplankton (1.6-4.0 mm ESD) was not conservative with mixing and suggested that their distributions were also influenced by their swimming behaviour. The biovolume of these species was high on both sides of the front, but lower within the front (although there were only a few data points). This observation suggests that the communities acclimatised to the conditions on either side were able to avoid by swimming unfavourable intermediate conditions in the front. The larger macrozooplankton, which are generally even stronger swimmers, also showed non-conservative distributions across the front. The distribution of phytoplankton was in partly conservative with the mixing, although appeared to be influenced by biological processes such as growth and grazing.

5.2.5.2 Conclusions

The evidence examined in this section indicates that both physical mixing and behavioural processes were responsible for determining the distribution of zooplankton across the front. The interaction of physical and biological forcing mechanisms varied with different sized mesozooplankton, and it is suggested that this relates to the greater swimming abilities of larger zooplankton. The calculations presented in the second part of this section indicate that mesozooplankton grazing does have an impact of phytoplankton standing stock in areas of high zooplankton abundance. These observations are discussed further in §6.2.

5.3 The affect of Variability caused by Internal waves at the boundary between the GOS and the STW on the Plankton

The horizontal boundary between the GOS and the STW is not a clearly defined sharp front (as exists between the AGO and STW, §5.2) but is in the form of a gradual gradient over 150 km (**Fig 4.1.1.i**). Superimposed on the smooth transition is sub-

mesoscale variability, indicated by vertical perturbations in the isotherms, over a range of 5-50 km. Much of this variability resulted from internal waves generated by the interaction of the tides with the topography particularly at the shelf break.

The aim of this section is to examine the evidence for physically and biologically mediated forcing on the distribution of zooplankton on the east side of the Strait of Hormuz. This objective is addressed with the following analysis: first, there is a description of the physical structure and distribution of plankton at the boundary between the GOS and STW. Then there is an examination of how the standing stock of zooplankton is affected by the proportion of GOS and STW in the water column. The role of mesozooplankton size on this relationship is also investigated. Finally, spectral analysis is used to diagnose correlations between the dominant scales in both the environmental and the plankton patchiness.

5.3.1 Description of the physical structure and plankton distributions

Fig 5.3.1.i shows contour plots of potential temperature and zooplankton abundance from a transect (Leg 3 of the SeaSoar survey) through the boundary between the GOS and STW. The upper contour plot shows the potential temperature structure and the lower plot shows the abundance of zooplankton between 0.41 and 4.1 mm ESD, both contoured as a function of distance and depth. The left hand side of the plot represents the NW (near the peninsula) and the right hand side represents the SE (above the shelf break at the northern end of the Gulf of Oman).

5.3.1.1. Temperature structure of the boundary between the GOS and STW

The GOS extends deepest in the SE of the survey, and forms a progressively shallower layer as it propagates through the Strait (**Fig 5.3.1.i**). By the time the GOS water reaches the tip of the Masandam peninsula the surface salinity has increased from 36.50 to 37.25 and the temperature has decreased from 23.3 to 22.6°C. The STW lies beneath the GOS and is approximately represented by green colours in **Fig 5.3.1.i**.

Superimposed on the smooth SE-NW temperature gradient is marked physical variability visible at a scale of 5-50 km, indicated by sharp vertical displacements of the isotherms (**Fig 5.3.1.i**). Internal waves, generated by the interaction of the tides with the topography, are responsible for this variability. In addition, some of the variability may have also been caused by small eddies and meanders in the NW flowing GOS. The variability results in horizontal temperature gradients of 0.6°C in less than 10 km, which are of a similar magnitude to the mean gradient from the shelf break to the tip of the peninsula.

Figure 5.3.1.i Variability in thermal structure and zooplankton abundance

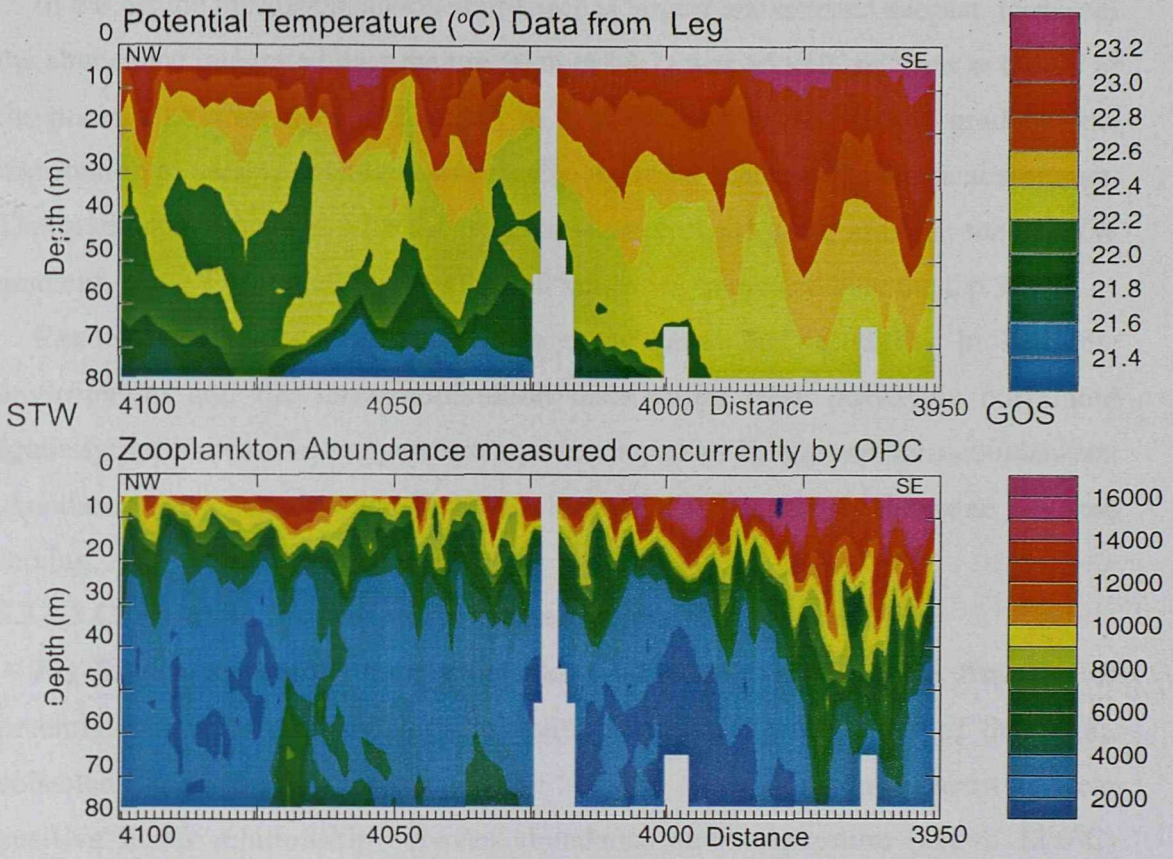

Figure 5.3.1.ii Zooplankton abundance (size range 0.4-4.1˚mm˚ESD) plotted as a function of potential temperature. Data from east side of the Strait of Hormuz

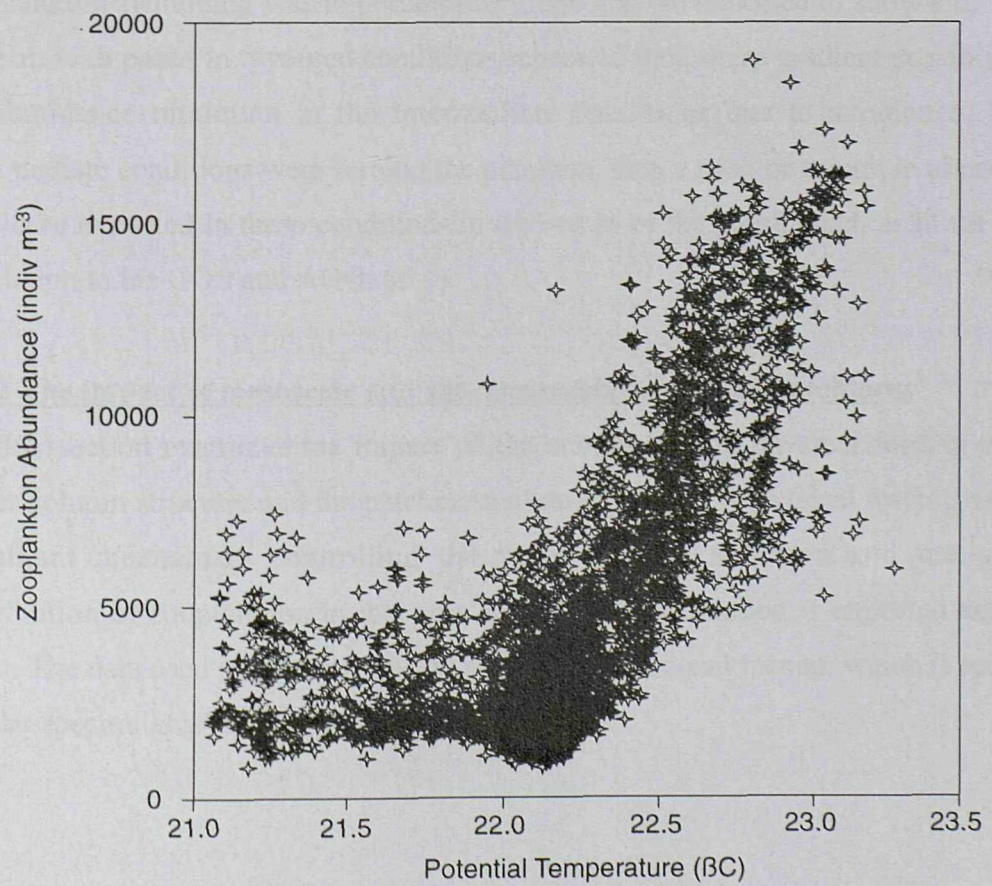

5.3.1.2 The distribution of mesozooplankton

In the SE the mesozooplankton abundance is largest and extends deepest. In the SE the abundance integrated over the top 50 m (§5.3.2) was >5 $x10^5$ m^{-2}, but at the tip of the peninsula (NW) it was <2.5 $x10^5$ m^{-2}. In addition to the SE/NW gradient, the distribution of mesozooplankton was patchy at similar scales to the physical structure. The gradients associated with the patchiness were of the same order as the SE/NW gradient, being 1-2 $x10^5$ m^{-2} in less than 10 km, when integrated over the top 50 m.

Examination by eye reveals that in many cases the variability in both the environment and the mesozooplankton distribution were positively correlated spatially: an increase in temperature was accompanied by greater mesozooplankton abundance. This suggests that both variables were influenced by the same physical forcing.

5.3.1.3 Correlation between temperature and abundance in the GOS

Fig 5.3.1.ii shows the mesozooplankton abundance plotted as a function of potential temperature. This figure contains data from the east side of the Strait, collected during the first four legs of the SeaSoar survey. This graph shows a clear positive linear relationship between abundance and temperature (above 22.0°C) indicating that for both the SE/NW gradient and the variability the majority of zooplankton in this size range were passively mixed between the water types. If zooplankton swimming was important this graph may be expected to show a different pattern: with peaks in favoured conditions separated by a sharp gradient possibly with an abundance minimum in the intermediate conditions due to avoidance. If the intermediate conditions were forcing the plankton, then a peak or trough in abundance would be expected in these conditions in the centre of the graph (such as in the STW in relation to the GOS and AGO: §5.1).

5.3.2 The impact of mesoscale and sub-mesoscale forcing on patchiness

This section examines the impact of the sub-mesoscale physical forcing on the water column structure and the patchiness of zooplankton. If physical forcing was the dominant mechanism controlling the water column structure and the spatial distribution of zooplankton in this area then a close correlation is expected between them. The data used in this analysis are in a two dimensional format, which is required for the spectral analysis performed in §5.3.4.

The passage of internal waves through this area displaces the isotherms up and down changing the proportion of GOS to STW in the water column. The 22.5°C isotherm is indicative of the boundary between them and its depth can be used to represent the proportion of GOS and STW in the water column. The deeper the isotherm the greater the proportion of GOS to STW. The upper graph of **Fig 5.3.2.i** shows the depth of the 22.5°C isotherm plotted against distance for a continuous section from legs 2 and 3 of the SeaSoar survey. The internal waves are moving the isotherm vertically through 20 to 30 m (**Fig 5.3.2.i**).

Zooplankton abundance was determined to a constant depth in the water column, below the boundary between the GOS and STW, by integrating the abundance of the size range 0.4–4.1 mm ESD from the surface down to 50 m. The upper 50 m includes the surface maximum but does not include biases from the presence of AGO in some places (such as 4050 km: **Fig 5.3.1.ib**). The lower graph of **Fig 5.3.2.i** shows this integrated zooplankton abundance plotted against distance.

The depth of the isotherm is deepest and zooplankton are most numerous in the SE (the centre of **Fig 5.3.2.i** at 3965 km). In addition both variables also show clear variability over scales of 5 to 50 km. This relationship would be expected from the observation of the contour plots in **Fig 5.3.1.i**. The data shown in **Fig 5.3.2.i** are re-plotted with mesozooplankton abundance as a function of the depth of the isotherm in **Fig 5.3.2.ii**. This graph shows that there was a positive correlation between the variables, quantified by a Pearson Correlation Coefficient (PCC) of 0.74. This strong relationship suggests that the forcing that shaped the temperature structure, primarily controlled the distribution of zooplankton abundance. This evidence suggests that the mechanism was primarily a direct physical redistribution of zooplankton, and there was not a significant behavioural response by the most numerous zooplankton.

5.3.2.1 The correlation between physical forcing and mesozooplankton size

The total mesozooplankton abundance is dominated by the smallest species, which in general behaved as passive tracers in the mixing between the AGO and STW. The larger mesozooplankton (>1 mm) have greater mobility and are more capable of determining their own position in the water column. In this section the spatial correlation between the depth of the 22.5°C isotherm and the integrated abundance of different size classes of mesozooplankton is examined. A weaker correlation would be expected for the larger species if their swimming ability is significant in comparison to the physical redistribution by the internal waves.

Figure 5.3.2.i Variability in the depth of the 22.5°C isotherm and the zooplankton abundance Integrated over the upper 50m of the water column in the GOS (data from legs 2 and 3)

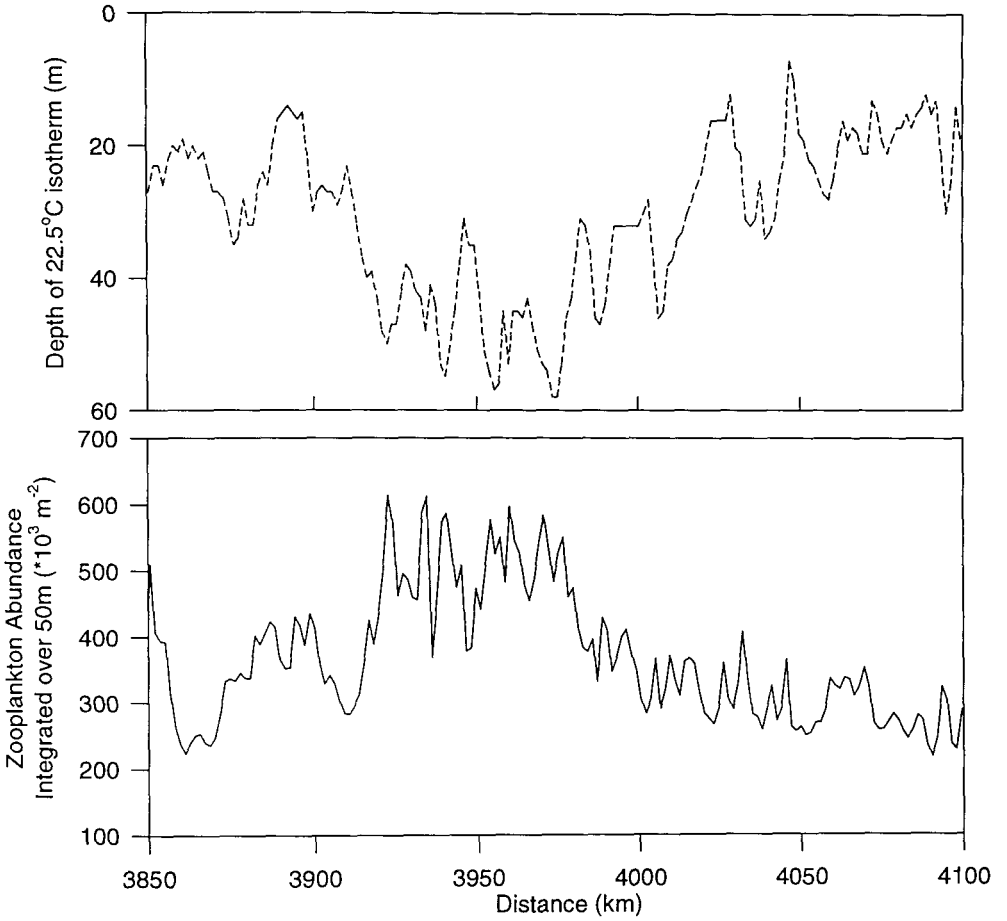

Figure 5.3.2.ii The relationship between the depth of the 22.5°C isotherm and zooplankton Abundance (integrated over upper 50m) in the Gulf of Oman inflow (data Legs 1 - 4)

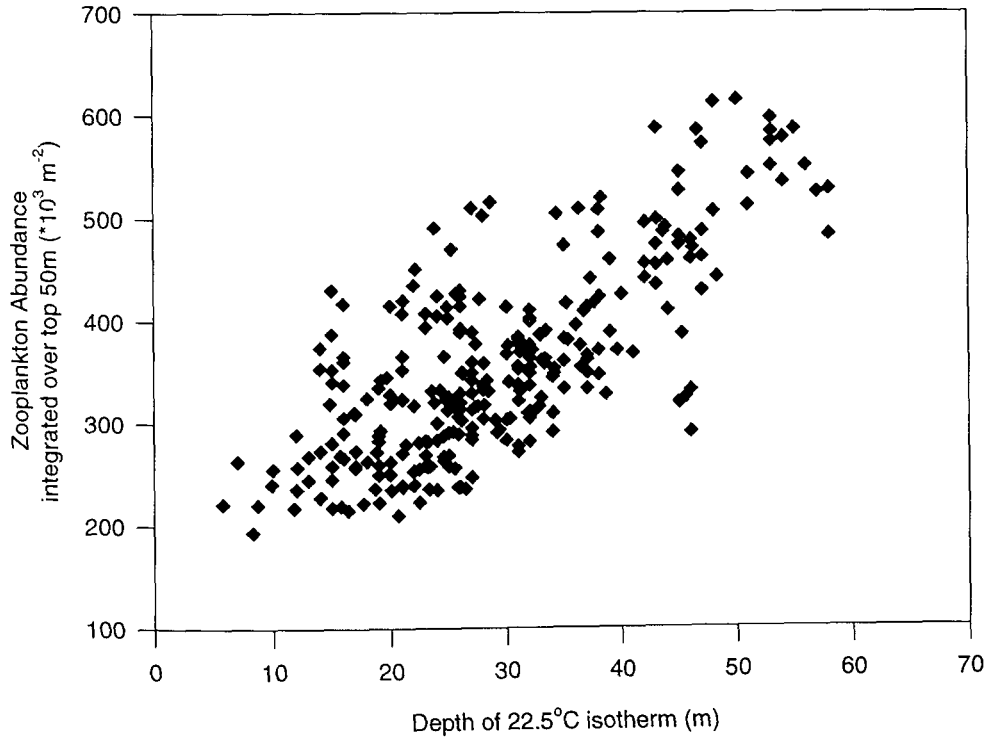

Figure 5.3.2.iii The Pearson correlation coefficient between mesozooplankton abundance in the upper 50m and the depth of the 22.5°C isotherm plotted as a function of organism size Data taken from the Gulf of Oman inflow, on the east side of the Strait

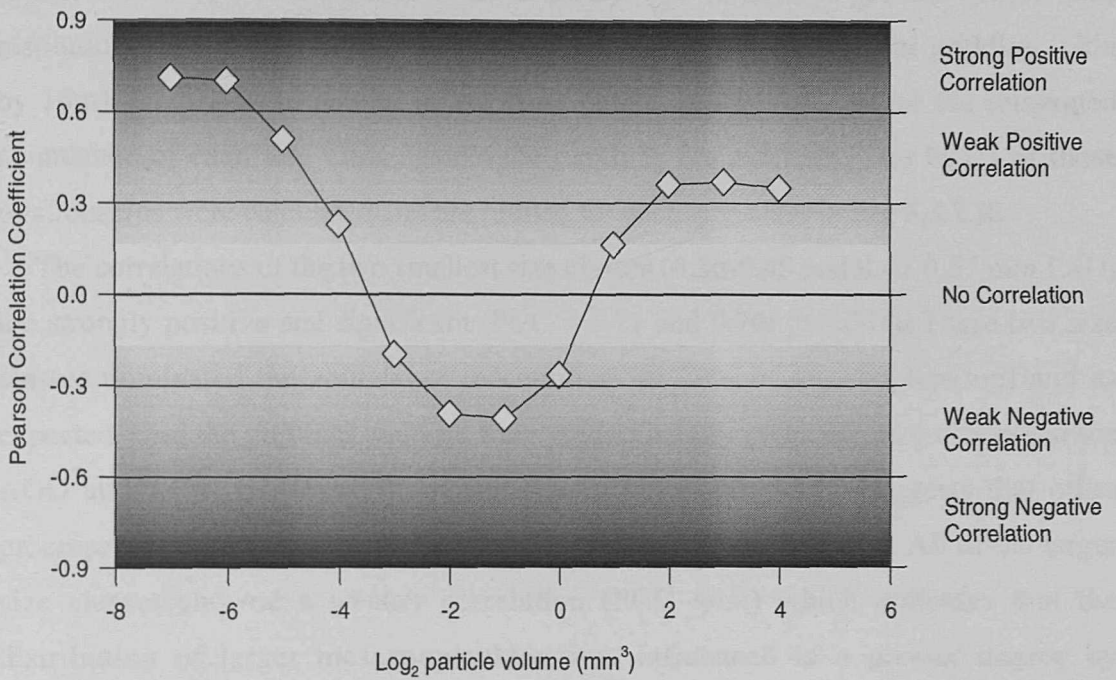

Figure 5.3.4.i The relationship between phytoplankton and temperature on the east side of the Strait
a) Chlorophyll a integrated over the top 50m plotted as a function of the depth of the 22.5°C isotherm
b) The ratio of phaeopigments to chlorophyll *a* in surface samples plotted as a function of the depth of the 22.5°C isotherm

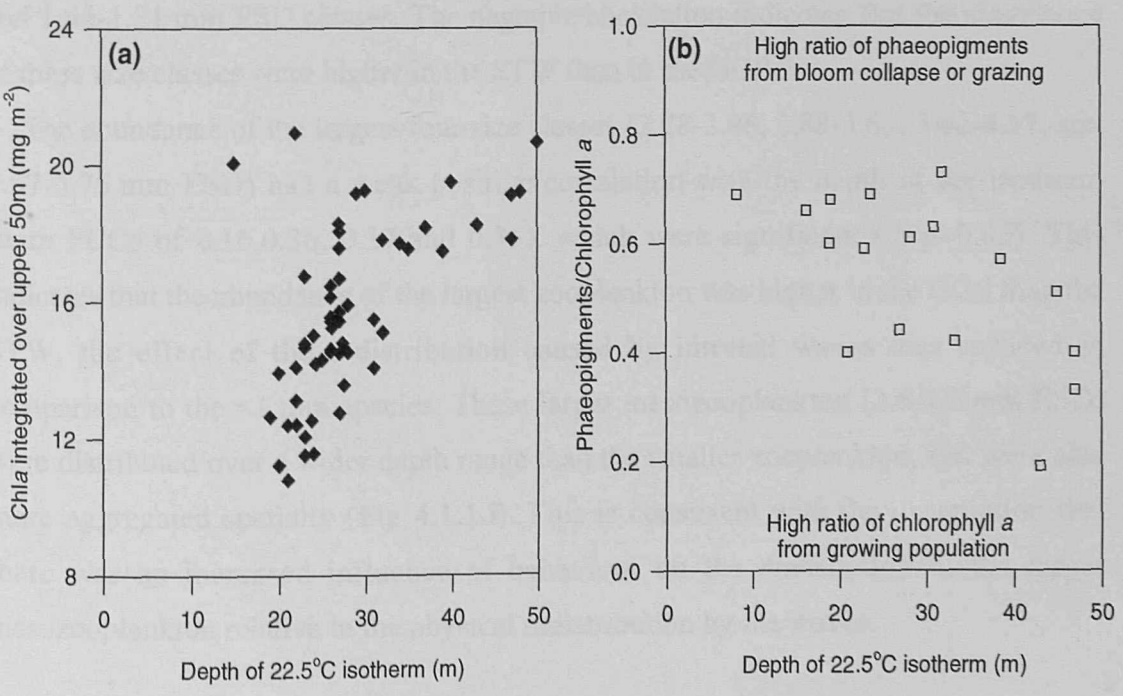

The mesozooplankton data from the OPC are divided into the 12 size classes (the same as used in **Fig 5.1.3.i**) which correspond to $\log_2$ increments of particle volume (Table 5.1.3.a shows the conversions to ESD). The 12 classes provide greater size resolution (than the standard 5) but are compromised by larger spatial gridding (6km by 16m). Graphs were plotted in the same format as **Fig 5.3.2.ii**, for the integrated abundance of each size class against the depth of the isotherm. The PCCs of these relationships were calculated and are plotted for each size class in **Fig 5.3.2.iii**.

The correlations of the two smallest size classes (0.36-0.45 and 0.45-0.57 mm ESD) are strongly positive and significant (PCC = 0.71 and 0.70: $p>0.001$). These two size classes dominated the abundance (accounting for 70% of the zooplankton) and as expected from the previous analysis were predominantly passively mixed between the AGO and STW. However, the correlation is not exact, which suggests that other processes were also important (these will investigated subsequently). All of the larger size classes showed a weaker correlation (PCC <0.6) which indicates that the distribution of larger mesozooplankton was influenced to a greater degree by processes other than physical redistribution by the internal waves, resulting in a reduced correlation with the physical structure of the water column.

The four size classes: 0.91-1.14, 1.14-1.44, 1.44-1.81 and 1.81-2.28 mm ESD had weak negative correlations with the depth of the isotherm (quantified with PCCs of –0.20, –0.40, –0.41 and –0.27), which were significant (to $p>0.01$) in the 1.14-1.44 and 1.44-1.81 mm ESD classes. The negative correlation indicates that the abundance of these size classes were higher in the STW than in the GOS.

The abundance of the largest four size classes (2.28-2.88, 2.88-3.62, 3.62-4.57, and 4.57-5.75 mm ESD) had a weak positive correlation with the depth of the isotherm (with PCCs of 0.16,0.36, 0.37 and 0.35), which were significant (to $p>0.05$). This indicates that the abundance of the largest zooplankton was higher in the GOS than the STW, the effect of the redistribution caused by internal waves was reduced in comparison to the <1 mm species. These larger mesozooplankton (2.6-4.1 mm ESD) were distributed over a wider depth range than the smaller zooplankton, and were also more aggregated spatially (**Fig 4.1.1.i**). This is consistent with the observation that there was an increased influence of behaviour on the distribution of the larger mesozooplankton relative to the physical redistribution by the waves.

5.3.2.2 The impact of physical forcing on macrozooplankton

The relationship between the macrozooplankton and the depth of the isotherm was determined in a similar way to the other variables. The MVBS determined from EK500 data was averaged between 18 and 50 m, for legs 1-4 on the east side of the Strait. The MVBS at 38 kHz had no correlation with the inflow (PCC = 0.14), indicating that the distribution of the larger species was not strongly influenced by the physical forcing (data not shown). These species are more mobile and are distributed throughout the water column (**Fig 4.1.1.i**), indicating the importance of behaviour in determining their distributions. The 120 and 200 kHz frequencies are weakly positively correlated with the depth of the isotherm (PCCs = 0.43 and 0.40) and the mesozooplankton abundance (PCCs = 0.55 and 0.56). These coefficients indicate a closer relationship with the distribution of the mesozooplankton in comparison with the physics. This is additional evidence for the importance of the swimming behaviour of the macrozooplankton, enabling them to aggregate more independently of the physical forcing. This evidence may indicate that some of the macrozooplankton were actively aggregating with the mesozooplankton, possibly to feed on them.

5.3.3 Spectral analysis of the variability of the temperature structure and the mesozooplankton and phytoplankton patchiness in the GOS

Spectral analysis is a numerical methodology that can be used to identify the scale of the component wavelengths (the power spectra) that make up a natural signal. A power or variance spectra can be determined using the Fast Fourier Transform - FFT (e.g. Jenkins and Watts, 1968; Brigham, 1974; Press *et al.*, 1992) which calculates the spectral density at each frequency (f) or wavelength (λ). To quantify a sine wave it must be sampled at least twice per cycle, therefore the lower limit of the spectra must be twice the sampling interval, known as the Nyquist critical frequency.

In this region spectral analysis can be used to identify the dominant scales of variability in the GOS and STW, and to determine if these scales corresponded in physical and biological variables. The correlation between variables can then be used to determine the dominant forcing mechanisms. In addition, if biological dynamics (e.g. zooplankton phytoplankton interactions) have the largest effect on the observed distributions, then regular scales of variability are unlikely.

5.3.3.1 The calculation of power spectra

Qualitative observation of the contour plots in **Fig 5.3.1.i** and the line graphs in **Fig 5.3.2.i** indicated regular scales of spatial heterogeneity in both variables at scales of 5 to 50 km. Spectral analysis was performed on the longest continuous section of SeaSoar data on the east side of the Strait, which was from legs 2 and 3, between 3840 and 4099 km distance run (**Fig 5.3.2.i**). Visual inspection of legs 1 and 4 identified that these contained similar scales of variability (data not shown).

Power spectra were calculated using the FFT for the depth of the 22.5°C isotherm, chlorophyll *a* concentration, and mesozooplankton abundance in 0.41-0.64, 0,64-1.02, 1.02-1.61, 1.61-2.56 and 2.56-4.1 mm ESD size classes. The power spectra are presented in **Fig 5.3.3.i** (excluding 2.56-4.1 mm) and the correlations are summarised in Table 5.3.3a. In **Fig 5.3.3.i** the x axis represents cycles per km (on a $\log_{10}$ scale) covering a range of 0.006 to 0.2 cycles per km. An additional x axes showing the equivalent wavelengths (160-5 km) are also plotted at the bottom of the page. The spectra below a 5 km wavelength are not presented because these are close to the Nyquist critical frequency (Press *et al.*, 1992). The wavelengths larger than 80 km are artefacts of the U shaped section of SeaSoar data. This section of data was only long enough to address the variability between 10 and 50 km. Because only a narrow range of scales can be resolved the spectral density is plotted on a linear scale.

5.3.3.2 Identification of the dominant scales of variability in the power spectra

The power spectra for the variability in the depth of the 22.5°C isotherm contains peaks at wavelengths of 40, 27, 17 and 9 km (marked on **Fig 5.3.3.i** as dashed lines). Peaks at a 40 km wavelength are also present in the spectra of chlorophyll *a*, and mesozooplankton abundance in the size classes 0.41-0.64 and 0.64-1.02 mm ESD. There are no equivalent peaks in the larger size classes 1.02-1.61, 1.61-2.56 and 2.56-4.10 mm ESD (the 2.56-4.10 mm size class is not presented in **Fig 5.3.3.i**, see Table 5.3.3a). But there are peaks in these size classes at 35 km, which correspond with low spectral density for the temperature, chlorophyll and the 0.41-0.64 and 0.64-1.02 mm ESD size classes. None of the variables correlate with the peak at 27 km in the spectrum for temperature. In the 0.41-0.64 and 0.64–1.02 mm ESD size classes there is a spectral density minimum at 27 km. The power spectra for chlorophyll peaks at 24 km, which does not correlate with a peak in the spectra for temperature. The spectra of the three zooplankton classes covering 0.41-1.61 mm ESD have medium spectral densities while those for 1.61-4.10 mm ESD contain low spectral densities.

Figure 5.3.3.i Power spectra of the spatial variability in the depth of the 22.5°C isotherm, chlorophyll *a* and the mesozooplankton abundance in each size class integrated over the upper 50 m

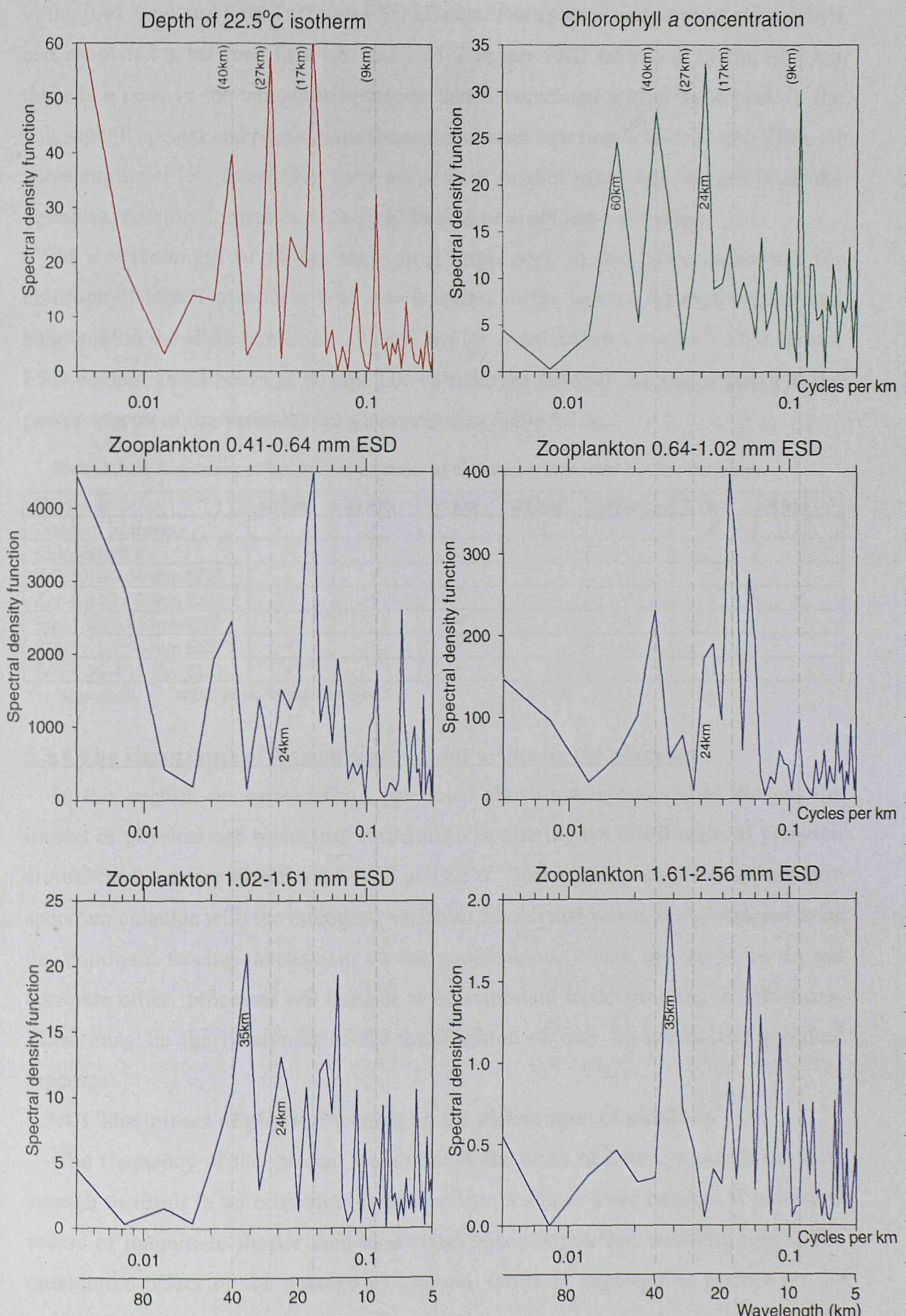

The power spectra for temperature also peaks at 17 km, which correlates with peaks in the 0.41-0.64 and 0.64-1.02 mm ESD classes. The spectral densities of chlorophyll and zooplankton between 1.02-1.61 and 1.61-2.56 mm ESD are low at 17 km. At 9 km there is a peak in the temperature spectra that is correlated with a large peak in the chlorophyll spectra and peaks in the three size classes covering 0.41-1.02 mm ESD. At wavelengths of less than 10km there are several smaller peaks and troughs in all the variables, possibly formed by biological forcing or result from aliassing.

At a wavelength of 60 km there is a large peak in the power spectrum for chlorophyll which correlates with low densities in the spectra for temperature and zooplankton 0.4–1.61 mm ESD. The spectra for zooplankton between 1.61-4.10 mm ESD contain small peaks at 60 km. The correlations between the major peaks in the power spectra of the variables are summarised in Table 5.3.3a.

Table 5.3.3a Summary of the dominant scales of high spectral density for the variables

Variable	60 km	40 km	35 km	27 km	24 km	17 km	9 km
Depth of isotherm		✓		✓		✓	✓
Chlorophyll *a*	✓	✓			✓		✓
Zoo 0.41-0.64 mm ESD		✓			✓	✓	✓
Zoo 0.64-1.02 mm ESD		✓			✓	✓	✓
Zoo 1.02-1.61 mm ESD			✓		✓		
Zoo 1.61-2.56 mm ESD	✓		✓				
Zoo 2.56-4.10 mm ESD	✓		✓				

✓ : large peak. ✓ : small peak. blank : no peak

5.3.4 The importance of forcing mechanisms acting on the plankton

In this section the relationships presented above are interpreted to discuss the impact of physical and biological mechanisms in altering the distribution of plankton around the boundary between the GOS and STW. Where the peaks in the temperature spectrum coincide with the biological variables the internal waves are considered to be the dominant forcing mechanism on the zooplankton. Where the variables do not correlate other processes are thought to be important in determining distributions. These may be the behaviour of the zooplankton or may be unresolved physical processes.

5.3.4.1 The impact of physical forcing on the distribution of plankton

The frequency of the internal waves are of the order of hours, which is not long enough to result in an ecosystem response from a single wave because it is several orders of magnitude shorter than mesozooplankton population doubling times. The cumulative affect of the passage of internal waves is expected to impact on the

ecosystem by causing greater vertical mixing and elevating nutrients in the euphotic zone. The main impact that is expected to be observed in this quasi-synoptic survey is the redistribution of the plankton by the passage of the waves.

The spectral density for temperature contained a peak at 27 km, that was not associated with any peaks in the spectra of the biological variables. This indicates that the physical process at this scale was not influencing the distribution of the plankton, which may indicate that this was a different physical process to the other peaks.

At scales of 40, 17 and 9 km there are peaks in the temperature spectra that are correlated with peaks in biological variables (**Fig 5.3.3.i** and Table 5.3.3a). At these scales the internal waves have an impact on the distribution of plankton. However, all the plankton do not act as passive tracers of this forcing, and the different sized plankton were not consistently correlated with temperature. The larger species have a reduced correlation with the physical structure which may have resulted from a greater interaction of behavioural processes or also unresolved physical processes.

The spectra for small zooplankton and phytoplankton are not identical to each other or the physical structure, although they are more correlated than the larger individuals. This indicates that both are affected by processes other than the spatially regular physical forcing by the internal waves. **Fig 5.3.4.ia** (p175) shows night time chlorophyll *a*, integrated over the upper 50m, plotted as a function of the depth of the 22.5°C isotherm. The limited data show a positive correlation with the depth of the isotherm (PCC = 0.58). This is lower than the correlation coefficients for the small mesozooplankton (PCCs = 0.71, 0.70: §5.3.2.1). The weaker PCC for the chlorophyll may result from the lower number of data points (as only night data were used), but may also show that the distribution of chlorophyll was influenced by other processes such as primary production and grazing by zooplankton.

At a wavelength of 17 km there is the largest peak in the temperature spectra that is correlated with the largest peak in the small mesozooplankton (0.41-0.64 and 0.64-1.02 mm ESD) spectra. However the chlorophyll spectra does not contain a large peak at this frequency. An explanation for these observations is that the chlorophyll that has been aggregated by the physical processes has been grazed by the aggregated zooplankton. Evidence for zooplankton grazing can be seen in **Fig 5.3.4.ib**, although the grazing cannot be related only to this spatial scale. **Fig 5.3.4.ib** shows the ratio of the concentration of phaeopigments to chlorophyll *a* as a function of the depth of the 22.5°C isotherm. As the depth of the isotherm decreased the total chlorophyll also

decreased, and the relative proportion of phaeopigments increased, suggesting grazing. However, the reduced phaeopigments with distance from the source of the internal waves may indicate a reduction in health of the phytoplankton with distance from the Gulf of Oman.

At a wavelength of 9 km there were peaks in the spectra of temperature and chlorophyll, but there were not large peaks in the mesozooplankton spectra. This may be evidence that the swimming of even the smallest mesozooplankton is important in relation to physical forcing at these scales. This de-coupling of the small zooplankton from the physical forcing would reduce the top-down control on the phytoplankton populations, which is provides an explanation for the particularly large peak in the chlorophyll spectra at 9 km.

5.3.4.2 The impact of biological processes on the distribution of plankton

The biological spectra also contain peaks that are not correlated with peaks in the temperature spectra. Such peaks are either evidence for additional forcing by biological processes, or by physical processes that do not influence the temperature structure. The spectra for chlorophyll contains a large peak at 24 km, which is not associated with a major peak in the temperature spectra. The spectra for the mesozooplankton size classes (0.64-1.02, 1.02-1.61 mm ESD) also show small peaks at this wavelength. From the data it is not clear what factor has lead to this patchiness in the phytoplankton. The regular scale of the variability suggests that the process may be physical, but the lack of correlation with the temperature is not consistent with this explanation.

A wavelength of 60 km corresponds to the scale of the day/night change in this section of data. Evidence for this change is seen as peaks in the chlorophyll spectra caused by quenching. In addition, there was a small peak in the spectrum for the 1.61-2.56 mm ESD size class, and a slightly larger peak in the 2.56-4.10 mm ESD size class (not shown) at 60 km. These may indicate small DVM signals, which would be expected to be stronger in the larger size classes (§4.1.4). Finally, the small peak in the spectra for the depth of the isotherm at 60 km might represent the day/night variation in solar heating.

5.3.4.3 The importance of size

The small mesozooplankton (0.41-1.02 mm ESD) were correlated with the physical processes at 40, 17 and 9 km, while the larger species (1.02-4.10 mm ESD) did not show a correlation with the temperature spectra at these scales. This pattern can be

explained by the different swimming abilities of the zooplankton. The smaller species were passively redistributed by the internal waves, while the larger species were more actively determining their own distributions by swimming. This hypothesis is supported by the correlation between the macrozooplankton and the physical structure, which also lessened with increasing animal size (§5.3.2.2). The largest macrozooplankton and micronekton (those that backscattered at 38 kHz) had no significant correlation with the physical forcing, suggesting that their behaviour decorrelates their distribution from the waves. An alternative hypothesis is that a physical process that was not observed in the temperature spectra was important in determining the distribution of the larger species. These hypotheses are discussed further in §6.2.4.

5.3.5 Summary and conclusions

A strong positive correlation was determined between the mesozooplankton abundance and the temperature of the GOS water. GOS water is the warmest water in the Strait, and both temperature and zooplankton abundance were reduced when this water mixed with the STW. Total zooplankton abundance showed strong correlations with the temperature structure, even when the isotherms were displaced vertically by the passage of internal waves. Which indicates that the majority of mesozooplankton were passive tracers of this process.

The larger mesozooplankton (>1 mm ESD) were less correlated with the physical structure, and other factors (such as behaviour) were hypothesised to be more important in determining their distribution. The distribution of macrozooplankton was more closely correlated with the mesozooplankton than the physical forcing, possibly suggesting these species were aggregating in this food source. The largest macrozooplankton, which would have the greatest mobility, showed the weakest correlation with the physical structure of the water column.

Spectral analysis indicated that the distributions of temperature, phytoplankton and <1 mm ESD zooplankton were characterised by wavelengths at 40, 17 and 9 km. This indicates the dominance of physical forcing by the internal waves at these scales. However there was considerable evidence for the importance of other processes because of the lack of exact agreements between variables, such as possible grazing of the phytoplankton at 17 km. Spectral analysis of the distribution of the larger mesozooplankton (>1 mm ESD) revealed that there were no correlations between their

spectra and temperature spectra, again indicating a reduced impact of the internal waves. Two mechanisms are proposed to explain the reduced correlation of the distribution of the larger zooplankton with the water column structure determined by the internal waves:

1) That the increased swimming ability of larger zooplankton means that they are more able to maintain their distribution in relation to the internal waves.

2) That other physical processes were determining the distributions of these species that did not result in regular scales of variability in the temperature spectra.

These mechanisms are not exclusive of each other and are discussed further in §6.2.4.

SUMMARY: THE INTERRELATIONSHIP BETWEEN ENVIRONMENTAL AND BIOLOGICAL FORCING DETERMINING THE DISTRIBUTION OF ZOOPLANKTON IN THE STRAIT

In this chapter, the analysis of the concurrent measurements of the physical environment and the distribution of plankton demonstrated that the interaction of environmental and biological mechanisms was important in determining the distribution of zooplankton in the Strait. The relative importance of these mechanisms varied with both the structure and the scale of the physical processes and size of the individual plankter.

The formation of the STW by the mixing of the AGO and GOS resulted in substantial change in the planktic community structure at the time of sampling. In comparison to the AGO and GOS the mesoscale frontal region represented by the STW contained more phytoplankton and less herbivorous mesozooplankton. The larger macrozooplankton showed no response in the STW, instead the MVBS showed a gradient from the GOS to the AGO, and possibly was influenced by Strait scale processes such as the shallowing of the depth, and the increasing salinity.

The front between the AGO and STW had a different impact on the zooplankton, with small mesozooplankton (<1.6 mm ESD) predominantly mixed passively from one side to the other, and the larger mesozooplankton (>1.6 mm) absent in the intermediate conditions. The MVBS from macrozooplankton also did not show a conservative gradient across the front. It is worth noting that even the small mesozooplankton were not entirely conservative with salinity in the front.

The sub-mesoscale variability associated with internal waves on the east side of the Strait also had a different impact on small and large zooplankton. The distribution of

small mesozooplankton (<1.0 mm ESD) was often correlated with the scales of the internal waves, indicating that they were redistributed passively by the physical forcing of the waves. The distribution of larger mesozooplankton (>1.0 mm) and macrozooplankton (measured by the EK500) was not as closely correlated with the internal waves. This indicates that other process such as their swimming behaviour and unresolved physical processes were more important in determining their distributions.

The wider implications of these findings are discussed in Chapter 6, where they are also compared with the observations of similar studies.

CHAPTER 6

Discussion of Observations and Findings

6.1 THE USE OF AN OPC TO DESCRIBE ZOOPLANKTON DISTRIBUTIONS AT THE MESOSCALE . 187
6.2 THE EFFECT OF THE PHYSICO-CHEMICAL ENVIRONMENT ON THE DISTRIBUTION OF ZOOPLANKTON 197
6.3 IMPLICATIONS FOR THE RELATIONSHIP BETWEEN ZOOPLANKTON AND THEIR PHYSICO-CHEMICAL ENVIRONMENT AT THE MESOSCALE 210
SUMMARY 216

In this chapter the findings presented in the previous chapters are compared with similar studies and the wider implications of the results are discussed. The first section (§6.1) refers specifically to the use of the OPC as a tool to describe the distribution of zooplankton at the mesoscale. This section recounts the findings and conclusions of the calibration of the OPC (Chapter 3) and compares these with the results of previous research. In addition, the limitations of the instrument and the methodology are discussed and solutions and future work are proposed. §6.2 recounts the main features of the distribution of zooplankton in relation to the mesoscale environment in the Strait of Hormuz (Chapters 4 and 5) and compares these findings with previous studies in this area and in other regions. Environmental and behavioural mechanisms that may determine mesoscale plankton distributions in the Strait are proposed and evaluated with the observations of this survey and compared with mesoscale studies in other regions. In §6.3 the implications of the findings of this study are discussed in the context of the impact of mesoscale forcing on the role of different sized zooplankton in trophic and biogeochemical processes.

6.1 Discussion of the use of an OPC to describe zooplankton distributions at the mesoscale

In chapter 3 a processing and calibration methodology was presented and used to estimate zooplankton abundance and biovolume from the optical plankton counter (OPC) data collected in the Strait of Hormuz. The accuracy of the calibration of the OPC was determined by comparison with netted samples of zooplankton collected with a Longhurst-Hardy Plankton Recorder (LHPR). Some previous studies have attempted to calibrate OPC data by fitting it directly with net measurements (§3.2.1). However a "standard" method has not yet arisen. The LHPR cannot be towed synchronously with the SeaSoar (fitted with the OPC) and no provision was made to mount the OPC on the LHPR. The resulting spatial and temporal differences between the datasets potentially make empirical fitting of the OPC data to the LHPR data unreliable. Instead, OPC data were calibrated using a model derived from estimates of the factors that influence the size of a particle recorded by an OPC (see §3.2) that included empirical measurements of animal dimensions from the nets. The resulting calibration was then compared with the LHPR net biovolume, but no further calibration was made. The accuracy of the calibration is discussed and errors

associated with the use of the OPC in mesoscale studies are summarised and improvements are suggested in §6.1.1. Methods for collection the more robust calibration datasets are discussed in §6.1.2, and future improvements to interdisciplinary mesoscale studies are briefly discussed in §6.1.3.

6.1.1 An assessment of the OPC calibration and improvements for future work

In this section the OPC calibration from this study is evaluated, and then problems associated with the OPC are listed and improvements are suggested.

6.1.1.1 The calibration of OPC data in this study

The OPC estimates of zooplankton abundance were in the same range as those determined by the enumeration of zooplankton in the LHPR samples in this study. An important step in the comparison was the standardisation of both datasets to the same size range of zooplankton. Standardisation is fundamental because the effective retention size range of a net varies with both mesh size and towing speed (Vannucci, 1965; §1.4). A number of other errors (e.g. filtered volume, avoidance) are associated with nets and should be quantified when net data are used for comparative assessment of the data collected by modern sampling technologies (Skjoldal *et al.*, 2000), such as the OPC. The LHPR and OPC data were standardised in terms of size and spatial resolution (§3.1). Net samples still provide the best source of information to evaluate OPC data because nets are widely used and their data are generally accepted.

The vertical profiles of zooplankton abundance determined by the OPC and LHPR were not identical (**Fig 3.1.3.i** and **iii**). The shapes of the profiles were generally consistent, but details differed, such as the magnitude and depth ranges of high and low abundances. The differences were mainly attributed to changes in the water column structure during the 4 to 7 day gap between sampling, but this is not evidence that a better correlation would have been obtained with concurrent sampling. However, the abundance measured by the OPC was close enough to the 1:1 line to be accepted as a reliable estimate describe the number of zooplankton in the Strait.

Zooplankton biovolume was initially determined from the sizes measured by the OPC with a spherical model (§3.2.1), but this was found to consistently overestimate biovolume compared with the biovolume measured in the LHPR samples. This is because zooplankton are not typically spheres. The OPC data were then calibrated with a spheroidal model, that was tuned with dimensional measurements of

zooplankton capture in the net samples. The calibrated biovolume from the OPC provided a good fit with the data, although the fit was not exact at all depths (**Fig 3.3.1.i**). Biovolume was highest in the upper 50 m, and at these depths the OPC estimates were equivalent to the net data. At the lower biovolume levels found below 50 m the OPC overestimated biovolume compared with the LHPR. This partly may have been a result of the low numbers of animals sampled by each instrument at these depths. This discrepancy cannot be attributed to the OPC counting non-zooplankton particles because the abundance profiles did not show as large a difference.

The calibrated OPC measurements of biovolume and abundance were also within the range of values measured in a net survey made by Gibson *et al.* (1980) in the Strait. The biovolume calibration factor (CF_{vol}: a factor relative to the spherical model, §3.2.3) for the OPC determined in this study ($CF_{vol} = 0.61$) is almost identical to other empirically derived factors (**Fig 3.4.2.i**) – 0.57 (Sprules *et al.*, 1998) and 0.60 (Pollard *et al.*, submitted). The consistency of these factors, from such different environments (sub-tropical shelf, freshwater lake and Antarctic Ocean) suggests that a standard OPC calibration factor in this range may be reliable in many environments for a first order calibration of the biovolume of mesozooplankton from OPC data. Stockwell and Sprules (1995) determined a calibration factor of 0.39 which is lower than the other three factors. Although the calibration by this factor was still within the range of the LHPR data (**Fig 3.4.2.i**) the better calibration samples collected for their 1998 study, produced an improved calibration (Sprules *et al.*, 1998).

The calibration equation that is proposed in this study is probably applicable for the OPC in a wide range of environments, and provides a useful calibration procedure for future studies. In the future, it is recommended that the parameters used in the calibration are more precisely quantified by empirical measurements. For example, the length to width ratio of the spheroid (r_{cop}) that represents zooplankton should be more accurately defined. Net samples should be used to determine if r_{cop} varies with zooplankton size and in different areas within the survey (such as water masses). Investigations are also required to determine if zooplankton are randomly or consistently orientated in the beam. In this study the calibration assumed that zooplankton were consistently orientated in the beam, but a calibration equation (Eq 3.2.4) is provided to calculate the CSA of a randomly orientated particles (which is expected to be the case for the bench top OPC). Empirical measurements should also

be used to quantify the importance of translucency and appendages of zooplankton on the CSA measured by the OPC.

The calibration of the OPC demonstrates that the OPC can be used to describe the distribution of zooplankton abundance and biovolume in the Strait. The calibrated OPC data provide a good measure of zooplankton abundance to examine the relationship between these organisms and the mesoscale environment in this study.

6.1.1.2 Problems associated with the OPC that still remain to be addressed

There were still notable discrepancies between the OPC and net data, for example at low *in situ* biovolumes. The following paragraphs list the problems associated with producing accurate zooplankton data with an OPC, the importance of these problems in this study and possible improvements for future work.

1) In order to quantify zooplankton abundance (and biovolume) from OPC data, the number of particle counts is standardised by the volume of water passing through the instrument. Unlike zooplankton nets the SeaSoar is not usually fitted with a flowmeter, which meant that the flow through the OPC was estimated from the ship's speed. Grant *et al.* (2000) found that by applying a correction for the flow through the OPC discrepancies as large as two orders of magnitude with net data could be accounted for, and state that "flow correction would appear to be a fundamental calibration requirement". In §3.1.2.2 it was demonstrated that the speed difference of SeaSoar between the up and down profiles can be as much as 70%, which will affect the estimates of abundance by the same amount. In this study this error was minimised by averaging the data over several up and down profiles which reduced the effect to about 2.5%. Because this effect is not exactly opposite on the up and down profiles, close attention is required to this problem in future studies.

Further improvements for quantifying the flow through an OPC are to use a flowmeter and to model the changes in speed of the SeaSoar. Rissik *et al.* (1997) and Sprules *et al.* (1998) have used a General Oceanics model 2031H flowmeter with the OPC to determine the volume sampled. However, this flowmeter is mounted outside the OPC sampling tunnel and Grant *et al.* (2000) found that the flow through an OPC can change when it is towed obliquely and the mouth of the OPC is not perpendicular to the flow. The same phenomenon is well know for net systems (e.g. Roe *et al.*, 1980). Ideally flow should be measured within the tunnel, possibly using miniature impeller, acoustic Doppler technologies or the passage time of particles through the

beam. These relatively simple procedures would correct both the problems in determining the flow due to the changing speed of the SeaSoar and the angle of the OPC relative to the flow. A second solution would be to accurately model the affect of the changing speed of SeaSoar, and correct the OPC data accordingly. Both of these techniques are recommended for more accurately determining the volume sampled by an OPC.

2) The OPC measures not only the zooplankton particles, but also any other material of similar size. Zhang *et al.* (2000) determined that the high levels of detritus found in estuarine waters could significantly increase the number of counts made by an OPC. In this study the zooplankton abundance determined from the net and the OPC were approximately equivalent indicating that non-zooplankton particles did not significantly enlarge the OPC counts. This is consistent with expectations for the region because the Strait receives little freshwater input and as a result terrigenous detritus levels are low. A similar situation would be expected in open ocean water. In certain areas of the Strait the counts increased close to the seabed, and it is possible that resuspended sediment was counted by the OPC. However, these increases were correlated with the AGO water and the LHPR samples at stn 54007 showed a larger increase in zooplankton numbers in the AGO close to the bottom, suggesting that the OPC counts were indeed zooplankton (**Fig 4.2.1.vii**). In areas where background detritus levels are expected to be large, their impact on OPC counts can be determined and corrected following the laboratory method developed by Zhang *et al.* (2000).

Large phytoplankton cells and colonies can also elevate OPC counts when they are numerous, such as in the Southern Ocean (Grant *et al.*, 2000; Pollard *et al.*, submitted). Taxonomic studies of the phytoplankton in the Arabian Gulf and Strait of Hormuz (reviewed by Rao and Al-Yamani, 1998) have shown that very large phytoplankton (>200 μm) are rare. Phytoplankton that are slightly smaller (≈ 100 μm) than the minimum detection limit of the OPC may also be counted when two or more cells pass through the sampling beam simultaneously and their combined size is within the OPC sensitivity range (Herman, 1992). This effect becomes significant when the phytoplankton are very abundant. The OPC was not thought to be counting phytoplankton in this study because the lowest count rate of the OPC in the upper 30 m coincided with the highest chlorophyll concentrations.

3) Zooplankton abundance and biovolume estimates are also affected when two or more individuals pass through the beam simultaneously. When zooplankters coincide in the beam their abundance is underestimated (by half for two individuals) but their biovolume is overestimated (Sprules *et al.*, 1998). The biovolume is overestimated because the volume of a particle with a certain diameter is larger than the summed volumes of two particles with same combined diameter as the first particle. Sprules *et al.* (1998) also determined that coincidence counts are unavoidable at count rates exceeding 167 sec^{-1}. The problem of coincidence counts was minimised in this study by reducing the sampling rate of the OPC to less than 100 sec^{-1} by reducing the volume of the sampling tunnel. This is a widespread solution in many studies, but results in a reduction of the total numbers of counts. As a consequence larger species are not encountered regularly enough for their distributions to be reliably determined. Coincidence can also be evaluated by comparing the size spectra determined by the OPC with one produced by detailed analysis of net samples (Sprules *et al.*, 1998).

4) An OPC does not produce any taxonomic information about the zooplankton that are counted. Zooplankton size was a major focus of this study and the OPC is well suited for producing this type of information. The LHPR samples showed that copepods were clearly the numerically dominant mesozooplankton in the Strait. A more rigorous determination of the species present was not attempted in this study because the animals in the net samples were damaged by collision with the LHPR net (§2.2.5). Taxonomic information can be inferred by cross correlating the sizes measured by the OPC with the dimensional measurements of dominant taxa and species captured by a detailed net survey (e.g. Herman, 1992; Rissik *et al.*, 1997). The dimensions can be determined with a microscope or with the use of the laboratory OPC (Wieland *et al.*, 1997). The measurement method has limitations with gelatinous species, which do not have a consistent relationships between dimensions and light blocked in an OPC. In addition zooplankton samples are usually preserved before the lab OPC analysis can be performed. Preservation not only influences zooplankton size (Beers, 1976) but also the size recorded by an OPC compared with fresh zooplankton (Beaulieu *et al.*, 1999). Taxonomic information would greatly enhance the interpretation of distribution of zooplankton at the mesoscale, and future studies should attempt to incorporate these measurements.

Alex Herman and Focal Technologies (the makers of the OPC) have been developing a new laser OPC for the past few years (Herman pers. comm.). This

instrument will solve several of these problems, but handling the data collected by this instrument continues to delay its production. First, the laser OPC can precisely measure the volume of seawater passing through the tunnel. The laser optics also work faster which results in a 100 fold reduction in the probability of coincidence counts. The LOPC is also capable of coarse taxonomic resolution of particles larger than 0.5 mm, and has worked well on copepods such as *Calanus finmarchicus* CIV, CV and euphausiids in tests (Herman, pers. comm.). The LOPC will clearly be advantageous compared with the standard OPC in mesoscale studies.

6.1.2 The use of the OPC in mesoscale studies, improvements in the collection of calibration and interpretation datasets

This section is divided into two parts: the first suggests improvements in the collection of a more reliable calibration dataset for OPC data, and the second briefly discusses other data that are useful in the interpretation of OPC measurements.

6.1.2.1 Sampling protocols for the calibration of the OPC in mesoscale studies

A serious short coming of this study was that the LHPR did not provide an ideal calibration dataset for the OPC. The main problems were that the LHPR samples were not concurrent with the OPC data, and second the LHPR did not capture the complete size range counted by the OPC. Recognising these difficulties, possible improved methodologies are discussed in this section.

To resolve the physical mesoscale structure of the upper ocean a survey must have adequate coverage and resolution and be completed in short enough period to provide a quasi-synoptic view of the environment. This is essential if zooplankton distributions at the mesoscale are to be studied. Typically these requirements are addressed by using a towed undulating vehicle, such as SeaSoar (Pollard, 1986). Although the details vary, a mesoscale survey usually consists of a grid of transects encompassing the feature(s) of interest, and takes 2 to 6 days to complete. Current technology does not allow nets (other than surface samplers, such as the CPR) to be deployed simultaneously with SeaSoar. The CPR is not suited as a calibration tool because it samples zooplankton just below the surface and does not collect spatially discrete samples (§1.4). A future solution would be to fit a discrete plankton sampling mechanism (PSM) to the SeaSoar thus collecting a concurrent calibration dataset. This solution is discussed at the end of this section, but first the benefits and costs of current technologies are discussed.

The synopticity of a mesoscale survey is significantly reduced by punctuating it to collect on station measurements, such as the net samples needed to calibrate and interpret OPC data. The relative importance of physical synopticity and the data needed for instrument calibration must be assessed during cruise planning in the context of the overall objectives of the study. In a survey of this nature there are two choices: first to stop at intervals during the survey and take samples accepting the loss in quality of physical data or second to only take net samples before and after the survey thus maximising physical synopticity.

If stops are made during a survey, the time consumed "on station" while samples are collected must be minimised. In reality this only provides time for the deployment of simple vertically hauled nets, which can be deployed and recovered in less than 20 minutes. More complicated samplers, such as the LHPR, provide much higher spatial resolution but consume too much time to be used during a SeaSoar survey (tows typically take several hours). Vertically hauled nets allow many independent calibration samples to be taken relatively quickly. In order to collect the smallest zooplankton sampled by an OPC, a fine mesh of between 80-110 μm is required. The positioning of the net sample can be guided by near real time OPC data processing, so that samples are targeted at diverse conditions. This method does not produce a concurrent calibration dataset and the calibration assumes that quantity of zooplankton was the same when net samples and OPC data were collected. The samples from vertically integrated net hauls only allow the performance of the OPC to be compared with the net for the average zooplankton concentration in the water column. Therefore these net samples do not provide data to assess the OPC data with the net at the highest and lowest *in situ* concentrations. In this study the largest discrepancy between the OPC and the net was at lowest concentrations.

More sophisticated samplers, such as multi-nets and the LHPR, can provide samples from different depths and can be fitted with a second OPC to collect a synchronous calibration dataset (e.g. Herman, 1992; Heath, 1995; Wieland *et al.*, 1997). For reasons stated above, these samplers can only be deployed before and after the SeaSoar surveys and therefore it is important to minimise the time gap between the collection of the datasets. The standard mesh that is fitted to most of these samplers does not catch the smaller species counted by the OPC. Both of these factors were problems with the LHPR used in this study. The OPC on the net system may not be directly comparable with the OPC on SeaSoar because of the different towing

conditions. Therefore an additional inter-calibration may be required between the two OPC datasets, and these datasets will not be concurrent. However the distribution of zooplankton at a station with 1-2 hours of survey work would be expected to be similar, especially if marked with a Lagrangian marker.

Concurrent calibration data for an OPC mounted on SeaSoar could be obtained from the other zooplankton sampling technologies deployed concurrently with the SeaSoar. For example high frequency acoustic instruments (e.g. TUBA/TAPS see §1.4.2.1) and optical technologies (such as the digital video or stills) could be used to collect independent datasets for comparison. These methods would not produce a precise calibration, because they also need calibration, but may be adequate to qualitatively assess OPC data. These techniques would be suitable when OPC data are needed for comparative and descriptive work which do not require a quantitative calibration.

Important future work should be developing a zooplankton sampling mechanism to take zooplankton samples on SeaSoar. Such a methodology would not only collect data suitable to calibrate the OPC, but would also save valuable ship time. The plankton sampling mechanism (PSM) of the U-Tow (Hays *et al.*, 1998) is a viable option as it is small enough to fit within the body of SeaSoar, is suitable for the towing speed of SeaSoar and can remain underwater for the typical length of a SeaSoar survey. This instrument collects a series of 50 discrete zooplankton samples, which will give a resolution of 20 km when spread through a typical 1000 km survey. Currently part of the instrument payload of the SeaSoar would have to be removed to accommodate the PSM. But with planned developments to enlarge SeaSoar to accommodate more instruments, the PSM should be identified as a significant addition to SeaSoar both for OPC calibration and as an independent survey tool.

The OPC is a useful tool for describing the distribution of mesozooplankton at the mesoscale with higher resolution and greater coverage than can be obtained from net surveys. OPC data are collected concurrently with other variables providing robust datasets for interdisciplinary studies and without the expense of extra ship time. Additional studies are still required to accurately evaluate and interpret the data produced by the OPC: areas for continued research are flow through the instrument, coincidence counts, species identification, the production of a standard method for the calibration of abundance and biovolume from OPC data and a standard method for the collection of suitable samples.

6.1.2.2 Improvements to the sampling strategy for understanding the relationship between the mesoscale environment and zooplankton

The use of modern zooplankton sampling technologies has greatly enhanced the observational capabilities of mesoscale studies. However, this study has shown that the distribution of different sized zooplankton can be explained by a number of hypotheses which have been difficult to test because of a lack of suitable evidence. In order to understand the mechanisms that cause these distributions, mesoscale studies must incorporate the measurement of a range of variables such as nutrient concentration, primary production, species present and grazing. At present many of these variables that are needed to understand the ecology of the pelagic community can only be collected on station. It is important to develop technologies and sampling methodologies that enable these variables, or at least proxies for them, to be collected concurrently with and at the same resolution as SeaSoar data. Instruments such as fast repetition rate fluorimeter (FRRF) and nutrient sensors are examples of the technologies that are beginning to become available for this use. Mesoscale studies should also make use of other sources of data, such as moorings and Lagrangian floats to better interpret temporal changes and to define boundary conditions, and also satellite and aircraft observations to produce truly synoptic spatial information. Future studies could also utilise autonomous vehicles or make surveys with multiple ships in order to collect station measurements during underway surveys.

6.2 DISCUSSION OF THE FINDINGS OF THIS STUDY: THE EFFECT OF THE PHYSICO-CHEMICAL ENVIRONMENT ON THE DISTRIBUTION OF ZOOPLANKTON

This study is the first in the Strait that attempted to observe mesoscale physical processes. It is also unique in the Strait because the distribution of zooplankton is described using data at a higher resolution than is provided by vertically integrated net samples from fixed stations. Most of the previous studies have had the objective of describing the distribution of zooplankton in the different geographic areas, but have found as large differences within each area as between them. Moreover these studies have determined contradictory geographic distributions of zooplankton biomass (§2.1.3). The investigation in this thesis has attempted to relate zooplankton distributions to hydrographic features by using biological data sampled at the same high spatial resolution and coverage as concurrent physical data. In doing so, this study has provided clear and detailed descriptions of zooplankton distributions in areas defined not by regional geography, but by the prevailing physical environment. Moreover, the data have been used to investigate the important physical and biological mechanisms that determine zooplankton distributions at the mesoscale.

The main physical features observed during this survey were a mesoscale two layered exchange between the Gulf of Oman and the Arabian Gulf, a mesoscale front in the western Strait marking the eastward surface extent of the high salinity outflow from the Arabian Gulf and sub-mesoscale variability associated with internal waves in the eastern Strait. The two layered exchange has been documented in previous studies (e.g. Leveau and Szekielda, 1968; Reynolds, 1993). In this study a third water type was defined: the STW, which was formed by mixing processes at the mesoscale between the end members (the AGO and GOS; see §5.1) and represents a frontal region between the AGO and GOS. Water with the temperature and salinity characteristics of the STW was only found in the Strait. The sharp front between the high salinity AGO and the STW is part of the larger frontal region represented by the STW, but is considered as a separate mesoscale feature because it forms a clear discontinuity to plankton distributions. This front can be seen to the west of the Masandam peninsular in the data presented by Leveau and Szekielda (1968) and Sultan and Elghribi (1996). However, in both these surveys the front fell between CTD stations and was not investigated in detail. Internal waves have been widely recorded associated with shelf areas with steep topography and large tides (Baines,

1982): features that are characteristic of the Strait of Hormuz (Sultan and Elghribi, 1996). No authors have investigated the internal waves in detail in the Strait, but their presence has been noted (e.g. Reynolds, 1993). The internal waves are a sub-mesoscale feature, and have been investigated in this study for comparison with the mesoscale features.

In this section the findings of chapters 4 and 5 are discussed. First, there is a summary of the trophic relationships between the plankton sampled by the fluorimeter, OPC and EK500. The possible mechanisms that are important in determining plankton distributions in the Strait are discussed for each of the water types, for the front and the internal waves. These mechanisms are evaluated with the observations and analysis presented in chapters 4 and 5 and are compared with the results of previous studies in the Strait and similar studies in other regions

6.2.1 Summary of expected trophic interactions of plankton in the Strait

It is important to determine the trophic interactions between the phytoplankton, mesozooplankton and macrozooplankton when interpreting their spatial distributions. This study has used size to categorise plankton, which is a useful tool because size is generally related to what an organism eats and what eats it (Sheldon *et al.*, 1977; §1.3.3). From this assumption we can generalise that the small (<2 mm) mesozooplankton sampled by the OPC were capable of feeding on phytoplankton, and also other food sources such as microzooplankton. In §5.2.3 calculations estimated that mesozooplankton herbivory in the STW was between <1 and 6% of chlorophyll standing stock per day (not primary production) but in the AGO was between 50 and >200% of chlorophyll standing stock per day. These calculations were supported by observations of phaeopigment to chlorophyll ratios, which indicated increased grazing in the AGO compared with the STW. These values are only estimates and no measurements were made of grazing rates or gut fluorescence during this study. In the open ocean mesozooplankton are thought to typically graze only a minor proportion of primary production (note figures above relate to standing stock): between 0.1 and 25% per day (Dam *et al.*, 1993; Roman *et al.*, 1993; Roman and Gauzens, 1997; Head *et al.*, 1999). However, Roman *et al.* (2000) found that mesozooplankton in the Arabian Sea grazed on average 40% of the primary production a day and measured a range of values between <10% and 120%. The increased significance of mesozooplankton

herbivory in this region was attributed to the high zooplankton biomass, the abundance of diatoms and the warm water temperature which results in high growth rates. Edwards *et al.* (1999) estimated a much lower rate of mesozooplankton herbivory in the Arabian Sea between 4 and 12% of primary production. The difference between these studies may in part be caused by the method used by Edwards *et al.*, who estimated herbivory from the product of zooplankton biomass and Smith's (1982) data for ingestion rates. Both studies reported greater mesozooplankton herbivory closer to the coast, and Roman *et al.* estimated it as 85% of primary production at their inshore station in the SE Gulf of Oman. Although primary production was not determined in the Strait the high mesozooplankton abundance is expected to be an important control of phytoplankton stocks in some areas.

In the LHPR samples carnivorous chaetognaths accounted for an increasingly greater proportion of abundance in the larger size classes (§4.2.3). Therefore, the larger mesozooplankton sampled by the OPC are expected to have a lower proportion of herbivores to carnivores. In the Gulf of Oman the dominant scatterers in the EK500 data were zooplanktivorous fish and decapods (§4.1.4.1). These mesopelagic species are not expected on the shelf, but the species that are present and scatter at the same frequencies, are also expected from their size to be mesozooplankton predators.

In reality the situation is not so straight forward: for their size raptorial feeders tend to prefer larger prey and filter feeders favour smaller prey (Hansen *et al.*, 1994). For example the small (<1 mm) copepod *Oithona* is a raptorial feeder; Lampitt and Gamble (1982) show that this species can feed on a wide range of particles from small phytoplankton (4 μm) to nauplii and copepodites (upto 300 μm). In this area, the euphausiid *Pseudeuphausia latifrons* grows to about 15 mm (Weigmann, 1971), but also feeds on phytoplankton and microzooplankton (by filtering) and small copepods (raptorially). As a result both the small counts from the OPC (*Oithona*) and the MVBS from the EK500 (120 kHz: *Pseudeuphausia*) may both represent animals feeding on the same food, despite a large difference in their sizes. Hansen *et al.* (1994) show that the ratio between organism size and prey size is variable between taxonomic groups, but suggest a ratio of 18:1 for copepods (that is a copepod with an ESD of 0.4 mm will favour particle of 22 μm). In this study, size provides a useful framework to generalise about expected trophic interactions, but in situ measurements made during the cruise are recommended in future studies interested in trophic interactions.

6.2.2 Possible mechanisms impacting of zooplankton distributions in the three water types defined in the Strait of Hormuz

In this section there is a discussion of mechanisms that can account for the observed distribution of zooplankton in the three water types defined in the Strait. The GOS is the warm, fresher oceanic water entering the Strait from the Gulf of Oman in the south east. The AGO is the cooler, high salinity water flowing out of the Arabian Gulf and into the Strait from the west. In the Strait, mixing processes at the mesoscale produce the STW which has intermediate temperature and salinity characteristics. The STW represents frontal region between the two flows. In the first part of this section possible mechanisms that can explain the biological characteristics in the end members are discussed. In the second part of this section, mechanisms are examined that may explain the differences in plankton community in the STW.

6.2.2.1 The biological characteristics of the end members: the GOS and AGO

The GOS was characterised by a high mesozooplankton standing stock and moderate chlorophyll *a* concentration (**Fig 5.1.1.ii** & **6.2.2.i**; Table 6.2.2a). Studies in the Gulf of Oman have found that zooplankton standing stock is large compared with the rest of the region (e.g. Lens, 1973; Kimor, 1973). This high standing stock is partly supported by a region of year round upwelling along the Iranian coast, which injects nutrients into the euphotic zone increasing production. The high mesozooplankton abundance and biovolume measured in the GOS in this study can be explained as typical of the NW Gulf of Oman. Another possibility is that nutrients are upwelled at the shelf break as a result of the internal waves promoting vertical mixing. At the shelf break in the Bay of Biscay (North Atlantic) elevated chlorophyll concentrations are thought to result from enhanced nutrient concentrations supplied by increased vertical mixing associated with internal waves (Pingree *et al.*, 1986). In this study both mesozooplankton abundance and the MVBS of macrozooplankton were reduced with distance away from the shelf break to the tip of the peninsula. The highest biovolume of zooplankton measured by Gibson *et al.* (1980) in the Gulf of Oman, Strait of Hormuz and the Arabian Gulf was above the shelf break on the east side of the Strait, which is consistent with this being a site of localised production.

The AGO contained similarly large mesozooplankton abundance and slightly larger mesozooplankton biovolume than the GOS. The chlorophyll concentration was also at a similar level (**Fig 5.1.1.ii** & **6.2.2.i**; Table 6.2.2a). The Arabian Gulf is characterised

by a zooplankton community that is low in diversity but high in biomass (Kimor, 1973). High primary production in the Arabian Gulf is supported by nutrients entering the basin through the eutrophic Shatt Al-Arab estuary and by rapid remineralisation in the warm, shallow sediments (El-Gindy and Dorgham, 1992; Rao and Al-Yamani, 1998). Leveau and Szekielda (1968) hypothesise that the euryhaline species that can tolerate the high salinities of the Arabian Gulf tend to flourish because of reduced competition. The high mesozooplankton abundance and biovolume measured in the AGO is consistent with these previous findings. However, the survey did not extend far enough into the Arabian Gulf to determine if the high standing stock of mesozooplankton was a consistent feature in this water, or was related to the front with the STW (examined in §6.2.3).

6.2.2.2 The impact of mesoscale mixing on the planktic community in the Strait

The STW was produced by mesoscale mixing between the AGO and GOS and as a result the temperature and salinity characteristics of the STW were intermediate of these end members. However, the standing stocks of phytoplankton and mesozooplankton differed dramatically from what would be expected from conservative mixing (**Fig 5.1.1.ii** & **6.2.2.i**; Table 6.2.2a). In the STW the chlorophyll concentration was about twice that in the AGO and the GOS. Conversely, the mean mesozooplankton abundance in the GOS and AGO was more than twice that in the STW. The STW also showed a distinct shaped mesozooplankton biomass size spectrum: the spectra in the GOS and AGO were similar with biovolume dominated by small species (0.3-0.9 mm ESD) but in the STW biovolume was dominated by larger species (2.3-5.0 mm ESD), which were at a concentration that was intermediate of the end members (**Fig 5.1.1.ii** & **6.2.2.i**; Table 6.2.2a). The stocks of phytoplankton and small mesozooplankton in the STW were distinct and not intermediate of the communities in the source waters: the AGO and GOS. The larger mesozooplankton (2.3-5.0 mm ESD) and the MVBS from the EK500 (representing macrozooplankton) showed a different pattern and were intermediate in the STW (Table 6.2.2a).

Table 6.2.2a Summary of characteristics of the water types in the Strait (averaged over top 30 m)

Water type	Salinity range	Chl*a* conc. (mg m^{-3})	0.4-4.0 mm zooplankton abundance (*10^3 m^{-3})	0.3-0.9 mm zooplankton biovolume (ml m^{-3})	2.3-5.0 mm zooplankton biovolume (ml m^{-3})	MVBS at 38 kHz (dB)
GOS	36.4 - 36.8	0.50	9.7	0.73	0.145	-64.6
STW	36.8 - 38.0	0.75	4.2	0.19	0.155	-66.8
AGO	38.0 - 40.5	0.40	10.0	0.79	0.165	-71.8

These observations indicate that in comparison to the end members the small mesozooplankton in the STW were relatively decoupled from the phytoplankton. This structure was relatively stable for at least the 5 days of the SeaSoar survey, and appeared to be consistent 9 days after the start of the SeaSoar survey, when CTDs and an LHPR were deployed in the STW. The CTD measured the highest chlorophyll concentration in the STW (**Fig 4.1.1.iii**, line B) and the LHPR caught less zooplankton in the STW than deeper in the AGO (**Fig 4.2.1.ii**). Zooplankton populations have doubling times several orders of magnitude longer than phytoplankton (e.g. Sheldon *et al.*, 1972) and may be temporally decoupled from transient and spatially confined bursts of phytoplankton growth at the mesoscale. Temporal decoupling of zooplankton occurs during the development of the spring bloom at temperate latitudes in the North Atlantic, when the biomass of the zooplankton population lags behind an increase in phytoplankton (Cushing, 1959). Spall and Richards (2000) show in a mesoscale physical/ecosystem model that microzooplankton grazers can lag behind new primary production when the initial stocks of zooplankton are low. Mesozooplankton have growth rates an order of magnitude longer than microzooplankton, and therefore have a greater potential to become decoupled from pulses of primary production.

Unfortunately, observations over a nine day period do not provide a long enough series to determine whether the physical mixing between the end members is modifying the STW at a rate that maintains the decoupling, or whether these observations represent a temporary situation where STW will develop into a similar state to the end members. The small mesozooplankton in the STW were about 4 times less abundant than in the GOS and AGO (Table 6.2.2a). The time needed for the mesozooplankton to "catch-up" with the conditions in the end members can be calculated using the estimated doubling rates from Roman *et al.* (2000) from the Arabian Sea. Roman *et al.* determined doubling rates between 0.14 and 0.19 day^{-1} for the size range 0.5-1.0 mm, and between 0.09 and 0.12 day^{-1} for the size range 1.0-2.0 mm. For the population in the STW to double twice it would take between 21 and 44 days, which is 2-4 times longer than the observations of this study. Without observations over a similar period it is unwise to comment on the temporal stability of the situation in the STW, other than to state that it persisted for 9 days.

The stocks of larger mesozooplankton and macrozooplankton were intermediate in the STW, which suggested that they were not effected in the same way by the

mesoscale formation of the STW. These groups showed gradients across the whole Strait, which indicates that larger scale processes may be important such as the overall salinity gradient through the Strait and the shallowing of the seafloor.

Five mechanisms that may account for the difference in the biological properties of the STW relative to the end members are considered in this section. These mechanisms are direct convergence, bottom-up, top-down, environmental tolerance and community interactions, and should **not** be considered as mutually exclusive.

1) *Advective convergence*: plankton are aggregated by converging currents. The mean flows of the GOS and AGO converge in the Strait, and these could be aggregating the plankton in the STW. Many studies investigating convergent fronts have found higher concentrations of chlorophyll than in the surrounding water (e.g. Bainbridge, 1957; Pingree *et al.*, 1975; Holligan *et al.*, 1984). The concentration of a particle tracer in a parcel of water is not changed directly by convergence, but requires additional factors affecting movement such as buoyancy, photo-tactic, DVM and depth maintenance swimming. Different size classes may be effected by convergence in different ways, depending on the balance of the factors listed above and the strength of the convergence. The small (<2 mm) mesozooplankton were the least abundant zooplankton in the STW, and were at lower concentrations than in the end members, while phytoplankton biomass was enhanced. This is not consistent with convergence acting as an aggregating mechanism. Convergence may account for the distribution of chlorophyll at the mesoscale in the Strait, but the zooplankton data indicates that this mechanism is not controlling their distributions. The mesoscale physical convergence and mixing can lead to other ecological effects, such as displacing species into unfavourable physico-chemical or biological conditions: considered in mechanisms 4 and 5.

2) *Bottom up*: mesoscale mixing processes enhance primary production by increasing nutrient supply, thus leading to more secondary production and increased zooplankton stocks. Measurements of the ratio of phaeopigments to chlorophyll (**Fig 5.2.3.ii**), and the high chlorophyll standing stock suggest that the phytoplankton in the STW were an actively growing population. Both horizontal and vertical mixing processes at the mesoscale can result in enhanced primary production by supplying of nutrients: for example Videau *et al.* (1994) and Fernández and Pingree (1996) have measured increased primary production and high phytoplankton standing stocks at

ocean fronts. The situation in the Strait is different because the water depth is shallow (≤100 m) and there is no obvious source for the nutrients to drive an increase in production. El-Gindy and Dorgham (1992) determined that different nutrients affected phytoplankton growth in upper and lower layers of the water column in the Strait. It is possible that vertical mixing in the STW could change the nutrient availability in the upper layer, resulting in greater primary production. Another possibility is that different nutrients limit the primary production in the GOS and AGO, but when mixed to form the STW the combination of nutrients was not limiting. No measurements of dissolved nutrients were made during this cruise, so there are no data suitable to further evaluate these hypotheses.

The distribution of mesozooplankton at the mesoscale in the Strait is inversely correlated with phytoplankton standing stock. These observations are not consistent with a bottom up forcing, although they do suggest, in conjunction with grazing rate estimates, that herbivory is important in determining the phytoplankton stock. Bottom up forcing of zooplankton at the mesoscale is not thought to be important during this survey, probably because nutrients were not limiting phytoplankton growth.

3) *Top down*: standing stocks of herbivorous mesozooplankton are controlled by predation by macrozooplankton and fish. Environmental manipulation experiments have shown that top-down controls can dominate in some areas, and standing stocks of phytoplankton and herbivorous zooplankton fluctuate in response to modifications of predation pressure from macrozooplankton (Christaki and Vanwambeke, 1995; Pitta *et al.*, 1998; Pace *et al.*, 1998). If a top-down mechanism was dominant in the Strait, then we would expect that the highest macrozooplankton abundance (estimated from EK500 data) would be correlated with the lowest mesozooplankton and highest chlorophyll stocks. This is not the case for the Strait as a whole (**Fig 5.1.1.ii** & **6.2.2.i**; Table 6.2.2a) and no such a correlation exist. Verity and Smetacek (1996) draw attention on the importance of gelatinous species exerting a top-down control of mesozooplankton. These species are not strong scatterers of sound (Stanton *et al.*, 1996) and are destroyed by nets, so may be important but would not be detected.

4) *Environmental tolerance*: the transitional STW region represented physico-chemical conditions that are unsuitable for species that are adapted to the conditions in either of the two end members. Salinity, for example, can have an important effect on the distribution of marine organisms, because their ability to osmoregulate determines

their environmental tolerance (Kinne, 1966). The high salinity of the Arabian Gulf water is thought to be a barrier to many planktic species (§2.1.3.3) and marks the limit of their ranges (Kimor, 1973). The changes in species present on either side of the Strait is indicated in Table 6.2.2b, which shows that the environmental gradients across the Strait are significant.

Table 6.2.2b Summary species present on either side of the Srait of Hormuz

Taxonomic group	No. species in the NW Gulf of Oman	No. species in the E Arabian Gulf	%	Reference
Phytoplankton	527	390	75	Al-Saadi & Hadi (1987); Dorgham & Muftah (1986)
Euphausiids	6	1	17	Weigmann (1970)
Ostracods	6	2	33	Leveau (1968)
Pteropods	13	3	23	Frontier (1963b)
Appendicularians	12	6	50	Fenaux (1964)

If the physico-chemical conditions in the STW were unsuitable for species with physiological adaptations to the conditions in the AGO and GOS then a lower stock may be expected. The abundance and biovolume of smaller zooplankton is lower in the STW, but larger mesozooplankton and macrozooplankton were intermediate in the STW (Table 6.2.2a). Possible mechanisms are that the small individuals avoided this water, their fitness, growth and reproduction was low, or their mortality was high in the unfavourable conditions. At the western extreme of the survey, the mesozooplankton were an order of magnitude more abundant in the AGO than they were just 10 metres above in the chlorophyll maximum in the STW (**Fig 5.2.1.i**). This distance is within the sensory and swimming capabilities of mesozooplankton (Bainbridge, 1953; Buskey, 1984) suggesting that some zooplankton were actively avoiding the STW. Cervetto *et al.* (1999) observe that the fitness and survivorship of the copepod *Acartia tonsa* in estuarine conditions is determined not only by the actual salinity, but also the rates of change in salinity it experiences. If similar processes are important for the zooplankton in the Strait, then the transition conditions in the STW may be particular unfavourable in comparison to the more stable end members.

If environmental tolerance is important, the observed distributions suggest that its effect was more adverse on small mesozooplankton than on larger individuals. Tester and Turner (1991) and Cervetto *et al.* (1999) show that nauplii and copepodite stages of *Acartia tonsa* were more sensitive to variations and extremes in salinity. A similar effect may explain why the larger zooplankton were intermediate in the STW.

Studies have shown that phytoplankton are influenced by changes in salinity, for example Lohrenz *et al.* (1999) observed the highest chlorophyll concentrations at intermediate salinities in the plume of the Mississippi. The standing stock of phytoplankton was highest in the STW, which suggests that the phytoplankton were not affected by the salinity gradient to the same degree. The data in Table 6.2.2b may support this explanation: the table shows that the number of phytoplankton species present in the eastern Arabian Gulf was 75% of that in the NW Gulf of Oman, which is a much larger proportion compared with the zooplankton groups (17-50%).

The species of plankton that were tolerant of the conditions in the STW might be expected to flourish because of lack of competition for resources. Because of their faster generation times phytoplankton would respond quicker than zooplankton, and in this way may become decoupled from mesozooplankton grazing. In addition, the species of phytoplankton present in the STW may be unsuited for mesozooplankton.

Information on the species present and their functional relationships with salinity are needed to understand if the phytoplankton and zooplankton are affected in different ways by the salinity change in the STW.

5) *Community interactions*: biological interactions caused by the mixing of the communities from the end members has resulted in a distinct community in the transition area. The transition zone between two communities is classified as an ecotone (Odum, 1971; Kolasa and Zalewski, 1995). In terms of biomass, ecotones are variable because they are transitions between more stable environments (Naiman, 1988), and both increases and decreases of biomass have been reported in ecotonal communities (Odum, 1971). In the STW the distinct communities from the AGO and GOS are mixed together, and this will cause species that do not usually interact to be brought together. This will result in unpredictable changes in the community structure because of the diverse interspecific interactions in natural systems. Changes will be forced by mechanisms such competition and predation. Many ecotones contain more diverse communities than the end members. The STW might be expected to contain more species than the AGO but not the GOS, because the plankton of the Arabian Gulf is a subset of euryhaline species that are present in the GOS. Although predominantly a term from terrestrial ecology, some frontal boundaries between water masses have been classified as ecotones (Brandt and Wadley, 1981; Meise and O'Reilly, 1996).

In the STW mechanisms of predation and competition may reduce and maintain the low standing stock of small mesozooplankton. Predation and competition can certainly

effect community structure, but because the observed distributions may result from the complex interactions between species this hypothesis is difficult to predict and to test. In the LHPR samples from the STW, the abundance of small mesozooplankton (copepods) showed an inverse relationship with that of the euphausiid *Pseudeuphausia latifrons* (≈15 mm). Both feed on phytoplankton and microzooplankton, and this may show competition (§6.2.1). In addition, Weigmann (1970) states that *P. latifrons* also feeds on small copepods suggesting that the presence of this species may lead to a reduction in copepod numbers by both predation and competition. The high density of *P. latifrons* in the LHPR samples from the STW suggests that this species may be an important "edge species", that is an organism that is characteristically abundant in an ecotone.

In conclusion: the formation of the STW had a large impact on the standing stock of phytoplankton and the biomass size spectra of mesozooplankton, giving rise to a different community structure in the STW. It is difficult to produce conclusive evidence for any mechanisms because it is not currently possible to measure the appropriate variables (e.g. primary productivity, grazing, environmental tolerances, species present) with the appropriate resolution, coverage and duration.

The main changes in the STW were associated with the phytoplankton and small mesozooplankton, while the larger zooplankton were intermediate in relation to the end members. These observations suggest that the larger zooplankton were affected by the overall gradients of the Strait, rather than mesoscale processes.

There is no evidence for bottom-up or top-down control of the small mesozooplankton, and the distribution of zooplankton is not consistent with advective convergence between the GOS and AGO. The environmental tolerance mechanism produces a good explanation for the low standing stock of mesozooplankton in STW, but relies on the larger mesozooplankton having different salinity tolerances. This suggests that in this area of large environmental gradients the zooplankton are not favoured in the variable conditions of mesoscale mixing. This may be because of the additional osmoregulatory energy expenditure and stress of the organisms. All of these mechanisms are rather simplistic, and in natural ecosystems, the interaction between communities in an ecotone is complex. However, the data collected are not sufficient to comment on this hypothesis. It is worth emphasising again that these mechanisms

are not expected to act independently in influencing the distribution of mesozooplankton at the mesoscale in the Strait.

6.2.3 Mechanisms affecting plankton at the front between the STW and AGO

The previous section demonstrated and discussed the differences between the STW and the end members. At the western extreme of the STW there is a sharp front with the AGO, characterised by a salinity change from 37.25 to 39.75 in 60-80 km horizontally. This front marked a clear boundary to the different planktic communities and therefore the effects of this mesoscale feature are considered separately in this section (**Fig 3.2.1.i**). Many studies have reported that fronts on a range of scales (0.001-100 kms) are often correlated with dramatic changes in the vertical and horizontal distribution of zooplankton, (e.g. Owen, 1981; Denmann and Powell, 1984; Olson *et al.*, 1994; Gallager *et al.*, 1996). In this respect, mesoscale fronts behave in a similar way to fronts at other scales. Mesoscale fronts can also be the sites of enhanced primary production (e.g. Videau *et al.*, 1994). The mechanism for this is the addition of nutrients to the euphotic zone as a result of ageostrophic vertical motion (Pollard and Regier, 1992; Strass, 1992). However, in the shallow Strait there is not a clear source for nutrients to be upwelled, and because no measurements of nutrients were made on this cruise this process cannot be confirmed.

It is important to consider that although fronts mark boundaries between different waters and communities, they are also the sites where these waters mix (Sournia, 1994). The small (0.4-1.6 mm ESD) and large (1.6-4.1 mm ESD) mesozooplankton showed different distributions across the front (**Fig 5.2.2.i**). Small species were generally conservative with salinity from one side of the front to the other indicating that they were predominantly passively mixed across the front. Larger species were not conservative, and were less abundant in intermediate conditions. This suggests that the larger species were actively avoiding unfavourable intermediate conditions, and were capable of altering their position relative to mixing. Vertical swimming in the steep vertical swimming gradients would allow zooplankton to remain in favoured salinity ranges. Alternatively the low concentration of zooplankton between 1.6-4.1 mm ESD in the front may have resulted from these conditions being unfavourable, and stocks declining because of reduced fitness. Haury *et al.* (1990) investigated the effect of wind driven mixing on the distribution of zooplankton off Monterey, California. Their study found that the small, non-migratory copepod *Oithona* was

passively redistributed by wind mixing, while the larger, migratory copepod *Metridia* maintained its preferred distribution. Although the frontal mixing is a different physical process to the wind driven mixing the results here are consistent with Haury *et al.*'s findings that zooplankton with different swimming capabilities do not have the same response to diffusive mixing.

In the region around the front the distributions of phytoplankton, mesozooplankton and macrozooplankton were inversely correlated (**Fig 5.2.1.i**). This may be evidence for a top down control of the community by macrozooplankton: where they were abundant their predation lowered the number of mesozooplankton, this in turn reduced herbivorous grazing which leads to a larger standing stock of phytoplankton. However, the correlations alone are not conclusive evidence for such processes because correlation does not prove cause. For example, the distributions may result from different environmental tolerances of the plankton.

6.2.4 The importance of the internal waves in determining plankton distributions

Internal waves were observed in the water column on the eastern side of the Strait. These sub-mesoscale physical features also effected the distribution of zooplankton in the Strait. The internal waves resulted in vertical displacement of isotherms by as much as 20-30 m. Spectral analysis, using the FFT, of the physical data showed peaks at wavelengths of 40, 17 and 9 km (§5.3.3), which were correlated with similar periodicities in phytoplankton and zooplankton distributions (**Fig 5.3.3.i**). SeaSoar is not an ideal vehicle to study the waves because it does not move fast enough to sample the waves synoptically. Internal waves of this magnitude typically have phase speeds of 1-2 m s^{-1} (e.g. New, 1988) which is significant compared with a SeaSoar speed of 4 m s^{-1}. If SeaSoar travelled orthogonally to the waves then the wavelengths may be incorrect by as much as 50%. This method of sampling is still robust for studying their correlation with plankton distributions, when sampled concurrently.

The analysis presented in §5.3.3 demonstrates that the distributions of small and large mesozooplankton were different in response to the internal waves. The phytoplankton and the small mesozooplankton (<1 mm ESD) showed spatial variability correlated with the internal waves, but the larger mesozooplankton (1-4 mm ESD) did not correlate. The general correlation of the spectra of the phytoplankton and small mesozooplankton indicates that these species were mainly

passively redistributed by the action of the waves. The larger zooplankton were not correlated with the periods of the waves, which indicates that their distribution was determined by either their behaviour or physical processes that were unresolved by the analysis.

The observation of the different size zooplankton being influenced in different ways by internal waves is a novel, although not unexpected finding. Haury *et al.* (1983) investigated the effect on the distribution of plankton caused by internal waves with wavelengths of 300 m in Massachusetts Bay. This study found that both phytoplankton and mesozooplankton appeared to be carried up and down passively with the waves. Their data reveal that different taxa showed different distributions in the waves, but their data were not sufficient to resolve an active response to the internal waves. A modelling study by Lennert-Cody and Franks (1999) shows that the maximum concentration of plankton will be above a trough of a wave, and therefore is out of phase (although at a correlating spatial scale) with the wave. The correlation of the patchiness of zooplankton with the phase of the waves has not been investigated in this study, but future work in this direction could be used to assess the model of Lennert-Cody and Franks (1999) and to clarify the physical processes that result in the observed distributions in the internal waves in the Strait.

6.3 Implications for the relationship between zooplankton and their physico-chemical environment at the mesoscale

The interrelationship between physical features and zooplankton in the Strait is influenced by the topography of the shallow sea bed and the large salinity gradients in this area and therefore there may be fundamental differences between the Strait and the typical open ocean. This section discusses the relevance of the findings of this study to the study of mesoscale processes in the open ocean. It is divided into three parts: the importance of different forcing mechanisms at the mesoscale, the importance and usefulness of mesozooplankton size, and the implications on upper ocean productivity and biogeochemistry.

6.3.1 The importance of different forcing mechanisms at the mesoscale

The boundaries of zooplankton distributions are often correlated with hydrographic boundaries in the oceans. It is only the recent advent of optical and acoustic sampling

technologies (§1.4) that has allowed the distribution of zooplankton to be described simultaneously and at the same resolution as physical variables, which is needed for the robust determination of the correlation between variables. However, the process measurements (e.g. primary production, species present, grazing, environmental tolerance) required to determine the causative mechanisms behind the correlations cannot be measured concurrently at present.

Direct physical forcing on zooplankton has been shown to be a dominant driving force on their distributions at a number of scales, including the mesoscale (e.g. Owen, 1981; Denmann and Powell, 1984; Franks, 1992). Direct physical forcing did not appear to be important for zooplankton in the STW, but appeared to dominate on the small (<1.5mm) mesozooplankton in mixing across the STW/AGO front and by redistributing plankton in the internal waves. The implications from this study are that direct forcing at the mesoscale (and sub-mesoscale) can dominate patchiness and overwrite the signals from other processes, but its importance depends not only on the type, strength and duration physical forcing, but also on the behaviour (swimming) of the zooplankton, which is correlated with changes in their size (§6.3.3).

Bottom up forcing of planktic communities by mesoscale features is an important processes because the allochthonous nutrients supplied by this mechanism increase the proportion of new versus regenerated production in the upper ocean, producing a shift to a higher *f* ratio (Strass, 1992; McGillicuddy and Robinson, 1997). This can not only increase secondary production, but also lead to a shift in the trophic pathway (Legendre *et al.*, 1999; §1.3). Bottom-up forcing did not appear to be particularly important at the mesoscale in this study because the area is not know to be nutrient limited and the seafloor was shallow with no clear nutricline in the water column (however, there were no measurements of nutrients made during this cruise). Bottom-up forcing is probably more important in the open ocean. Primary production has been shown to increase at fronts, indicating that phytoplankton enhancement can result from growth (Videau *et al.*, 1994; Fernández and Pingree, 1996). And in modelling studies chlorophyll distributions have been shown to correlate more closely with primary production than passive tracers (e.g. Strutton *et al.*, 1997).

Studies have found that mesozooplankton biomass is not consistently correlated with phytoplankton at the mesoscale. Boucher (1984) measured high densities of phytoplankton and copepods (especially late copepodites, which were probably the most active herbivores) at the Ligurian front in the Mediterranean. In addition,

Thibault *et al.* (1994) found greater copepod abundance and herbivorous feeding associated with increased production of diatoms associated with the Almeria-Oran frontal jet in the Mediterranean. However, at the Ushant front in the channel, a large number have studies have found no consistent correlation between phytoplankton and zooplankton (e.g. Holligan *et al.*, 1984; Le Fèvre, 1986). In this study zooplankton were decoupled from primary production in the STW relative the other water types.

Top-down mechanisms have not been widely investigated at the mesoscale in natural ecosystems, because of the difficulties associated with studying the processes at the appropriate scales (Verity and Smetacek, 1996). However, mesocosm studies and field observations in the last two decades have begun to reveal evidence for the importance of top-down forcing in marine plankton communities (e.g. Behrends and Schneider, 1995; Pitta *et al.*, 1998). On either side of the AGO/STW front the distribution of adjacent trophic levels were inversely correlated, which may suggest that top-down control was structuring the ecosystem in this area. Atkinson *et al.* (1998) determined inverse correlations between krill and copepods at the mesoscale (and other scales), and concluded that the presence of krill was detrimental to copepods. Possible mechanisms were competition for resources, where the presence of krill affected the fitness of copepod populations, and predation, where the krill were reducing copepod stocks by grazing. Top-down mechanisms require more attention in mesoscale studies, but correlative analysis should be backed up with process measurements of feeding rates and gut content.

Physico-chemical environmental tolerance is important in determining the distribution of many zooplankton species in the Strait of Hormuz. The Strait contains large environmental gradients in comparison to other regions, and this mechanism is not expected to be as important in all environments. Gulf Stream Rings, that pinch off shelf water and advect it into the Sargasso Sea, subject the "captured" community to unfavourable conditions, although these are both physico-chemical and trophic (Wiebe *et al.*, 1976a). The euphausiid *Nematoscelis megalops* is characteristic of the slope waters and its fitness declines with time in the ring, showing lower total body lipids, carbon and nitrogen and also a lower respiration rate (Boyd *et al.*, 1978). As a ring warms up *N. megalops* moves deeper into the water column, remaining in its optimum temperature range. But at these depths Wiebe and Boyd (1976) report that there is insufficient food for growth and reproduction, and the euphausiids starve. Temperature preference may also determine fish distributions at fronts (Brandt and Wadley, 1981).

Phytoplankton production may also be reduced by the physico-chemical stress at fronts: Brunet *et al.* (1992) determined that although algae were accumulated at a front in English Channel, production was low at the front, and pigment analysis indicated that the phytoplankton were stressed.

The interaction of communities brought together by mesoscale forcing is expected to have significant, but variable influences on the zooplankton. This mechanism requires extensive datasets detailing species present and their interactions, and has rarely been investigated at the mesoscale. In Gulf Stream Rings herbivorous zooplankton from the Sargasso sea out compete and replace shelf species within the ring, but carnivores species take much longer (Wiebe *et al.*, 1976a; Ortner *et al.*, 1979). Frontal zones can also develop distinct ecotonal communities (Backus, 1986) and certain species may be predominantly restricted to the intermediate conditions. For example, the euphausiid *Nematoscelis megalops* exists in the Kuroshio current across the Pacific and down the Californian current (Brandt and Wadely, 1981).

The work here has highlighted a number of mechanisms that could be important in determining the distribution of zooplankton at the mesoscale. This has been summarised by the theory proposed by Haury *et al.* (1978) and the multiple driving force hypothesis of Pinel-Alloul (1995). In any instance a number of mechanisms may interact, or a single mechanism may dominate (such as direct physical advection).

6.3.2 Effect of zooplankton size on their relationship with the environment

It is well established that many aspects of zooplankton biology are correlated with their body size, for example population doubling times (growth), mobility, trophic status and food size preferences (e.g. Eberhardt, 1969; Sheldon *et al.*, 1972; Fenchel, 1974; Banse, 1976; Hirst and Sheader, 1997). In this study, it has been shown that the populations of different sized zooplankton respond in different ways to physical and biological processes at the mesoscale and sub-mesoscale. Such a finding is consistent with the expectations from the work referenced above, but it is only the advent of modern optical and acoustic zooplankton sampling technologies that have allowed such observations to be made. In this study, the small (0.4-1 mm ESD) zooplankton were in general passively redistributed by the internal waves and mixing across the front between the AGO and STW. The larger species (1-4.1 mm ESD) were not as precisely correlated with the physics suggesting that their distributions were

determined to a greater extent by their behaviour. In the STW the abundance of mesozooplankton smaller than 1.8 mm ESD was reduced in comparison to the other water types, while the abundance of the larger species 1.8-4.5 mm ESD was intermediate. Several mechanisms have been proposed to account for these differences (§6.2.2.2), but whichever mechanisms were important, it is clear that the different sized zooplankton were effected differently by these processes at the mesoscale.

This study has presented evidence that indicates that small mesozooplankton (0.3-1 mm ESD) were important herbivorous grazers in this area at the time of the survey. This size range of mesozooplankton is not reliably retained by commonly used zooplankton nets with mesh sizes in the range 0.20-0.33 mm (Barnes and Tranter, 1965). As a result their role as grazers has been overlooked in some studies. During the last decade studies (particularly those in the Joint Global Ocean Flux Study, JGOFS) have quantified the herbivory of different sized mesozooplankton in the ocean. Some of these studies found that small species (<1 mm) can be the dominant mesozooplankton herbivores (e.g. Morales *et al.*, 1991; Head *et al.*, 1999). In addition, these small mesozooplankton can feed omnivorously, possibly on nauplii and copepodite stages of larger mesozooplankton (e.g. Lampitt and Gamble, 1982) and in this way affect the populations of the larger species.

The diel migration behaviour of the small mesozooplankton (0.3-1 mm ESD) also differed from larger species in this study. No migration could be detected in the smallest species but the day-night differences in the larger mesozooplankton (1.0-4.0 mm ESD) showed evidence that a part of their biovolume was migrating (**Figs 4.1.4.iii** and **iv**). The migration of macrozooplankton was more pronounced (shown by the EK500), and as expected the extent of DVM was found to increase with body size. DVM was also different in the open ocean and the shelf environments. In the Gulf of Oman (ocean depths) the majority of the acoustic scatterers (at 38 kHz) migrated from 250 m during the day to the upper 50 m at night, but in the Strait (shelf depths) the migrations of scatterers at the same frequency were greatly reduced (**Fig 4.1.4.i**). Although this change in DVM correlated with the depth of the seafloor, it may have been caused by either a change in the behaviour of the migrators or because different species were present on the shelf and in the open ocean.

The results presented in this thesis show that mesozooplankton cannot be regarded as a homogeneous group in their relationship with the mesoscale environment. In this

study the zooplankton community has been divided by size, and this has proved a useful method for simplifying the diverse planktic community because many biological and behaviour processes are correlated with size. For example, small and large mesozooplankton populations showed different distributions relative to mesoscale and sub mesoscale mixing, diel vertical migration and in their importance as herbivores. This size based classification was not without problems, for example, in terms of size distributions it was difficult to distinguish between the mesozooplankton communities in the GOS and AGO. Taxonomic information would be useful for differentiating between these water types. Also the relationship between size and biological processes has been shown to change between taxonomic groups (e.g. Paffenhöfer, 1993; Hensen *et al.*, 1994). An integration between a sized based and a taxonomic based approach is advised for future studies of the interaction of zooplankton with the mesoscale physico-chemical environment. This study has also highlighted the need for more research into small mesozooplankton, which have often been overlooked by sampling methods in many studies.

6.3.3 Implications for upper ocean productivity and biogeochemistry

The nutrients supplied by mesoscale processes (e.g. Falkowski *et al.*, 1991; Pollard and Regier, 1992) can have a dramatic affect on the trophic pathway of the ecosystem (Cushing, 1989). Where new nutrients are supplied to the euphotic zone larger autotrophs, such as diatoms, are favoured. These in turn are more suitable food for mesozooplankton rather than microzooplankton (e.g. Legendre *et al.*, 1999; §1.3). This process has consequences for the biological pump because mesozooplankton produce larger, more rapidly sinking faecal pellets, which results in greater export.

Mesozooplankton grazing can be decoupled from primary production when the normal equilibrium is perturbed by physical forcing at the mesoscale. In the STW mesoscale processes acted to decouple the small mesozooplankton from the phytoplankton. Decoupling of herbivory from primary production may lead to the direct sedimentation of phytoplankton, which results in a large export flux via the biological pump (Legendre and Lefévre, 1989; Karl, 1999). Direct sedimentation of algae is also important because it transports suitable food to the deep sea benthos (Billett *et al.*, 1983). Possible mechanisms for this decoupling include different responses to advection, bottom-up, top-down, environmental tolerance and community

interactions in an ecotone. Mesoscale processes can also cause an advective subduction of biomass out of the euphotic zone, which may make a significant contribution to the total flux (Spall and Richards, 2000).

DVM can affect the biological pump if the migrants traverse the pycnocline and food consumed above is released below it (Longhurst and Harrison, 1989). Some estimates have shown that interzonal migrants contribute considerably to the total export flux (e.g. Morales, 1999). In this study the different sized zooplankton were shown to have different migration behaviours, with migration increasing with animal size. In the STW the mesozooplankton community shifted from one dominated by <1 mm species to one dominated by >1 mm species. The difference in the DVM behaviour between these zooplankton of different sizes, also demonstrated in this study, could have a significant impact on the export via migration.

The smaller scale processes associated with the internal waves are not expected to have such a large impact on the ecosystem. The redistribution of zooplankton is a temporary effect and is expected to mainly dissipate when the forcing is relaxed, but the raising of the nutricline and the changes in the light environment during undulations can promote primary productivity. Sub-mesoscale physical processes can also impact on zooplankton distributions by direct and indirect mechanisms.

Summary

The work presented in this thesis has highlighted many avenues for future work. In general terms similar studies in the future would be enhanced by: gaining a better understanding (and calibration) of the data produced by optical and acoustic zooplankton sampling technologies, and by measuring more variables concurrently and at the same resolution as the physical environment.

The observations made in this study show that mesoscale physico-chemical processes are correlated with changes in distribution of zooplankton. However zooplankton do not act as passive tracers and their distributions in the Strait are also influenced by biological processes such as behaviour, growth and mortality. This interaction of abiotic and biotic forcing on zooplankton at the mesoscale is consistent with the theory proposed by Haury *et al.* (1978). The analysis in this study has also shown that different sized zooplankton show distinct distributions in response to physical forcing, indicating that influence of biological processes on their distributions also varies with organism size.

REFERENCES

AHMAD, F., SULTAN, S.A.R., (1991) Annual mean surface heat fluxes in the Arabian Gulf and the net heat transport through the Strait of Hormuz. Atmosphere -Ocean **29**: 54-61.

AINLEY, D.G., JACOBS, S.S., (1981) Seabirds, pack ice and the Antarctic Slope Front in the Ross Sea. Deep Sea Research. **28**: 1173-1185.

AL-HAJRI, K.R., (1990) The circulation of the Arabian (Persian) Gulf: A model study of its dynamics. The Catholic University of America, Washington DC. PhD dissertation.

AL-HAJRI, K.R., CHAO, S.Y., KAO, T.W., (1997) Circulation of the Arabian Gulf: A three dimensional study. Arabian Journal for Science and Engineering. **22** (1B): 105-128.

AL-KAISI, K.A., (1976) On the phytoplankton of the Arabian Gulf, p 125 *In*: Book of Abstracts of papers presented at Joint Oceanographic Assembly, Edinburgh, UK. 13-14 September 1976. FAO, Rome.

ALDERSON, S.G., (1997) see www.soc.soton.ac.uk/JRD/PEXEC/pexec.html

ALLEN, J.T., (1997) Scheherezade – an interdisciplinary study of the Gulf of Oman, Strait of Hormuz and the southern Arabian Gulf. Charles Darwin Cruise 104. No 3. Surface temperature from the shipboard thermosalinograph. Leg 1, 12 Feb – 19 March. Southampton Oceanography Centre. Research and Consultancy Report No. **12**.

ALLEN, J.T., GRIFFITHS, G., (1997) Scheherezade – an interdisciplinary study of the Gulf of Oman, Strait of Hormuz and the southern Arabian Gulf. Charles Darwin Cruise 104. No 4. Current vectors from the vessel mounted acoustic Doppler current meter. Leg 1, 12 Feb – 19 March. Southampton Oceanography Centre. Research and Consultancy Report No. **13**.

ALLEN, J.T., SMEED, D.A., (1996) Potential vorticity and vertical velocity at the Iceland – Færœs Front. Journal of Physical Oceanography **26**: 2611-2634.

ALLEN, J.T., SMEED, D.A., TINTORE, J., RUIZ,, S., (submitted, 2000) Mesoscale subduction at the Almeria-Oran front. Part 1: ageostrophic flow.

AL-ROBAAE, K., (1969) The whales and dolphins of the Arabian Gulf (Cetacea) Bulletin of the College of Science, University of Basrah, **12**: 61-73.

AL-SAADI, H.A., HADI, R.A., (1987) Ecological and taxonomical studies on phytoplankton in the Arabian Gulf. Arabic section. Journal of Biological Scientific Research. **18**: 7-31.

AL-SAADI, H.A., HADI, R.A., SCHIEWER, U., AL-MOUSAWI, A.H (1989) On the influence of the sewage drainage from Basrah City on the phytoplankton and related nutrients in the Shatt Al-Arab estuary, Iraq Archives of Hydrobiology. **114**: 443-452.

AL-YAMANI F.Y., AL-RIFAIE, K., ISMAIL, W., (1993) Post-spill zooplankton distribution in the NW Gulf. Marine Pollution Bulletin **27**:239-243.

ANGEL, M.V., (1986) Vertical migrations in the oceanic realm: possible causes and probable effects. pp. 45-70 *In*: Migration mechanisms and adaptive significance, Rankin, M.A., (Ed.) Contributions in Marine Science, Supplement to volume **27**.

ARON, W., (1958) The use of a large portable pump for plankton sampling, with note on plankton patchiness. Journal of Marine Research. **16**: 158-173.

ATKINSON, A., WARD, P., HILL, A., BRIERLEY, A.S., CRIPPS, G.C., (1999) Krill-copepod interactions at South Georgia, Antarctica, II. *Euphausia superba* as a major control on copepod abundance. Marine Ecology Progress Series **176**: 63-79.

AZAM, F., FENCHEL, T., FIELD, J.G., GRAY, J.S., MEYER REIL, L.A., THINGSTAD, F., (1983) The ecological role of water column microbes in the sea. Marine Ecology Progress Series, **10**: 257-263.

BACKUS, R.H., (1986) Biogeographic boundaries in the ocean. *In*: Pelagic Biogeography UNESCO Techniques in Marine Science **49**: 9-13.

BAINBRIDGE, R., (1953) Studies on the interrelationships of zooplankton and phytoplankton. Journal of the Marine Biological Association of the UK. **32**: 385-447.

BAINBRIDGE, R., (1957) The size, shape and density of marine phytoplankton distributions. Biological Review **32**: 91-115.

BAINES, P.G., (1982) On internal tide generation models. Deep-Sea Research. **29**(A): 307-338.

BAKER, A.DE C., BODEN, B.P., BRINTON, E., (1990) A practical guide to the euphausiids of the world. London: Natural History Museum Publications. 96pp.

BÅMSTEDT, U., (1986) Chemical composition and energy content. p. 1 – 58. In: Corner, E.D.S., and S.C.M., O'Hara (eds.)The biological chemistry of marine copepods. Oxford Univ. Press.

BANSE, K., (1976) Rates of growth, respiration and photosynthesis of unicellular algae as related to cell size. Journal of Phycology, **12**: 135-140.

BANSE, K., (1977) Determining the carbon-to-chlorophyll ratio of natural phytoplankton. Marine Biology. **41**: 199-212.

BANSE, K., (1982) Cell volume, maximal growth rates of unicellular algae and ciliates, and the role of ciliates in the marine pelagial. Limnology and. Oceanography **27**: 1059-1071.

BANSE, K., (1984) Overview of the hydrography and associated biological phenomena in the Arabian Sea, off Pakistan. *In*: Marine Geology and Oceanography of the Arabian Sea and Coastal Pakistan, Haq, B.U., Milliman, J.D., (Eds.) Van Nostrand Reinhold, New York, pp. 271-303.

BANSE, K., (1997) The irregular flow of Persian (Arabian) Gulf water to the Arabian Sea. Journal of Marine Research, **55**: 1049-1067.

BARLOW, R.G., MANTOURA, R.F.C., CUMMINGS, D.G., (1999) Monsoonal influence on the distribution of phytoplankton pigments in the Arabian Sea. Deep–Sea Research II. **46**: 677-699.

BARLOW, R.G., MANTOURA, R.F.C., GOUGH, M.A., FILEMAN, T.W., (1993) Phaeopigment distribution during the 1990 spring bloom in the north eastern Atlantic. Deep-Sea Research, **40**: 2229-2242.

BARNES, H., TRANTER, D.J., (1965) A statistical examination of the catches, numbers and biomass taken by three commonly used plankton nets. Australian Journal of Marine and Freshwater Research. **16**: 293-306.

BARRY, J.P., DAYTON, P.K., (1991) Physical heterogeneity and the organisation of marine communities. *In*: Ecological heterogeneity. J. Kolasa, S.T.A. Pickett, (Eds.) Springer-Verlag, New York. **14**: 270-320.

BARY, B.M., (1966) Back scattering at 12 kc/s in relation to biomass and numbers of zooplanktonic organisms in Saanich Inlet, British Colombia. Deep – Sea Research, **13**: 655-666.

BASSON, P.W., BURCHARD, J.E., HARDY, PRICE, A.R.G., (1977) Biotopes of the western Arabian Gulf: Marine Life and Environments of Saudi Arabia, Aramco, Dhahran, Saudi Arabia.

BEAULIEU, S.E., MULLIN, M.M., TANG, V.T., PYNE, S.M., KING, A.L., TWINNING, B.S., (1999) Using an optical plankton counter to determine the size distributions of preserved zooplankton samples. Journal of Plankton Research, **21**: 1939-1956.

BEERS, J.R., (1976) Determination of zooplankton biomass. In: Steedman, H.F., (ed.) Zooplankton fixation and preservation. Monographs on Oceanographic Methodology 4. The UNESCO Press, Paris, pp. 35-84.

BEERS, J.R., STEWART, G.L., (1970) The ecology of the plankton of LaJolla, California in the period April through September, 1967. Bulletin of the Scripps Institution of Oceanography. **17**: 76-87

BEERS, J.R., STEWART, G.L., (1971) Micro-zooplankters in the upper waters of the eastern tropical Pacific. Deep-Sea Research. **18**: 861-883.

BEHRENDS, G., SCHNEIDER, G., (1995) Impact of *Aurelia aurita* medusae (Cnidaria, Scyphozoa) on the standing stock and community composition of mesozooplankton in the Kiel Bight (western Baltic Sea). Marine Ecology Progress Series **127**: 39-45.

BENFIELD, M.C., DAVIS, C.S., GALLAGER, S.M., (2000) Estimating the in-situ orientation of *Calanus finmarchicus* on Georges Bank using the Video Plankton Recorder. Plankton Biology and Ecology **47**: 69-72.

BERNARD, M., MÖLLER, F., NASSOGNE, A., ZETTERA, A., (1973) Influence of pore size of plankton nets and towing speed on the sampling performance of two high-speed samplers (Delfino I and II) and its consequences for the assessment of plankton populations. Marine Biology. **20**: 109-136.

BERNSTEIN, O., SHAPIRO, M., (1994) Direct determination of the orientation distribution function of cylindrical particles immersed in laminar and turbulent shear flows. Journal of Aerosol Science. **25**: 113-136.

BILLETT, D.S.M., LAMPITT, R.S., RICE, A.L. MANTOURA, R.F.C., (1983) Seasonal sedimentation of phytoplankton to the deep-sea benthos. Nature, **302**: 520-522.

BISHOP, J.K.B., SMITH, R.C., BAKER, K.S., (1992) Springtime distributions and variability of biogenic particulate matter in Gulf Stream warm-core ring 82B and surrounding N.W. Atlantic waters. Deep-Sea Research. **39**: S295-S325.

BODHOLT, H., NES, H., SOLLI, H., (1989) A new echo-sounder system. Proc. IOA **11**: 123-130.

BOGOROV, B.G., (1959) On the standardisation of marine plankton investigations. Int. Rev. Ges. Hydrobiol. Hydrogr. **44**: 621-642.

BOHM, E., MORRISON, J.M., MANGNANI, V., KIM, H.S., FLAGG, C.N., (1999) The Ras al Hadd Jet: Remotely sensed and acoustic Doppler current profiler observations in 1994-1995. Deep – Sea Research II. **46** (8-9): 1531-1549.

BOLLENS, S.M., FROST, B.W., CORDELL, J.R., (1994) Chemical, mechanical and visual cues in the vertical migration behaviour of marine planktonic copepod, *Acartia hudsonica*. Journal of Plankton Research, **16**: 555-564.

BOUCHER, J., (1984) Localisation of zooplankton populations in the Ligurian marine front: role of ontogenetic migration. Deep-Sea Research. **31**: 469-484.

BOUR, W., FRONTIER, S., (1974) Zooplankton de la région de Nosy Bé. IX. Répartition spatio-temporelle des chaetognathes dans la provice néritique. Cahiers ORSTOM, Océanographie, **12**: 207-219.

BOYD, C.M., JOHNSON, G.W., (1969) Studying zooplankton populations with an electronic zooplankton counting device and the LINC-8 computer. Transactions of applications of sea going computers. 83-90.

BOYD, S.H., WIEBE, P.H., COX, J.H., (1978) Limits of *Nematoscelis megalops* in NW Atlantic in relation to the Gulf Stream cold core rings. II Physiological and biochemical effects of expatriation. Journal of Marine Research **36**: 143-159.

BRANDT, S.B., WADELY, V.A., (1981) Thermal fronts as ecotones and zoogeographic barriers in marine and freshwater systems. Proceeding of Ecological Society of Australia **11**: 13-26.

BRETTSCHNEIDER, G., GRASSHOFF, K., KOSKE, P.H., VON TREPKA, L., (1970) Physikalische und chemiche Daten nach Beobachtungen des Forschungsschiffes "Meteor" im Persischen Golf 1965. '*Meteor*' Forschungsergebnisse, Series **A**, (8) 43-90.

BREWER, P.G., DYRSSEN, D., (1985) Chemical Oceanography of the Persian Gulf. Progress in Oceanography. **14**: 41-55.

BREWER, P.G., FLEER, A.P., KADAR, S., SHAFER, D.K., SMITH, C.L., (1978) Chemical Oceanography data from the Persian Gulf and the Gulf of Oman. Woods Hole Oceanographic Institution Technical Report No. WHOI 81-37, 105pp.

BRIERLEY, A.S., WARD, P., WATKINS, J.L., GOSS, C., (1998) Acoustic discrimination of Southern Ocean zooplankton. Deep-Sea Research II **45**: 1155-1173.

BRIGHAM, E.O., (1974) The Fast Fourier Transform. Englewood Cliffs. Prentice Hall.

BRINTON, E., (1975) Euphausiids of south east Asian Waters. Naga Report **4**: 1-287.

BRUNET, C., BRYLINSKI, J.M., FRONTIER, S., (1992) Productivity, photosynthetic pigments and hydrology in the coastal front of the Eastern English Channel. Journal of Plankton Research. **14**: 1541-1552.

BUCK, K.R., CHAVEZ, F.P., CAMBELL, L., (1996) Basin-wide distributions of living carbon components and the inverted trophic pyramid of the central gyre of the North Atlantic Ocean, summer 1993. Aquatic Microbial Ecology **10**: 283-298.

BURKILL, P.H., (1999) ARABESQUE: an overview. Deep–Sea Research II. **46**: 529-547.

BUSKEY, E.J., (1984) Swimming pattern as an indicator of the roles of copepod sensory systems in the recognition of food. Marine Biology. **79**: 165-175.

CARPENTER, S.R., BERQUIST, A.M., (1985) Experimental tests of grazing indicators based on chlorophyll *a* degradation products. Archiv fur Hydrobiologie, **102**: 303-307.

CASSIE, R.M., (1959) Micro-distribution of plankton. N. Z. J. Sci. **2**: 398-409.

CASSIE, R.M., (1963) Microdistribution of plankton. Oceanography and Marine Biology Annual Review. **1**: 223-252.

CERVETTO, G., GAUDY, R., PAGANO, M., (1999) Influence of salinity on the distribution of *Acartia tonsa* (Copepoda, Calanoida). Journal of Experimental Marine Biology and Ecology. **239**: 33-45.

CHAN, A.T., (1980) Comparative physiological study of marine diatoms and dinoflagellates in relation to irradiance and cell size. II. Relationship between photosynthesis, growth and carbon/chlorophyll *a* ratio. Phycology **16**: 428-432

CHECKLEY, D.C., ORTNER, P.B., SETTLE, L.R., CUMMINGS, S.R., (1997) A continuous underway fish egg sampler. Fisheries Oceanography. **6**: 58-73.

CHRISTAKI, U., VANWAMBEKE, F., (1995) Simulated phytoplankton bloom input in top-down manipulated microcosms – comparative effect of zooflagellates, ciliates and copepods. Aquatic Microbial Ecology. **9**: 137-147.

CHU, D., FOOTE, K.G., STANTON, T.K., (1993) Further analysis of target strength measurements of Antarctic krill at 38 and 120kHz: comparison with deformed cylinder model and inference of orientation distribution. Journal of the Acoustic Society of America. **93**: 2985-2988.

CLARKE, G.L., BUMPUS, D.F., (1950) The plankton sampler – an instrument for quantitative plankton investigations. Special Publications of the American Society of Limnology and Oceanography **5**: 1-8.

CLARKE, M.R., (1969) A new midwater trawl for sampling discrete depth horizons. Journal of the Marine Biological Association of the U.K. **49**: 945-960.

CLAY, C.S., MEDWIN, H., (1977) Acoustic oceanography: principles and applications. Wiley-Interscience, New York. 554pp.

CLUTTER, R.I., ANRAKU, M., (1968) Avoidance of samplers. *In*: D.J. Tranter and J.H. Fraser (eds.) Zooplankton sampling. Monographs on Oceanographic Methodology 2. UNESCO, Paris, pp57-76.

COAD, B.W., (1993) Fishes of the Persian Gulf and the Gulf of Oman: Checklist and bibliography.

CONVERSI, A., HAMEED, S., (1998) Common signals between physical and atmospheric variables and zooplankton biomass in the Subarctic Pacific. ICES Journal of Marine Sciences. **55**: 739-747.

COOKE, R.A., TREHUNE, L.B.D., FORD, J.S., BELL,W.H., (1970) An opto-electronic plankton sizer. Fisheries Research Board Canada Technical Report. No. **172**: 40pp.

CRISP, N.A., ALLEN, J.T., GRIFFITHS, G., MUSTARD, A.T., ROE, H.S.J., SMEED, D.A., (1998) Scheherezade – an interdisciplinary study of the Gulf of Oman, Strait of Hormuz and the southern Arabian Gulf. Charles Darwin Cruise 104. No 12. Calibrated multifrequency backscatter and concurrent hydrography. Leg 1, 12 Feb – 19 March. Southampton Oceanography Centre. Research and Consultancy Report No. **31**.

CULBERSON, C.H., (1991) WOCE Operations Manual (WHP Operations and Methods). WHPO 91/1 Woods Hole. 15pp.

CULBERSON, C.H., HUANG, S., (1987) Automated amperometric oxygen titration. Deep–Sea Research. **34**: 875-880.

CULLEN, J.J., RENGER, E.H., (1979) Continuous measurement of DCMU-induced fluorescence response of natural phytoplankton populations. Marine Biology **53**: 13 – 20.

CURRIE, R.I., (1963) The Indian Ocean Standard Net. Deep–Sea Research. **10**: 27-32.

CURRIE, R.I., (1992) Circulation and upwelling off the coast of South-East Arabia. Oceanologica Acta, **15**: 43-60.

CURRIE, W.J.S., CLAEREBOUDT, M.R., ROFF, J.C., (1998) Gaps and patches in the ocean: a one-dimensional analysis of planktonic distributions. Marine Ecology Progress Series, **171**: 15-21.

CUSHING, D.H., (1959) The seasonal variation in oceanic production as a problem in population dynamics. Journal du Conseil International pour L' Exploration de la Mer. **24**: 455-464.

CUSHING, D.H., (1989) A difference in structure between ecosystems in strongly stratified waters and in those that are only weakly stratified. Journal of Plankton Research, **11**: 1-13.

DAGG, M.J., FROST, B.W., NEWTON, J.A., (1997) Vertical migration and feeding behaviour of *Calanus pacificus* females during a phytoplankton bloom in Dabob Bay, U.S. Limnology and Oceanography **42**: 974-980

DALEY, R.J., (1973) Experimental characterisation of lacustrine chlorophyll diagenesis: II. Bacterial, viral and herbivore grazing effects. Archiv für Hydrobiologie, **72**: 409-439.

DAM, H.G., PETERSON, W.T., (1988) The effect of temperature on the gut clearance rate constant of planktonic copepods. Journal of Experimental Marine Biology and Ecology, **123**, 1-14.

DAM, H.G., MILLER, C.A., JONASDOTTIR, S.H., (1993) The trophic role of mesozooplankton at 47°N, 20°W during the North Atlantic Bloom Experiment. Deep-Sea Research, **40**: 197-212.

DAVIS, C.S., FLIERL, G.R., WIEBE, P.H., FRANKS, P.J.S., (1991) Micro-patches, turbulence and recruitment in plankton. Journal of Marine Research **49**: 109-151.

DAVIS, C.S., GALLAGER, S.M., BURMAN, M.S., HAURY, L.R., STRICKLER, J.R., (1992a) The Video Plankton Recorder (VPR): design and initial results. Archiv für Hydrobiologie, Beihefte, Ergebnisse der Limnologie **36**: 67-81.

DAVIS, C.S., GALLAGER, S.M., SOLOW, A., (1992b) Microaggregations of oceanic plankton observed by towed video microscopy. Science **257**: 230-232.

DE SYLVA, D.P., (1979) A bibliography of oceanography of the Arabian Gulf. 1959-1978. Miami: University of Miami, 33pp.

DENMAN, K.L., (1976) Covariability of chlorophyll and temperature in the sea. Deep–Sea Research, **23**: 539-550.

DENMAN, K.L., POWELL, T.M., (1984) Effects of physical processes on planktonic ecosystems in the coastal ocean. Oceanography and Marine Biology Annual Review **22**: 125-168.

DICKEY, T., (1991) The emergence of concurrent physical and bio-optical measurements in the upper ocean. Revs. Geophys. **29**: 383-413.

EBERHARDT, L.L., (1969) Similarity, allometry and food chains. Journal of Theoretical Biology, **24**: 43-55.

EDWARDS, E.S., BURKILL, P.H., STELFOX, C.E., (1999) Zooplankton herbivory in the Arabian Sea during and after the SW monsoon, 1994. Deep-Sea Research II, **46**: 843-863.

EID, F.M., ELGINDY, A.A., (1998) The seasonal changes of the circulation pattern in the Arabian Gulf deduced from the field of mass. Arab Gulf Journal of Scientific Research, **16**: 45-63.

EL GINDY, A.H.H., DORGHAM, M.M., (1992) Interrelations of phytoplankton, chlorophyll and physiochemical factors in Arabian Gulf and Gulf of Oman during Summer. Indian Journal of Marine Science, **21**: 257-261.

EMERY, K.O., (1956) Sediments and water of the Persian Gulf. Bulletin of American Petrology and Geology. **40**: 2354-2383.

EPPLEY, R.W., HARRISON, W.G., CHISHOLM, S.W., STEWART, E., (1977). Particulate organic matter in surface waters off Southern California and its relationship to phytoplankton. Journal of Plankton Research. **35**: 671-696.

EPPLEY, R.W., PETERSON, B.J., (1979) Particulate organic matter flux and planktonic new production in the deep ocean. Nature. **282**: 677-680.

FAGER, E.W., MCGOWAN, J.A., (1963) Zooplankton species groupings in the North Pacific. Science, **140**: 453-460.

FALKOWSKI, P.G., (1984) Physiological responses of phytoplankton to natural light regimes. Journal of Plankton Research. **6**: 295-308.

FALKOWSKI, P.G., ZIEMANN, D., KOLBER, Z., BIENFANG, P.K., (1991) Role of eddy pumping in enhancing primary production in the ocean. Nature **352**: 55-57.

FAO (1966) A bibliography of the fisheries of the near east with special reference to the major water bodies. Food and Agriculture Organisation of the United Nations report **FID: FRN/66/INF 10**, 25 pp.

FAO (1976) Bibliography of living marine resources. Food and Agriculture Organisation of the United Nations report **FI: DP/REM/71/278/2**, 47 pp

FARMER, A.S.D., DOCKSEY, J.E., (1983) A bibliography of the marine and maritime environment of the Arabian Gulf and Gulf of Oman. Kuwait Bulletin of Marine Science 4: 1-121.

FASHAM, M.J.R., ANGEL, M.V., ROE, H.S.J., (1974) An investigation of the spatial pattern of zooplankton using the Longhurst-Hardy Plankton Recorder. Journal of Experimental Marine Biology and Ecology. **16**: 93-112.

FENAUX, R., (1964) Les Appendiculaires de la troisième campagne du Ct *Robert Giraud* en mer d'Arabie. Bulletin d'Insititute Océanographie Monaco. **62**: 1-14.

FENAUX, R., (1973) Appendicularia from the Indian Ocean, the Red Sea and the Persian Gulf. *In*: The Biology of the Indian Ocean. B., Zeitzschel (Ed.). Chapman and Hall Limited, London. Springer-Verlag Berlin-Heidelberg-New York. 544pp.

FENCHEL, T., (1974) Intrinsic rate of natural increase: the relationship with body size. Oecologia **14**: 317-326.

FERNÁNDEZ, E., PINGREE, R.D., (1996) Coupling between physical and biological fields in the North Atlantic subtropical front southeast of the Azores. Deep-Sea Research I, **43**(9): 1369-1393.

FIELDING, S., CRISP, N., ALLEN, J.T., HARTMAN, M.C., RABE, B., ROE, H.S.J., (submitted, 2000) Mesoscale subduction at the Almeria-Oran front. Part 2. Biophysical Interactions.

FLAGG, C.N., SMITH, S.L., (1989) On the use of the acoustic Doppler current profiler to measure zooplankton abundance. Deep–Sea Research. **36**:455-474.

FLEMER, D.A., (1969) Continuous measurement of in vivo chlorophyll of a dinoflagellate bloom in Chesapeake Bay. Chesapeake Science, **10**: 99-103

FLEMINGER, A., CLUTTER, R.I., (1965) Avoidance of towed nets by zooplankton. Limnology and Oceanography. **10**: 96-104.

FOLT, C., SCHULZE, P.C., BAUMGARTNER, K., (1993) Characterising a zooplankton neighbourhood: small-scale patterns of association and abundance. Freshwater Biology, **30**: 289-300.

FOLT, C.L., BURNS, C.W., (1999) Biological drivers of zooplankton patchiness. Trends in Ecology and Evolution, **14(8)**: 300-305.

FOOTE, K.G., STANTON, T.K., (2000) Acoustical methods. pp 223-258. *In*: Harris, R., Wiebe, P.H., Lenz, J., Skjoldal, H.R., Huntley, M.A., (Eds.) ICES zooplankton methodology manual. Academic Press, London. pp 684.

FOWLER, J., COHEN, L., (1990) Practical statistics for field biology. John Wiley and Sons Ltd. Chichester, England. pp 227.

FRANKS, P.J.S. (1992) Sink or swim: accumulation of biomass at fronts. Marine Ecology Progress Series **82**: 1-12.

FRASER, J.H., (1968) Standardisation of zooplankton sampling methods at sea. *In* D.J. Tranter and J.H. Fraser (Eds.) Zooplankton Sampling. Monographs on Oceanographic Methodology 2. UNESCO, Paris, pp 145-169.

FROLANDER, H.F., (1957) A plankton volume indicator. Journal du Conseil International pour L' Exploration de la Mer. **22**: 278-283.

FRONTIER, S., (1963a) Zooplankton récolté en mer d' Arabie, golfe Persique et golfe d' Aden. I. Données généralés. Répartition quantitative. Cahiers ORSTOM, Océanographie, **3**: 17-30.

FRONTIER, S., (1963b) Zooplankton récolté en mer d' Arabie, golfe Persique et golfe d' Aden. I. Ptéropodes Systematique et Répartition. Cahiers ORSTOM, Océanographie, **6**: 233-254.

FUDGE , H., (1968) Biochemical analysis of preserved zooplankton. Nature. **219**: 380-381.

FUHRMAN, J.A., SLEETER, T.D., CARLSON, C.A., PROCTOR, L.M., (1989) Dominance of bacterial biomass in the Sargasso sea and its ecological implications. Marine Ecology Progress Series. **57**: 207-217.

FURNESTIN, M.L., CODACCIONI, J.C., (1968) Chaetognatha du nord-ouest de L' Océan Indien (Golf d' Aden – Mer d' Arabie – Golfe d' Oman – Golf Persique) Cahiers ORSROM, Océanoraphie, **6**: 143-171.

GALE, W.F., MOHR, H.W., (1978) Larval fish drift in a large river with a comparison of sampling methods. Transaction of the American Fisheries Society. **107**: 46-55.

GALLAGER, S.M., DAVIS, C.S., EPSTEIN, A.W., SOLOW, A., BEARDSLEY, R.C., (1996) High resolution observations of plankton spatial distributions correlated with hydrography in the Great South Channel, Georges Bank. Deep Sea Research II 43: 1627-1663.

GALLAGHER, M.D., (1975) The dugong, *Dugong dugon* (Sirenia) at Bahrain, Persian (Arabain) Gulf. Journal of the Bombay Natural History Society, **73**: 211-212.

GALLIENNE, C.P., ROBINS, D.B., (1998) Trans-oceanic characterisation of zooplankton community size structure using an optical plankton counter. Fisheries Oceanography, 7: 147-178.

GALLIENNE, C.P., ROBINS, D.B., PILGRIM, D.A., (1996) Measuring abundance and size distribution of zooplankton using the Optical Plankton Counter in underway mode. Underwater Technology. **21**:15-21.

GALLIENNE, C.P., ROBINS, D.B., WOODD-WALKER, R.S., (2001) Abundance, distribution and size structure of zooplankton along a 20° west meridional transect of the northeast Atlantic Ocean in July. Deep-Sea Research II **48**: 925-949.

GASOL, J.M., DEL GIORGIO, P.A., DUARTE, C.M., (1997) Biomass distribution in marine planktonic communities. Limnology and Oceanography. **42**: 1353-1363.

GASPERETTI, J., (1988) Snakes of Arabia. Fauna of Saudi Arabia **9**: 169-400.

GEHRINGER, J.W., An all-metal plankton sampler (model Gulf III) Spec. Scient. Rep.U.S. Fish. Wildl. Serv. Fisheries. **88**: 7-12.

GEIDER, R.J., MACINTYRE, H.L., KANA, T.M., (1998) A dynamic regulatory model of phytoplanktonic acclimation to light, nutrients and temperature. Limnology and Oceanography. **43**: 679-694.

GIBSON, V.R., GRICE, G.D., GRAHAM, S.J., (1980) Zooplankton investigation in Gulf Waters North and South of the Strait of Hormuz. p501-517. *In*: The Coastal and Marine Environment of the Red Sea, Gulf of Aden and Tropical Western Indian Ocean vol. II.

GOES, J.I., CAEIRO, S., GOMES, H.R., (1999) Phytoplankton-zooplankton inter-relationships in tropical waters – grazing and gut pigment dynamics. Indian Journal of Marine Sciences, **28**: 116-124.

GORSKY, G., ALDORF, C., KAGE, M., PICHERAL, M., GARCIA, Y., FAVOLE, J., (1992) Vertical distribution of suspended aggregates determined by a new underwater video profiler. Annales de l' Institut Oceanographique, **68**: 275-280.

GOVONI, J.J., GRIMES, C.B., (1992) The surface accumulation of larval fishes by hydrodynamic convergence within the Mississippi River plume front. Continental Shelf Research, **12**: 1265-1276.

GOWEN, R.J., MCCULLOUGH, G., KLEPPEL, G.S., HOUCHIN, L., ELLIOTT, P., (1999) Are copepods important grazers of the spring bloom in the western Irish Sea? Journal of Plankton Research, **21**: 465-483.

GRANT, S., WARD, P., MURPHY, E., BONE, D., ABBOTT, S., (2000) Field comparison of an LHPR net sampling system and an Optical Plankton Counter (OPC) in the Southern Ocean. Journal of Plankton Research. **22**: 619-638.

GRICE, G.D., GIBSON, V.R., (1978) General biological oceanographic data from the Persian Gulf and Gulf of Oman Report B, Woods Hole Oceanographic Institution, Technical Report. WHOI 78-38 37pp.

GRIFFITHS, G., CRISP, N., BISHOP, D., (1996) Trials of a Simrad EK500 Scientific Echo Sounder on RRS *Charles Darwin* Cruise 98a. Southampton Oceanography Centre, Internal Documents No. 1, 111pp.

GRIFFITHS, G., HARRIS, A.J.K., MANSFIELD, R., SOMERS, M.L., CRISP, N.A., ROE, H.S.J., SMITH, B.V., (1997) A Multifrequency Echo Sounder for use within a towed undulating vehicle to study oceanic zooplankton abundance. Proceedings of the 7th International Conference. on Electronic Engineering in Oceanography 23 - 25 June 1997. Southampton Oceanography Centre, 79-85.

GUNDERSEN, J.S., GARDNER, W.D., RICHARDSON, M.J., WALSH, I.D., (1998) Effects of monsoons on the seasonal and spatial distributions of POC and chlorophyll in the Arabian Sea. Deep-Sea Research II. **45**: 2103-2132.

HADI, R.A., AL-SABOONCHI, A.A., HAROON, A.Y.K., (1984) Diatoms of the Shatt Al-Arab River, Iraq. Nova Hedwigia. **39**: 513-558.

HALIM, Y., (1984) Plankton of the Red Sea and the Arabian Gulf. Deep Sea Research **34**: 969-982.

HAMNER, W.M., HAMNER, P.P., STRAND, S.W., GILMER, R.W., (1983) Behaviour of Antarctic krill, *Euphausia superba*: chemo-reception, feeding, schooling and moulting. Science **220**: 433-435.

HANSEN, B., BJØRNSEN, P.K., HANSEN, P.J., (1994) The size ratio between planktonic predators and their prey. Limnology and Oceanography, **39**: 395-403.

HARDY, A.C., (1924) The herring in relation to its animate environment. I The food and feeding habits of the herring with special reference to the east coast of England. Fisheries Investigations London. Series. **2**. **7**: 1-53.

HARDY, A.C., (1936) The continuous plankton recorder. Discovery Reports **11**: 457-510.

HARDY, A.C., (1956) The open sea: its natural history. Part 1: The world of plankton. Collins, St James' Palace, London, 335pp.

HARDY, A.C., GUNTHER, E.R., (1935) The plankton of the South Georgia whaling grounds and adjacent waters, 1926-1927. Discovery Report, **11**: 1-456.

HARRIS, R.P., BOYD, P., HARBOUR, D.S., HEAD, R.N., PINGREE, R.D., POMROY, A.J., (1998) Physical, chemical and biological features of a cyclonic eddy in the region of 60°10'N, 19°50'W in the North Atlantic. Deep-Sea Research. **44**: 1815-1839.

HARRIS, R.P., WIEBE, P.H., LENZ, J., SKJOLDAL, H.R., HUNTLEY, M.A., (2000) ICES zooplankton methodology manual. Academic Press, London. pp 684.

HAURY, L.R., (1973) Sampling bias of a Longhurst-Hardy plankton recorder. Limnology and Oceanography **18**: 500-506.

HAURY, L.R., M^{C}GOWAN, J.A., WIEBE, P.H., (1978) Patterns and processes in time-space scales of plankton distributions, *In*: Spatial Patterns in Plankton Communities, J.H. Steele (Ed.) Plenum Press NY pp 277-328.

HAURY, L.R., WIEBE, P.H., BOYD, S.H., (1976) Longhurst-Hardy Plankton Recorders: their design and use for minimum bias. Deep–Sea Research **23**: 1217-1229.

HAURY, L.R., WIEBE, P.H., ORR, M.H., BRISCOE, M.G., (1983) Tidally generated high-frequency internal wave packets and their effects on plankton in Massachusetts Bay. Journal of Marine Research. **41**: 65-112.

HAURY, L.R., YAMAZAKI, H., ITSWEIRE, E.C., (1990) Effects of turbulent shear flow on zooplankton distribution. Deep Sea Research. **37A**: 447-461.

HAYS, G.C., WALNE, A.W., QUARTLEY, C.P., (1998) The U-tow: a system for sampling mesozooplankton over extended spatial scales. Journal of Plankton Research, **20**: 135-144.

HEAD, E.J.H.. HARGRAVE, B.T., SUBBA RAO, D.V., (1994) Accumulation of a pheophorbide *a* like pigment in sediment traps during the late stage of a spring bloom: A product of dying algae? Limnology and Oceanography, **39**: 176-181.

HEAD, R.N., HARRIS, R.P., BONNET, D., IRIGOIEN, X., (1999) A comparative study of size-fractionated mesozooplankton biomass and grazing in the North East Atlantic. Journal of Plankton Research. **21**: 2285-2308.

HEATH, M.R., (1995) Size spectrum dynamics and the plankton ecosystem of Loch Linnhe. ICES Journal of Marine Science. **52**: 627-642.

HENSEN, V., (1887) Über die Bestimmung des Planktons, oder des im Meere treibende Materials und Planzen und Thieren. – V. Ber. Komm. Wiss. Unters. Deutsch. Meere **5**:1-107.

HERBLAND A., (1988) The deep phaeophytin maximum in the ocean – reality or illusion? *In*: Toward a Theory on biological-physical interactions in the World Ocean, B. Rothschild, editor, Kluwer Academic Publishers. pp. 157-172.

HERMAN, A.W., (1988) Simultaneous measurement of zooplankton and light attenuance with a new optical plankton counter. Continental Shelf Research. **8**: 205-221.

HERMAN, A.W., (1992) Design and calibration of a new optical plankton counter capable of sizing small zooplankton. Deep-Sea Research., **39**: 395-415.

HERMAN, A.W., COCHRANE, N.A., SAMEOTO, D.D., (1993) Detection and abundance estimation of euphausiids using an optical plankton counter. Marine Ecology Progress Series. **94**: 165-173.

HERMAN, A.W., DAUPHINE, E., (1980) Continuous and rapid profiling of zooplankton with an electronic counter mounted on a Batfish vehicle. Deep–Sea Research. **27**: 79-96.

HERMAN, A.W., PLATT, T. (1980) Meso-scale spatial distribution of plankton: co-evolution of concepts and instrumentation. *In*: Oceanography: the past, present and future. M. Sears, D. Merriman, (Eds.) pp 204-225.

HERMAN, A.W., SAMEOTO, D.D., CHEN SHUNNIAN, MITCHELL, M.R., PETRIE, B., COCHRANE, N., (1991) Sources of zooplankton on the Nova Scotia Shelf and their aggregations within deep-shelf basins. Continental Shelf Research. **11**: 211-238.

HERRING, P.J., (1997) "Red tides" water discolouration and bioluminescence in the Gulf of Oman and Strait of Hormuz. Marine Observer, **68**: 19-25.

HERRING, P.J., HOWELL, P.R., PUGH, P, R., (1999) Scheherezade: an interdisciplinary study of the Gulf of Oman, Strait of Hormuz and the southern Arabian Gulf. No. 16. Fish, decapod shrimps and siphonophores: abundance and size data. Leg 1, 12 Feb – 19 March. Southampton Oceanography Centre No. **42**.

HERRING, P.J., HOWELL, P.R., ROE, H.S.J., (1998) Scheherezade: an interdisciplinary study of the Gulf of Oman, Strait of Hormuz and the southern Arabian Gulf. No. 11. Biomass data. Leg 1, 12 Feb – 19 March. Southampton Oceanography Centre No. **25**.

HERRING, P.J., ROE, H.S.J., GRIFFITHS, G., BOORMAN, B. MUSTARD, A.T., (1997) The effects of the oxygen minimum on the distribution of the mesopelagic fauna in the Gulf of Oman. Abstract and presentation at: The 8th Deep Sea Biology Symposium. Monterey, California, USA.

HEWES, C.D., SAKSHAUG, E., REID, F.M.H., HOLM-HANSEN, O., (1990) Microbial autotrophs and heterotroph eukaryotes in Antarctic waters: relationships between biomass and chlorophyll, adenosine triphosphate and particulate organic carbon. Marine Ecology Progress Series. **63**: 27-35.

HEYWOOD, K.J., SCROPE-HOWE, S., BARTON, E.D., (1991) Estimation of zooplankton abundance from shipborne ADCP backscatter. Deep-Sea Research, **38**: 677-691.

HILLMANN-KITALONG, A., BIRKLAND, C., (1987) Comparative biases from pushnet and pullnet zooplankton samples. Marine Ecology Progress Series **38**: 131-135.

HITCHCOCK, G.L., MARIANO, A.J., ROSSBY, T., (1993) Mesoscale pigment fields in the Gulf Stream: observations in a meander crest and trough. Journal of Geophysical Research **98**: 8425-8445.

HOLLIDAY, D.V., (1977) Extracting bio-physical information from acoustic signatures of marine organisms. *In*: Ocean sound scattering prediction, N. R. Anderson and B. J. Zahuranec (eds.) Plenum Press, New York, pp. 619-624.

HOLLIDAY, D.V., PIEPER, R.E., (1995) Bioacoustical oceanography at high frequencies. ICES Journal of Marine Science, **52**: 279-296.

HOLLIGAN, P.M., HARRIS, R.P., NEWELL, R.C., HARBOUR, D.S., HEAD, R.N., LINLEY, E.A.S., LUCAS, M.I., TRANTER, P.R.G., WEEKLEY, C.M., (1984) Vertical distribution and partitioning of organic carbon in mixed, frontal and stratified waters of the English Channel. Marine Ecology Progress Series. **14**: 111-127.

HOPKINS, T.L., (1968) Carbon and nitrogen content of fresh and preserved *Nematoscelis difficilis*, an euphausiid crustacean. Journal du Conseil International pour L' Exploration de la Mer. **31**: 300-304.

HOWELL, D.C., (1995) Fundamental statistics for the behavioural sciences. Wadsworth Inc. California. pp 458.

HULBERT, E.M., MOHMOODIAN, F., RUSSELL, M., STALCUP, F., LALZARY, S., AMIRHOR, P., (1981) Attributes of plankton flora at Bushehr, Iran. Hydrobiologia, **79**: 51-63.

HUNTER, J.R., (1983) Aspects of the dynamics of residual circulation in the Arabian Gulf. *In*: Coastal Oceanography, H. Grade, A. Edwards, H. Svendsen, (eds.) Plenum Press, New York, p 31-42.

HUNTLEY, M.E., ZHOU, M., NORDHAUSEN, W., (1995) Mesoscale distribution of zooplankton in the California Current in late spring, observed by Optical Plankton Counter. Journal of Marine Research, **53**: 647 – 674.

HUQ, M.F., AL-SAADI, H.A., HADI, R.A., (1978) Preliminary studies on the primary production of the north west Persian Gulf during a post monsoon period. Journal of the Oceanography Society of Japan. **34**: 78-80.

HUQ, M.F., AL-SAADI, H.A., HAMEED, H.A., (1981) Studies on the primary production of the river Shatt Al-Arab at Basrah, Iraq. Hydrobiologia. **77**: 25-29.

IUCN (1987) Saudi Arabia: an assessment of biotopes and coastal zone management requirements for the Arabian Gulf coast. MEPA Coastal and Marine Management Series, Reports 5.

JACOB, P.G., AL-MULZAINI, S., (1990) Marine plants of the Arabian Gulf: A literature review. KISR technical report, Safat, No. 3426, 122pp.

JACOB, P.G., ZARBA, M.A., ANDERLINI, V., (1980) Observations on the plankton and hydrography of the Kuwait waters. Mahasagar. **13**: 325-334.

JENKINS, G.M., WATTS, D.G., (1968) Spectral analysis and its applications, Holden-Day, 525pp.

JOSEPH, P.S., LEE, W., (1989) Seasonal variability of heat capacity in Kuwait coastal water. Kuwait Bulletin of Marine Science **10**: 213-221.

JOYCE, T.M., (1983) Varieties of ocean fronts. In: Baroclinic instability and ocean fronts. M.E. Stern and F.K. Mellor (Eds.) Woods Hole Oceanographic Institute Technical Report No. **83-41**.

JUMARS, P.A., (1993) Concepts in biological Oceanography. An interdisciplinary primer. Oxford Univ. Press.

KARL, D.M., (1999) A sea of change: biogeochemical variability in the North Pacific Subtropical Gyre. Ecosystems. **2**: 181-214.

KATZ, J., DONAGHAY, P.L., ZHANG, J., KING, S., RUSSELL, K., (1999) Submersible holocamera for the detection of particle characteristics and motions in the ocean. Deep-Sea Reasearch I. **46**: 1455-1481.

KIEFER, D.A., (1973) Chlorophyll a fluorescence in marine centric diatoms: response of chloroplasts to light and nutrient stress. Marine Biology **23**: 39-46.

KIERSTEAD, H., SLODODKIN, L.B., (1953) The size of water masses containing plankton blooms. Journal of Marine Research **12**: 141.

KILS, U., (1993) Formation of micropatches by zooplankton-driven microturbulences. Bulletin of Marine Science, **53(1)**, 160-169.

KIMOR, B., (1973) Plankton relations of the Red Sea, Persian Gulf and Arabian Sea. *In*: The Biology of the Indian Ocean. B., Zeitzschel (Ed.). Chapman and Hall Limited, London. Springer-Verlag Berlin-Heidelberg-New York. 544pp.

KINNE, O., (1966) Physiological aspects of animal life in estuaries with special reference to salinity. Netherlands Journal of Sea Research. **3**: 222-244.

KIRK, J.T.O., (1976) A theoretical analysis of the contribution of algal cells to the attenuation of light within natural waters. III Cylindrical and spheroidal cells. New Phytology **77**: 341-358.

KOGELER, J.M., FALK-PETERSON, S., KRISTENSEN, A., PETTERSEN, F., DALEN, J., (1987) Density and sound speed contrasts in sub-Arctic zooplankton. Polar Biology **7**: 231-235.

KOLASA, J., ZALEWSKI, M., (1995) Notes on ecotone attributes and functions. Hydrobiologia, **303**: 1-7.

KREMBS, C., JUHL, A.R., STRICKLER, J.R., (1998) The spatial information preservation method: Sampling the nanoscale spatial distribution of micro-organisms. Limnology and Oceanography, **43**: 298-306.

KREY, J., (1973) Primary production in the Indian Ocean I. *In*: The Biology of the Indian Ocean. B., Zeitzschel (Ed.). Chapman and Hall Limited, London. Springer-Verlag Berlin-Heidelberg-New York. 544pp.

LAMPERT, W., (1993) Ultimate causes of diel vertical migration of zooplankton: new evidence for the predator-avoidance hypothesis. Archiv für Hydrobiologie, **39**: 79-88.

LAMPITT, R.S., GAMBLE, J.C., (1982) Diet and respiration of the small planktonic marine copepod *Oithona nana*. Marine Biology **66**: 185-190.

LAMPITT, R.S., NOJI, T., BODUNGEN, B.VON., (1990) What happens to zooplankton faecal pellets? Implications for material flux. Marine Biology **104**: 15-23.

LAURS, R.M., FIEDLER, P.C., MONTGOMERY, D.R., (1984) Albacore tuna catch distributions relative to environmental features observed from satellites. Deep Sea Research **31**: 1085-1099.

LE FÈVRE, J., (1986) Aspects of the biology of frontal systems. Advances in Marine Biology. **23**: 163–299.

LEGENDRE, L., LE FÈVRE, J., (1989) Hydrodynamical singularities as controls of recycled versus export production in oceans. *In*: W.H. Berger, V.S. Smetacek, G. Wefer, (Eds.) Productivity of the ocean: past and present. New York: John Wiley & Sons. p 49-63.

LEGENDRE, L., RASSOULZADEGAN, F., MICHAUD, J., (1999) Identifying the dominant processes (physical versus biological) in pelagic marine ecosystems from field estimates of chlorophyll *a* and phytoplankton production. Journal of Plankton Research, **21**(9): 1643-1658.

LENNERT-CODY, C.E., FRANKS, P.J.S., (1999) Plankton patchiness in high frequency internal waves. Marine Ecology Progress Series. **186**: 59-66.

LENZ, J., (1972) A new-type of plankton pump on the vacuum principle. Deep–Sea Research. **19**: 453–459.

LENZ, J., Introduction. 1-32. *In*: Harris, R., Wiebe, P.H., Lenz, J., Skjoldal, H.R., Huntley, M.A., (Eds.) ICES zooplankton methodology manual. Academic Press, London. pp 684.

LENZ, J., MORALES, A., GUNKEL, J., (1993) Mesozooplankton standing stock during the North Atlantic spring bloom study in 1989 and its potential grazing pressure on phytoplankton: a comparison between, low, medium and high latitudes. Deep-Sea Research, **40**: 559-572.

LEVEAU, M., (1968) Ostracodes pélagiques récueilles lors de la 3eme campagne de l' Aviso Ct. *Robert Giraud*. Récuil des Traveux de la Station Marine Marseille. **8**: 127-142.

LEVEAU, M., SZEKIELDA, K.-H., (1968) Situation hydrologique et distribution du zooplankton dans le N.W. de la Mer d' Arabie. Sarsia, **34**: 285-298.

LI, W.K.W., DICKIE, P.M., IRWIN, B.D., WOOD, A.M., (1992) Biomass of bacteria, cyanobacteria, prochlorophytes and photosynthetic eukaryotes in the Sargasso Sea. Deep–Sea Research. **39**: 501-519.

LILLIBRIDGE, J.L., HITCHCOCK, G., ROSSBY, R., LESSARD, E., MORK, M., GOLMAN, L.,(1990) Entrainment and mixing of shelf/slope waters in the near-surface Gulf Stream. Journal of Geophysical Research **95**: 13026-13087.

LOHRENZ, S.E., FAHNENSTIEL, G.L., REDALJE, D.G., LANG, G.A., DAGG, M.J., WHITLEDGE, T.E., DORTCH, Q., (1999) Nutrients, irradiance, and mixing as factors regulating primary production in coastal waters impacted by the Mississippi River plume. Continental Shelf Research, **19**(9): 1113-1141.

LOHRENZ, S.E., WIESENBURG, D.A., DE PALMA, I.P., JOHNSON, K.S., GUSTAFSON, D.E.JR., (1988) Interrelationship among primary production, chlorophyll, and environmental conditions in frontal regions of the Western Mediterranean. Deep-Sea Research I. **35**: 793-810.

LONGHURST, A.R., (1967) Vertical distribution of zooplankton in relation to the eastern Pacific oxygen minimum. Deep–Sea Research. **14**: 51-63.

LONGHURST, A.R., HARRISON, W.G., (1989) The biological pump: profiles of plankton production and consumption in the upper ocean. Progress in Oceanography. **22**: 47-123.

LONGHURST, A.R., REITH, A.D., BOWER, R.E., SIEBERT, D.L.R., (1966) A new system for the collection of multiple serial plankton samples. Deep–Sea Research. **13**: 213-222.

LONGHURST, A.R., WILLIAMS, R., (1976) Improved filtration system for multiple-serial plankton samplers and their development. Deep–Sea Research. **23**: 1067-1073.

LORENZEN, C.J., (1966) A method for the continuous measurement of *in vivo* chlorophyll concentration. Deep–Sea Research. **13**: 223-227.

LORENZEN, C.J., (1967) Vertical distribution of chlorophyll and phaeopigments: Baja California. Deep-Sea Research, **14**: 735-745.

LUDWIG, J.A., REYNOLDS, J.F., (1988) Statistical Ecology: a primer on methods and computing. Wiley, New York.

LUO, J., ORTNER, P.B., FORCUCCI, D., CUMMINGS, S.R., (2000) Diel vertical migration of zooplankton and mesopelagic fish in the Arabian Sea. Deep-Sea Research II **47**: 1451-1473.

MACAULAY, M.C., (1994) A generalised target strength model for euphausiids, with applications to other zooplankton. Journal of the Acoustic society of America. **95**: 2452-2466.

MACAULAY, M.C., WISHNER, K.F., DALY, K.L., (1995) Acoustic scattering from zooplankton and micronekton in relation to a whale feeding site near Georges Bank and Cape Cod. Continental Shelf Research. **15**, (4/5), 509-537.

MACKAS, D.L., BOHRER, R., (1976) Fluorescence analysis of zooplankton gut contents and an investigation of diel feeding patterns. Journal of Experimental Marine Biology and Ecology, **25**, 77-85.

MACKAS, D.L., BOYD, C.M., (1979) Spectral analysis of zooplankton spatial heterogeneity. Science, **204**: 62-64.

MACKAS, D.L., DENMAN, K.L., ABBOTT, M.R., (1985) Plankton patchiness: biology in the physical vernacular. Bulletin of Marine Sciences **37**: 652-674.

MACLENNAN, D.N., (1990) Acoustic measurement of fish abundance. Journal of the Acoustic Society of America. **87**: 1-15.

MADDUX, W.S., KANWISHER, J.W., (1965) An *in situ* particle counter. Limnology and Oceanography **10**:162-168.

MAHNKEN, C.V.W., JOSSI, J.W., Flume experiments on the hydrodynamics of plankton nets. Journal du Conseil International pour L' Exploration de la Mer. **31**: 38-45.

MARGALEF, R., (1978) Sampling design: Some examples. *In* A. Sournia (ed.) Phytoplankton Manual. Monographs on Oceanographic Methodology 6. UNESCO, Paris, pp 17-31.

MATONDKAR, S.G.P., BHAT, K.L., ANSARI, Z.A., PARULEKAR, A.H., (1995) Elemental (C, H, N) composition of the zooplankton from north Arabian Sea. Indian Journal of Marine Science **24**: 68-72.

MAUCHLINE, J., (1980) The biology of mysids and euphausiids. Advances in Marine Biology **18**: 1–687.

MAUCHLINE, J., FISHER, L.R., (1969) The biology of euphausiids. Advances in Marine Biology. **7**: 454-495.

MCCLAIN, C.R., ISHIZAKA, J., HOFMANN, E.E., (1990) Estimation of the processes controlling variability in plankton pigment distributions on the south west US continental shelf. Journal of Geophysical Research **95**: 20213-20236.

MCGEHEE, D.E., GREENLAW, C.F., HOLLIDAY, D.V., PIEPER, R.E., (2000) Multifrequency acoustical volume backscattering patterns in the Arabian Sea-265 kHz to 3 MHz. Journal of the Acoustic Society of America. **107**: 193-200.

MCGILLICUDDY, D.J.JR., ROBINSON, A.R., (1997) Eddy-induced nutrient supply and new production in the Sargasso Sea. Deep-Sea Research. **44**(8): 1427-1450.

McGILLICUDDY, D.J.JR., ROBINSON, A.R., SIEGEL, D.A., JANNASCH, H.W., JOHNSON, R., DICKEY, T.D., MCNEIL, J., MICHAELS, A.F., KNAP, A.H., (1998) Influence of mesoscale eddies on new production in the Sargasso Sea. Nature. **394**: 263-266.

McGOWAN, J.A., BROWN, D.M., (1966) A new opening-closing paired zooplankton net. Univ. Calif. Scripps Inst. Ref 66-23.

MEISE, C.J., O'REILLY, J.E., (1996) Spatial and seasonal patterns in abundance and age-composition of *Calanus finmarchicus* in the Gulf of Maine and on Georges Bank. Deep-Sea Reseach II **43**: 1473-1501.

MESHAL, A.H., HASSAN, H.M., (1986) Evaporation from the coastal water in the central part of the Gulf. Arabian Gulf Journal of Scientific Research **4**: 649-655.

MICHEL, H.B., BEHBEHANI, M., HERRING, D., ARAR, M., AL-SHOUSHANI, M., BRAKONIECKI, T., (1981) Zooplankton diversity, distribution and abundance in Kuwaiti waters. Kuwait: Kuwait Institute for Scientific Research, 154pp.

MICHEL, H.B., BEHBEHANI, M., HERRING, D., ARAR, M., AL-SHOUSHANI, M., BRAKONIECKI, T., (1986a) Zooplankton diversity, distribution and abundance in Kuwait waters. Kuwait Bulletin of Marine Science. **8**: 37-105.

MICHEL, H.B., BEHBEHANI, M., HERRING, D., (1986b) Zooplankton of the western Arabian Gulf south of Kuwait waters. Kuwait Bulletin of Marine Science. **8**: 1-36.

MILLER, C.B., JUDKINS, D.C., (1981) Design of pumping systems for sampling zooplankton, with descriptions of two high capacity samplers for coastal studies. Biological Oceanography **1**: 29–56.

MOAT, B.I., PASCAL, R.W., GUYMER, T.H., (1997) Scheherezade – an interdisciplinary study of the Gulf of Oman, Strait of Hormuz and the southern Arabian Gulf. Charles Darwin Cruise 104. No 8. Surface meteorological parameters. Leg 1, 12 Feb – 19 March. Southampton Oceanography Centre. Research & Consultancy Report No. **17**.

MØLENBERG, F., (1987) A submersible net-pump for quantitative zooplankton sampling; comparison with conventional net sampling. Ophelia **27**: 101-110.

MORALES, C.E., (1999) Carbon and nitrogen fluxes in the oceans: the contribution by zooplankton migrants to active transport in the North Atlantic during the Joint Global Ocean Flux Study. Journal of Plankton Research. **21**: 1799-1808.

MORALES, C.E., BEDO, A., HARRIS, R.P., TRANTER, P.R.G., (1991) Grazing of copepod assemblages in the north-east Atlantic: the importance of the small size fraction. Journal of Plankton Research. **13**: 455-472.

MOTODA, S., (1959) Devices of simple plankton apparatus. Mem. Fac. Fish. Hokkaido Univ. **7**: 73-94.

MULLIN, M.M., BROOKS, E.R., (1976) Some consequences of distributional heterogeneity of phytoplankton. Limnology and Oceanography. **21**: 784-796.

MUSAEVA, E.I., NEZLIN, N.P., (1996) Comparison of various zooplankton sampling tools based on catches in the Bering Sea. Oceanology **35**: 857-861.

MUSTARD, A.T., (1997) Scheherezade – an interdisciplinary study of the Gulf of Oman, Strait of Hormuz and the southern Arabian Gulf. Charles Darwin Cruise 104. No 7. Optical plankton counter data. Leg 1, 12 Feb – 19 March. Southampton Oceanography Centre. Research & Consultancy Report No. **16**.

NAIMAN, R.J., (1988) The potential importance of boundaries to fluvial ecosystems. Journal of North American Benthology Society. **7**: 289-306.

NEW, A.L., (1988) Internal tidal mixing in the Bay of Biscay. Deep-Sea Research **35A**(5): 691-709.

NEWELL, G.E., NEWELL, R.C., (1963) Marine Plankton. A Practical Guide. Hutchinson Educational Ltd. London. pp 207.

NICHOLS, J.H., THOMPSON, A.B., (1991) Mesh selection of copepodite and nauplius stages of four calanoid copepod species. Journal of Plankton Research. **13**: 661-671.

O'NEILL, R.V., DEANGELIS, D.L., (1981) Comparative productivity and biomass relations of forest ecosystems, p 411-449. *In*: D.E. Reichle (ed.) Dynamic properties of forest ecosystems. Cambridge Univ. Press.

ODUM, E.P., (1971) Fundamentals of ecology. Saunders.

OLSON, D.B., BACKUS, R.H., (1985) The concentrating of organisms at fronts: a cold water fish and a warm-core Gulf Stream ring. Journal of Marine Research **43**: 113-137.

OLSON, D.B., HITCHCOCK, G.L., MARIANO, A.J., CARIN, A.J., GE, P., REDWOOD, N.W., GUILLER, M.O., (1994) Life on the edge: marine life and fronts. Oceanography **7**: 52-60.

OMORI, M., IKEDA, (1992) Methods in Marine Zooplankton Ecology. Wiley, New York. pp 311.

OMORI, M., MARUM, O.R., AIZAWA, Y., (1965) A 160cm opening-closing plankton net II. Some notes on towing behaviour of the net. Journal of the Oceanographical Society of Japan. **21**: 245-252.

ORTNER, P.B., (1993) Integration of video imaging with optical plankton counting: "Smart Sampling". US GLOBEC News. **5**: 9-11.

ORTNER, P.B., WIEBE, P.H., HAURY, L., BOYD, S., (1978) Variability in zooplankton biomass distribution in the Northern Sargasso Sea: the contribution of the Gulf Stream cold core rings. Fishery Bulletin **76**: 323-334.

OWEN, R.W., (1981) Fronts and eddies in the sea: mechanisms, interactions and biological effects. *In*: analysis of marine ecosystems. p197-233. A.R., Longhurst, (Ed.) Academic Press London.

PACE, M.L., COLE, J.J., CARPENTER, S.R., (1998) Trophic cascades and compensation: differential responses of microzooplankton in whole-lake experiments. Ecology, **79**: 138-152.

PAFFENHÖFER, G.A., (1993) On the ecology of marine cyclopoid copepods (Crustacea, Copepoda). Journal of Plankton Research, **15**: 37-55.

PAKHOMOV, E.A., VERHEYE, H.M., ATKINSON, A., LAUBSCHER, R.K., TAUNTON-CLARK, J., (1997) Structure and grazing impact of the mesozooplankton community during late summer 1994 near South Georgia, Antarctica. Polar Biology, **18**: 180-192.

PARKER, R.E., (1983) Introductory Statistics for Biology. 2nd Edition. Edward Arnold Ltd. London. pp 122.

PARSONS, T.R., LEBRASSEUR, R.J., FULTON, J., (1967) Some observations on the dependence of zooplankton grazing on the cell size and concentration of phytoplankton blooms. Journal of the Oceanography Society of Japan. **23**: 10-17.

PARSONS, T.R., TAKAHASHI, M., HARGRAVE, B.E., (1977) Biological oceanographic processes. 2nd edition, Pergamon Press. New York, 332pp.

PAULINOSE, V.T., ARAVINDAKSHAN, P.N., (1977) Zooplankton biomass, abundance and distribution in the north and north eastern Arabian Sea. Proceedings of the Symposium on Warm Water Zooplankton, special publication, National Institute of Oceanography, Goa India, p 132-136.

PEARCY, W.G., MESECAR, R.S., (1971) Scattering layers and the vertical distribution of oceanic animals off Oregon. *In*: Proceedings of the Internatiional Symposium of Biological Sound Scattering in the Ocean. U.S. Dept. Navy, MC Rept. 005, pp 381-394.

PIEPER, R.E., HOLLIDAY, D.V., KLEPPEL, G.S., (1990) Quantitative zooplankton distributions from multifrequency acoustics. Journal of Plankton Research, **12**: 433-441.

PIERROT-BULTS, A.C., SPOEL, S.VAN DER., ZAHURANEC, B.J., JOHNSON, R.K., (Eds) (1986) Pelagic biogeography. Proceedings of an international conference, The Netherlands, 29 May - 5 June 1985. Unesco Technical Papers in Marine Science, No. **49**, 295pp.

PIJANOWSKI, J., KOWALCZEWSKI, A., (1997) Predators can influence swarming behaviour in and locomotory responses in *Daphnia*. Freshwater Biology **37**: 649-656.

PINEL-ALLOUL, B., (1995) Spatial heterogeneity as a multiscale characteristic of zooplankton community. *In*: Space partition within aquatic ecosystems. G., Balvay. (Ed.) Dordrecht: Kluwer Academic. pp.17-42 (Reprinted from: Hydrobiologia, 300/301, 1995)

PINGREE, R.D., HOLLIGAN, P.M., HEAD, R.N., (1977) Survival of dinoflagellate blooms in the western English Channel. Nature **265**: 266-269.

PINGREE, R.D., MARDELL, G.T., NEW, A.L., (1986) Propagation of internal tides from upper slopes of the Bay of Biscay. Nature **321**: 154-158.

PINGREE, R.D., PUGH, P.R., HOLLIGAN, P.M., FORSTER, G.R., (1975) Summer phytoplankton blooms and red tides along tidal fronts in the approaches of the English Channel. Nature **258**: 672-677.

PITTA, P., GIANNAKOUROU, A., DIVANACH, P., KENTOURI, M., (1998) Planktonic food web in marine mesocosms in the eastern Mediterranean: bottom-up or top-down regulation? Hydrobiologia **363**: 97-105.

PLATT, T., (1985) Structure of the marine ecosystem: its allometric basis. In: Ecosystem theory for biological oceanography. Canadian Bulletin of Fishery Aquatic Science **213**.

PLATT, T., DENMAN, K., (1978) The structure of pelagic marine ecosystems. Journal du Conseil International pour L' Exploration de la Mer. **173**: 60-65.

PLUEDDEMANN, A.J., PINKEL, R., (1989) Characterisation of the patterns of diel migration using a Doppler Sonar. Deep-Sea Research. **36**: 509-530.

PODESTA, G.P., BROWDER, J.A., HOEY, J.J., (1993) Exploring the association between swordfish catch and thermal fronts on the US long-line grounds in the Western North Atlantic. Continental Shelf Research **13**: 253-270.

POLLARD, R.T., (1986) Frontal surveys with a towed profiling conductivity/ temperature/ depth measurement package (SeaSoar) Nature, **323**: 433-435.

POLLARD, R.T., BATHMANN, U., DUBISCHAR, C., READ, J.F., LUCAS, M., (2000, in press) Spatial surveys in the Southern Oceans with a towed Optical Plankton Counter. Submitted for special edition of Deep Sea Research.

POLLARD, R.T., GRIFFITH, M.J., GWILLAM, T.J.P., READ, J.F., (1996) Optical Plankton Counter SeaSoar data collected on Polarstern Cruise Antares XIII/2. Southampton Oceanography Centre Internal Report.

POLLARD, R.T., REGIER, L., (1992) Vorticity and vertical circulation at an ocean front. Journal of Physical Oceanography **22**: 609-625.

POSTEL, L., (1990) The mesozooplankton response to coastal upwelling off West Africa with particular regard to biomass. Marine Science Reports. **1**: 1-127.

POSTEL, L., FOCK, H., HAGEN, W., (2000) Biomass and abundance. 83-192. *In*: Harris, R., Wiebe, P.H., Lenz, J., Skjoldal, H.R., Huntley, M.A., (Eds.) ICES zooplankton methodology manual. Academic Press, London. pp 684.

POULET, S.A., WILLAMS, R., CONWAY, D.V.P., VIDEAU, C., (1991) Co-occurrence of copepods and dissolved amino acids in shelf sea waters. Marine Biology. **108**: 373-385.

PRESS, W.H., TEUKOLSKY, S.A., VETTERLING, W.T., FLANNERY, B.P., (1994) Numerical recipes in Fortran 77. 2nd Ed. Cambridge University Press. 931pp.

PRICE, A.R.G., COLES, S.L., (1992) Aspects of sea-grass ecology along the western Arabian Gulf. Hydrobiologica **234**: 129-141.

PRICE, A.R.G., MATTHEWS, C.P., INGLE, R.W., AL-RASHEED, K., (1993a) Abundance of zooplankton and penaid shrimp larvae in the Western Gulf: Analysis of pre-war and post-war data. Marine Pollution Bulletin **27**: 273-278.

PRICE, A.R.G., SHEPPARD, C.R.C., ROBERTS, C.M., (1993b) The Gulf: its biological setting. Marine Pollution Bulletin **27**: 9-15.

PRIEUR, L., COPIN-MONTEGUT, C., CLAUSTRE, H., (1993) Biophysical aspects of "Almofront-1", an intensive study of geostrophic frontal jet. Ann. Inst. Oceanogr. **69**: 71-86.

PROTOCOLS FOR THE JOINT GLOBAL OCEAN FLUX (JGOFS), (1994). Intergovernmental Oceanographic Commission manual and guides no. 29. 170 pp.

PUGH, P.R., (1978) The application of particle counting to an understanding of the small scale distribution of the plankton. *In*: Steele, J.H., (ed.) Spatial Patterns *In*: Plankton Communities. Plenum Press, N.Y.

RABE, B., MUSTARD, A.T., ALDERSON, S.G., ALLEN, J.T., (1998) Towed, undulating Optical Plankton Counter (OPC), attenuance and fluorimeter observations during RRS *Discovery* Cruise 224, 15 Nov 96 – 17 Jan 97. Southampton Oceanography Centre Internal Document **42**. pp 166.

RAO, D.V.S., AL-YAMANI, F., (1998) Phytoplankton ecology in the waters between Shatt Al-Arab and Straits of Hormuz, Arabian Gulf: A review. Plankton Biology and Ecology, **45**: 101-116.

READ, J.F., POLLARD, R.T., BATHMANN, U., (2000, in press) Physical and biological patchiness of an upper ocean transect from South Africa to the ice edge near the Greenwich Meridian. Submitted for special issue of Deep Sea Research.

REYNOLDS, M.R., (1993) Physical oceanography of the Persian Gulf, the Strait of Hormuz, and the Gulf of Oman. Results of the Mt Mitchell Expedition. Marine Pollution Bulletin, **27**: 35-59.

RICHARDS, K.J., GOULD, W.J., (1996) Ocean weather – eddies in the sea. pp.59-68 *In*: Oceanography: an illustrated guide. C.P., Summerhayes & S.A., Thorpe (Eds.) London: Manson. 352pp.

RIEMANN, B., SIMONSEN, P., STENSGAARD, L., (1989) The carbon and chlorophyll content of phytoplankton from various nutrient regimes. Journal of Plankton Research. **11**: 1037-1045.

RISSIK, D., SUTHERS, I.M, TAGGART, C.T., (1997) Enhanced zooplankton abundance in the lee of an isolated reef in the south Coral Sea: the role of flow disturbance. Journal of Plankton Research. **19**: 1347-1368.

RODRIGUEZ, J., MULLIN, M.M., (1986) Relation between biomass and body weight of plankton in a steady state oceanic ecosystem. Limnology and Oceanography. **31**: 361-370.

ROE, H. S. J., *et al.*, (1997). Scheherezade – an interdisciplinary study of the Gulf of Oman, Strait of Hormuz and the southern Arabian Gulf. R.R.S. *Charles Darwin* Cruise 104, Leg 1. Cruise Report No. 9. Southampton Oceanography Centre.

ROE, H.S.J., (1974) Observations on the diurnal vertical migrations of an oceanic animal community. Marine Biology **28**: 99-113.

ROE, H.S.J., BAKER, A. DE C., CARSON, R.M., WILD, R., SHALE, D., (1980) Behaviour of the Institute of Oceanographic Science's Rectangular Midwater Trawls: theoretical aspects and experimental observations. Marine Biology **56**: 247-259.

ROE, H.S.J., GRIFFITHS, G., (1993) Biological information from an acoustic Doppler current profiler. Marine Biology **115**: 339-346.

ROE, H.S.J., GRIFFITHS, G., CRISP, N., FIELDING, S., (1998) Recent observations in the North West Indian Ocean. In: Colloquium on recent advances in sonar applied to biological oceanography.

ROE, H.S.J., GRIFFITHS, G., HARTMAN, M., CRISP, N., (1996) Variability in biological distributions and hydrography from concurrent acoustic doppler current profiler and SeaSoar surveys. ICES Journal of Marine Science. **53**, No. 2, pp 131-138.

ROE, H.S.J., SHALE, D.M., (1979) A new multiple rectangular midwater trawl (RMT 1 + 8 m) and some modifications to the Institute of Oceanographic Science's RMT 1 + 8. Marine Biology. **50**: 283-288.

ROMAN, M.R., DAM, H.G., GAUZENS, A.L., NAPP, J., (1993) Zooplankton biomass and grazing at the JGOFS Sargasso Sea time series station. Deep-Sea Research **40**: 833-901.

ROMAN, M.R., GAUZENS, A.L., (1997) Copepod grazing in the equatorial Pacific. Limnology and Oceanography **42**: 623-634.

ROMAN, M.R., SMITH, S., WISHNER, K., ZHANG, X, GOWING, M., (2000) Mesozooplankton production and grazing in the Arabian Sea. Deep-Sea Research **47**(B): 1423-1450.

ROY, S., HARRIS, R.P., POULET, S.A., (1989) Inefficient feeding by *Calanus helgolandicus* and *Temora longicornis* on *Coscinodiscus wailesii*: quantitative estimation using chlorophyll-type pigments and effects on dissolved free amino acids. Marine Ecology Progress Series, **52**: 145-153.

RUDNICK, D.L., (1996) Intensive surveys of the Azores Front. 2. Inferring the geostrophic and vertical velocity field. Journal of Geophysical Research, **101**: 16291-16303.

RUSSELL, F.S., (1927) The vertical distribution of plankton in the sea. Biological Reviews, **2**: 213-262.

RYTHER, J.H., (1969) The relationship of photosynthesis to fish production in the sea. Science **166**: 72–76.

SAAD, M.A.H., (1976) Observations on the problems of pollution in Shatt Al-Arab, Iraq. Rev. Intern. Oceanogr. Med. **43**: 3-11.

SAVILLE, A., (1958) Mesh selection in plankton nets. Journal du Conseil International pour L' Exploration de la Mer. **23**: 192-201.

SCHIEWER, U., AL-SAADI, H.A., HAMEED, H.A., (1982) On the diel rhythm of phytoplankton productivity in Shatt Al-Arab at Basrah, Iraq. Archiv fur Hydrobiologie. **93**: 158-172.

SCHMIDT-NIELSEN, K., (1997) Animal physiology: adaptation and environment. 5th Edition. Cambridge University Press. pp 612.

SEIBOLD, E., (1973) Biogenic sediments of the Persian Gulf. *In*: The Biology of the Indian Ocean. B., Zeitzschel (Ed.). Chapman and Hall Limited, London. Springer-Verlag Berlin-Heidelberg-New York. 544pp.

SHELDON, R.W., PARSONS, T.R., (1967) A continuous size spectrum for particulate matter in the sea. Journal of the Fisheries Research Board Canada. **24** (5): 909-915.

SHELDON, R.W., PRAKASH, A., SUTCLIFFE, W.H., (1972) The size distribution of particles in the ocean. Limnology and Oceanography. **17**: 327-340.

SHELDON, R.W., SUTCLIFFE, W.H., PARANJAPE, M.A., (1977) Structure of the pelagic food chain and the relationship between plankton and fish production. Journal of the Fisheries Research Board Canada. **34**: 2344-2353.

SHEPPARD, C.R.C., PRICE, A.R.G., ROBERTS, C.M., (1992) Marine ecology of the Arabian region. Patterns and Processes in Extreme Tropical Environments. Academic Press, London.

SHUMAN, F.R., LORENZEN, C.J., (1975) Quantitative degradation of chlorophyll by a marine herbivore. Limnology and Oceanography **20**: 580-586.

SKJOLDAL, H.-R., WIEBE, P.H., FOOTE, K.G., (2000) Sampling and experimental design, pp 33-53. *In*: Harris, R., Wiebe, P.H., Lenz, J., Skjoldal, H.R., Huntley, M.A., (Eds.) ICES zooplankton methodology manual. Academic Press, London. pp 684.

SMEED, D.A., (1997) Scheherezade: an interdisciplinary study of the Gulf of Oman, Strait of Hormuz and the southern Arabian Gulf. No. 1 CTD Data. Research and Consultancy Report No. 7. Southampton Oceanography Centre.

SMEED, D.A., ALLEN, J.T., CRISP, N.A., (1997) Scheherezade – an interdisciplinary study of the Gulf of Oman, Strait of Hormuz and the southern Arabian Gulf. No. 2 SeaSoar Data. Research and Consultancy Report No. 11. Southampton Oceanography Centre.

SMITH, P.E., COUNTS, R.C., CLUTTER, R.I., (1968) Changes in filtering efficiency of plankton nets due to clogging under tow. Journal du Conseil International pour L' Exploration de la Mer. **32**: 232-248.

SMITH, R.J., (1968) Upwelling. Oceanography and Marine Biology Annual Review **6**: 11-46.

SMITH, S.L., (1982) The northwestern Indian Ocean during the monsoons of 1979: distribution, abundance and feeding of zooplankton. Deep-Sea Research, II, **29**: 1331-1353.

SMITH, S.L., PIEPER, R.E., MOORE, M.V., RUDSTRAM, L.G., GREENE, C.E., ZANON, J.E., FLAGG, C.M., WILLIAMSON, C.E., (1992) Acoustic techniques for the in situ observations of zooplankton. Archiv für Hydrobiologie Theoretische und Angewante Limnologie, **36**: 23-43.

SNYDER, D.E., (1983) Fish eggs and larvae, p. 165-197. *In*: L. A. Nielsen and D. L. Johnson [eds.] Fisheries techniques. American Fisheries Society, Bethesda, MD. 468 pp.

SOLEMDAL, P., ELLERTSEN, B., (1984) Sampling fish larvae with large pumps; quantitative and qualitative comparisons with traditional gear. – *In*: E. Dahl *et al.*, [eds.]: The Propagation of cod *Gadus morhua* L., pp. 335-364. Flodevigen Rapporter **1**.

SOURNIA, A., (1994) Pelagic biogeography and fronts. Progress in Oceanography. **34**: 109-120.

SPALL, S.A., RICHARDS, K.J., (2000) A numerical model of mesoscale frontal instabilities and plankton dynamics – I. Model formulation and initial experiments. Deep-Sea Research **47**: 1261-1301.

SPOEL, S.VAN DER., HEYMAN, R.P., (1983) A comparative atlas of zooplankton. Biological patterns in the oceans. Wetenschappelijke uitgeverij Bunge, Utrecht. The Netherlands. pp 186.

SPRULES, W.G., BERGSTROM, B., CYR, H., ET AL., (1992) Non-video optical instruments for studying zooplankton distribution and abundance. Arch. Hydrobiol. Beih. Ergebn. Limnol. **36**: 45-58.

SPRULES, W.G., BRANDT, S.B., STEWART, D.J., MUNWAAR, M., JIN, E.H., LOVE, J., (1991). Biomass size spectrum of Lake Michigan pelagic food web. Canadian Journal of Fisheries and Aquatic Science. **48**: 105-115.

SPRULES, W.G., CASSELMAN, J.M., SHUTER, B.J., (1983) Size distribution of pelagic particles in lakes. Canadian Journal of Fisheries and Aquatic Science. **40**: 1761-1769.

SPRULES, W.G., JIN, E.H., HERMAN, A.W., STOCKWELL, J.D., (1998) Calibration of an optical plankton counter for use in fresh water. Limnology and Oceanography. **43**: 726-733.

STANTON, T.K., CHU, D., WIEBE, P.H., (1996) Acoustic scattering characteristics of several zooplankton groups. ICES Journal of Marine Sciences, **53**(2): 289-295.

STANTON, T.K., WIEBE, P.H., CHU, D., BENFIELD, M.C., SCANLON, L., MARTIN, L., EASTWOOD, R.L., (1994) On acoustic estimate of zooplankton biomass. ICES Journal of Marine Science, **51**: 505-512.

STEELE, J.H., (1978) Some comments on plankton patchiness. *In*: Spatial patterns in plankton communities. J.H. Steele (ed.) Plenum Press NY pp 1-20.

STEELE, J.H., (1991) Can ecological theory cross the land-sea boundary? Journal of Theoretical Biology. **153**: 425-436.

STEELE, J.H., FROST, B.W., (1977) The structure of plankton communities.

STOCKWELL, J.D., SPRULES, W.G., (1995) Spatial and temporal patterns of zooplankton biomass in Lake Erie. ICES Journal Marine Science **52**: 557-564.

STRASS, V.H., (1990) On the calibration of large-scale fluorometric chlorophyll measurements from towed undulating vehicles. Deep-Sea Research. **37**: 525-540.

STRASS, V.H., (1992) Chlorophyll patchiness caused by mesoscale upwelling at fronts. Deep-Sea Research **39**: 75-96.

STRICKLER, J.R., (1977) Observation of swimming performances of planktonic copepods. Limnology and Oceanography, **22**: 165-170.

STRICKLER, J.R., (1998) Observing free-swimming copepods mating. Philosophical Transactions of the Royal Society of London. Series B: **353**: 671-680.

STRUTTON, P.G., MITCHELL, J.G., PARSLOW, J.S., GREENE, R.M., (1997) Phytoplankton patchiness: quantifying the biological contribution using fast repetition rate fluorometry. Journal Plankton Research, **19**: 1265-1274.

SULTAN, S.A.R., ELGHRIBI, N.M., (1996) Temperature inversion in the Arabian Gulf and the Gulf of Oman. Continental Shelf Research **16**: 1521-1544.

SVERDRUP, H.U., (1953) On conditions for the vernal blooming of phytoplankton. Journal du Conseil International pour L' Exploration de la Mer. **18**: 287-295.

SWALLOW, J.C., (1984) Some aspects of the physical oceanography of the Indian Ocean. Deep–Sea Research, **31**: 639-650.

TAGGART, C.T., LEGGETT, W.C., (1984) Efficiency of large volume pumps and evaluation of a design suitable for deployment from a small boat. Canadian Journal of Fisheries and Aquatic Science, **41**: 1428-1435.

TAYLOR, A.H., GEIDER, R.J., GILBERT, F.J.H., (1997) Seasonal and latitudinal dependencies of phytoplankton carbon-to-chlorophyll a ratios: results of a modelling study. Marine Ecology Progress Series. **152**: 51-66.

TESTER, P., TURNER, J.T., (1991) Why is *Acartia tonsa* restricted to estuarine habits. *In*: Proceedings of the Forth International Conference Copepoda. Bulletin of the Plankton Society of Japan. Special Volume pp 603-611.

THE RING GROUP (which includes BACKUS, R.H., FLIERL, G.., KESTER, D.R., OLSON, D.B., RICHARDSON, P.L., VASTANO, A.C., WIEBE, P.H., WORMUTH, J.H.,), (1981) Gulf Stream cold-core rings: their physics, chemistry and biology. Science, **212**: 1091-1100.

THIBAULT, D., GAUDY, R., LE FEVRE, J., (1993) Zooplankton biomass, feeding and metabolism in a geostrophic frontal area (Almera-Oran Front, western Mediterranean). Significance to pelagic food webs. Journal of Marine Systems, **5**: 297-311.

TIMONIN, A.G., (1983) Closing plankton nets for vertical mesoplankton catches. *In*: Sovremennyye metody kolichestvennoy otsenki raspredeleniya morskogo planktona (Current Methods for Qualitative Determination of the Distribution of Marine Plankton). Moscow, Nauka Press, 158-173.

TISELIUS, P., (1992) Behaviour of *Acartia tonsa* in patchy food environments. Limnology and Oceanography. **37**: 1640-1651.

TISELIUS, P., (1998) An in situ camera for plankton studies: design and preliminary observations. Marine Ecology Progress Series. **164**: 293-299.

TRANTER, D.J., FRASER, J.H., (1986) Zooplankton sampling – UNESCO, Paris. 174pp.

TRANTER, D.J., HERON, A.C., (1967) Experiments on filtration in plankton nets. Australian Journal of Marine and Freshwater Research. **18**: 89-111.

TRANTER, D.J., SMITH, P.E., (1968) Filtration performance. *In:* D.J. Tranter and Fraser J.H. (eds.) Zooplankton Sampling. Monographs on Oceanographic Methodology 2. UNESCO, Paris, pp 27-56.

TUTUBALIN, V.E., UGER, E.G., VINOGRADOV, M.E., (1987) A statistical model for the comparison of the results of mesoplankton sampling by the water bottle and net. Oceanology English Translation. **27**: 507-512.

VAN DORN, W.G., (1957) Large-volume water sampler. Transactions of the American Geophysical Union, **37**: 682-684.

VAN DUREN, L.A., VIDELER, J.J., (1995) Swimming behaviour of developmental stages of the calanoid copepod *Temora longicornis* at different food concentrations. Marine Ecology Progress Series. **126**: 153-161.

VAN DUREN, L.A., VIDELER, J.J., (1996) The trade-off between feeding, mate seeking and predator avoidance in copepods: behavioural responses to chemical cues. Journal of Plankton Research, **18**: 805-818.

VANNUCCI, M., (1965) Loss of organisms through the meshes. *In:* D.J. Tranter and Fraser J.H. (eds.) Zooplankton Sampling. Monographs on Oceanographic Methodology 2. UNESCO, Paris, pp 77-86.

VERITY, P.G., SMETACEK, V., (1996) Organism life cycles, predation, and the structure of marine pelagic ecosystems. Marine Ecology Progress Series. **130**: 277-293.

VIDEAU, C., SOURNIA, A., PRIEUR, L., FIALA, M., (1994) Phytoplankton and primary production characteristics at selected sites in the geostrophic Almeria-Oran front system (SW Mediterranean Sea). Journal of Marine Systems **5**: 235-250.

VINDONDO, B., PRAIRIE, Y.T., BLANCO, J.M., DUARTE, C.M., (1997) Some aspects of the analysis of size spectra in aquatic ecology. Limnology and Oceanography, **42**: 184-192.

VINOGRADOV, M.E., FLINT, M.V., SHUSHKINA, E.A., (1987) Comparative sampling efficiency of the water bottles of large volume and plankton nets of vertical hauls, Oceanology Engl. Transl. **27**: 329-337. Same as: VINOGRADOV, M.E., FLINT, M.V., SHUSHKINA, E.A., TUTUBALIN, V.N., (1987B) Comparative catch efficiency of large volume sampling bottles and vertical catch plankton nets. Oceanology **27**: 242-247.

VINOGRADOV, M.E., SHUSHKINA, E.A., (1983) Collection of mesoplankton with large-volume sampling bottles. *In*: Sovremennyye metody kolichestvennoy otsenki raspredeleniya morskogo planktona (Current Methods for Qualitative Determination of the Distribution of Marine Plankton). Moscow, Nauka Press, 154-158.

VOLTERRA, V., (1926) Variazionie fluttuazioni del numero d'individui in specie animali convivienti. Mem. Acad. Lincei. **2**: 31-113.

WAITE, S.W., O'GRADY, S.M., (1980) Description of a new submersible filter pump apparatus for sampling plankton. Hydrobiology. **74**: 187-191.

WANG, R., CHEN, K.-Z., (1963) Description of a new species of the genus *Pseudeuphausia* (Crustacea) *Pseudeuphausia sinica* sp. nov. Oceanolgia et Limnologia Sinica. 5: 353-358.

WARNER, A.J., HAYS, G.C., (1994). Sampling by the Continuous Plankton Recorder Survey. Progress in Oceanography, **34**, 237-256.

WATSON, A.J., ROBINSON, C., ROBINSON, J.E., WILLIAMS, P.J.LE B., FASHAM, M.J.R., (1991) Spatial variability in the sink for atmospheric carbon dioxide in the North Atlantic. Nature. **350**: 50–53.

WEIGMANN, R., (1970) Zur Ökologie und Ernährungsbiologie der Euphausiaceen (Crustacea) im Arabischen Meer. '*Meteor*' Forschungsergebnisse, Series D, (5) 11-52.

WEIGMANN, R., (1971) Eine isolierte population von *Pseudeuphausia latifrons* (Crustacea: Euphausiacea) im Persischen Golf. Marine Biology 8: 351-355.

WELSCHMEYER, N.A., LORENZEN, C.J., (1984) Carbon-14 labelling of phytoplankton carbon and chlorophyll *a* carbon: determination of specific growth rates. Limnology and Oceanography **29**: 135-145.

WIBORG, K.F., (1948) Experiments with the Clarke-Bumpus sampler and with a plankton pump in the Loften area in northern Norway. Fisk. Dir. Skr. **9**: 1-33.

WIEBE, P.H., (1988) Functional regression equations for zooplankton displacement volume, wet weight, dry weight and carbon, a correction. Fishery Bulletin **86**: 833-835

WIEBE, P.H., BOYD, S., COX, J.L., (1975) Relationships between zooplankton displacement volume, wet weight, dry weight and carbon. Fishery Bulletin **73**: 777-786.

WIEBE, P.H., BOYD, S.H., (1978) Limits of *Nematoscelis megalops* in the north western Atlantic in relation to Gulf Stream cold core rings. Part I. Horizontal and vertical distributions. Journal of Marine Research. **36**: 119-142.

WIEBE, P.H., BURT, K.H., BOYD, S.H., MORTON, A.W., (1976b) A multiple opening/closing net and environmental sensing system for sampling zooplankton. Journal of Marine Research. **34**: 313-326.

WIEBE, P.H., HULBURT, E.M., CARPENTER, E.J., JAHN, A.E., KNAPP, G.P., BOYD, S.H., ORTNER, P.B., COX. J.L., (1976a) Gulf Stream cold core rings: large-scale interaction sites for open ocean plankton communities. Deep Sea Research **23**: 685-710.

WIEBE, P.H., MOUNTAIN, D.G., STANTON, T.K., GREENE, C.H., LOUGH, G., KAARTVEDT, S., DAWSON, J., COPLEY, N., (1996) Acoustical study of the spatial distribution of plankton on Georges Bank and the relationship between volume backscattering strength and the taxonomic composition of the plankton. Deep–Sea Research **43**: 1971-2001.

WIELAND, K., PETERSEN, D., SCHNACK, D., (1997) Estimates of zooplankton abundance and size distribution with the Optical Plankton Counter (OPC). Arch. Fish. Mar. Res. **45**: 271-280.

WILLIAMS, R., COLLINS, N.R., CONWAY, D.V.P., (1983) The double LHPR system, a high speed micro- and macroplankton sampler. Deep–Sea Research **30**: 331-342

WISHNER, K., DURBAN, E., DURBIN, A., MACAULAY, M., WINN, H., KENNEY, R., (1988) Copepod patches and right whales in the Great South Channel off New England. Bulletin of Marine Science. **43**: 825-844.

WYRTKI, K., (1973) Physical Oceanography of the Indian Ocean. *In*: The Biology of the Indian Ocean. B., Zeitzschel (Ed.). Chapman and Hall Limited, London. Springer-Verlag Berlin-Heidelberg-New York. 544pp.

YAMAZI, I., (1974) Analysis of the data on temperature, salinity and chemical properties of the surface water, and the zooplankton communities in the Arabian Gulf in December, 1968, Trans. Tokyo Univ. Fish. **1**: 25-51

YODER, J.A., MCCLAIN, C.R., FELDMAN, G.C., ESAIAS, W.E., (1992) Annual cycles of phytoplankton chlorophyll concentrations in the global ocean: a satellite view. Global Biogeochemical Cycles. **7**: 181-193.

ZHANG, X., ROMAN, M., SANFORD, A., ADOLF, H., LASCARA, C., BURGETT, R., (2000) Can an optical plankton counter produce reliable estimates of zooplankton abundance and biovolume in water with high detritus? Journal of Plankton Research, **22**: 137-150.

APPENDIX

Appendices to the thesis

1 PEXEC PROCESSING OF OPC DATA FROM CD 104 235
2 THE RELATIONSHIP BETWEEN THE LENGTH AND WIDTH OF COPEPODS . . . 236
3 QUANTIFYING AND CORRECTING THE LHPR SAMPLE SHRINKAGE . . . 240
4 COMPARISON BETWEEN THE BIOVOLUME TO CARBON CONVERSIONS FOR ZOOPLANKTON . 241
5 RELATING ESD SIZES TO LENGTHS AND LHPR SAMPLES 243

FIGURES

Appen.i Copepod length and width measurements from the preserved LHPR samples taken in the Strait of Hormuz 238
Appen.ii Quantifying zooplankton sample shrinkage from RMT samples collected at stns 54001 and 54002. 238
Appen.iii Zooplankton carbon plotted as a function of biovolume, determined by the calibrations of Wiebe (1988) and Parsons *et al* (1977) 242

Appendix 1 Pexec Processing of OPC data from CD104

A series of PEXEC programs were used to process the OPC data collected during the first leg of R.R.S. *Charles Darwin* cruise 104 (CD 104). The majority of the programs are standard PEXEC programs, although several (*popcin, popcain, gropc3, pverts* and *pverti*) were written by Raymond Pollard, and one (*pinvxy*) by Jane Read to aid OPC data processing. Details of programs are available on PSTAR manual pages. All the scripts to run the programs were written by Alexander Mustard.

Reading Data from PC data files, and merging with spatial data:

FUNCTION	PROGRAM	SCRIPT
Read in OPC count data from binary PC data file	*popcin*	*popc0*
Read in OPC attenuance data from binary PC data file	*popcain*	*popc0*
Subtract 50 seconds from the time in the counts file	*pcalib*	*popc1*
Merge counts data with concurrent SeaSoar file's press & distrun	*pmerge*	*popc1*
Subtract 50 seconds from the time in the attenuance file	*pcalib*	*popc1*
Merge attenuance data with SeaSoar file's press & distrun	*pmerge*	*popc1*
Grid attenuance file this is the end of attenuance procssing	*pgrids*	*popc1*

Main processing steps to produce the files for contouring:

FUNCTION	PROGRAM	SCRIPT
List header of file	*plisth*	*popcgrid.c*
Grid OPC file in 3 dimensions, calculate volume filtered, zooplankton abundance & uncalib'd biovolume (volratio) into 5 useful (7 total) logarithmically incrementing size classes.	*gropc3*	*popcgrid.c*
Add latitude and longitude data from the navigation file	*pmerge*	*popcgrid.c*
Calibrate size class values from digital size to ESD in mm	*tabcal*	*popcalib.c*
Change the name and units of this variable to size_lg2 and mm3	*pheadr*	*popcalib.c*
Multiply variable volratio by factor of 0.61 to produce calibrated biovolume in mm3/m3	*pcalib*	*popcalib.c*
Triplicate the variable volratio to calculate the carbon values (as Wiebe '88 & Parsons et al '77)	*pcopya*	*popcalib.c*
Add a small constant to second volratio (Wiebe's carbon) and divide by 1000	*pcalib*	*popcalib.c*
Calculate $\log_{10}$ of this variable, and rename carbonW	*psoup*	*popcalib.c*
Multiply this variable by 1.2195 and add 1.7488	*pcalib*	*popcalib.c*
Inverse log10 of this variable	*psoup*	*popcalib.c*
Remove the small constant	*pcalib*	*popcalib.c*
Rename variable 1st volratio as biovol and change units of carbonW to mg/m3	*pheadr*	*popcalib.c*
Determine Parsons carbon from third volratio: Multiply by 1.03, then 0.0916, then 0.446, values from Matondkar et al., (1995)	*pcalib*	*popcalib.c*
Rename this volratio (3rd) as carbonP and change units to mg/m3	*pheadr*	*popcalib.c*
View header of output file	*plisth*	*popcalib.c*
Reorder variables in file order changes from spd to psd	*pinvxy*	
Reorder variables in file order changes from psd to pds	*pinvxy*	
Data cycles for size class 1 selected and variables copied (press, distrun, lat and long too)	*pcopya*	*3dto2d.c*
Variables of biovol and abundnce renamed to indicate represent size class 1	*pheadr*	*3dto2d.c*
Data cycles for size class 2 selected and biovol and abundnce	*pcopya*	*3dto2d.c*

variables only copied		
Variables of biovol and abundnce renamed to indicate represent size class 2	*pheadr*	*3dto2d.c*
Data cycles for size class 3, 4 & 5 selected and biovol and abundnce variables only copied	*pcopya* *3	*3dto2d.c*
Variables of biovol and abundnce renamed to indicate represent size class 3, 4 & 5	*pheadr* *3	*3dto2d.c*
Rejoin all files created for each class by *pcopya* making a file with each size class separately displaying abundance and biovolume	*pjoin* *4	*3dto2d.c*
Reset nplane to 0	*pheadr*	*3dto2d.c*
Attach physical data (potemp, salin, sigma0 and light), and chlorophyll from SeaSoar file	*pjoin*	

These processing steps were repeated to produce the data file needed for size spectra analysis, except with a different gridding parameters in *gropc3*, and with more repetitions of *pcopya*, *pheadr* and *pjoin*. This processing used the scripts *popcgrid.s*, *popcalib.s*, and *3dto2d.s*.

The main processing steps involved in vertically integrating, and size class summing the data:

From .pds input file: remove unwanted size classes	*pcopya*	*popcvert1*
Change nplane to new number of size classes	*pheadr*	*popcvert1*
Reorder variables into psd order	*pinvxy*	*popcvert1*
Integrate over depth for both biovol, carbonW and carbonP	*pverti*	*popcvert1*
Change units to $mm^3\ m^{-2}$ and $mgC\ m^{-2}$ respectively (output 1)	*pheadr*	*popcvert1*
Sum biovol, carbonW and carbonP of all the size classes of file output 1	*pverts*	*popcvert1*
Change units to $mm^3\ m^{-2}$ and $mgC\ m^{-2}$ respectively (output 2)	*pheadr*	*popcvert1*
Reorder input file to spd format	*pinvxy*	*popcvert1*
Sum biovol, carbonW and carbonP of all the size classes	*pverts*	*popcvert1*
Change units to $mm^3\ m^{-3}$ and $mgC\ m^{-3}$ respectively (output 3)	*pheadr*	*popcvert1*

Appendix 2 The relationship between the length and width of copepods

It is important to determine the shape of the dominant zooplankton in order to calculate zooplankton biovolume from the ESD size measured by the OPC (§3.3). During CD 104 copepods were the numerically dominant mesozooplankton caught by the LHPR samples from the Strait of Hormuz. In these samples copepods accounted for more than 90% of all individuals. Moreover, previous studies in the region (Michel *et al.*, 1986b) have shown that copepods can be even more numerous in the <1 mm size classes detected by the OPC, but missed by the LHPR.

A copepod can be approximated as an spheroid when sized by an OPC (Herman, 1992; Sprules *et al.*, 1998), and therefore an spheroid model is used to determine

biovolume in this study. To determine the typical dimensions of copepods in the Strait length and width measurements were made of preserved copepods from the LHPR samples. These measurements are used to define the dimensions of the spheroid. The shape of the spheroid is important because it will effect both the volume of the spheroid, and the CSA measured for a particle at different orientations in the beam.

These measurements were made using a binocular microscope and a calibrated Hitachi digitising tablet, controlled by the Jandel Scientific program Sigmascan. The maximum length and width of 75 copepods were measured. Length was determined along the median line from the anterior tip of the cephalothorax to the posterior end of the urosome (setae were not included). Width was measured as the maximum width of the prosome. Other appendages were not included in these measurements. The data are presented in Table 2a.1.i and **Fig Appen.i**.

The average length to width ratio of these measurements was **2.72:1** (with a standard deviation of 0.4). This is less than the usual 3:1 ratio that is often quoted as a length to width ratio of copepods (Herman 1992), and in some regions values as high as 4:1 have been used for this relationship, (Pollard *et al.*, submitted). The spread of values was relatively consistent below 2 mm, which represents the numerically dominant zooplankton sampled by the OPC. The ratio showed a wider spread above this size.

Fig Appen.i also shows that the LHPR net does not retain zooplankton smaller than 1mm, the smallest zooplankton after preservation was 0.95 mm. This is consistent with the findings of Barnes and Tranter's (1965), who determined the minimum retention size of a 333 μm IOSN net as 1 mm.

More importantly these dimensions of the dominant species do not include measurements made of species smaller that 1 mm, although the biovolume of zooplankton of this size have been determined by extrapolating this calibration. In future studies it is recommended that spheroid calibration factors are determined for from the whole size range. Also if different sized zooplankton show different relationships then different calibrations should be applied to the size classes. This is also important in areas where copepods do not dominate the counts of the OPC.

Figure Appen.i Copepod length and width measurements from the preserved LHPR samples taken in the Strait of Hormuz. The solid line represents the mean ratio (2.72:1) and the dashed llines show the standard deviation of the ratio

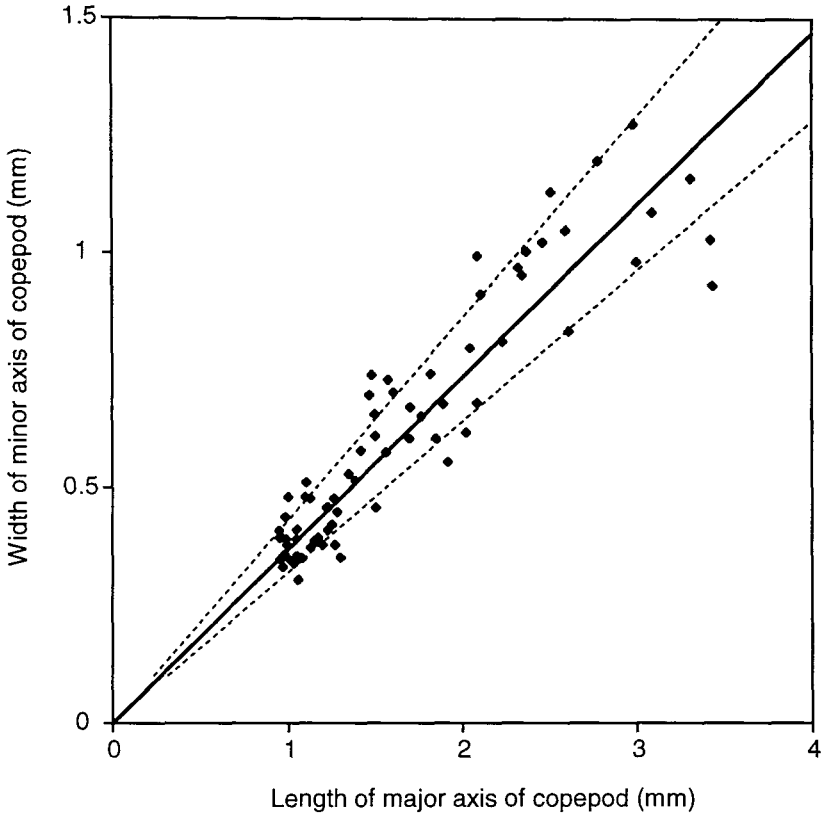

Figure Appen.ii Quantifying zooplankton sample shrinkage from RMT samples collected at stns 54001 and 54002

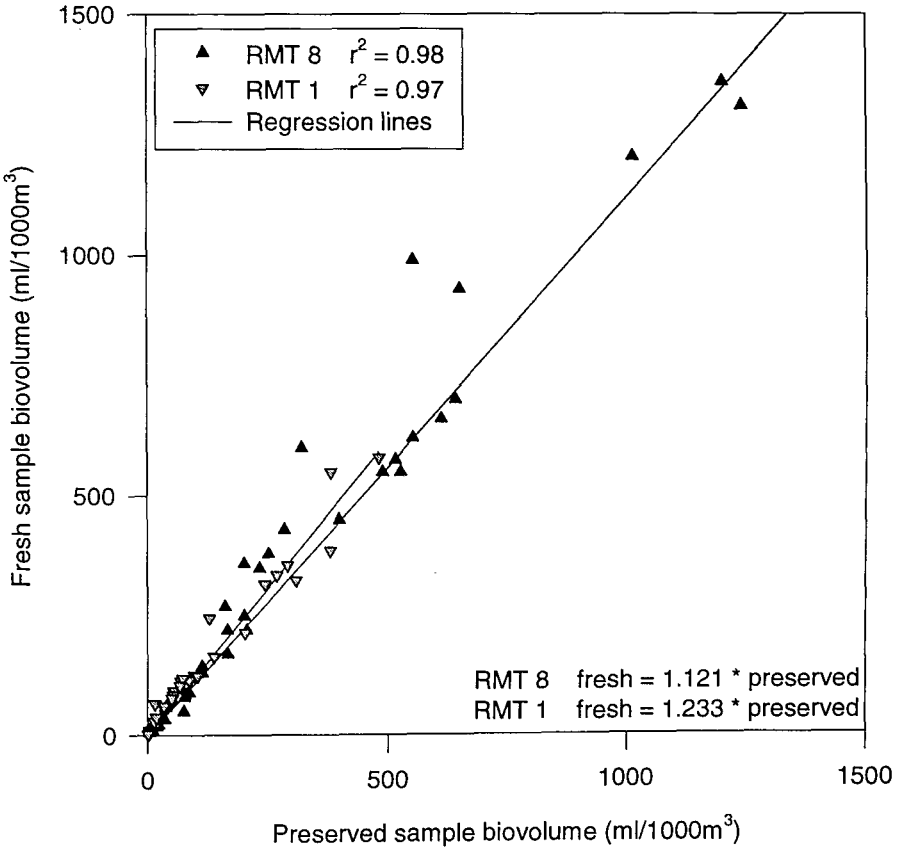

Table 2a.1.i Length and width measurements of copepods from LHPR samples in the Strait

Length (mm)	Width (mm)	Ratio a:b	Length (mm)	Width (mm)	Ratio a:b
3.435	0.932	3.69	1.351	0.530	2.55
3.424	1.030	3.32	1.300	0.352	3.69
3.309	1.161	2.85	1.282	0.449	2.86
3.091	1.088	2.84	1.271	0.379	3.36
3.001	0.982	3.06	1.264	0.478	2.64
2.984	1.276	2.34	1.254	0.422	2.97
2.780	1.198	2.32	1.229	0.459	2.68
2.614	0.834	3.13	1.227	0.410	2.99
2.595	1.049	2.47	1.222	0.458	2.67
2.512	1.132	2.22	1.198	0.379	3.16
2.464	1.024	2.41	1.174	0.394	2.98
2.371	1.004	2.36	1.165	0.385	3.03
2.349	0.954	2.46	1.152	0.387	2.98
2.326	0.970	2.40	1.132	0.373	3.04
2.236	0.812	2.75	1.126	0.478	2.36
2.110	0.913	2.31	1.107	0.512	2.16
2.092	0.995	2.10	1.099	0.481	2.28
2.089	0.682	3.06	1.080	0.350	3.09
2.050	0.799	2.57	1.076	0.350	3.07
2.023	0.619	3.27	1.066	0.350	3.04
1.920	0.556	3.45	1.057	0.304	3.48
1.894	0.680	2.79	1.051	0.411	2.55
1.850	0.606	3.05	1.049	0.355	2.96
1.822	0.744	2.45	1.047	0.391	2.68
1.769	0.654	2.70	1.030	0.340	3.03
1.705	0.673	2.54	1.012	0.346	2.93
1.698	0.606	2.80	1.001	0.481	2.08
1.608	0.704	2.28	0.995	0.379	2.63
1.577	0.731	2.16	0.990	0.391	2.53
1.564	0.576	2.71	0.985	0.438	2.25
1.504	0.458	3.28	0.983	0.359	2.74
1.502	0.611	2.46	0.969	0.332	2.92
1.502	0.657	2.29	0.962	0.395	2.43
1.483	0.741	2.00	0.953	0.348	2.74
1.470	0.698	2.11	0.951	0.394	2.41
1.419	0.580	2.44	0.950	0.409	2.32
1.388	0.517	2.68			

Mean ratio of a:b, this is r_{cop} : 2.715

Standard deviation : 0.4

Appendix 3 Quantifying and correcting the shrinkage of LHPR samples

Zooplankton preserved in formaldehyde change considerably over time, both physically and chemically (Fudge 1968; Hopkins, 1968; Beers, 1976; Omori and Ikeda, 1992). Zooplankton samples consistently show a significant reduction in the volume as a result of preservation in formaldehyde, with typical shrinkage of 5 to 40% (Beers, 1976; Omori and Ikeda, 1992; Beaulieu *et al.*, 1999). This varies with a number of factors including the taxa present in the sample, the size of the zooplankton and the region and time of year sampled. Before any comparison was made with the OPC data it is essential to correct for shrinkage the LHPR biovolume.

During the CD104 zooplankton samples were collected using both a rectangular midwater trawl (RMT) net system and a LHPR. It was not possible to volume the zooplankton at sea before preservation because LHPR samples are collected into a long sandwich of sampling gauze, and cannot be retrieved on board. As a result, LHPR biovolume measurements were only obtained after preservation shrinkage had occurred, when the samples were returned to the UK 3 months after the cruise.

The RMT zooplankton samples were volumed at sea just after preservation in a 4% formaldehyde solution, and then again 3 months later when the samples were returned to the UK. The RMT samples provide a dataset that can be used to quantify and correct the preservation shrinkage of the LHPR samples. The RMT1 collected a more comparable size range of zooplankton to the LHPR than the RMT8, however both have been included in this analysis as the larger animals from the RMT1 were removed before the samples were re-volumed after preservation the SOC. Therefore, the shrinkage calibration factor combines the data from both the RMT 1 and 8.

Fig Appen.ii, shows the data and regression lines of the biovolume before preservation as a function of the biovolume after preservation. The RMT8 biovolume shrank by 12% and the RMT1 shrank by 23% as a result of preservation. The removal of the larger organisms from the RMT1 samples probably accounts for the larger shrinkage of these samples. Therefore a value close to the RMT8 shrinkage, of 15%, has been used to correct the LHPR biovolume for the effect of preservation.

Appendix 4 Comparison of conversions for zooplankton biovolume to carbon

Two conversion methods were used to calculate carbon biomass from the zooplankton biovolume measurements from the OPC. The first was the conversion equation of Wiebe (1988), which is a correction of Wiebe *et al.* (1975) and is determined from empirical zooplankton studies in diverse ocean environments:

$$Log_{10}(Carbon(mg)) = 1.2.195 Log_{10}(Volume(ml)) + 1.7488 \quad . \quad . \quad \text{Eq. App.1}$$

Pollard *et al.* (submitted) argue that such calibration factors are unsuitable for OPC data because they are derived from net samples which have an increased volume resulting from interstitial water. However, the OPC data here have been calibrated to fit the biovolume measured by the net, before the conversion to carbon. Pollard *et al.* (1999) calculate wet weight from volume assuming the zooplankton have a density equal to seawater, then the dry weight as 10% of the wet, and finally carbon as 50% of the dry weight in a method similar to that developed by Parsons *et al.* (1977) for Coulter counter data. In this study, these values are modified to better represent the zooplankton sampled in the Strait of Hormuz by using data collected in the same month 5 years earlier in the Arabian Sea (Matondkar *et al.*, 1995). In Matondkar *et al.*'s dataset, the dry weight of copepod dominated samples accounted for 9.16% of wet weight, and carbon represented 44.6% of dry weight.

These two conversions are compared in **Fig Appen.iii**. At the typical biovolume values represented by each size class in **Fig 4.1.1.i** (a range of 0.1 to 0.7 ml m^{-3}) the two calibrations produce equivalent carbon biomass. At higher biovolume values Wiebe's equation produces higher carbon biomass than the method of Parsons *et al.*

Figure Appen.iii Zooplankton carbon plotted as a function of biovolume determined from the calibrations of Wiebe (1988) and Parsons *et al.* (1977)

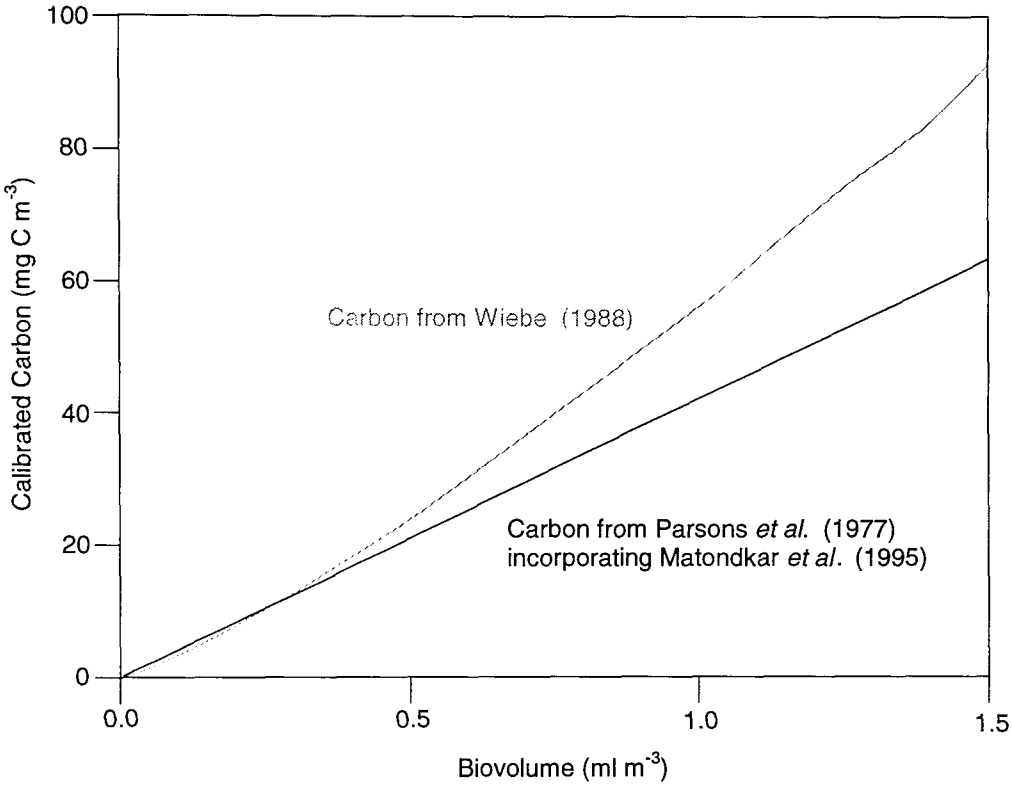

Appendix 5 Relating ESD sizes to lengths and LHPR samples

Zooplankton size is commonly specified either in terms of ability to pass through nets of known mesh size, or length determined microscopically. In this thesis zooplankton size measured by the Optical Plankton Counter is presented as an equivalent spherical diameter (ESD). ESD is widely used to quantify zooplankton size from the OPC (e.g. Herman, 1992; Wieland *et al.*, 1997; Gallienne *et al.*, 2001). (Details of how the OPC measures ESD are presented in §3.2.2). ESD has also been used for describing net samples and for classifying the pelagic community over several orders of magnitude (e.g. Sheldon *et al.*, 1972; Steele, 1977; Lenz, 2000).

A conversion table is presented in this section to relate mesozooplankton lengths and size fractions separated by nets to ESD, using the data for this study. In addition, the ESD measurements from the OPC are qualitatively compared with the LHPR samples to identify the dominant taxa in each size class. The way that the OPC and the LHPR measure size gives rise to different biases because of the way different species are divided into size classes. For example, the ESD recorded for a partly transparent chaetognath will be smaller than an ESD determined from its measured dimensions. In addition, a long and thin chaetognath may be retained by a mesh that is much large that its cross section because when side on it will not pass through, and therefore be placed in a larger size class. For this reason this is not a precise conversion between OPC sizes and LHPR size fractions. The conversion table presented below should be viewed as a guide.

The length of each particle of given ESD can be calculated if it is assumed that the particle is spheroidal (§3.2.2) and its major axis is perpendicular to the beam (i.e. $\theta=0°$). The dimensions of the spheroid are defined by r_{cop} (§3.2.2).

From Eq 3.2.2 and Eq 3.2.5 it is known that:

$$\left(\frac{ESD}{2}\right)^2 = ab \quad . \quad . \quad . \quad . \quad . \quad . \quad . \quad . \quad \text{Eq App. 2}$$

It is also know that $b=a/r_{cop}$ (p 78) therefore Eq App. 2 can be solved for a:

$$a = \sqrt{\left(\frac{ESD}{2}\right)^2 r_{cop}} \quad . \quad . \quad . \quad . \quad . \quad . \quad . \quad . \quad \text{Eq App. 3}$$

The particles equivalent spheroid length (ESL) is $2a$.

The conversion table 5a.1.i correlates the ESD sizes measured by the OPC to the particle lengths, approximate LHPR size fractions, and the dominant species and taxonomic groups expected to be present (data from LHPR and Michel *et al.*, 1986b).

Table 5a.1.i Conversion data for OPC measured ESD with lengths, LHPR samples and taxa

ESD size from OPC (mm)	Spheroid length (mm) {r_{cop}=2.72}	LHPR Size Fraction (mm)	Dominant Taxonomic Groups and Species from LHPR and Michel *et al.* (1986b)
0.40-0.64	0.66-1.06	Too small (not measured)	Copepoda >90% (e.g. *Onacea, Oithona*)
0.64-1.02	1.06-1.68	<1.5	Copepoda >90% (e.g. *Paracalanus, Corycaeus*)
1.02-1.61	1.68-2.66	<1.5, 1.5-4.5	Copepoda >90% (*Temora, Euterpina*)
1.61-2.56	2.66-4.22	1.5-4.5	Copepoda 60-80%
2.56-4.07	4.22-6.71	1.5-4.5, >4.5	Chaetognatha (*Sagitta*), Euphausiacea, Decapoda, Ostracoda,

N.B. Dominant copepods species are given for adult sizes, nauplii and copepodites will occupy smaller size classes.

This table is specific to the zooplankton of this study. Areas dominated by other species of zooplankton (i.e. not copepods) maybe expected to have different relationships between ESD and other measures of size.